

Aus dem Institut für Transfusionsmedizin und Immunologie
der Medizinischen Fakultät Mannheim
(Direktor: Prof. Dr. med. Harald Klüter)

Development of a noninvasive prenatal test for the determination of fetal
blood cell antigens

Inauguraldissertation
zur Erlangung des Doctor scientiarum humanarum (Dr. sc. hum.)
der
Medizinischen Fakultät Mannheim
der Ruprecht-Karls-Universität
zu
Heidelberg

vorgelegt von
Marion Eryilmaz, geb. Nimz

aus
Neustadt in Holstein
2021

Dekan: Prof. Dr. med. Sergij Goerd
Referent: Prof. (apl) Dr. rer. nat. Peter Bugert

Mother is the name for God in the lips and hearts of little children.

William Makepeace Thackeray

TABLE OF CONTENT

	Seite
LIST OF ABBREVIATIONS	1
1 INTRODUCTION	4
1.1 Red Blood Cell Antigens	4
1.1.1 RH System	4
1.1.2 KEL Sytem	5
1.2 Erythroblastosis Fetalis	6
1.3 Human Platelet Antigens	8
1.3.1 Nomenclature of HPA	8
1.3.2 HPA-1	10
1.3.3 HPA-2	11
1.3.4 HPA-3	11
1.3.5 HPA-5	12
1.3.6 HPA-15	12
1.4 Fetal and Neonatal Alloimmune Thrombocytopenia	13
1.5 Noninvasive Prenatal Diagnosis	13
1.5.1 Quantitative Real Time PCR	15
1.5.2 Massive Parallel Sequencing	15
1.5.3 Fetal Control Markers	17
1.5.4 Internal PCR Control	18
1.6 Aim of the dissertation	19
2 MATERIAL AND METHODS	20
2.1 Reagents and Devices	20
2.2 Consumables	24
2.3 Primer Mixtures	26
2.4 Primer Sequences for Preamplification and dPCR	30
2.5 Primer Sequences for PCR-SSP	31
2.6 Preparation and Storage of Cell-Free Plasma	33
2.7 DNA Isolation Methods	33
2.7.1 Genomic DNA Isolation Methods	34
2.7.2 Cell-Free DNA Extraction Methods	34
2.8 DNA Amplification Methods	36
2.8.1 Multiple Displacement Amplification	36
2.8.2 Whole Genome Amplification with REPLI-g Mini Kit	37
2.8.3 Whole Genome Amplification with REPLI-g FFPE Kit	37
2.8.4 Targeted Preamplification PCR	38
2.9 PCR Purification	38
2.10 Digital PCR	39
2.11 Sequence-Specific Primer PCR for Maternal Pretyping	41
2.12 RHD Zygosity Test with qPCR	44
2.13 SRY Verification with PCR	45
2.14 Calculations for dPCR Evaluation	45
2.15 Calculations for the Number of Molecules After Preamplification PCR	46
2.16 Simulation of Pregnancies for Technical Validation	46
3 RESULTS	48
3.1 Protocol Development for Noninvasive Prenatal Antigen Testing	48
3.1.1 Influence of Different Elution Liquids on dPCR Results	48
3.1.2 Influence of Plasma Volume on dPCR Results	49
3.1.3 Investigation of Different Cell-Free DNA Isolation Methods	51
3.1.4 Signal Amplification Using Different PCR Methods	56
3.1.5 Optimization of Molecule Density	66
3.1.6 Comparison Between Automatic and Manual Cell-Free DNA Isolation	68
3.2 Summary of Protocol Development	72
3.3 Validation Process of Red Blood Cell and Platelet Antigens	73

3.3.1	Validation of the <i>RHD</i> Assays	73
3.3.2.	Validation of the <i>KEL</i> Assay.....	77
3.4	Validation of <i>HPA</i> Assays.....	79
3.4.1	Validation of <i>HPA-1</i>	79
3.4.2	Validation of <i>HPA-2</i>	80
3.4.3	Validation of <i>HPA-3</i>	81
3.4.4	Validation of <i>HPA-5</i>	82
3.4.5	Validation of <i>HPA-15</i>	83
3.5	Validation of Gonosomal and Autosomal Markers	83
3.5.1	Validation of Amelogenin	84
3.5.2	Validation of Autosomal SNPs	85
3.6	Summary of Technical Validation	88
3.7	Preliminary Results from Clinical Validation.....	89
3.7.1	Clinical Validation of the <i>RHD</i> Assays.....	90
3.7.2	Clinical Validation of the <i>KEL</i> Assay	91
3.7.3	Clinical Validation of the <i>HPA</i> Assays	92
3.7.4	Clinical Validation of Amelogenin.....	98
3.7.5	Clinical Validation of the Autosomal SNP Assays	100
3.8	Summary of Clinical Validation	112
4	DISCUSSION.....	114
4.1	Optimization of the Protocol	114
4.2	Technical Validation of the Assays	115
4.3	Clinical Validation of the Assays.....	117
4.4	Conclusion and Outlook	124
5	ABSTRACT	125
6	LITERATURE LIST	127
7	SUPPLEMENTAL MATERIAL	142
8	CURRICULUM VITAE	145
9	ACKNOWLEDGEMENTS	147

LIST OF ABBREVIATIONS

%	Percent
°C	Centigrade
µg	Micrograms
µl	Microliter
µM	Mikromol
aa	Amino acid
ag	Attogram (10 ⁻¹⁸)
AMEL	Amelogenin
AMEL-X	Amelogenin from the X-chromosome
AMEL-Y	Amelogenin from the Y-chromosome
anti-D	Antibody against the rhesus D antigen
Anti-K	Antibody against the KEL antigen
anti-Rh	Antibody against the rhesus antigen
bar	Bar
BCT	Blood collection tubes
BFU-E	Erythroid burst-forming units
bp	Base pairs
CD109	Cluster of Differentiation 109
CD34	Cluster of Differentiation 34
cells/L	Number of cells in one liter
cFAM	Concentration of FAM molekules
cfDNA	Cell-free DNA
cffDNA	Cell-free fetal DNA
CFU	Colony-forming units
CFU-E	Colony-forming unit erythroid
(COLD) HRM PCR	(Coamplification at lower temperature) High-resolution melting PCR
copies/µl	Number of copies from a molecule in one µl
Cr ₅₁	Chromium-51
ct	Cycle threshold, is the point at which the exponential growth of a curve begins and the signal leaves the background
cVIC	Concentration of VIC molekules
D	Rhesus antigen
ddH ₂ O	Double-distilled water
DNA	Deoxyribonucleic acid
D-negative	No rhesus D-antigen present
dNTP	Desoxyribonukleosid Triphosphate
dPCR	Digital PCR
D-positive	Rhesus D antigen is present

LIST OF ABBREVIATIONS

e.g.	Exempli gratia = for example
EDTA	Ethylenediaminetetraacetic acid
EtOH	Ethanol
FAM	6-Carboxyfluorescein
FFPE	Formalin-Fixed Paraffin-Embedded
FNAIT	Fetal/neonatal alloimmune thrombocytopenia
FRET	Förster resonance energy transfer
g	Gravitational force
g	Gram
GAPDH	Glyceraldehyde 3-phosphate dehydrogenase enzyme
gDNA	Genomic DNA
Gov	HPA-15
GPI α	Glycoprotein 1alpha
GPI β	Glycoprotein 1beta alpha
GPII	Glycoprotein 2
GPIIb	Glycoprotein 2 beta
GPIIb/IIIa	Glycoprotein 2beta / 3 alpha
GPIII	Glycoprotein 3
GPIIIa	Glycoprotein 3 alpha
h	Hour
HPA	Human platelet antigen
ICH	Intracranial hemorrhage
IgG	Immunoglobulin G
ISBT	International Society of Blood Transfusion
K	KEL antigen
kb	Kilobases
kDa	Kilodalton
KEL	Blood group
<i>KEL</i>	KEL gene
KEL	KEL blood group
KEL1	KEL1 allele
KEL2	KEL2 allele
Kell	KEL antigen
MDA	Multiple displacement amplification
mg	Milligram
MHN	Morbus haemolyticus neonatorum or erythroblastosis foetalis
MPS	Massive parallel sequencing
NAD	Nicotinamide adenine dinucleotide
ng	Nanogram
NGS	Next-Generation Sequencing

LIST OF ABBREVIATIONS

NIPT	Noninvasive prenatal test
No.	Number
PBS	Phosphate-buffered saline
PCR	Polymerase chain reaction
pg	Pikogram
pl	Pikoliter
qPCR	Quantitative PCR
RASSF1A	Ras association domain-containing protein 1A
RBC	Red blood cell
RH	Blood group
RHD	Rh(D) polypeptide, blood group
RhD	Rhesus antigen
<i>RHD</i>	Rhesus gene
ROX	5- and 6-carboxy-X-rhodamin;
rpm	Revolutions per minute
RT	Room temperature
SBS	Sequencing by synthesis (SBS)
SDS	Sodium dodecyl sulfate
sec	Second
SNP	Single Nucleotide Polymorphism
SRY	Sex-determining region Y
SSP-PCR	Sequence-specific primer PCR
STR	Short tandem repeats
™	Trademark
V	Volt
VIC	2'-chloro-7'phenyl-1,4-dichloro-6-carboxy-fluorescein;
VLA-2	Very Late Activation Antigens-2
WGA	Whole Genome Amplification
Δ	Delta

1 INTRODUCTION

This thesis's subject is the analysis of blood cell and platelet antigens of unborn children using cell-free DNA (cfDNA) isolated from the mother's plasma. This introduction chapter should give an overview of the analyzed antigens, complications in case of an incompatibility between the blood or platelet antigens of mother and child, and about cfDNA.

1.1 Red Blood Cell Antigens

Red blood cells (RBC) are mainly responsible for the transportation of oxygen from the lung to the cells in the body. These cells contain neither a nucleus nor any organelles. On the erythrocytes' surface are different antigens responsible for the different blood groups, like the ABO, RH or KEL system (Figure 1). An incompatibility between the antigens of one person with another can lead, e.g., to complications in pregnancy or blood transfusions. In the following, the antigens of the RH and KEL system will

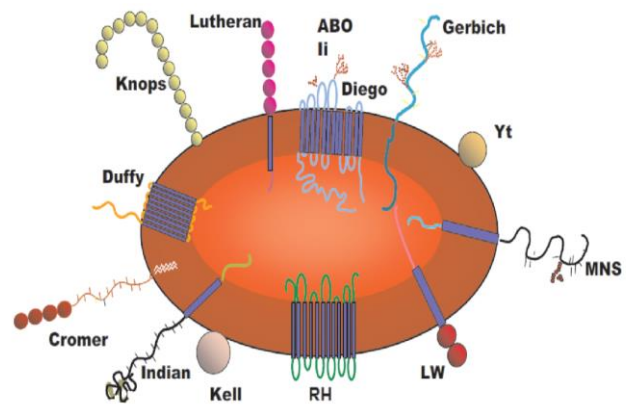


Figure 1: Surface of an erythrocyte with blood antigens [1].

be introduced. The clinical manifestation of the blood cell incompatibility between mother and child is the Erythroblastosis fetalis, which will also be explained (chapter 1.2).

1.1.1 RH System

The history of the Rhesus factor (RhD) started with the description of a hemolytic reaction in 1939 by Levine and Stetson. A Woman received after stillbirth blood from her husband and showed transfusion reactions, like chill and pain, although both had the same blood group. Further tests indicated that the response was independent of the known general blood groups. Therefore, they postulated that the mother was immunized during pregnancy by a fetal antigen inherited from the father [2, 3]. One year later, Landsteiner and Wiener obtained an anti-Rh by injecting red blood cells from a rhesus monkey into rabbits. This antibody agglutinated rhesus monkey red blood cells as well as 85 % of the white New Yorkers [3, 4]. The RH system is genetically defined by two highly homologous genes [5]. The *RHCE* gene encodes the RhCE subgroup antigens, the *RHD* gene encodes the RhD antigen. Both consist of 10 exons and are located on chromosome 1 p34.3-1p36.1 [6, 7]. Interestingly, the *RHD* and *RHCE* genes are arranged in the opposite orientation [8]. The *RHD* gene is flanked by two segments, called rhesus boxes, in which the origin of the *RHD* deletion is [9]. Therefore, an RhD negative phenotype is characterized by the absence of the *RHD* gene [5] (Figure 2). The inheritance of the Rh factor is dominant Mendelian and not sex-linked [10]. The proteins encoded by *RHD* and *RHCE* are out of 417 amino acids and differ in only 36 amino acids [11, 12]. Each of these proteins comprises twelve membrane-spanning domains whereby the N and the C-terminus are located in the cytoplasm [13] (Figure 2). The occurrence of the RhD antigen in blood cell development was shown in vitro cultures. Here, it was demonstrated that after 9-11 days of culture, the RhD antigen could be detected. Additionally, it was demonstrated that the RhC antigen was present before the RhD antigen, and both are expressed after the Kell antigen [14].

There are several different RhD variants. The most important for the prenatal diagnosis are the D weak and partial D variants. Partial D are characterized by a D-positive phenotype, but can form anti-D. This variant was first described in 1962 by Tippett et al. [15].

A change of the amino acid sequence in the *RHD* gene results in a difference in the protein folding and can cause an epitope loss [16]. Due to the ability of anti-D formation, women with partial D should receive immunoglobulins.

The other type is the weak-D, which was described by Stratton [17]. This type is characterized by a reduced D-protein expression on the surface of erythrocytes [18]. The reason for a weak-D is based on the amino acid substitution positioned in the transmembranous and intracellular protein segments [19]. The antigen density of weak-D samples varies between less than 100 in weak-D type 12 and about 4,000 RhD antigens per cell in weak-D type 4.1 [20].

Weak-D results in no antibody formation because the protein structure is intact, and only the quantitative amount of the protein is reduced. Women with weak D do not need immunoglobulins.

1.1.2 KEL System

Anti-Kell was first mentioned by Coombs et al. in 1946 [22]. A few years later, the anti-Cellano antibody was described [23]. The *KEL* gene is located on chromosome 7q33-q35 [24-26]. The Kell (KEL1, K) and Cellano (KEL2, k) antigens are defined by a SNP located in exon 6 in which a C is substituted to a T. This results in the amino acid sequence a change from Threonine to Methionine at position 193 [27] (Figure 3).

K2: Asn Phe Asn Arg **Thr** Leu Arg
AAC TTT AAC CGA **ACG** CTG AGA

AAC TTT AAC CGA **ATG** CTG AGA

K1: Asn Phe Asn Arg **Met** Leu Arg

Figure 3: The difference between K1 and K2 is an amino acid sequence change from C to T.

The Kell protein consists of 732 amino acids, and its sequence shows strong homology with zinc-binding neutral endopeptidases. The resulting glycoprotein is 93 kDa and is characterized as a type II single-pass transmembrane spanning protein, indicated by an N-terminus situated on the cytoplasmatic side. [28] (Figure 4).

The frequency of distribution in the caucasian population for the Cellano antigen is 91.2 % Cellano homozygous (kk), meaning they are negative for Kell. 8.6 % are Kell/Cellano heterozygous (Kk), and only 0.2 % are Kell homozygous (KK), therefore, negative for Cellano [23].

The occurrence of Kell antigen based of the KEL2 allele was found in fetuses between 6-7 weeks of gestation, whereas the Kell protein from the KEL1 allele was detected between 10-11 weeks of gestation [29].

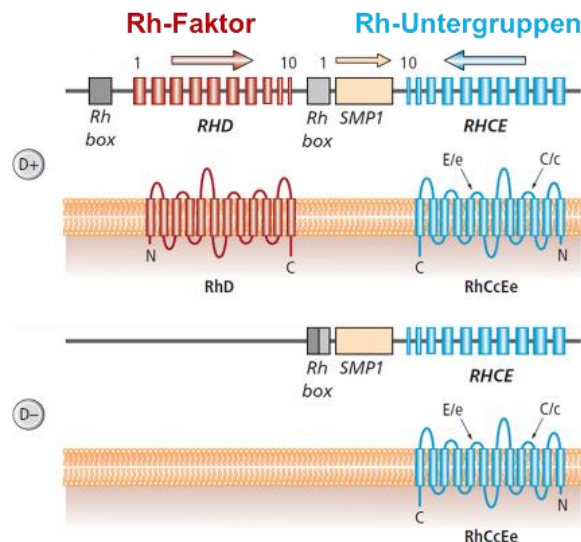


Figure 2: Rhesus positive and rhesus negative phenotype on the surface of an erythrocyte [21].

Cell culture with placental cord blood indicated progenitor cells (BFU-E and CFU-E) with high Kell antigens levels from KEL1 allele but CD34 negative after six days of culture. Indicating that KEL1 is the first erythroid-specific epitope shown in vitro cultures of cord blood cells [14].

In the case of a KEL2 (kk) mother carrying a KEL1/KEL2 (Kk) child, the process of Erythroblastosis fetalis development is different as in RhD incompatibility. The anti-K antibody inhibits the growth of KEL1 positive erythroid progenitor cells (erythroid burst-forming units (BFU) and colony-forming units (CFU) in a dose-dependent manner. Nevertheless, the anti-K antibody titer is not in correlation to the strength of inhibition in erythroid progenitor cells [30]. Due to the antibodies, erythropoiesis is blocked at a very early level and results in fetal anemia [30]. A consequence of this is a low number of circulating reticulocytes compared to fetuses with an anti-D [31].

Also, bilirubin concentration in fetal serum is lower due to the early inhibition in erythropoiesis because the cells are immature non-homoglobinized erythroid precursors [31]. This is also a difference from the fetus with RhD because the erythrocytes were attacked here in a mature stage, and the hemolysis results in a high level of bilirubin [31].

1.2 Erythroblastosis Fetalis

The earliest description of an Erythroblastosis fetalis was made in 1609 by the French midwife Louise Bourgeois. She described newborn twins, one with signs of hydrops fetalis, the other jaundiced, and neurologic symptoms (kernicterus) [32]. All different manifestations of Erythroblastosis fetalis like the mentioned symptoms hydrops fetalis, jaundice, kernicterus, and fetal anemia were not seen as the same disease until Diamond et al. connects these conditions as aspects of the same disease [33] (Figure 5).

The trigger of Erythroblastosis fetalis was a long time in discussion. Ruth Darrow made the first clue in the right direction in 1938. She postulated an antigen-antibody interaction as the cause of Erythroblastosis fetalis induced by the mother's immunization against the fetus. However, her theory mentioned fetal hemoglobin as an antigen [34]. As mentioned before, Landsteiner and Wiener discovered the RH system, and subsequently, Levine et al. identified RhD as the offending antigen for Erythroblastosis fetalis [35]. The primary mechanism for Erythroblastosis fetalis is that D-positive fetal red blood cells (RBCs) enter into the D-negative circulation of the mother. This, for the mother's immune system, unknown antigen triggers the production of anti-D. The IgG can pass the placenta and attack the fetal RBC leading to hemolysis of these cells and the manifestation of Erythroblastosis fetalis. To prevent the anti-D formation, Stern et al. injected RH-positive blood previously coated with RhD antibodies and showed anti-D formation [36]. The mechanism of Erythroblastosis fetalis prevention was shown by Finn et al. They injected Cr₅₁ labeled RhD positive RBC in RhD negative volunteers, and shortly after this injection, they administered anti-D. A control group didn't receive the anti-D treatment. The group with the anti-D treatment revealed clearance of 50 % of the labeled Erythrocytes in two days. Finn et al. postulated that a D-prophylaxis administration would prevent the mother's immunization and inhibit Erythroblastosis fetalis. [37].

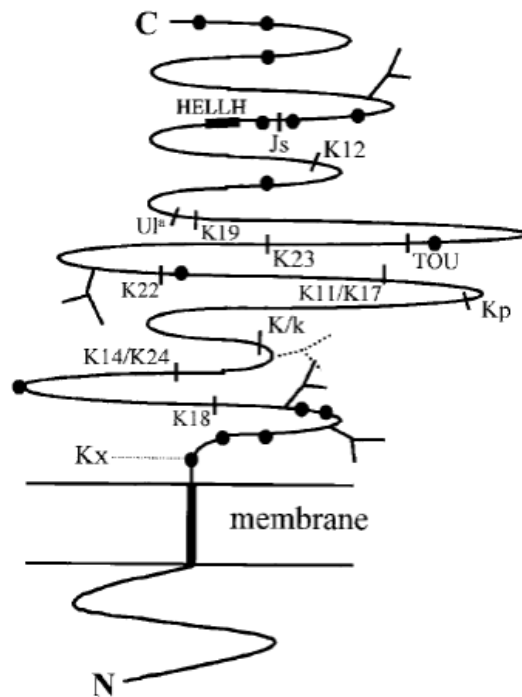


Figure 4: Kell protein with marked positions of known antigens [3].

It was repeatedly shown from different groups that anti-D administration to male RhD negative volunteers results in the prevention of isoimmunization [38, 39]. Before anti-D prophylaxis, 50 % of the children died of Erythroblastosis fetalis. The probability of a pregnant *RhD* negative women with ABO compatible D-positive fetus to immunize is 16 %. If the D-positive fetus is ABO incompatible, the likelihood reduces to 2 %. So the overall risk of an *RhD* negative woman of immunization is 13.2 % [40]. After the routine administration of the D-prophylaxis, the immunization rate was reduced to 0.18 % [41]. Therefore, the success rate of immunization is 98.4-99 % [40]. The basis for the first approval of rhesus-prophylaxis was the Western Canadian Rh Trail, in which the effectiveness of anti-D administration was successfully investigated [42]. The routine anti-D administration license was given both in America and Europe in 1968 [40].



Figure 5: An Affected fetus with Erythroblastosis fetalis [43].

Since the beginning of routine anti-D administration, the rhesus immunoglobulin is produced from pooled plasma from immunized donors [44, 45]. That kind of product comes with the risk of transferring diseases to the patient, e.g., Creutzfeld Jacob or Hepatitis C, which will be determined years later [44, 46]. Therefore, the UK imports their plasma for fractionation from North America to circumvent the possibility that UK donors may carry prions for Creutzfeld Jacob disease [44, 47]. Additionally, there are concerns about using human pooled plasma for newly emerging viruses and the risk of infecting women by the anti-D administration [47]. The possibility of transferring unknown infections and the anti-D administration itself can lead to anaphylaxis, rash, or dyspnoea [48, 49]. Germany's anti-D plasma supply is covered by importing pooled plasma outside the European Economic Area [50].

Until today the alternative production of monoclonal or recombinant IgG anti-D is not successful [44]. One cause could be the glycosylation pattern, which has an essential effect on the antibodies' bioactivity. So non-human oligosaccharides are indicated in a differed glycosylation pattern as in natural human pooled plasmas [44].

Germany's guidelines recommend the administration of anti-D globulins between the 28-30th week of gestation with a dose of 300 µg. After birth, a blood group determination of the child is recommended. In the case of an RhD positive child, the mother receives another anti-D globulin shot within 72 h postpartum with a dose of 300 µg [51].

1.3 Human Platelet Antigens

The human platelet antigens (HPA) are part of the integrin family. These transmembrane glycoproteins (GP) are essential for cell adhesion and signaling transduction. These molecules are expressed on the cell surface except on erythrocytes. As a heterodimer, it consists of two noncovalently associated subunits (α and β). Whereas the C-terminal is intracellular, and the N-terminal forms the extracellular domain [52] (Figure 6). The glycoproteins on platelets are mostly responsible for hemostasis but also play a role in inflammation, innate and adaptive immunity, and different diseases. Glycoproteins on the platelet surface are polymorphic caused by SNPs in the genes resulting in a change in the amino acid sequence and, therefore, in the glycoproteins' folding. This results in the formation of different platelet antigens causing the

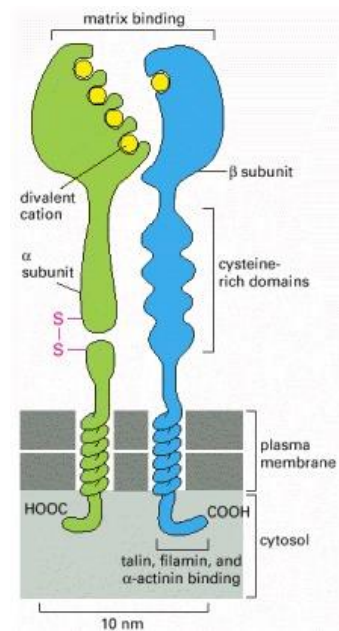


Figure 6: Principle of an integrin heterodimer [52].

appearance of alloantibodies in case of exposure in platelet transfusions or pregnancy. Clinically relevant are posttransfusion purpura (PTP) or fetal and neonatal alloimmune thrombocytopenia (FNAIT) [53].

1.3.1 Nomenclature of HPA

The first discovered antigens were named after the patient who first was immunized against a specific antigen. But publications were submitted from different groups at the same time with their antigen term. This leads to multiple names for the same antigen, e.g., Zw and PI for HPA-1 or Br, Hc, Zav for HPA-5. In order to reduce confusion regarding the different names, von dem Borne and Décary suggest a new nomenclature for platelet antigens [54], which determined that the antigen-systems are called HPA and are numbered chronically in order of their first publication. Additionally, they are listed alphabetically, corresponding to their frequency. New HPA systems need approval from the working party of the ISBT.

Up to today, there are more than 24 platelet specific alloantigens defined. Twelve of them are grouped into six biallelic systems, HPA-1 to -5 and HPA-15 [55]. Important in this thesis are five of the six biallelic groups namely HPA-1,-2,-3,-5, and 15. Table 1 introduces the HPA SNPs. The higher frequency allele is defined with 'a,' and the mutation is designated with 'b'.

Table 1: List of the biallelic Human Platelet Antigens. 1.[56], 2 [57], 3 [58].

Blood group	Glycoprotein	SNP ¹	Nucleotide (coding sequence)	Amino acid (mature protein)	HPA-antigen	Allele frequency ²
HPA-1	GPIIIa	rs5918	196 T	33 Leu	HPA-1a	0.834
			196 C	33 Pro	HPA-1b	0.116
HPA-2	GPIIb	rs6065	434 C	145 Thr	HPA-2a	0.940
			434 T	145 Met	HPA-2b	0.060
HPA-3	GPIIb	rs5911	2622 T	843 Ile	HPA-3a	0.616
			2622 G	843 Ser	HPA-3b	0.383
HPA-4	GPIIIa	rs5917	506 G	143 Arg	HPA-4a	0.999
			506 A	143 Gln	HPA-4b	0.001
HPA-5	GPIa	rs1801106	1648 A	505 Glu	HPA-5a	0.899
			1648 G	505 Lys	HPA-5b	0.111
HPA-15	CD109	rs10455097	2108 C	682 Ser	HPA-15a	0.532 ³
			2108 A	682 Tyr	HPA-15b	0.468 ³

Figure 7 visualizes the location of the SNPs on the glycoproteins resulting in human platelet antigens. The underlined HPAs are presented in more detail in the following subsections.

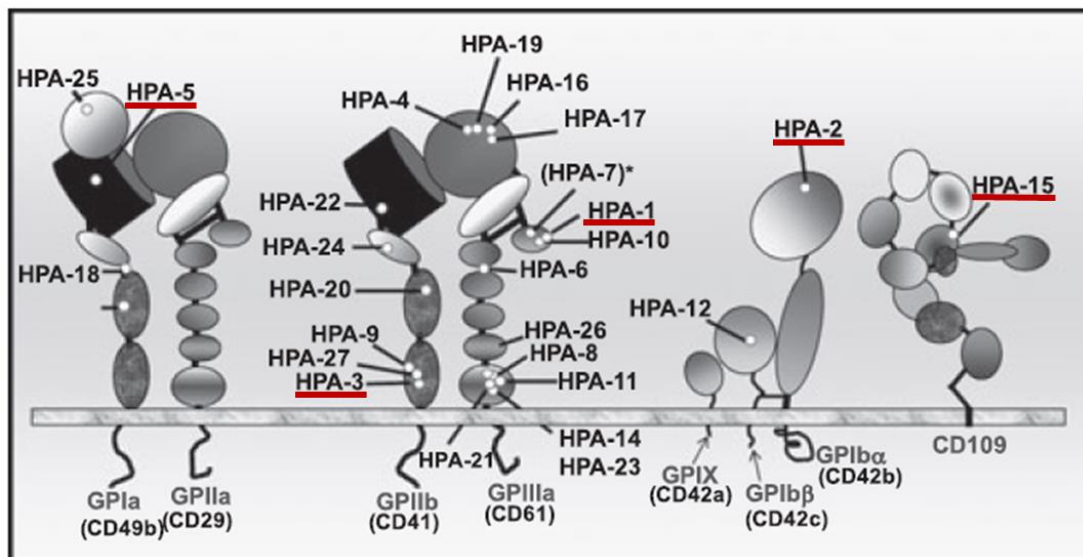


Figure 7: Visualization of the GP with the known SNPs. The highlighted HPAs are explained in more detail in the following subsections 1.3.1 -1.3.5. Figure adapted from [53].

1.3.2 HPA-1

The first description of an alloantibody against platelets was by Zucker et al. [59]. A short time later, van Loghem identified a platelet isoagglutinin, which they called "Zw". Today it is known as the HPA-1a antibody [60]. Almost simultaneously, Shulman et al. identified a platelet antigen they called PI(A1). An analysis of the two antigens revealed that Zw and PI(A1) are the same [61]. In 1990 a nomenclature for Platelets was published, and Zw(a) or PI(A1) were renamed to HPA-1a. Additionally the counterparts Zw(b) or PI(A2) were renamed to HPA-1b [54].

A suggestion where HPA-1 is located was published in 1978. Kunicki et al. realized that patients with Glazmanns type I disease express no glycoprotein II and III and are HPA-1 negative [62]. Due to the separation of GPIIb and GPIIIa, it was shown that the HPA-1a antibodies bind to GPIIIa and are located on the membrane surface with approximately

50,000 copies per platelet [63]. GPIIb/IIIa is a receptor for the ligand molecules fibrinogen, vitronectin, fibronectin, and von Willebrand factor [64-69]. The GPIIIa subunit consists of 762 amino acids with 84,5 kDa. The intracellular carboxyl-terminal segment is 41 aa, followed by the transmembrane region with 29 aa. The large amino-terminal region is located extracellular [70] (Figure 8). On this side, Newman et al. identified an SNP at position 196 from T to C, resulting in an amino acid substitution from leucine to proline resulting in the formation of HPA1-a or HPA-1b, respectively [71]. The majority of the Caucasian population has the HPA-1a phenotype with 98 %, and this trait is inherited dominantly [60]. The reason why HPA-1a is so strongly immunogenic could be that GPIIIa is also expressed on the syncytiotrophoblast. These cells are directly connected to the maternal system so that dead cell parts and DNA of these cells enter the maternal circulation and induce an immune response in the spleen. If there are now antigens on these cell debris that are unknown to the mother's immune system, an alloimmunization occurs, leading to FNAIT [72].

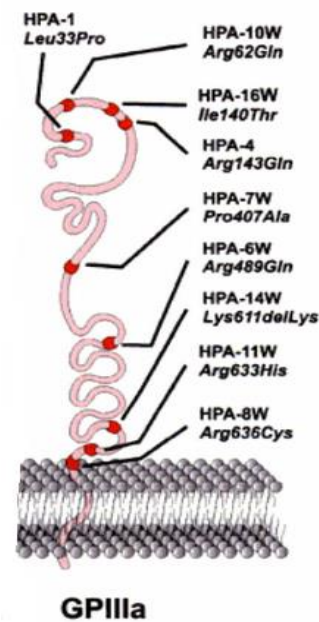


Figure 8: Scheme of the GPIIIa with the location of the amino acid substitution for HPA-1 [73].

1.3.3 HPA-2

The HPA-2 alloantigens were first mentioned in 1961 and was named Ko system [74, 75]. In the late 1980s, an antigen called Sib^a was described in a case of platelet transfusion refractoriness of a multiply transfused patient [76]. Kuijpers and co-workers showed that Ko^a and Sib^a are identical antigens [77]. The localization for the HPA-2 alloantigens were determined on the N-terminal globular fragment of the GPIIb α molecule. This molecule has a molecular weight of 45 kDa and is present with around 25,000 copies/GPIb/IX [56, 77, 78]. The gene for GPIIb is located on chromosome 17p17-12 [79]. GPIIb contains binding sites for thrombin as well as for the von Willebrand factor [78, 80-82]. The mature protein GPIIb consists of 610 aa. The intracellular domain contains approximately 100 aa, followed by a transmembrane segment of 29 aa, and around 485 aa are part of the extracytoplasmic domain [83] (Figure 9). Experiments indicated that the change from HPA-2a to HPA-2b is caused by a SNP at position 434 of the GPIIb gene. The exchange from a T to a C resulting in a change in the aa sequence from threonine in HPA-2a to methionine in HPA-2b at position 145 [84].

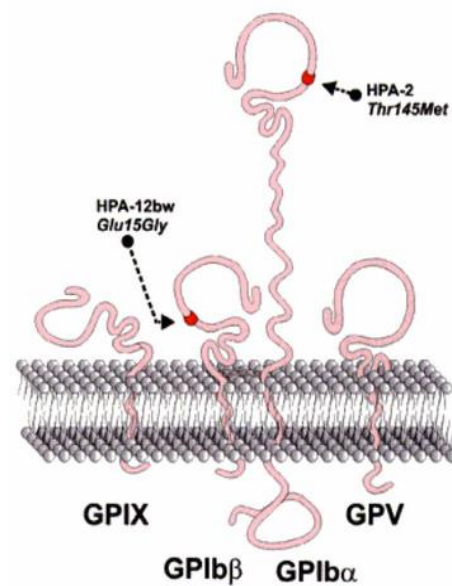


Figure 9: Scheme of the GPIIb with the location of the amino acid substitution for HPA-2 [73].

1.3.4 HPA-3

The HPA-3a antigen was first described in 1980 with the name Bak^a in a case of FNAIT [85]. A few years later, Leka's antibody was described, but it appears that Bak^a and Lek^a are identical [85-87]. The Bak^b (HPA-3b) antibody was discovered in 1988 in the case of posttransfusion purpura [88].

Analysis of the location of the antigen revealed the heavy chain of GPIIb [89, 90]. GPIIb is part of the GPIIb/IIIa complex, which is a receptor for fibrinogen, vitronectin, fibronectin, and von Willebrand factor [64-69]. The genes encoding for GPIIb/IIIa are found on chromosome 17q21-22 [91]. The GPIIb consists of 1,039 amino acids subdivided in a light chain with 137 aa with a molecular weight of 15,5 kDa and a heavy chain with 871 aa with 94,5 kDa, and a smaller unit with 26 aa, which encodes for the transmembranous domain [92] (Figure 10). Altogether, the coding DNA sequence consists of 3,311 bp, and in this, at position 2,622, HPA-3a is indicated by a T and HPA-3b by a G. This results in a substitution from isoleucine to serin in the amino acid sequence at position 843 [92, 93].

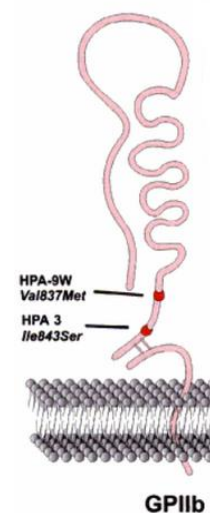


Figure 10: Scheme of the GPIIb with the location of the amino acid substitution for HPA-3 [73].

1.3.5 HPA-5

The HPA-5b antigen named Br^a was described in the late 1980s in four cases of FNAIT with a new alloantibody [94]. HPA-5b antibodies are the second most common cause for Fetal/neonatal alloimmune thrombocytopenia (FNAIT), right behind the HPA-1 antibodies [95]. In the early 1990s, the counterpart Br^b (HPA-5b) was identified [96]. Different other groups detected alloantibodies against the HPA-5 system like Hc^a and Zav^a [97, 98].

The HPA-5 antigen is expressed with 2,000 copies and is relatively low compared to the HPA-1 antigen with 40,000-50,000 copies per platelet [99, 100]. Alloantigens of HPA-5 are expressed on the Very Late Activation Antigens 2 (VLA-2) of activated T-lymphocytes and endothelial cells [101, 102]. The location of the Br-system was identified on the glycoprotein Ia (GPIa) [99, 103]. This protein is responsible for the binding and aggregation of the collagen of nonactivated platelets [104-106]. The GPIa coding sequence consists of 3,543 bp, which are 1,181 amino acids for the protein [107]. A nucleotide sequence analysis of the GPIa revealed at base 1648 a substitution from A to G (Figure 11). This results in a change in the amino acid sequence on the peptide position 505 from glutamic acid in Br^a to lysin for Br^b [108].

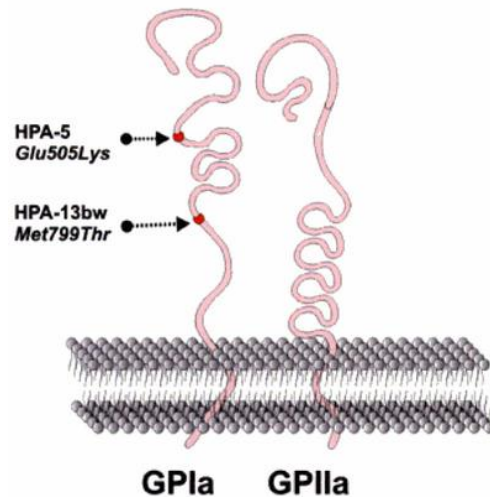


Figure 11: Scheme of the GPIa with the location of the amino acid substitution for HPA-5 [73].

1.3.6 HPA-15

The history of the Gov (HPA-15) antigens started in 1990 with the description of antibody development in patients with multiple platelet transfusions [58]. The authors identified a 175 kDa protein with a frequency of 0.532 for Gov^a (HPA-15b) and 0.468 for Gov^b (HPA-15a) [58]. The HPA-15 immunogenicity is the third most frequently described cause for FNAIT [109]. The antigen was identified on CD109, which is present on activated T-lymphoblasts and activated platelets, bone marrow CD34⁺ cells, and endothelial cells [110-112]. The function of CD109 is still not resolved, but recent publications identified it as a member of the α 2 macroglobulin/C3, C4, C5 family of thioester-containing proteins [113, 114]. It is suggested that the CD109 antigens are expressed in a low number of 2000±400 molecules per activated platelet [110]. The CD109 cDNA consists of 4335 bp resulting in 1445 amino acids for one protein [114]. In this sequence at position 2,108, the substitution of C to an A occurred, resulting in an amino acid change from serine to tyrosine at position 703 of the protein [115] (Figure 12).

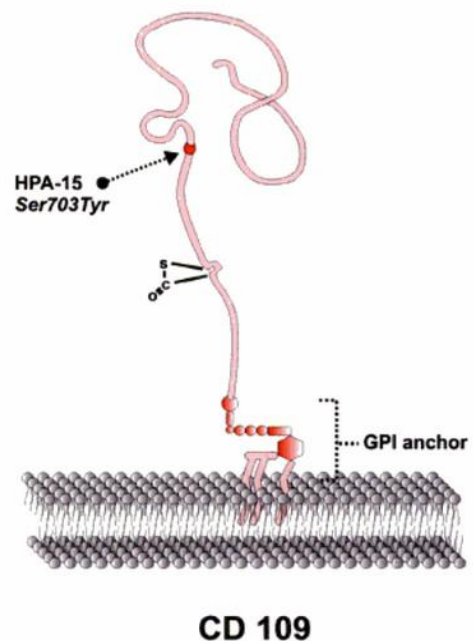


Figure 12: Scheme of the CD109 with the location of the amino acid substitution for HPA-15 [73].

1.4 Fetal and Neonatal Alloimmune Thrombocytopenia

The first description of severe cases with newborns with thrombocytopenia was published in 1953 [116]. The mother's immunization against antigens on fetal platelets as a mechanism behind the thrombocytopenia was reported in 1962 [117]. The erythroblastosis fetalis affects only children in the second pregnancy; however, FNAIT already affects women during the first pregnancy [95, 118].

The clinical description of FNAIT in the neonate is purpura and hemorrhagic signs like gastrointestinal bleeding or haematuria. The most severe complication in FNAIT is the intracranial hemorrhage (ICH), leading to neurological dysfunction (sequelae) or death [95, 118-120] (Figure 13).

In healthy human fetuses, the platelet count in the first trimester was identified as $>150 \times 10^9$ cells/L [121]. After the 18th week of gestation, the platelet count is around 250×10^9 cells/L and never below 150×10^9 cells/L [122]. Therefore, thrombocytopenia was defined as a platelet count below 150×10^9 cells/L and a severe thrombocytopenia $\leq 50 \times 10^9$ cells/L. Severe fetal thrombocytopenia is characterized by $\leq 50 \times 10^9$ cells/L and is mostly caused by neonatal immune thrombocytopenia [123]. A study of 5,623 newborn indicated 0.9 % of thrombocytopenic cases, 0.3 % of them are due to immune incompatibility [124]. The most crucial platelet antigens responsible for FNAIT are the 12 biallelic polymorphisms from HPA-1, -2, -3, -4, -5, and -15. Whereas HPA-1 is the most immunogenic [95]. Until today there is no prophylactic treatment for FNAIT. The main treatment of fetal alloimmune thrombocytopenia is the administration of

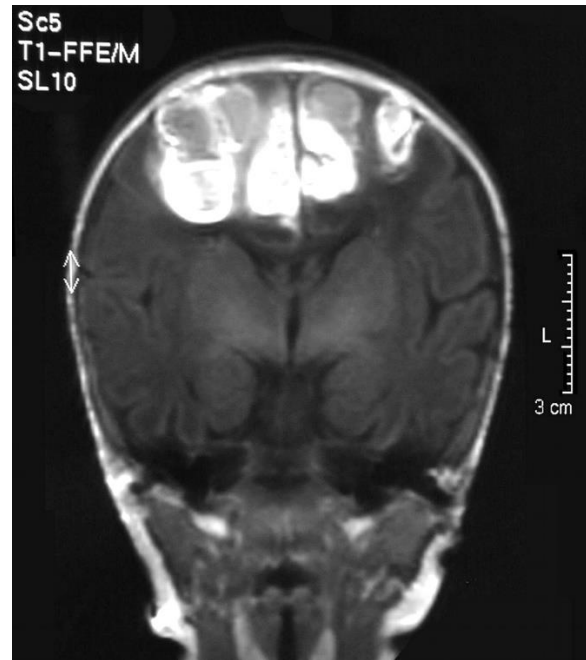


Figure 13 Picture of a hemorrhage of a two days old newborn [125].

intravenous immunoglobulin of 1 g/kg weekly to circumvent ICH [126, 127]. If this treatment is not successful, an in utero platelet transfusion is another possibility [128-131].

Platelet antigens are fully expressed at 18 weeks of gestation onwards [132]. The earliest detection of an anti-HPA-1a was the 6th week of gestation, but it usually is detected around the 20th week [133]. The most feared effect of FNAIT is the ICH, which can occur in extreme cases at the end of the 1st trimester but usually occurs late in the second trimester [130, 134].

1.5 Noninvasive Prenatal Diagnosis

As early as 1948, the first evidence of cell-free DNA (cfDNA) was published by Mandel and Métais [135]. But at the time, this was not considered a relevant discovery in science. Until the 1960s, the subject of cfDNA was revived by the discovery that patients with systemic lupus erythematosus showed DNA in cell-free plasma and serum from cell-free plasma [136]. It took over a decade until researchers become evidence of increased levels of cfDNA in metastatic cancer patients [137]. Finally, 20 years later, Lo et al. identified fetal DNA in pregnant women's plasma [138]. Fetal DNA can be detected in pregnancy as early as the 7th week of gestation, and the amount of fetal DNA in early pregnancy (11-17 week of gestation) was 3.4 % of total plasma DNA. This amount rises in late pregnancy (37-43 weeks of gestation) to approximately 6.2 % [139].

Investigations on anembryonic pregnancies showed that the primary source of cffDNA are the trophoblasts. An anembryonic pregnancy consists only of the placenta and no fetus, but the amount of cfDNA in the maternal plasma amount was normal, and sex determination was possible with cfDNA [140].

The size of the cffDNA was found to be in a range of 145-201 bp and whereas maternal DNA was found to be up to 20 kb [141, 142]. Other measurements indicated a fetal length of 143 bp and for the maternal one 166 bp [143]. Circulatory DNA shows an apoptotic pattern resulting from the nucleosomal cleavage of the DNA [142]. Usually, the degraded DNA is packed in vesicles and released for further elimination by macrophages [144]. This different length between the cfDNA of mother and fetus is a result of a different degradation mechanism. Because fetal cfDNA was cut within the nucleosomal core, whereas maternal cfDNA is cut in the linker region [145]. In case of an enhanced turnover, the procedure is overloaded, and free DNA enters the plasma in different shapes: a) free DNA sections, b) DNA packed as nucleosome, c) DNA bound to other plasma proteins d) in apoptotic bodies [144]. The nucleosomes are especially characterized by a size of 146 bp, which matches the detected size of the cffDNA. So it can be suspected that cffDNA is mostly of nucleosomal origin. After birth, the presence of cffDNA is undetectable after two hours with a half-life of 16.30 min [146].

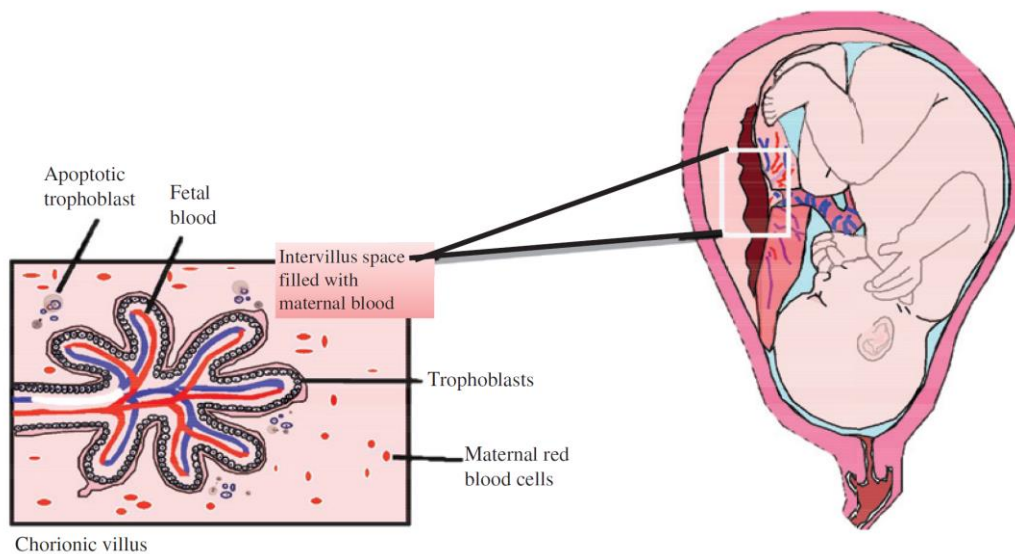


Figure 14: Placental chorionic villous syncytiotrophoblast is the origin of the cfDNA [147].

The placental chorionic villous syncytiotrophoblast is in direct contact with maternal blood (Figure 14). GPIIIa is expressed on placental syncytiotrophoblast, which carries the antigens of the fetus. Three types of fetal material enter the maternal circulation: a) syncytiotrophoblast microparticulate matter, b) DNA derived from syncytiotrophoblast nuclei. c) Fetal blood cells [72].

As mentioned before, the amount of cffDNA rises during pregnancy, but it can also indicate a fetal disorder, placental dysfunction, or other pregnancy complications. E.g., it was shown that women with preterm labor are showing significantly increased levels of cffDNA [148, 149]. Preeclampsia, a disease with hypertension, albuminuria, and edema, can lead to mother and child life-threatening conditions. It could be shown that in patients with this disorder, the level of fetal DNA in the maternal serum is increased [150, 151]. Also, chromosomal aberrations like trisomy 21 are accompanied by an increased amount of cfDNA [152, 153]. Soon after discovering the cffDNA, the fetus's *RHD* genotyping was published [154, 155]. Nowadays, this testing is established in several European countries [156-158].

1.5.1 Quantitative Real Time PCR

In NIPT, the use of qPCR is standard and explained in detail in chapter 2.12. A routine examination of all RhD negative women to determine whether they are expecting a RhD positive child and thus require immunoglobulin is already being carried out routinely in Denmark, the Netherlands, Norway and Finland [156-161]. In other countries this service is only offered in parts or to a limited extent, such as England, Slovenia, Spain, Sweden and Brazil [162-165]. In Germany, every RhD negative pregnant woman is offered a NIPT to determine the fetal RhD status [166]. The annual external quality assurance testing for fetal *RHD* genotyping carried out by the Department of Clinical Immunology of the Copenhagen University Hospital was attended in 2016 by 22 laboratories and all of them used qPCR for the *RHD* analysis [167]. Only two years later, 31 laboratories participated whereas 29 used qPCR and 2 laboratories -including our group- used dPCR [168].

Evaluation of the fetal *KEL* status is routinely offered with the qPCR method only in England [169]. The Netherlands and Germany offer this service only to immunized women [165]. The *KEL* determination with qPCR was also successfully examined in Italy, but has not yet been implemented in the clinical routine [170].

An HPA-1a analysis is offered in the Netherlands, Spain and Sweden. Germany offers immunized pregnant women an analysis of the HPA-1a, 5b and 15a via NGS see chapter 1.5.2 [165].

1.5.2 Massive Parallel Sequencing

The first DNA sequencing was published in 1970 by Ray Wu and required a location-specific primer [171]. A long time the sequencing according to Sanger as well as Maxam and Gilbert were the basis of the various NGS methods. Sequencing according to Sanger works on the basis of chain-terminating inhibitors [172]. The sequencing by Maxman and Gilbert uses chemical treatment of the DNA sample to remove specific nucleotides [173].

Nowadays the classic NGS is rarely used, they are replaced by newly developed massive parallel sequencing (MPS) methods. To mention here the development of nanopore sequencing of single stranded DNA [174], sequencing by ligation [175], sequencing by synthesis (SBS) [176], or ion semiconductor sequencing [177].

In contrast to Sanger sequencing, where only a single DNA fragment is analyzed, with the MPS millions of fragments are sequenced at the same time. In the following, sequencing by synthesis (SBS) and ion semiconductor sequencing are presented in more detail.

The basic concept of SBS was already published in 1988 through the detection of the pyrophosphate that arises during the reaction of the DNA polymerization [178]. This concept was further developed and the first SBS was successfully used in the sequencing of the *Mycoplasma genitalium* [176]. An important development step at SBS is the use of reversible terminators at the 3'-end. This method gives the opportunity to use all 4 nucleotides at the same time. Furthermore, the reversible terminator at the 3'-end prevents a further synthesis of the polymerase. Therefore, the incorporated nucleotide can be identified and subsequently the cap is removed [179, 180]. The Illumina solex for example uses before SBS an isothermal bridging amplification. For the reversible termination they use 3'-O-azidomethyl 2'-deoxynucleoside triphosphates (A, C, G and T). Firstly, the DNA is fragmented, adaptors are ligated and subsequently the product is amplified. The adaptors include binding sites for the sequencing primers and regions which are complementary to the flow cell oligo for immobilization. After the sequence templates were annealed to the complementary oligonucleotides on the flow cell a cluster is produced by clonal amplification. The bound template is copied by the polymerase and thus bound to the surface of the flow cell. The original strand is removed by denaturing and washing. The 3'-end binds to another complementary oligonucleotide by forming a bridge and the complementary strand is produced. Through denaturation, these are converted into two single strands and the bridge amplification repeats resulting in clusters on the flow cell. Finally, the reverse strands are removed to start the SBS. After the sequencing primer annealed the four differently labeled

nucleotides with reversible terminators are added. Due to the blocked 3'-end only one nucleotide can bind and the imaging step reveals the incorporated nucleotide. In the next step the 3'-end is uncapped and the synthesis starts a new cycle (Figure 15) [181, 182].

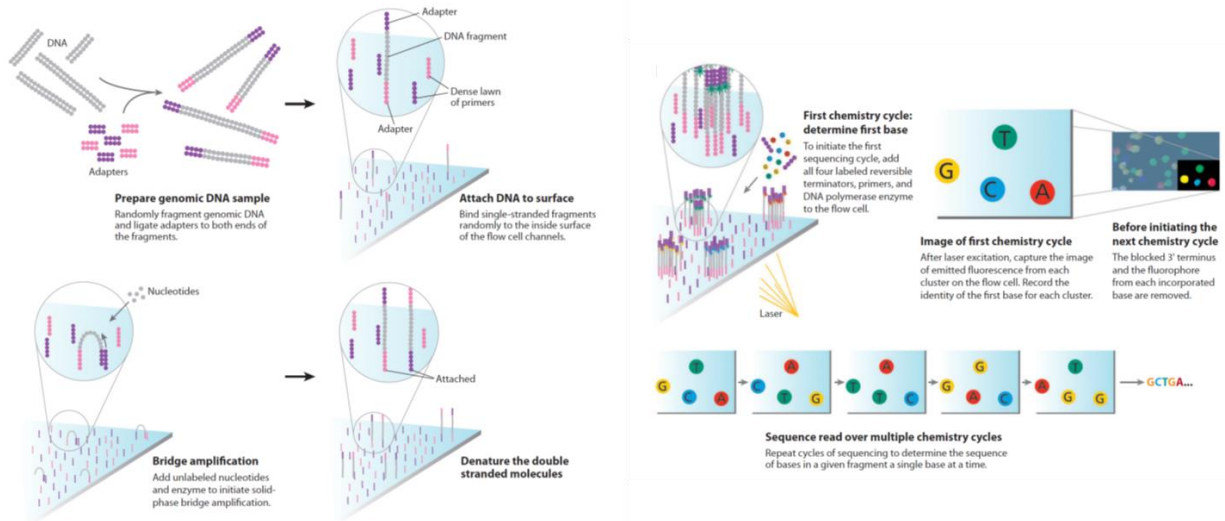


Figure 15: Principle of Illumina sequencing [182]

The other commonly used MPS method is the semiconductor sequencing developed by Ion Torrent. After the DNA is fragmented it is ligated to adapters. The prepared DNA then binds complementarily to the 2 mm acrylamide bead and is clonally amplified by emulsion PCR. Sequencing primers and polymerase are then added to the loaded beads and then loaded into individual sensor wells. In contrast to Illumina sequencing, the four nucleotides are added one after the other. If a nucleotide in the flow is incorporated by the polymerase, the hydrolysis of the nucleotide releases a proton for each nucleotide. Resulting in a pH change of 0.02 pH for each incorporated base which is measured by the sensor on the bottom of the well. This pH change is then converted into voltage and recorded by an special software which assign the signal to the base that was added. Then wash steps ensure that all unbound nucleotides have been removed before the well is flooded with the next nucleotide (Figure 16) [177].

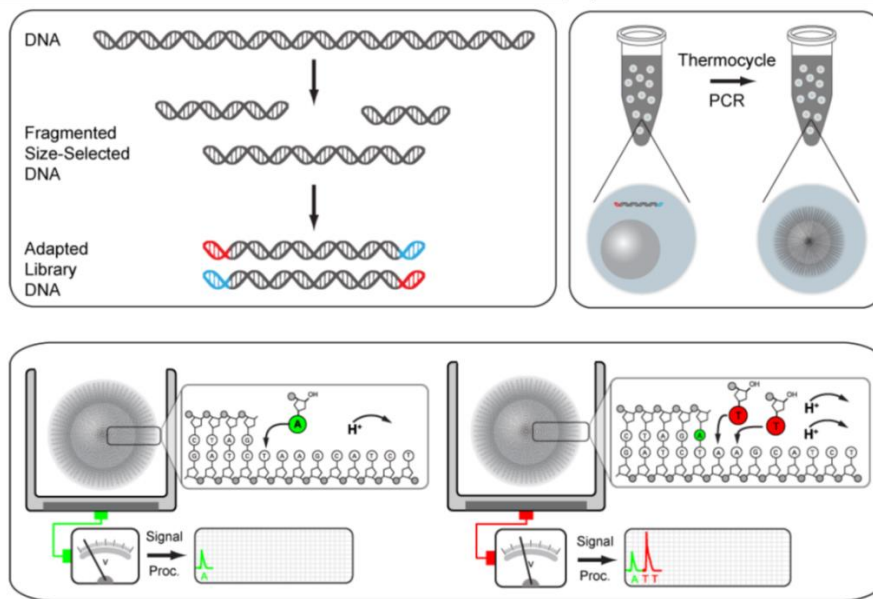


Figure 16: principle of semiconductor sequencing by Ion Torrent [177]

The main differences between sequencing and PCR are listed in table 2.

Table 2: Differences between qPCR and DNA sequencing

PCR	MPS
Needs two primers (forward and reverse) on both DNA strands	Uses one primer, for reading the sequence in one direction only
Is an exponentially amplification of the targeted region due to the two primers.	Has no, exponential amplification, it is linear
Has a low number of DNA templates	Has a large number of DNA templates
Is the amplification of a low number of known target sequences	Elucidates the DNA sequence
Only detection of a known sequence is possible	Knowledge of the sequence is not necessary

NGS is also used routinely at NIPT, so in Denmark the fetal status of KEL-immunized women is examined via MPS [183]. In Germany, the HPA-1a, -3, -5 and -15 are offered for immunized women [184].

1.5.3. Fetal Control Markers

For the analysis of blood cell- and platelet antigens, additional use of control markers is necessary. For calculations, the total DNA amount is essential, and the ubiquitary expressed enzyme GAPDH was chosen as a marker for the total amount of cfDNA.

In case of a negative test result, a fetal marker is recommended to verify a sufficient and intact amount of cell-free fetal DNA. One marker could be the analysis of the fetal gender in this thesis amelogenin was used. However, in the case of a female fetus, the signal merges with the mother. Therefore, another, gender independent marker, the SNPforID 52-plex, is introduced. On the following pages, the used control markers are presented in more detail.

Amelogenin

The most common marker for the analysis of the fetal gender is the sex-determining region Y (SRY) gene [185]. In this thesis, a different gender marker was established. The amelogenin gene (AMEL) is a widely used marker for gender identification in forensics. Amelogenin encodes for the protein forming tooth enamel. It is located on the X-chromosome in the p22.1-p22.3 region and on the Y chromosome at p11 [186]. The sequence between the two genes differs in the X-chromosomal version. Here, a 6 bp deletion compared to the Y-chromosome sequence is present [187, 188]. Resulting in one PCR product for a female of 106 bp and the male one product of 106 bp and one with 112 bp [188, 189]. Both genes come with equal copy numbers, which give the quantification a huge advantage.

SNPforID 52-plex as anonymous marker

A fetal control is essential to prove that the fetal DNA is analyzed and in sufficient quantities available. In the case of a male fetus, a signal in the AMEL-Y channel occurs. If the fetus is female, the X-chromosomal signal is melted with the AMEL-X signal of the mother and therefore not representable. To exclude failure of the dPCR or rule out the possibility of DNA damage, a gender-neutral marker for identifying an individual is useful. In forensics, identifying an unknown person is performed by using STRs, but in the last years, the use of SNPs is more and more in focus.

In 2002 the *SNPforID* consortium consisting of five European forensic laboratories supported by the European Community was formed in order to develop an SNP typing assay for the identification of human individuals. The criteria for the chosen SNPs are:

- SNPs must be biallelic
- SNPs are highly polymorphic in the majority of the population [190].
- SNPs are not in linkage disequilibrium [190].
- SNPs are not associated with commonly used STR loci and are indicated by a 100 kb distance to genes for cellular functions [191].
- All SNPs can be amplified in one multiplex PCR reaction [190, 192].
- SNPs are selected from the distal parts of each chromosome's p and q arms [191].

The result was the *SNPforID* 52 plex with a PCR product length between 59 to 115 bp [191, 192]. To discriminate close individuals or relatives with SNPs as good as with the gold standard of 12 STRs, at least 50 SNP loci are needed [193]. It could be shown that the use of SNPs complements the use of STR [194]. The 52 *SNPforID* plex is mostly used in the paternity test [194-196] and forensic casework [197, 198].

The advantage of SNP over STR is indicated by fewer mutations and the amplicon's lower size, which is for STR in a range between 100 to 400 bp [191, 196]. In forensic casework, DNA is highly degraded and shows low copy numbers, and with STRs, the analysis is more difficult due to the greater PCR products. The *SNPforID* panel, on the other hand, has a small PCR product, which makes it possible to identify in a highly degraded DNA mixture single individuals [197-199]. The use of the *SNPforID* 52-plex as an internal gender-neutral marker in prenatal diagnostics was recently shown by Doescher et al. [200].

1.5.4 Internal PCR Control

The Glyceraldehyde 3-phosphate dehydrogenase (GAPDH) gene's use as a reference for the total DNA amount was shown in other studies for the *RHD* zygosity test and noninvasive prenatal *RHD* testing [164, 201-203]. It has the advantage of two copies from each chromosome, making it easy to compare it with the copy number of an *RHD* homozygous individual. An advantage of dPCR is the possibility of internal control and target sequence on the same chip for absolute quantification. This means the internal control GAPDH with one copy of each chromosome 12 equals the copy number of a homozygous *RHD* positive person.

The GAPDH gene encodes for the Glyceraldehyde 3-phosphate dehydrogenase enzyme, which catalyzes the sixth step in the glycolysis. This reversible reaction of glyceraldehyde-3-phosphate with NAD⁺ Phosphate to 1,3-bisphosphoglycerate + NADH+H⁺. Glycolysis is one of the central biochemical reactions of the breakdown of glucose to lactate. Therefore, the gene is ubiquitously expressed.

1.6 Aim of the dissertation

Incompatibility of the blood cell and platelet antigens between mother and unborn child can lead to complications during pregnancy like MHN or FNAIT. The standard procedure to sample fetal material is invasive for mother and child, like amniocentesis or the umbilical cord's puncture. But these methods carry the risk of infections or miscarriage and are only used in cases of particular urgency. The procedure for noninvasive prenatal testing (NIPT) is noninvasive for the fetus because the blood taken from the mother contains cfDNA. With this, a genetic analysis of the fetus is possible. For several years now, noninvasive blood tests for determining the fetus's *RHD* status have been carried out in some countries to administer the immunoglobulin prophylaxis only to women that require them. Because the injected globulins are produced of pooled globulins of immunized individuals, they can transfer infections like Hepatitis C or other today not known infections. Additionally, there is also the possibility of an allergic reaction after the administration of the prophylaxis. Besides the RhD antigen, the Kell antigen can cause MHN, too. A noninvasive test for this blood group is not available yet. Another complication based on the incompatibility between mother and child is FNAIT, which is caused by different human platelet antigens. For these involved HPAs is no noninvasive test available.

This thesis aims to develop a NIPT to determine the genomic status of the fetal blood cell antigens RhD and Kell and the five biallelic platelet antigens HPA-1 -2, -3, -5, and -15. Furthermore, the test will include fetal markers AMEL-X/Y and nine SNPs from the SNPforID panel. For this test, further development of the qPCR, namely the digital PCR (dPCR), was chosen to obtain a test-system as sensitive as possible. Thus it should be possible to get a reliable diagnosis in the 1st trimester instead of the 25th week of gestation that is currently standard in many countries.

To show the road to such a test, this thesis is subdivided into three main sections. The first part of the dissertation is about developing the protocol, including optimal cfDNA isolation and the best dPCR conditions. The second part is the technical validation of the single assays. Because the amount of cfDNA in pregnant women varies, the simulation of pregnancy was chosen in order to analyze the strength and the weaknesses of the assays with a sample of known cfDNA distributions. Therefore, the dilution series from the plasma of tested volunteers was mixed from 5.00 % down to 0.10 % to test the sensitivity of the dPCR. In the third work package, blood samples from 50 pregnant women were tested. The mothers were pretested with PCR-SSP for the blood- and platelet antigen status as well as their SNP marker status. The *RHD* status was verified with a zygosity test. In cases where the women are homozygous for the characteristics, a dPCR with the plasma's cfDNA was applied to examine the fetus's status.

The results of these two validations were compared and analyzed to confirm that this test is very sensitive and a new important step in the noninvasive diagnostic.

2 MATERIAL AND METHODS

In this chapter, the used methods are explained in detail. Furthermore, all used materials and primers with their sequences are listed. Additionally, all recipes for the used solutions are documented. Figure 17 should give an overview of the applied methods.

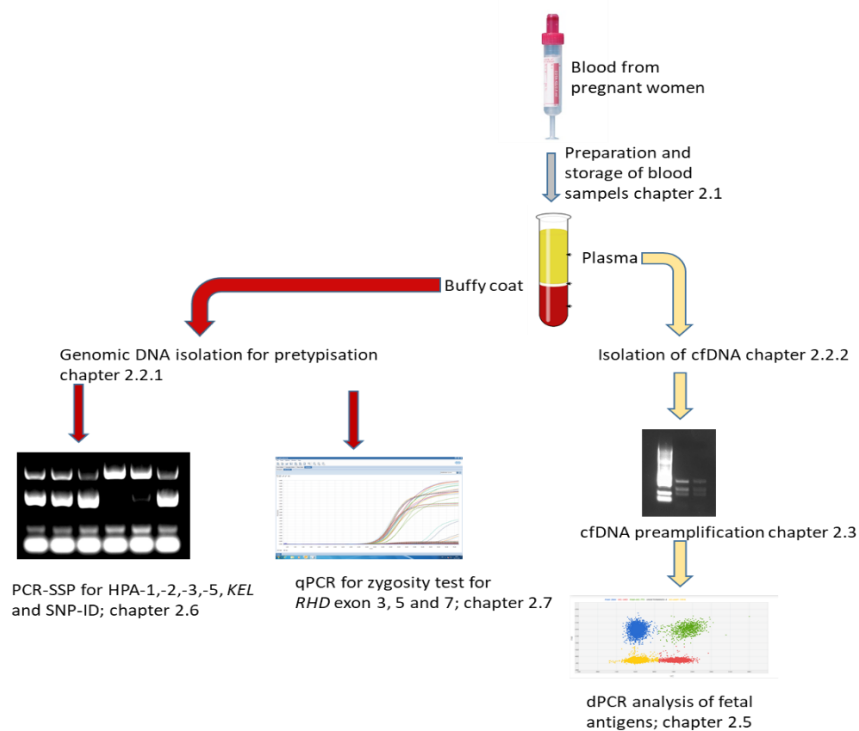


Figure 17: Scheme of the experimental setup.

2.1 Reagents and Devices

Application	Reagents and devices	Manufacturer
cfDNA isolation with Maxwell	Maxwell® RSC ccfDNA Plasma Kit	
	<ul style="list-style-type: none"> • 48 Maxwell® RSC Cartridges (RSCG) • 1 Maxwell® RSC Plunger Pack (48 Plungers) • 50 Elution Tubes (0.5 ml) • 20 ml Elution Buffer 	Promega GmbH
	Maxwell® RSC device	Promega GmbH

cfDNA isolation with Qiagen

QIAamp Circulating Nucleic Acid Kit

- 50 QIAGEN® Mini columns
- 50 Tube extenders (20 ml) 2 x 25
- 50 Collection tubes (2.0 ml)
- 50 Elution tubes (1.5 ml)
- 50 VacConnectors
- 220 ml Buffer ACL
- 300 ml Buffer ACB (concentrate)
- 19 ml Buffer ACW1 (concentrate)
- 13 ml Buffer ACW2 (concentrate)
- 5 x 2 ml Buffer AVE (purple caps)
- 4 x 7 ml Qiagen proteinase K
- 310 µg Carrier RNA (red caps)

Qiagen GmbH

2-Propanol

Merck KGaA

Ethanol absolute

Merck KGaA

QIAvac 24 Plus

Qiagen GmbH

KNF N86 KTP Corrosion-Resistant Vacuum Pump

KNF Neuberger GmbH

Eppendorf Thermomixer™ comfort

Eppendorf AG

Water bath

VWR International GmbH

cfDNA isolation with MagMAX™

MagMAX™ Cell-Free DNA Isolation Kit

- 1.5 ml MagMAX™ Cell-Free DNA Magnetic Beads
- 125 ml MagMAX™ Cell-Free DNA Lysis/Binding solution
- 100 ml MagMAX™ Cell-Free DNA Wash Solution
- 5 ml MagMAX™ Cell-Free DNA Elution Solution

Thermo Fisher Scientific Inc.

SDS 20 %

- 20 g SDS
- 100 ml ddH₂O

GERBU Biotechnik GmbH

VWR International

Ethanol 80 %

- 80 ml Ethanol absolute ≥99,9%
- 100 ml ddH₂O

Merck KGaA

VWR International

DynaMag™ Magnet

Thermo Fisher Scientific Inc.

Digital PCR

QuantStudio™ 3D Digital PCR 20K Chipkit v2

- 12 QuantStudio 3D Digital PCR 20K Chips v2
- 12 QuantStudio 3D Digital PCR Chip Lids v2
- 12 QuantStudio 3D Digital PCR Sample Loading Blades
- 3 syringes Immersion Fluid
- 3 Immersion Fluid Tips

Thermo Fisher Scientific Inc.

ProFlex™ 2x Flat PCR System

Thermo Fisher Scientific

QuantStudio™ 3D Digital PCR Chip Loader

Qiagen GmbH

QuantStudio™ 3D Digital PCR Instrument

Qiagen GmbH

Ultrapure Water

Merck KGaA

QuantStudio™ 3D Digital PCR Master Mix v2

Thermo Fisher Scientific Inc.

Primer and probes (chapter 2.4)

DNA - Isolation

QIAamp DNA Blood Mini Kit

- 250 QIAamp Mini Spin Columns
 - 250 Collection Tubes (2 ml)
 - 2 x 33 ml Buffer AL
 - 98 ml BufferAW1 (concentrate)
 - 66 ml BufferAW2 (concentrate)
 - 60 ml BufferAE
 - 1 vial Qiagen®Protease1
 - 5,5 ml ProteaseSolvent
- Qiagen GmbH

Ethanol absolute

Merck KGaA

1XPBS

- 8.00 g Sodium chloride (NaCl) ≥99,5 %, p.a., ACS, ISO
 - 1.44 g Di-sodium hydrogen phosphate dihydrate (Na₂HPO₄*2H₂O)
 - 0.20 g Potassium chloride (KCl)
 - 0.20 g Di-Potassium hydrogen phosphate (KH₂PO₄)
 - Adjust to Ph 7.4
- Carl Roth GmbH + Co. KG
Carl Roth GmbH + Co. KG
Carl Roth GmbH + Co. KG
Carl Roth GmbH + Co. KG

Gel electrophoresis

2 % Agarose

- 8.00 g Agarose NEED ultra-quality
- Carl Roth GmbH + Co. KG

- 400 ml 1x TAE buffer (selfmade)

GelRed® Nucleic Acid Gel Stain

Biotium, Inc.

DNA leader MWM-2

Bilatec AG

50x TAE- Puffer

- 242 g TRIS, PUFFERAN®
 - 100 ml 0.5mol EDTA (selfmade)
 - 57.10 ml Acetic acid absolute
 - fill up to 1 liter with ddH₂O
- Carl Roth GmbH + Co. KG
Carl Roth GmbH + Co. KG
VWR International

1x TAE buffer

- 9800 ml ddH₂O
 - 200 ml 50xTAE buffer (selfmade)
- VWR International

0.5 mol EDTA

- 186,1 g EDTA disodium salt dihydrate
 - 700 ml ddH₂O
 - adjust to pH 8.0
- VWR International
VWR International

Electrophoresis chamber Cascade

Biologics Inc. Portland, OR

Consort E815 Powersupply

GENEO BioTechProducts GmbH

Multiple displacement amplification with REPLI-g FFPE Kit

REPLI-g FFPE Kit

- 25 µl REPLI-g Midi DNA Polymerase
- 725 µl REPLI-g Midi Reaction Buffer
- 25 µl FFPE Enzyme
- 25 µl Ligation Enzyme
- 200 µl FFPE Buffer
- 1.9 ml FFPE Lysis Solution, 10x
- 250 µl Proteinase K

Qiagen GmbH

PCR Device Life ECO

Hangzhou Bioer Technology Co. Ltd.

Multiple displacement amplification with REPLI-g Mini Kit

REPLI-g Mini Kit

- 25 µl REPLI-g Mini DNA Polymerase (blue lid)
- 725 µl REPLI-g Mini Reaction Buffer (yellow lid)
- 1 tube Buffer DLB (clear lid)
- 1.8 ml Stop Solution (red lid)
- 1.8 ml PBS, 1x (clear lid)
- 1 ml DTT, 1 M (lilac lid)

Qiagen GmbH

PCR Device Life ECO

Hangzhou Bioer Technology Co. Ltd.

PCR for SRY

Hot Star mix

Qiagen GmbH

Primer mix (chapter 2.3)

PCR Device Life ECO

Hangzhou Bioer Technology Co. Ltd.

PCR purification

QIAquick PCR Purification Kit

- 250 QIAquick Spin Columns
- 150 ml Buffer PB 30 ml
- 55 ml Buffer PE (concentrate)
- 55 ml Buffer EB
- 800 µl pH Indicator I
- 250 Collection Tubes (2 ml)
- 550 µl Loading Dye

Qiagen GmbH

Heraeus™ Pico™ 17 Microcentrifuge

Thermo Fisher Scientific

PCR-SSP

10x PCR-Puffer for PCR-SSP

- 100 mM Tris/HCl pH 8.3
- 500 mM KCl
- 15 mM MgCl₂
- 0.1 % BSA
- filter sterile

Carl Roth GmbH + Co. KG
 Carl Roth GmbH + Co. KG
 Merck KGaA
 Carl Roth GmbH + Co. KG

dNTP-Mix (2 mM each):

- 10 µl dATP (100 mM stock solution)
- 10 µl dCTP (100 mM stock solution)
- 10 µl dGTP (100 mM stock solution)
- 10 µl dTTP (100 mM stock solution)

Eurofins Genomics Germany GmbH
 Eurofins Genomics Germany GmbH
 Eurofins Genomics Germany GmbH
 Eurofins Genomics Germany GmbH

MATERIAL AND METHODS

<ul style="list-style-type: none"> • 460 µl dd H₂O 	VWR International
Reagent mix	
<ul style="list-style-type: none"> • 200 µl 10x PCR-Puffer 	
<ul style="list-style-type: none"> • 200 µl dNTP (2 mM each) <ul style="list-style-type: none"> • 200 µl loading dye (50% glycerin, 1 mg/ml Cresol red) • Primer mix (see chapter 2.3) 	
Taq Polymerase, 5 U/µl	BIORON GmbH
PCR Device Life ECO	Hangzhou Bioer Technology Co. Ltd.
Targeted preamplification PCR	
Multiplex PCR MasterMix 2x	Qiagen GmbH
Primer mix (selfmade, see chapter 2.3)	Eurofins Genomics Germany GmbH
PCR Device Life ECO	Hangzhou Bioer Technology Co. Ltd.
Zygosity test	
Taq Polymerase, 5 U/µl	BIORON GmbH
SensiFAST™ Probe Lo-ROX Kit	Bioline GmbH
Primer and probes (chapter 2.4)	
LightCycler® 96 System	Roche Deutschland Holding GmbH
Commonly used devices	
Pipette 2,5 µl, 0,5-10 µl, 10-100 µl, 100-1000 µl	Eppendorf AG
3-Speed Mini Centrifuge D-6015	neoLab Migge GmbH
Centrifuge KR25i	JOUAN GmbH
Vortex-1 Gene Touch-Mixer	Scientific Industries Inc.

2.2 Consumables

Consumables	Manufacturer
Cryo-Babies	DIVERSIFIED BIOTECH
Domed 12 cap stripes	Thermo Fisher Scientific Inc.
Eppendorf Conical Tubes, 50 ml	Eppendorf AG
Eppendorf Safe-Lock Tubes, 1.5 ml	Eppendorf AG
Eppendorf Tube 1.5 ml	Eppendorf AG
Eppendorf Tubes® 5.0 ml	Eppendorf AG
Eppendorftubes (biopure) 1,5 ml, 5 ml	Eppendorf AG
Falcon tubes 50 ml	Greiner Bio-One International GmbH
Foliodress® Mask Protect	PAUL HARTMANN AG
Lint-free wipes	Kimberly-Clark Professional
MagMAX™ Cell-Free DNA Isolation Kit <ul style="list-style-type: none"> • 1.5 ml MagMAX™ Cell-Free DNA Magnetic Beads • 125 ml MagMAX™ Cell-Free DNA Lysis/BindingSolution • 100 ml MagMAX™ Cell-Free DNA Wash Solution • 5 ml MagMAX™ Cell-Free DNA Elution Solution 	Thermo Fisher Scientific Inc.
Maxwell® RSC ccfDNA Plasma Kit	Promega GmbH

MATERIAL AND METHODS

- 48 Maxwell® RSC Cartridges (RSCG)
- 1 Maxwell® RSC Plunger Pack (48 Plungers)
- 50 Elution Tubes (0.5 ml)
- 20 ml Elution Buffer

Micro Screw Tube 2 ml, PP	Sarstedt AG & Co. KG
Nalgene Round-bottom tube; 50 mL;	Thermo Fisher Scientific Inc.
Pasteur-Plast pipettes, 3,0 ml Makro	ratiolab GmbH
PCR-Plate, 96-well, für Roche® LightCycler® 480	BRAND GMBH + CO KG
Peha-soft® nitrile fino powder-free gloves	PAUL HARTMANN AG
Prionics (Forensics) BasicDry-Spuren (150 mm)	Voigtländer Polizei- und Kriminaltechnik GmbH

QIAamp Circulating Nucleic Acid Kit

- 50 QIAGEN® Mini columns
- 50 Tube extenders (20 ml) 2 x 25
- 50 Collection tubes (2.0 ml)
- 50 Elution tubes (1.5 ml)
- 50 VacConnectors
- 220 ml Buffer ACL
- 300 ml Buffer ACB (concentrate)
- 19 ml Buffer ACW1 (concentrate)
- 13 ml Buffer ACW2 (concentrate)
- 5 x 2 ml Buffer AVE (purple caps)
- 4 x 7 ml Qiagen proteinase K
- 310 µg Carrier RNA (red caps)

Qiagen GmbH

QIAamp DNA Blood Mini Kit

- 250 QIAamp Mini Spin Columns
- 250 Collection Tubes (2 ml)
- 2 x 33 ml Buffer AL
- 98 ml BufferAW1 (concentrate)
- 66 ml BufferAW2 (concentrate)
- 60 ml BufferAE
- 1 vial Qiagen®Protease1
- 5,5 ml ProteaseSolvent

Qiagen GmbH

QIAquick PCR Purification Kit

- 250 QIAquick Spin Columns
 - 150 ml Buffer PB 30 ml
 - 55 ml Buffer PE (concentrate)
 - 55 ml Buffer EB
 - 800 µl pH Indicator I
 - 250 Collection Tubes (2 ml)
 - 550 µl Loading Dye

Qiagen GmbH

QuantStudio™ 3D Digital PCR 20K Chipkit v2	Thermo Fisher Scientific Inc.
<ul style="list-style-type: none"> • 12 QuantStudio 3D Digital PCR 20K Chips v2 • 12 QuantStudio 3D Digital PCR Chip Lids v2 • 12 QuantStudio 3D Digital PCR Sample Loading Blades • 3 syringes Immersion Fluid • 3 Immersion Fluid Tips 	
REPLI-g FFPE Kit from Quagen	
<ul style="list-style-type: none"> • 25 µl REPLI-g Midi DNA Polymerase <ul style="list-style-type: none"> • 725 µl REPLI-g Midi Reaction Buffer • 25 µl FFPE Enzyme • 25 µl Ligation Enzyme • 200 µl FFPE Buffer • 1.9 ml FFPE Lysis Solution, 10x • 250 µl Proteinase K 	Qiagen GmbH
REPLI-g Mini Kit from Quiagen	
<ul style="list-style-type: none"> • 25 µl REPLI-g Mini DNA Polymerase (blue lid) • 725 µl REPLI-g Mini Reaction Buffer (yellow lid) • 1 tube Buffer DLB (clear lid) • 1.8 ml Stop Solution (red lid) • 1.8 ml PBS, 1x (clear lid) • 1 ml DTT, 1 M (lilac lid) 	Qiagen GmbH
SafeSeal Surphob tips, sterile, 10 µl, 100 µl, 1000 µl,	Biozym Scientific GmbH
Sealing film, self-adhesive for Real-Time-PCR (qPCR)	BRAND GMBH + CO KG
S-Monovette 9 ml	Sarstedt AG & Co. KG
SP-0029 Non-skirted Low Profile 96-well PCR Plate	Thermo Fisher Scientific Inc.

2.3 Primer Mixtures

Primer mix	Content	Manufacturer
KEL2	1 µl β-Globin -R	Eurofins Genomics Germany GmbH
	1 µl β-Globin -F	Eurofins Genomics Germany GmbH
	5 µl KEL-F	Eurofins Genomics Germany GmbH
	1 µl KEL-R(G)	Eurofins Genomics Germany GmbH
	246 µl ddH ₂ O	Merck KGaA
KEL1	1 µl β-Globin -R	Eurofins Genomics Germany GmbH
	1 µl β-Globin -F	Eurofins Genomics Germany GmbH
	5 µl KEL-F	Eurofins Genomics Germany GmbH
	1 µl KEL-R(A)	Eurofins Genomics Germany GmbH
	246 µl ddH ₂ O	Merck KGaA
HPA-1a	10 µl HPA-1a-F	Eurofins Genomics Germany GmbH
	10 µl HPA-1-R	Eurofins Genomics Germany GmbH
	2 µl HGH-F	Eurofins Genomics Germany GmbH
	2 µl HGH-R	Eurofins Genomics Germany GmbH
	476 µl Aqua dest.	Merck KGaA
HPA-1b	10 µl HPA-1b-F	Eurofins Genomics Germany GmbH

MATERIAL AND METHODS

	10 µl HPA-1-R	Eurofins Genomics Germany GmbH
	2 µl HGH-F	Eurofins Genomics Germany GmbH
	2 µl HGH-R	Eurofins Genomics Germany GmbH
	476 µl Aqua dest.	Merck KGaA
HPA-2a	10 µl HPA-2a-F	Eurofins Genomics Germany GmbH
	10 µl HPA-2-R	Eurofins Genomics Germany GmbH
	2 µl HGH-F	Eurofins Genomics Germany GmbH
	2 µl HGH-R	Eurofins Genomics Germany GmbH
	476 µl Aqua dest	Merck KGaA
HPA-2b	10 µl HPA-2b-F	Eurofins Genomics Germany GmbH
	10 µl HPA-2-R	Eurofins Genomics Germany GmbH
	2 µl HGH-F	Eurofins Genomics Germany GmbH
	2 µl HGH-R	Eurofins Genomics Germany GmbH
	476 µl Aqua dest.	Merck KGaA
HPA-3a:	10 µl HPA-3a-F	Eurofins Genomics Germany GmbH
	10 µl HPA-3-R	Eurofins Genomics Germany GmbH
	2 µl HGH-F	Eurofins Genomics Germany GmbH
	2 µl HGH-R	Eurofins Genomics Germany GmbH
	476 µl Aqua dest.	Merck KGaA
HPA-3b:	10 µl HPA-3b-F	Eurofins Genomics Germany GmbH
	10 µl HPA-3-R	Eurofins Genomics Germany GmbH
	2 µl HGH-F	Eurofins Genomics Germany GmbH
	2 µl HGH-R	Eurofins Genomics Germany GmbH
	476µl Aqua dest.	Merck KGaA
HPA-5a	20 µl HPA-5a-F	Eurofins Genomics Germany GmbH
	20 µl HPA-5-R	Eurofins Genomics Germany GmbH
	2 µl HGH-F	Eurofins Genomics Germany GmbH
	2 µl HGH-R	Eurofins Genomics Germany GmbH
	456 µl Aqua dest.	Merck KGaA
HPA-5b	20 µl HPA-5b-F	Eurofins Genomics Germany GmbH
	20 µl HPA-5-R2	Eurofins Genomics Germany GmbH
	2 µl HGH-F	Eurofins Genomics Germany GmbH
	2 µl HGH-R	Eurofins Genomics Germany GmbH
	456 µl Aqua dest.	Merck KGaA
HPA-15a:	30 µl HPA-15a-F	Eurofins Genomics Germany GmbH
	30 µl HPA-15-R	Eurofins Genomics Germany GmbH
	2 µl HGH-F	Eurofins Genomics Germany GmbH
	2 µl HGH-R	Eurofins Genomics Germany GmbH
	436 µl Aqua dest	Merck KGaA
HPA-15b:	30 µl HPA-15b-F	Eurofins Genomics Germany GmbH
	30 µl HPA-15-R	Eurofins Genomics Germany GmbH
	2 µl HGH-F	Eurofins Genomics Germany GmbH
	2 µl HGH-R	Eurofins Genomics Germany GmbH
	436 µl Aqua dest	Merck KGaA
SNP1a	1 µl β-Globin -R	Eurofins Genomics Germany GmbH
	1 µl β-Globin -F	Eurofins Genomics Germany GmbH
	5 µl SNP1-F	Eurofins Genomics Germany GmbH
	5 µl SNP1-R(T)	Eurofins Genomics Germany GmbH
	238 µl ddH ₂ O	Merck KGaA

MATERIAL AND METHODS

SNP1b	1 µl β-Globin -R	Eurofins Genomics Germany GmbH
	1 µl β-Globin -F	Eurofins Genomics Germany GmbH
	5 µl SNP1-F	Eurofins Genomics Germany GmbH
	5 µl SNP1-R(A)	Eurofins Genomics Germany GmbH
	238 µl ddH ₂ O	Merck KGaA
SNP2a	1 µl β-Globin -R	Eurofins Genomics Germany GmbH
	1 µl β-Globin -F	Eurofins Genomics Germany GmbH
	2.5 µl SNP2-F(C)	Eurofins Genomics Germany GmbH
	2.5 µl SNP2-R	Eurofins Genomics Germany GmbH
	243 µl ddH ₂ O	Merck KGaA
SNP2b	1 µl β-Globin -R	Eurofins Genomics Germany GmbH
	1 µl β-Globin -F	Eurofins Genomics Germany GmbH
	2.5 µl SNP2-F(T)	Eurofins Genomics Germany GmbH
	2.5 µl SNP2-R	Eurofins Genomics Germany GmbH
	243 µl ddH ₂ O	Merck KGaA
SNP3a	1 µl β-Globin -R	Eurofins Genomics Germany GmbH
	1 µl β-Globin -F	Eurofins Genomics Germany GmbH
	5 µl SNP3-F(G)	Eurofins Genomics Germany GmbH
	5 µl SNP3-R	Eurofins Genomics Germany GmbH
	238 µl ddH ₂ O	Merck KGaA
SNP3b	1 µl β-Globin -R	Eurofins Genomics Germany GmbH
	1 µl β-Globin -F	Eurofins Genomics Germany GmbH
	5 µl SNP3-F(C)	Eurofins Genomics Germany GmbH
	5 µl SNP3-R	Eurofins Genomics Germany GmbH
	238 µl ddH ₂ O	Merck KGaA
SNP4a	1 µl β-Globin -R	Eurofins Genomics Germany GmbH
	1µl β-Globin -F	Eurofins Genomics Germany GmbH
	5µl SNP4-F(A)	Eurofins Genomics Germany GmbH
	5µl SNP4-R	Eurofins Genomics Germany GmbH
	238µl ddH ₂ O	
SNP4b	1µl β-Globin -R	Eurofins Genomics Germany GmbH
	1 µl β-Globin -F	Eurofins Genomics Germany GmbH
	5 µl SNP4-F(G)	Eurofins Genomics Germany GmbH
	5 µl SNP4-R	Eurofins Genomics Germany GmbH
	238 µl ddH ₂ O	Merck KGaA
SNP5a	1 µl β-Globin -R	Eurofins Genomics Germany GmbH
	1 µl β-Globin -F	Eurofins Genomics Germany GmbH
	5 µl SNP5-F(G)	Eurofins Genomics Germany GmbH
	5 µl SNP5-R	Eurofins Genomics Germany GmbH
	238 µl ddH ₂ O	Merck KGaA
SNP5b	1 µl β-Globin -R	Eurofins Genomics Germany GmbH
	1 µl β-Globin -F	Eurofins Genomics Germany GmbH
	5 µl SNP5-F(A)	Eurofins Genomics Germany GmbH
	5 µl SNP5-R	Eurofins Genomics Germany GmbH
	238 µl ddH ₂ O	Merck KGaA
SNP6a	1 µl β-Globin -R	Eurofins Genomics Germany GmbH
	1 µl β-Globin -F	Eurofins Genomics Germany GmbH
	2.5 µl SNP6-F(C)	Eurofins Genomics Germany GmbH
	2.5 µl SNP6-R	Eurofins Genomics Germany GmbH

MATERIAL AND METHODS

	243 µl ddH ₂ O	Merck KGaA
SNP6b	1 µl β-Globin -R	Eurofins Genomics Germany GmbH
	1 µl β-Globin -F	Eurofins Genomics Germany GmbH
	2.5 µl SNP6-F(T)	Eurofins Genomics Germany GmbH
	2.5 µl SNP6-R	Eurofins Genomics Germany GmbH
	243 µl ddH ₂ O	Merck KGaA
SNP7a	1 µl β-Globin -R	Eurofins Genomics Germany GmbH
	1 µl β-Globin -F	Eurofins Genomics Germany GmbH
	5 µl SNP7-F(T)	Eurofins Genomics Germany GmbH
	5 µl SNP7-R	Eurofins Genomics Germany GmbH
	238 µl ddH ₂ O	Merck KGaA
SNP7b	1 µl β-Globin -R	Eurofins Genomics Germany GmbH
	1 µl β-Globin -F	Eurofins Genomics Germany GmbH
	5 µl SNP7-F(C)	Eurofins Genomics Germany GmbH
	5 µl SNP7-R	Eurofins Genomics Germany GmbH
	238 µl ddH ₂ O	Merck KGaA
SNP8a	1 µl β-Globin -R	Eurofins Genomics Germany GmbH
	1 µl β-Globin -F	Eurofins Genomics Germany GmbH
	5 µl SNP8-F(A)	Eurofins Genomics Germany GmbH
	5 µl SNP8-R	Eurofins Genomics Germany GmbH
	238 µl ddH ₂ O	Merck KGaA
SNP8b	1 µl β-Globin -R	Eurofins Genomics Germany GmbH
	1 µl β-Globin -F	Eurofins Genomics Germany GmbH
	5 µl SNP8-F(G)	Eurofins Genomics Germany GmbH
	5 µl SNP8-R	Eurofins Genomics Germany GmbH
	238 µl ddH ₂ O	Merck KGaA
SNP9a	1 µl β-Globin -R	Eurofins Genomics Germany GmbH
	1 µl β-Globin -F	Eurofins Genomics Germany GmbH
	5 µl SNP9-F(A)	Eurofins Genomics Germany GmbH
	5 µl SNP9-R	Eurofins Genomics Germany GmbH
	238 µl ddH ₂ O	Merck KGaA
SNP9b	1 µl β-Globin -R	Eurofins Genomics Germany GmbH
	1 µl β-Globin -F	Eurofins Genomics Germany GmbH
	1 µl SNP9-F(G)	Eurofins Genomics Germany GmbH
	1 µl SNP9-R	Eurofins Genomics Germany GmbH
	246 µl ddH ₂ O	Merck KGaA
SRY-1	5 µl SRY-F1	Eurofins Genomics Germany GmbH
	5 µl SRY-R1	Eurofins Genomics Germany GmbH
	240 µl ddH ₂ O	Merck KGaA
SRY-2	5 µl SRY-F2	Eurofins Genomics Germany GmbH
	5 µl SRY-R2	Eurofins Genomics Germany GmbH
	240 µl ddH ₂ O	Merck KGaA
SRY-3	5 µl SRY-F1	Eurofins Genomics Germany GmbH
	5 µl SRY-R3	Eurofins Genomics Germany GmbH
	240 µl ddH ₂ O	Merck KGaA

All primer stock solutions with 100 µM concentration

2.4 Primer Sequences for Pre-amplification and dPCR

Target	Primer sequence for pre-amplification (5'–3') and amplicon size	Primer and probe sequence (5'–3') or commercial assay code (FAM or VIC label as indicated)
<i>RHD</i> exon 3	for: TCTCAGTCGTCTGGCTCTC rev: TTA CTGATGACCATCCTCAGGT amplicon size: 175 bp	for: GGCCACCATGAGTGCTTTG rev: CTCCACCAGCACCATCACC P: FAM-TGCTGATCTCAGTGGATG-MGB
<i>RHD</i> exon 5	for: TTCTGGCCAACCACCCTCTC rev: GTCACCACGCTGACTGCTAC amplicon size: 148 bp	for: CGCCCTCTTCTTGTGGATG rev: GAACACGGCATTCTTCCTTTT P: FAM-TCTGGCCAAGTTTCAAC-MGB
<i>RHD</i> exon 7	for: CAGCTCCATCATGGGCTACAA rev: GGGTAAGCCCAGTGACCC amplicon size: 122 bp	for: TGTGCTGCTGGTGCTTGA rev: AGTGACCCACATGCCATTG P: FAM-ACCGTCGGAGCCG-MGB
GAPDH	for: CCATCCCTTCTCCCCACAC rev: GCTGTATTTTAACCCCTAGTCC amplicon size: 123 bp	for: CCCCACACACATGCACTTACC rev: CCTAGTCCCAGGGCTTTGATT P: VIC-TAGGAAGGACAGGCAAC-MGB
AMEL	for: CTGGGCACCCTGGTTATATC rev: CTTGAGGCCAACCATCAGAG amplicon size: 201 bp	for: CCCTGGGCTCTGTAAAGAATAGTG rev: ATCAGAGCTTAACTGGGAAGCTG Px: VIC-TATCCCAGATGTTTCTC-MGB Py: FAM-CCAAATAAAGTGGTTTCTC-MGB
KEL1/2 (rs8176058)	for: GGCTCCACGGATCCTTATG rev: TGTGTGGAGAGGCAGGATG amplicon size: 178 bp	C_1719_20 KEL1: FAM; KEL2: VIC
HPA-1a/b (rs5918)	for: TGGACTTCTCTTTGGGCTCC rev: TTGAGTGACCTGGGAGCTG amplicon size: 189 bp	C_818008_30 HPA-1a: FAM; HPA-1b: VIC
HPA-2a/b	for: TTGCGAACTCCAAGAGC rev: GATTCTCCAGCCATTCAGG amplicon size: 153 bp	C_11442703_10 HPA-2a: VIC; HPA-2b: FAM
HPA-3a/b	for: CTGCGATCCCCTTGTGATG rev: TGGGCTGACCACTCCTTTG amplicon size: 97 bp	C_3017440_10 HPA-3a: FAM; HPA-3b: VIC
HPA-5a/b (rs1801106)	for: ACACCATTACAGACGTGCTC rev: CTTTCAAATGCAAGTTAAATTACC amplicon size: 165 bp	C_27862812_10 HPA-5a: FAM; HPA-5b: VIC
HPA-15a/b	for: GTTTAGATTATTTTGGCTTATTTCAAATGTATC rev: ACCAGTAGCCACCCAAGAAG amplicon size: 145 bp	C_3226894_10 HPA-15a: FAM; HPA-15b: VIC
SNP1 (rs1357617)	for: CTCATTGGCAGCTGATGCAG rev: GTCTCAAACGCCATCAGTATAG amplicon size: 169 bp	C_11354314_10 rs1357617-T: FAM; rs1357617-A: VIC
SNP2 rs917118	for: CTCCACTTCACTGATGTCC rev: GAGAAGCTTGAGCAAAGGC amplicon size: 194 bp	C_7608025_10 rs917118-T: FAM; rs917118-C: VIC

MATERIAL AND METHODS

SNP3 rs1015250	for: CATGTAACCTCCCTTAGGG rev: GATGTTCTTGTGACCGACATG amplicon size: 163 bp	C___1881082_10 rs1015250-G: FAM; rs1015250-C: VIC
SNP4 rs722098	for: TGCCAGCTTGCCAAGGAAGG rev: CCCATTCCCACAGATAGG amplicon size: 198 bp	C___2349786_10 rs722098-G: FAM; rs722098-A: VIC
SNP5 rs733164	for: GGCACAGCTTCTTGACTCT rev: GCTAGGGGTTGAGTCCAT amplicon size: 194 bp	C___27044_1_ rs733164-G: FAM; rs733164-A: VIC
SNP6 rs2056277	for: CTGCTTCATTCAATCCGTGAG rev:GTGGCAGGCGTTCTGTATAG amplicon size: 185 bp	C___408450_10 rs2056277-T: Fam; rs2056277-C: VIC
SNP7 rs938283	for: CCGTGCACCCTTCTATTATG rev: GTGCATGTCTGTGTCTAATC amplicon size: 185 bp	C___7475537_10 rs938283-T: FAM; rs938283-C: VIC
SNP8 (rs2830795)	for: GGCTGCAGGTTGATGATTC rev: TCTACCCAGATGCCTGAAATATG amplicon size: 189 bp	C_3086569_20 rs2830795-G: FAM; rs2830795-A: VIC
SNP9 (rs1028528)	for: AACAGATGTCCACAGCTGATG rev: AGCAAGGGCATGGGATCCA amplicon size: 177 bp	C_2988456_20 rs1028528-G: FAM; rs1028528-A: VIC

2.5 Primer Sequences for PCR-SSP

Target	Primer sequence for sequence-specific primer PCR (5'-3') and amplicon size
KEL1/2 (rs8176058)	for: GGGAGATGGAGATGGAAATGG rev: GACTCATCAGAAGTCTCAGCG rev: GACTCATCAGAAGTCTCAGCA amplicon size: 280 bp
β -Globin KEL assay	for: GGTTGGCCAATCTACTCCCAGG rev: GCTCACTCAGTGTGGCAAAG amplicon size: 540 bp
β -Globin SNP assay	for: GCTTACCAAGCTGTGATTCC rev: GCTCACTCAGTGTGGCAAAG amplicon size: 748 bp
HPA-1a/b (rs5918)	for HPA-1a: GACTTACAGGCCCTGCCTCT for HPA-1b: ACTTACAGGCCCTGCCTCC rev: GTGCAATCCTCTGGGGAC amplicon size HPA-1a: 190 bp amplicon size HPA-1b: 189 bp
HPA-2a/b (rs6065)	for HPA-2a: CCCCCAGGGCTCCTGAC for HPA-2b: CCCCCAGGGCTCCTGAT rev: GCCAGCGACGAAAATAGAGG amplicon size HPA-2a: 241 bp amplicon size HPA-2b: 241 bp

MATERIAL AND METHODS

HPA-3a/b (rs5911)	for HPA-3a: GGACTGGGGGCTGCCCAT for HPA-3b: TGGACTGGGGGCTGCCCAG rev: ACCAGAGAGCCTGCTCACTAC amplicon size HPA-3a: 142 bp amplicon size HPA-3b: 143 bp
HPA-5a/b (rs1801106)	for HPA-5a: AAGGAAGAGTCTACCTGTTTACTATCAAAG for HPA-5b: AAGGAAGAGTCTACCTGTTTACTATCAAAA rev: GGCAGTACACTATACATTCAACTC amplicon size HPA-5a: 244 bp amplicon size HPA-5b: 243 bp
HPA-15a/b (rs10455097)	for HPA-15a: GTTACTTCAAATTCTTGGTAAATCCTGG for HPA-15b: GTTACTTCAAATTCTTGGTAAATCCTGT rev: CAGTATTATGACCTTATGATGACCTATTC amplicon size HPA-15a: 229 bp amplicon size HPA-15b: 229 bp
HGH	for: GCCTTCCCAACCATTCCCTTA rev: TCACGGATTTCTGTTGTGTTTC amplicon size: 429 bp
SNP1 (rs1357617)	for: GAATCAGACACTCACTTTCACAGC rev SNP1-T: GCTGATAAGAAACATGACCAAGCT rev SNP1-A: GCTGATAAGAAACATGACCAAGCA amplicon size: 212 bp
SNP2 (rs917118)	for SNP2-C: AAGATGGAGTCAACATTTTACAAGAC for SNP2-T: AAGATGGAGTCAACATTTTACAAGAT rev: GACTCTGAGCTCAGAAAGGTG amplicon size: 181 bp
SNP3 (rs1015250)	for SNP3-G: GGAAAAGAACCCAGGTGTTTTATTG for SNP3-C: GGAAAAGAACCCAGGTGTTTTATTG rev: GTGCATTGCAGAATCGACAGC amplicon size: 362 bp
SNP4 (rs722098)	for SNP4-A: CTGTTGACAGTAATGAAATATCCTTGA for SNP4-G: CTGTTGACAGTAATGAAATATCCTTGG rev: GACATGCTGATCAGAAGATCCC amplicon size: 186 bp
SNP5 (rs733164)	for SNP5-G: CAGGCCATCCCCTTGGAAAAG for SNP5-A: CAGGCCATCCCCTTGGAAAA rev: GGTTGAGTCCATGCCAAGAC amplicon size: 97 bp
SNP6 (rs2056277)	for SNP6-C: GGAGACAGGCATGAATGAGAC for SNP6-T: GGAGACAGGCATGAATGAGAT rev: CTCCTACTCAGCCAACTCC amplicon size: 370 bp
SNP7 (rs938283)	for SNP7-T: CTAGTACGTTAGATGTGACCGT for SNP7-C: CTAGTACGTTAGATGTGACCGC rev: GTGAAGCCCCTCAGCCTG amplicon size: 290 bp
SNP8 (rs2830795)	for SNP8-A: GGACACACCATTTTATTGTCTAAWGA for SNP8-G: GGACACACCATTTTATTGTCTAAWGG rev: GGGAGGTTGTCATCAGAGAAG

	amplicon size: 179 bp
SNP9 (rs1028528)	for SNP9-A: GAAAGGTCCTTACTCGACATCA for SNP9-G: GAAAGGTCCTTACTCGACATCG rev: CCTGCAAGATAGATGCTAGTGC
	amplicon size: 285 bp
SRY-1	for: TGGCGATTAAGTCAAATTCGC rev: CCCCTAGTACCCTGACAATGTAT
	amplicon size: 137 bp
SRY-2	for: CAGGACAGCAGTAGAGCAGTC rev: TTCTACCAGATTCTTTGTTACG
	amplicon size: 200 bp
SRY-3	for: TGGCGATTAAGTCAAATTCGC rev: GCATATGATTGCATTGTCAAAAAC
	amplicon size: 316 bp

2.6 Preparation and Storage of Cell-Free Plasma

The preparation of the cell-free plasma in this lab is based on the QIAamp® Circulating Nucleic Acid instructions for use, Appendix A. In this protocol, the EDTA-blood was centrifuged at RT for 10 min at 2,000 g. Subsequently, the plasma was transferred into a Nalgene round-bottom tube by using a Pasteur pipette. The plasma was centrifuged for 10 min at 4 °C at 16,000 g. After centrifugation, the cell-free plasma was transferred into cryotubes and stored at -80 °C until use. The remaining blood was transferred in cryotubes and stored at -80 °C as well.

2.7 DNA Isolation Methods

In this work, different DNA isolation methods for cell-free DNA and genomic DNA were used. Some are based on columns, and others work with magnetic beads. Both isolation methods bind DNA on silica particles. Either a membrane in the column or a magnetic bead coated with a silica layer (Figure 18).

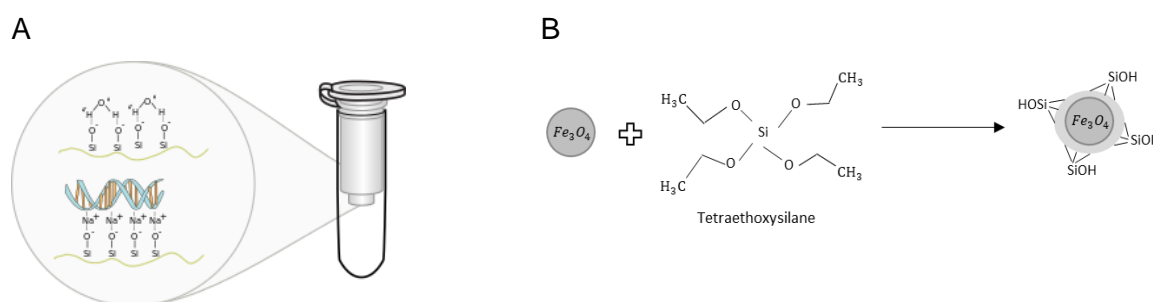


Figure 18: A: Example of a spin column with a silica B: Example of a magnetic bead coated with a silica layer [204].

The use of DNA extraction with silica was first published in 1990 [205]. In principle, the DNA binds to the silica under a low acidic pH combined with alcohol and high chaotropic salt content. Impurities were eliminated by reducing chaotropic salts and wash steps with 70-80 % ethanol. The DNA is released with water or elution buffer [206]. This is the extraction principle for all DNA isolation methods, regardless of if genomic or cell-free DNA is used. However, the membrane can clog in case of a sample with high impurity, like an incomplete homogenization. This is not the case with magnetic beads because there is no filter membrane. But after isolation with magnetic beads, some beads can stay in the solution with the isolated DNA and disturb further analysis.

The following section is subdivided into protocols for genomic DNA isolation and the isolation protocols for cell-free DNA.

2.7.1 Genomic DNA Isolation Methods

To determine the volunteers' and newborns' blood cell antigen status, genomic DNA was isolated from the whole blood or umbilical cord blood, and PCR analysis was performed. Another protocol presented here is the genomic DNA isolation from the buccal swabs. This was mainly done on newborns, from whom no umbilical cord blood was available. The DNA from the newborns was used to verify the results of the prenatal analyses.

2.7.1.1 DNA Extraction from EDTA Blood

The following protocol for the DNA extraction was conducted after the manufacturer's instructions. The used Kit from Qiagen is called the QIAamp DNA Blood Mini Kit (50) with Cat No./ID: 51104.

In a 1.5 ml Eppendorf tube, 20 μ l protease and 200 μ l EDTA blood were added and mixed gently before adding 200 μ l AL puffer. The mixture was vortexed and incubated for 10 min at 56 °C. 200 μ l EtOH was added and vortexed shortly. The lysate was transferred to a mini-column and centrifuged for 1 min at 10,000 rpm. The column was placed in a new tube, 500 μ l AW1 buffer was added and centrifuged for 1 min at 10,000 rpm. Afterward, the column was transferred in a new tube, 500 μ l AW2 buffer was added and centrifuged for 2 min at 13,000 rpm. Subsequently, the column was placed in a new 1.5 ml Eppendorf tube. Then 200 μ l AE buffer was added and incubated for 1 min at room temperature. The sample was centrifuged for 1 min at 10,000 rpm. Finally, the column was discarded, and the DNA was stored at 4 °C until use.

2.7.1.2 DNA Extraction from a Buccal Swab

For this protocol, the same kit as for the DNA extraction from EDTA blood was used. The difference between the whole blood extraction can be found at the beginning of the protocol. In order to solve the cells from the buccal swab, the swap was incubated for 10 min in 350 μ l PBS at room temperature and subsequently squeezed out. In a separate Eppendorf tube were 20 μ l protease mixed with 200 μ l of the squeezed PBS and gently mixed. Afterward, 200 μ l AL buffer was added, vortexed, and then incubated for 10 min at 56 °C. Subsequently, 200 μ l EtOH was added and vortexed. The lysate was transferred onto the spin column and centrifuged for 1 min at 10,000 rpm. Then the column was placed in a new tube. 500 μ l AW1 buffer was added and centrifuged for 1 min at 10,000 rpm. The column was transferred into a new tube. 500 μ l AW2 buffer was added and centrifuged for 2 min at 13,000 rpm. Afterward, the column was placed in a new labeled 1.5 ml Eppendorf tube, and a 50 μ l AE buffer was added. After 1 min incubation at room temperature, the tube was centrifuged for 1 min at 10,000 rpm, and the isolated DNA was stored at 4 °C until use.

2.7.2 Cell-Free DNA Extraction Methods

During the technical validation and later for the clinical validation, the cell-free DNA was isolated from plasma out of volunteers. Various applications were tested to determine the most suitable DNA extraction method. The aim was a high DNA content and low impurity to be well compatible with the dPCR. In this subsection, the cell-free DNA extraction was conducted with magnetic beads with various methods like a manual protocol or an automated device. Last but not least, a column-based manual extraction method was tested, too.

2.7.2.1 Cell-Free DNA Isolation with MagMax

One manual method is the isolation of cfDNA with magnetic beads, which uses magnetic force to separate the DNA from other contaminations or substances. The following protocol was according to the instructions from the manufacturer ThermoFisher. The kit used is called MagMAX™ CellFree DNA Isolation Kit and is available under the catalog number A29319.

Binding DNA to the magnet beads

In a 1.5 ml tube, 15 µl Proteinase K (20 mg/ml), 1 ml plasma sample, and 50 µl SDS (20 %) were mixed and incubated for 20 min. At 60 °C in the Eppendorf Thermomixer™. Afterward, the sample was incubated for 5 min. On ice and a binding solution/beads Mix, containing 1.25 ml MagMAX™ cell-free DNA lysis/binding solution and 15 µl MagMAX™ cell-free DNA magnetic beads was added to each sample and mixed by inverting the tube ten times. Subsequently, the sample was vortexed for 10 min on a vortexer with a tube adaptor. The tube was then placed on the DynaMag™-2 Magnet for 5 min. or until the solution was cleared, and the supernatant was discarded.

Washing of the beads

The beads were resuspended in 1 ml MagMAX™ cell-free DNA wash solution and were transferred into a new Eppendorf tube, whereas the old tube containing the lysis/binding solutions was saved. The new tube was placed on the DynaMag™-2 Magnet for 20 sec, and the supernatant was used to rinse the saved lysis/binding tube. The collected residual beads were transferred to the new tube, and the lysis/binding tube was discarded. The tube was incubated for 2 min or until the solution was cleared on the DynaMag™-2 Magnet. Subsequently, the supernatant was discarded, and the magnet was tapped on the benchtop, and the residual supernatant was removed. The tube was eliminated from the magnet stand, and 1 ml MagMAX™ cell-free DNA wash solution was added and vortexed for 30 sec. Now, the tube was placed back to the DynaMag™-2 Magnet for at least 2 min, or the solution had cleared. The supernatant was removed, and the magnet stand was tapped on the benchtop. Then the residual supernatant was removed. The tube was eliminated from the DynaMag™-2 Magnet, 1 ml 80 % ethanol was added, and subsequently vortexed for 30 sec. Afterward, the tube was placed on the magnet stand for 2 min or until the solution was clear. The supernatant was discarded, the magnet stand was taped on the benchtop, and the residual supernatant was removed. The washing step was repeated with 80 % ethanol. Afterward, the beads were air-dried for 3-5 min on the DynaMag™-2 Magnet.

Elution of the cfDNA

15 µl MagMAX™ cell-free DNA elution solution was added and vortexed for 5 min. The tube was placed on the DynaMag™-2 Magnet for 2 min or until the solution was clear. Finally, the supernatant was transferred in a new labeled Eppendorf tube and stored at -20 °C until use.

2.7.2.2 Cell-Free DNA Isolation with Maxwell

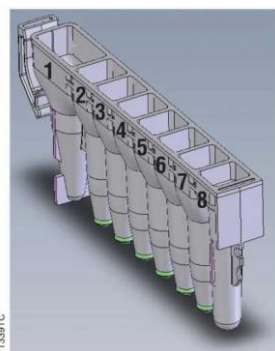
For the automated cell-free DNA extraction, the Maxwell® RSC device was tested. This DNA extraction is based on magnetic beads and is mostly automated. The used Maxwell® RSC ccfDNA Plasma Kit can be ordered with the catalog number AS1480. The following instruction was proceeded to prepare the samples before starting the device and was taken from the manufacturer's instructions.

The Maxwell® Instrument and Tablet PC were turned on, and the Maxwell® software was opened by double-touching the Maxwell® RSC icon.

The cartridges were placed into the deck tray and pressed down until it snaps into position. The seal was peeled off, and 1 ml plasma was added into the 1st well. One plunger was placed into the 8th well of the cartridge (Figure 19). The elution tube was placed in the deck tray, and 50 µl ddH₂O was added.

The “start” button was touched to access the ‘Methods’ screen and select the ccfDNA Plasma program or scan the barcode from the kit box. After the “proceed” button was pressed, the cartridge setup opens. In this mode, it is possible to select the cartridge's position in the deck tray and add tracking information from the sample. By using the “proceed” button, the door of the Maxwell[®] opened, and the deck tray was placed into the Maxwell[®] instrument. After the button “start” was pressed, the door closes, and the extraction started. After the isolation was finished, the cartridge was discarded, and the tube containing the isolated cfDNA was stored at -30 °C until use.

A



B



Figure 19: A: Maxwell[®] RSC Cartridge. B: Elution tubes in the deck tray [207].

2.7.2.3 Cell-Free DNA Extraction with QIAmp Circulating Nucleic Acids Kit

The last cell-free extraction method is a manual extraction based on column and vacuum pressure. The protocol was adopted from the QIAmp Circulating Nucleic Acids Kit instructions and is available from Qiagen with the catalog number 55114.

In a 5 ml Eppendorf tube, 100 μ l Protease K and 1 ml plasma were gently mixed. Then 800 μ l ACL buffer was added, vortexed, and incubated for 30 min at 60 °C. Subsequently, 1,800 μ l ACB buffer was added, vortexed, and incubated for 5 min on ice. The lysate was transferred to the column, placed on the QIAvac 24 Plus, and the vacuum pump was started until all lysate has passed the column. The vacuum system's pressure was released to 0 bar, and 600 μ l ACW1 buffer was added to the column. The vacuum pump was started until all buffer was drawn through the column, and the pressure of the vacuum system was released. 750 μ l ACW2 buffer was applied to the column, and the vacuum pump was started until all buffer was drawn through the column. The pressure in the system was released to 0 bar, and 750 μ l EtOH was added. The vacuum pump was started until all buffer was drawn through the column, and the pressure of the vacuum system was released until 0 bar. The column was then centrifuged for 3 min at 13,000 rpm, placed in a new 1.5 ml Eppendorf tube, and 10 min incubated at 56 °C. Finally, 100 μ l ddH₂O was applied, incubated for 3 min at room temperature, and centrifuged for 1 min at 13,000 rpm. The isolated DNA was stored at -30 °C until use.

2.8 DNA Amplification Methods

The amount of cell-free DNA is very low. To increase the DNA content, multiple-displacement amplification and targeted DNA amplification was tested.

2.8.1 Multiple Displacement Amplification

The multiple displacement amplification (MDA) is a non-PCR based method for DNA amplification [208, 209]. It uses the Φ 29 DNA polymerase derived from *Bacillus subtilis* [210]. The primers are hexamers, which randomly bind to the DNA. These primers are covered by thiophosphate linkages in the two 3' terminal nucleotides to prevent degradation of the 3'-

5' exonuclease proofreading activity [211, 212]. In principle, the random hexamer primer anneals to the template, and the polymerase starts with the synthesis and elongates the strand until it reaches the next primer. It displaces this primer and elongates further on. The newly replicated and displaced strand acts as a new template for primer, and so a hyper-branched DNA network of DNA arises [209] (Figure 20). For this type of amplification, a thermocycler is unnecessary because the thermal conditions are constant at 30 °C.

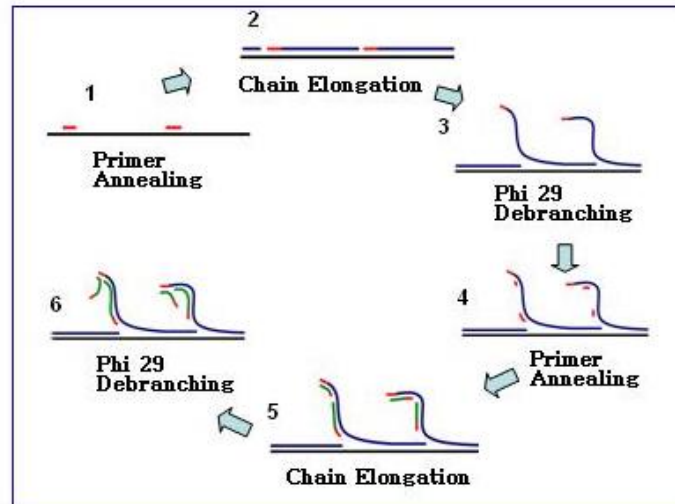


Figure 20: MDA steps: 1. The random hexamer primer hybridizes to the template DNA. 2. Φ 29 DNA polymerase binds and synthesizes the complementary strand. 3. The polymerase reaches the next primer and displaces the strand, and elongates further on. 4. The newly displaced DNA strand functions as a new template for primer annealing. 5. Φ 29 DNA polymerase binds and synthesizes the complementary strand. 6. The polymerase reaches the next primer and displaces the strand. Source: [213].

2.8.2 Whole Genome Amplification with REPLI-g Mini Kit

The protocol for the REPLI-g Mini Kit is developed to use DNA from whole blood and tissue culture cells. The following protocol is according to the REPLI-g Mini Kit protocol from Qiagen.

The procedure starts with the preparation of the buffer D1 containing 9 μ l reconstituted buffer DLB, 32 μ l nuclease-free water, and buffer N1 consisting of 12 μ l stop solution and 68 μ l nuclease-free water. The master mix was prepared on ice with 29 μ l REPLI-g Mini Reaction Buffer and 1 μ l REPLI-g Mini DNA Polymerase. In a 1.5 ml Eppendorf tube, 5 μ l template DNA and 5 μ l D1 buffer were added, vortexed and centrifuged briefly. The DNA was denatured by incubation for 3 min at room temperature. Subsequently, 10 μ l N1 buffer was added, vortexed, and centrifuged. To stop the denaturation step, 30 μ l master mix was added to the denatured DNA and incubated for 10-16 h at 30 °C. The REPLI-g Mini DNA Polymerase was inactivated by heating the sample to 65 °C for 3 min. The DNA was stored at -20 °C until use.

2.8.3 Whole Genome Amplification with REPLI-g FFPE Kit

The REPLI-g FFPE Kit is developed to amplify DNA from formalin-fixed, paraffin-embedded (FFPE) tissue. The DNA in this sample is strongly degraded, and it was tested if this method was more suitable to amplify cell-free DNA. The following protocol was taken from the REPLI-g FFPE Kit handbook.

The procedure started with preparing the FFPE master mix on ice containing 8 μ l FFPE Buffer, 1 μ l Ligation Enzyme, and 1 μ l FFPE Enzyme. The mixture was vortexed, briefly centrifuged, and subsequently the REPLI-g master mix containing 29 μ l REPLI-g Midi

Reaction Buffer and 1 μ l REPLI-g Midi DNA Polymerase was produced. Both mixtures are stored on ice until use. In an Eppendorf tube 10 μ l of the cfDNA and 10 μ l of the FFPE master mix were added, vortexed, and briefly centrifuged. During the 30 min incubation at 24 $^{\circ}$ C, the DNA fragments ligated randomly onto the denatured DNA. This ligation process was stopped by incubation at 95 $^{\circ}$ C for 5 min and cooled down to 4 $^{\circ}$ C in a thermal block. Then 30 μ l of the REPLI-g master mix was added and incubated at 30 $^{\circ}$ C for 8 h. Finally, the reaction was stopped by a 10 min incubation at 95 $^{\circ}$ C, and the DNA was stored at -20 $^{\circ}$ C until use.

2.8.4 Targeted Preamplification PCR

As mentioned before, the cell-free DNA amount is very low. This is accompanied by a small amount of fetal DNA as well as the desired target sequence. Another DNA amplification method is the targeted amplification with nested PCR. To increase the desired DNA sequence, two consecutive amplifications are performed. In the 1st PCR, the primers lay outside the desired PCR fragment, so a huge amplicon results. In the second PCR, the primer is placed in the region of interest, and only the desired sequence is amplified (Figure 21) [214, 215].

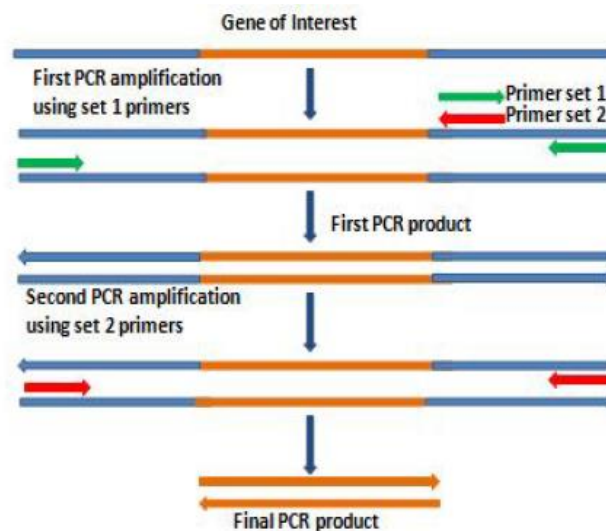


Figure 21: Principle of the nested PCR. In the 1st PCR, the primers are placed outside the targeted sequence. The 2nd PCR included different primers, which are placed in the targeted region [216].

The following protocol is taken from the QIAGEN[®] Multiplex PCR handbook, catalog number 206143.

Per approach, 12.5 μ l Multiplex Master mix, 2.5 μ l primer mix, and 10 μ l cfDNA were added to one reaction tube and placed in a thermal cycler. The cycling program started with 15 min at 95 $^{\circ}$ C and then 30 cycles with 30 sec. at 94 $^{\circ}$ C, 90 sec. at 63 $^{\circ}$ C and 90 sec. at 72 $^{\circ}$ C. Finally, the polymerase was inactivated by heating up to 72 $^{\circ}$ C for 10 min. Three different multiplex mixes were established for different targets. Multiplex I included primers for *RHD* exons 3, 5 and 7, *GAPDH*, and *AMEL-Y*, multiplex II consists of the primers for *KEL*, *HPA-1*, *HPA-5*, and *AMEL-Y*, and multiplex III contained the primers for the control SNP1-9. The assays for *HPA-2*, *-3*, and *-15* were not performed in a multiplex reaction.

2.9 PCR Purification

A purification after the preamplification PCR is necessary. In addition to the amplified DNA, there are primer dimers, unspecific PCR products, primer residues, unused dNTPs, and salts, and the DNA-polymerase. To get rid of them, the spin-column based PCR purification was applied. In this method, salt, primer, and unspecific DNA fragments below 100 bp were removed [217]. In the presence of high chaotropic salts, the DNA binds to the silica

membrane, and impurities were washed away by reducing the salt concentration. A wash step, including ethanol, removed other salts. Finally, the DNA is eluted with water. The following protocol was taken from the QIAquick PCR Purification Kit handbook from Qiagen and is usually used in this laboratory for PCR purification.

25 μ l PCR product was mixed with 125 μ l PB buffer, transferred onto the spin column, and centrifuged for 1 min at 13,200 rpm. The flow-through was discarded, 750 μ l PE buffer was added to the column and centrifuged for 1 min at 13,200 rpm. Again, the flow-through was discarded, and the membrane was air-dried for 2 min at room temperature and centrifuged for 2 min at 13,200 rpm. The column was placed in a new Eppendorf tube, and 50 μ l H₂O was added to the column. After 1 min incubation at RT, the DNA was eluted by centrifugation for 1 min at 13,200 rpm. The column was discarded, and the DNA was stored at -20 °C until use.

2.10 Digital PCR

The first step towards digital PCR was published in 1992. A quantification for target genes by combining a two-stage PCR in combination with limiting dilution and Poisson statistics was described [218]. A further step was reducing PCR volume by using glass capillaries in combination with the TaqMan chemistry. In this combination, it was possible to detect a single molecule template in a small volume of 10 nl [219]. The first digital PCR was published in 1999 by Vogelstein et al. They used 384-well plates with diluted DNA and added fluorescent probes that differentiated between wild types and mutations. By measuring the sample after PCR, they revealed an unambiguous signal for each well, e.g., WT PCR product or mutant PCR product, or no PCR product [220].

Nowadays, the isolated DNA is diluted and divided into independent partitions so that in a partition is at least one or no target sequence. During the PCR process, the target DNA is amplified, and the fluorescence signal is detected. In the end, it is resulting in positive signals where the target DNA is present or no signals if the target is not present (Figure 22). The amount of target sequences is then approximated by Poisson's statistics (chapter 2.14).

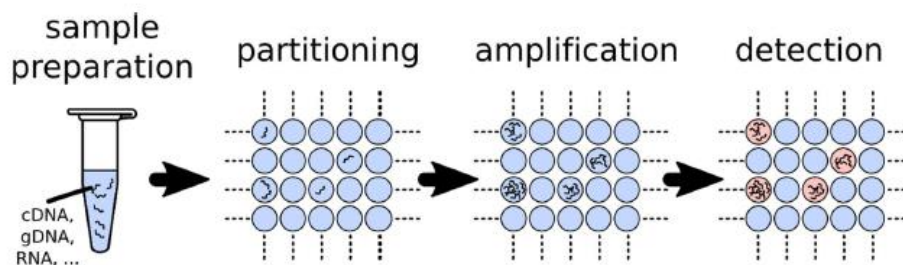


Figure 22: Principle of digital PCR [221].

Today there are different dPCR systems available. The best known are the digital droplet PCR in which water-oil-droplets are generated and the chip-based dPCR. In this thesis, chip-based digital PCR was used. One chip consists of 20,000 reaction cavities with a reaction volume of 755 pl. The signal generation in this approach is the TaqMan[®] chemistry, which will be explained now in detail.

The TaqMan system is based on ordinary PCR (chapter 2.11). However, in this PCR, the used polymerase is the *Thermus aquaticus* DNA Polymerase [222, 223]. This polymerase has a 5'→3' exonuclease activity, which cleaves the 5' terminal nucleotides of dsDNA. This results in a degradation of the probe into smaller fragments [222, 223]. The probe's labeling with a fluorescent dye was introduced in 1993 by Lee et al. [224]. The reporter's optimal position at the 5' and the quencher at the 3' end was published in 1995 [225]. The reporter and quencher can come close together in an unbound state, and no signal is received. After binding the probe to the target sequence, the 5'-exonuclease activity of the Taq-polymerase

claves the probe to smaller pieces, and the signal appears (Figure 23). The quenching is a result of the fluorescence energy transfer (FRET) [226].

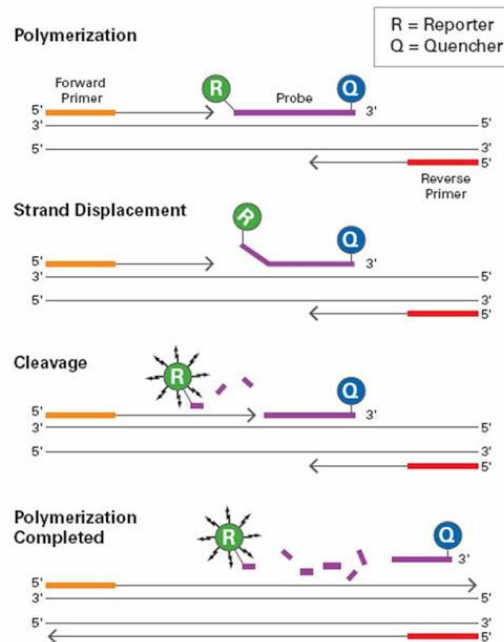


Figure 23: Principle of TaqMan chemistry [227].

The comparison of the characteristics of the different PCR techniques (PCR, qPCR, and dPCR) is shown in Figure 24. The conventional PCR is an end-point detection by gel electrophoresis and is a semi-quantitative assay. In qPCR and dPCR, the fluorescence is obtained by TaqMan[®] chemistry. The signal development is observed by real-time detection after each cycle in qPCR, and quantification is only possible with a standard curve. In contrast, the dPCR is an end-point detection method, and an absolute quantification is possible without a standard curve.

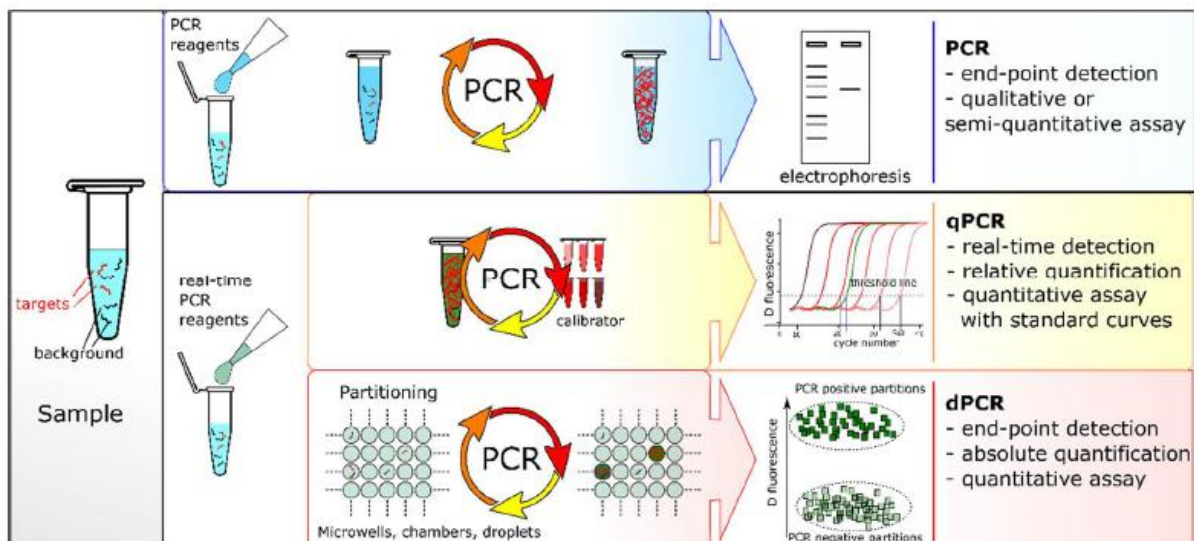


Figure 24: Comparison of PCR techniques [221].

The advantage of dPCR against qPCR is characterized by a higher reproducibility when performed at different times [228]. Another advantage of dPCR over qPCR is the possibility of absolute quantification because there is no standard curve needed [228-230]. The internal control runs on the same chip as the target sequence. Due to the dilution is the dPCR more robust against PCR inhibitory substances as qPCR [230]. Finally, the dPCR is characterized

by a higher sensitivity compared to qPCR [231]. Because due to the partitioning of the sample, the primer's dimerization is circumvented, and the template competition is reduced, so the mutations can be detected in a majority of wild-type sequences [221].

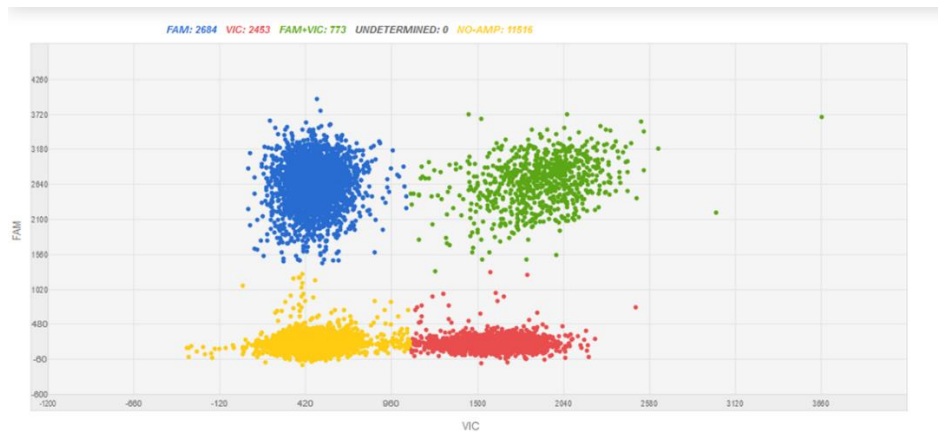


Figure 25: Example of the scatter plot of a PCR result.

The Poisson corrected results of the dPCR are presented in values of copies/ μ l or target/total in %. Besides, the uncorrected raw data is displayed in a scatter plot. In Figure 25, a representative result of an *RHD* exon 7 is depicted. The yellow dots indicate ROX positive vessels with no amplification of any target. The red dots show VIC signals, which indicate, in this case, the internal control GAPDH. The FAM signals are shown in blue and represent reaction vessels with the target's amplification, e.g., *RHD* exon 7. Reaction vessels containing the internal control and target sequence are indicated in green.

The applied protocol for the digital PCR was taken from the QuantStudio™ 3D Digital PCR System according to the instructions from ThermoFisher.

The DNA sample was diluted to the desired molecule density to a final volume of 7.1 μ l (chapter 2.15). 7.5 μ l Master Mix v2 and 0.375 μ l primer were added. This mixture was then applied to the chip using the QuantStudio™ 3D Digital PCR Chip Loader. Afterward, the chip was placed into the ProFlex™ 2x Flat PCR System. The thermal cycling program for the assays HPA-1, -2, -3, -5, and -15, *RHD* exon 3, and *RHD* exon 5 started with 96 °C for 10 min and 40 cycles with 2 min at 52 °C and 30 sec at 98 °C and a final elongation step at 52 °C for 2 min. The protocol for the assays *RHD* exon 7, AMX-Y, KEL 1, and SNP differed in the temperature for the elongation. Here, 56 °C was used instead of 52 C.

2.11 Sequence-Specific Primer PCR for Maternal Pretyping

For the identification of the maternal status of the different antigens and the nine SNPs markers, sequence-specific primer PCR (PCR-SSP) was conducted. The DNA was isolated from the mother's blood and analyzed with PCR-SSP. In the following, the principle of PCR and the peculiarity of the sequence-specific primer is explained. Subsequently, the used protocol is written down.

The PCR principle was first described by Mullis et al. in 1985 [232, 233]. The process of DNA amplification is divided into three steps. In the beginning, the DNA is heated up for denaturation. The two complementary DNA strands separate, and after cooling down, the primers can anneal to the single-stranded DNA. The temperature is now elevated to the optimal heat for the DNA polymerase, which binds to the 3'-end of the Primer and elongates the complementary strand. During the next cycles, the targeted DNA sequence is amplified exponentially (Figure 26) [232].

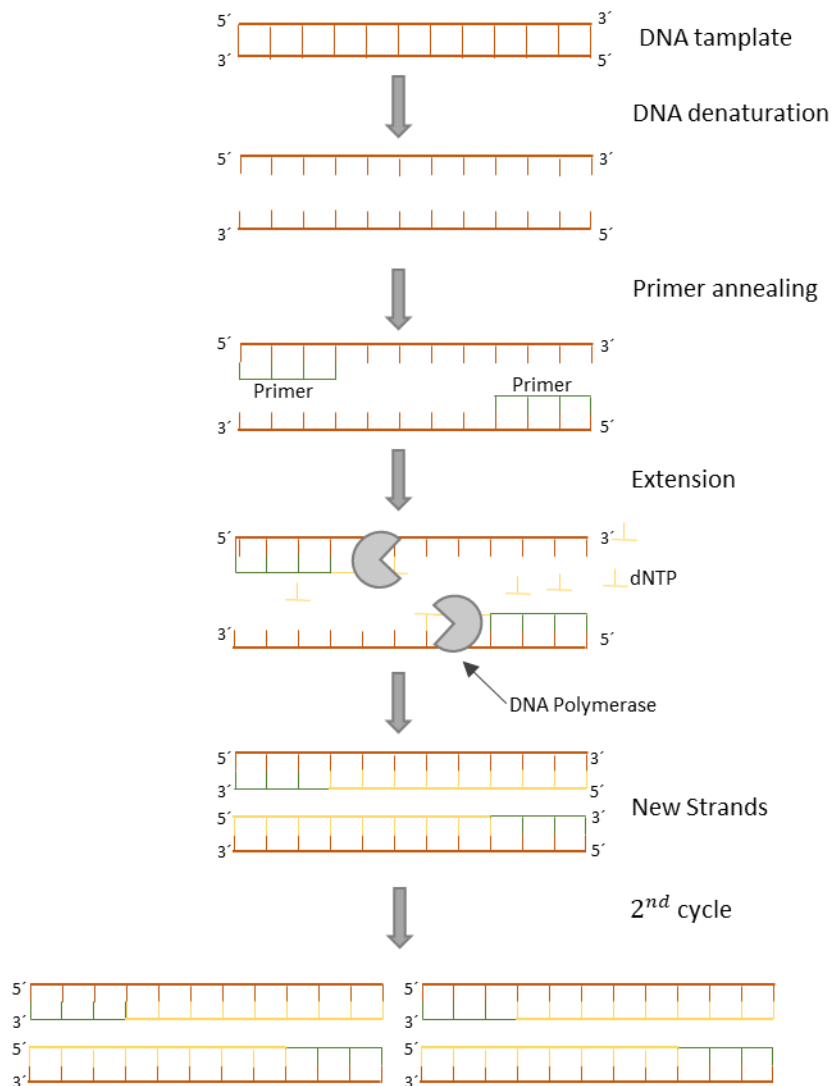


Figure 26: Principle of the PCR.

The difference between HPA a/b, KEL1/KEL2, and other SNPs from the SNPforID panel is the exchange of a single nucleotide. The first description of sequence-specific primers (SSP) to discriminate between the wild type and the mutation in point mutations was published in 1989 [234, 235]. The principle of SSP is depicted in Figure 27. Two different forward primers were designed. For example, the primer 1 corresponds to the wild type sequence at the 3'-end and primer 2 for the mutant. The reverse primer is the same for both reactions. In the case of a homozygous type for the wild type, the primer 1 bind and amplifies the sequence exponentially. In the reaction containing primer 2, the primer cannot bind properly, and therefore the polymerase cannot amplify. The wild-type reaction becomes positive while the other one shows no signal (Figure 27).

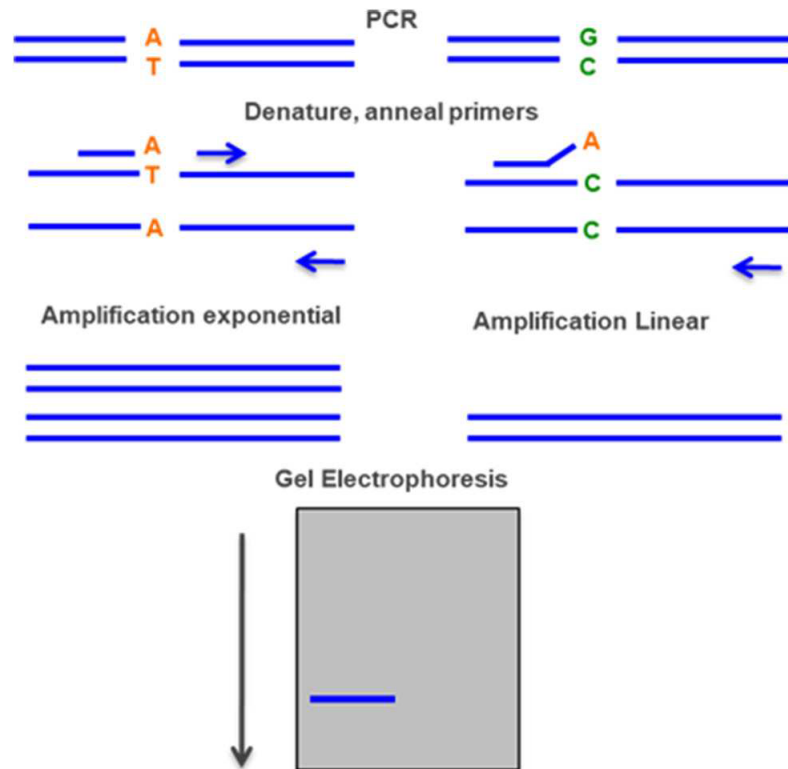


Figure 27: Principle of the PCR-SSP [236].

In the case of a heterozygous phenotype, each primer can bind to the target sequence, and the analysis in the gel reveals a signal for both reactions.

Figure 28 shows an example of an PCR-SSP result. The first horizontal line shows the internal control β -globin in the second horizontal row are the PCR results, and the third and fourth lines are primer and primer dimers. The first two vertical lines indicated a signal resulting in a heterozygous phenotype. Lines 3 and 4 revealed a signal for the a-allele and no signal for the b-allele resulting in a homozygous genotype for the a-allele. The last two rows show no signal for a-allele and a signal for b-allele, so the sample is homozygous for b.

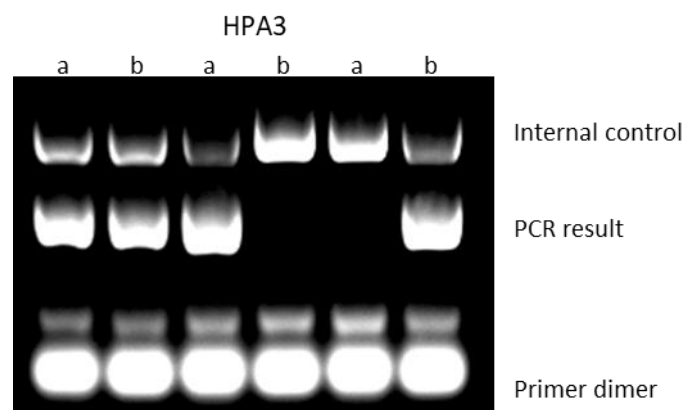


Figure 28: Example of an PCR-SSP of HPA-3.

The following protocol for the PCR-SSP is usually applied in the laboratory of Prof. Bugert and is a self-designed in-house application.

For each reaction, 5 μ l of the desired primer mix a-allele and 5 μ l primer mix b-allele were placed in different tubes. Then a master mix consisting of 22 μ l DNA in a concentration of 10 ng/ μ l, 33 μ l reagent mix for PCR-SSP, and 1 μ l Taq polymerase were gently mixed. Of this master mix, 5 μ l were added to each primer mix, and the tubes were sealed. The cycling

program started with 2 min at 94 °C and 10 cycles with 20 sec at 94 °C and 1 min at 65 °C for targeted amplification. This was subsequently followed by 20 cycles with 20 sec at 94 °C, 1 min at 65 °C, and 30 sec at 72 °C to increase the amplified target sequence. The PCR product was analyzed in 2 % agarose gel in an electrophoresis chamber Cascade for 10 min at 275 V.

2.12 RHD Zygosity Test with qPCR

In order to test if the pregnant women are a carrier of the *RHD* gene, a test for zygosity was performed with genomic DNA from the women. This was accomplished by qPCR, which was first established in 1996 [237]. The principle of PCR was already explained in chapter 2.11. QPCR works with TaqMan chemistry (chapter 2.10). The fluorescent reporter dye change is measured after each cycle, resulting in an amplification plot (Figure 29). On the X-axis are the number of PCR cycles, and on the y-axis are the fluorescent signals, which are proportional to the target amplification. In the first cycles, the fluorescence is hardly measurable and disappears in the baseline. As the amount of the amplified product increases, the fluorescence increases proportionally and breaks the threshold, which is called C_T . After the C_T was reached, the amplification is exponentially and results in later cycles in a plateau phase [237].

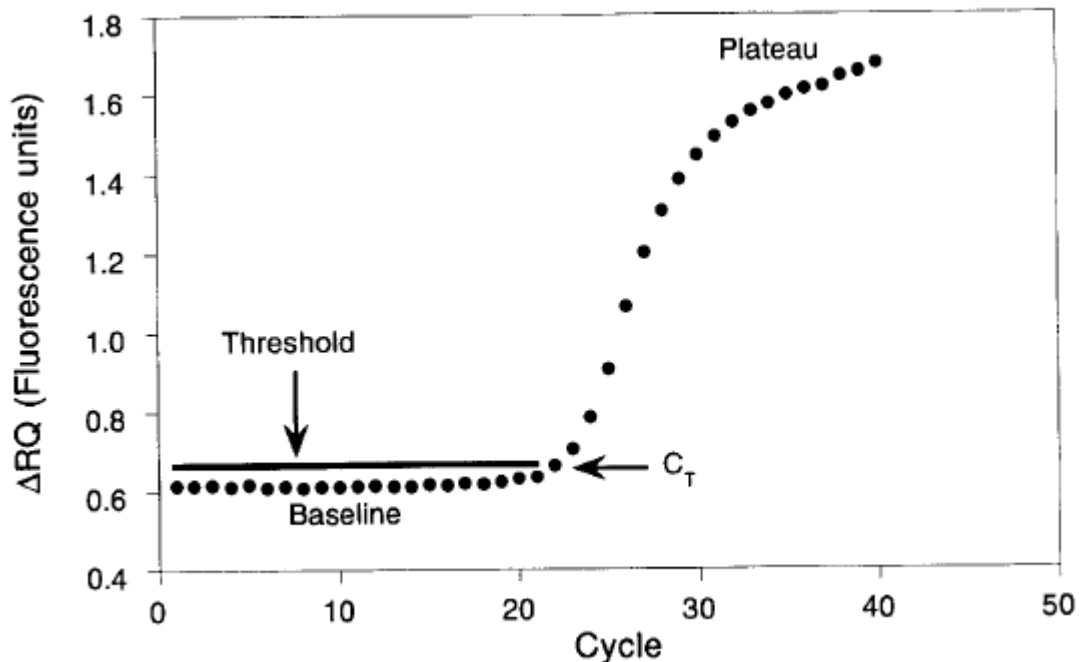


Figure 29: Amplification plot of qPCR [237].

The following protocol is, according to Krog et al. [202].

Per approach, 2 μ l DNA (10 ng/ μ l) were mixed with 0.375 μ l primer mix, 7.5 μ l master mix, and 5.125 μ l sterile water. Tubes were placed into the Light cycler with the thermal profile of 10 min at 95 °C followed by 45 cycles with 10 sec at 95 °C and 30 sec at 60 °C.

The approach for the determination of the *RHD* zygosity was first published in 2001 [238]. They used a multiplex real-time Taqman PCR with albumin as internal control. In the evaluation, they calculated the *RHD* gene's dosage by the difference between the C_T values of albumin and *RHD* [238]. Another group used GAPDH as an internal control because the gene is present in 2 copies [201]. They subtracted the C_T values ($\Delta C_T = C_T(RHD) - C_T(GAPDH)$) too, but they included in their calculations that one cycle entails the doubling of the PCR product, so the *RHD*/GAPDH ratio is $2^{-\Delta C_T}$, meaning the ratio is 1 for a homozygote

and 0.5 for a hemizygote [201]. The analysis of the zygosity in this thesis was conducted after the instructions from Li et al. from 2003.

2.13 SRY Verification with PCR

To verify the gender of the sent material of the born children, a PCR for the evidence of the SRY gene was used. The SRY gene stands for sex-determining region Y and is located on the Y-chromosome [239]. It is responsible for the development of a male phenotype [240]. The following protocol is according to Scheffer et al. [241].

Place 2.5 µl primer mix SRY-1, SRY-2, and SRY-3 in different reaction vessels. The concentration of each forward and reverse primer was 5 µM. Subsequently, 2.5 µl DNA (10 ng/µl) and 5 µl Hotstar Taq master mix were added to each reaction tube. The thermal cycling program started with 2 min at 94 °C, followed by 30 cycles with 30 sec at 94 °C, 30 sec at 60 °C, and 20 sec at 72 °C. In the last step, the amount of the amplified target sequence was increased by 2 min at 72 °C. The PCR result was analyzed in 2 % agarose gel in an electrophoresis chamber for 10 min at 275 V (Figure 30). In the samples of a female, the result should be negative, precisely the same as in water. Only in a male sample, the SRY signal is positive.

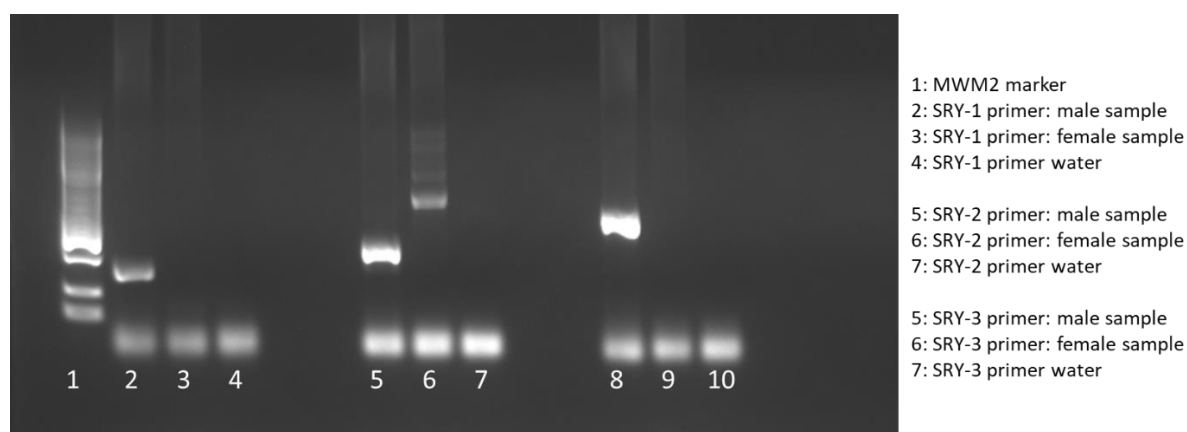


Figure 30: Result of the primer test for the SRY-PCR. The SRY-1 primer has an amplicon size of 137 bp, SRY-2 200 bp, and SRY-3 316 bp. 5 µl of the PCR product was mixed with 5 µl 2 x loading dye and analyzed in 2 % agarose gel.

2.14 Calculations for dPCR Evaluation

After dPCR, the chips were scanned for the FAM and VIC signals within the chip reader. For further analysis, the data were uploaded to the QuantStudio 3D AnalysisSuite cloud software. This software analyzes the fluorescence signals and uses Poisson distribution for statistical correction. This correction is necessary in order to consider reaction cavities, which contain more than one target molecule [242]. The QuantStudio 3D AnalysisSuite cloud software gives the analyzed results target copies per µL and target/total (%). The program calculates the data, but the calculation is explained in the following for a deeper understanding.

In principle, the calculation uses the number of VIC/FAM negative wells to calculate the target molecules' concentration. The first step is the calculation of P_0 . Here the number of filled wells (ROX positive) and wells negative for FAM or VIC were determined and calculated using formula (1).

$$(1) \quad P_0 = \frac{\# \text{ of FAM or VIC negative wells}}{\# \text{ of filled wells}}$$

In the next step, the correction factor λ is used to consider the probability of more than one target molecule in a reaction well using formula (2).

$$(2) \quad \lambda = -\ln P_0$$

For the calculation of the concentration c (copies/ μ L), formula (3) was used.

$$(3) \quad c = \frac{\lambda}{V}$$

*Reaction volume (V) of a single well on the chip is 755 pL = 7.55*10⁻⁴ μ L*

These calculations are accomplished for the FAM and VIC channel.

For the calculation of the target/total ratio, the concentration of molecules (cFAM and cVIC) are used in formula (4) for the FAM and (5) for VIC channel:

$$(4) \quad \frac{\text{target}}{\text{total}} (\%) = \frac{c_{FAM}}{c_{FAM} + c_{VIC}} * 100$$

$$(5) \quad \frac{\text{target}}{\text{total}} (\%) = \frac{c_{VIC}}{c_{FAM} + c_{VIC}} * 100$$

2.15 Calculations for the Number of Molecules After Pre-amplification PCR

After the pre-amplification, the chips were overloaded (chapter 3.1.4.3). Therefore, it made sense to determine the optimal number of molecules per chip (chapter 3.1.5). For this purpose, different amounts of molecules were loaded onto the chip in a series of experiments (n=3). The following formula was used to calculate the number of molecules:

$$\text{DNA molecules}/\mu\text{l} = \frac{(\text{ng}/\mu\text{l pre-amplification product}) * \text{Avogadro constant}}{(\text{mean bp size of PCR products}) * 660 * 10^9}$$

Avogadro constant = 6.022 \times 10²³ molecules/mol;
660 g/mol = average mass of 1 bp double-stranded DNA;
10⁹ = factor for g to ng

2.16 Simulation of Pregnancies for Technical Validation

The aim of this thesis is the identification of the blood cell antigens of a fetus. This means an investigation of two individuals. One is the mother, and the other is the unborn child. Plasma mixtures were used for all steps of protocol development and technical validation. At the beginning of the experiments, we solve fundamental challenges concerning the used plasma volume, best DNA isolation method, or suitable liquids for DNA elution. Afterward, the differentiation between the high cfDNA of the mother and the low cfDNA comes into focus.

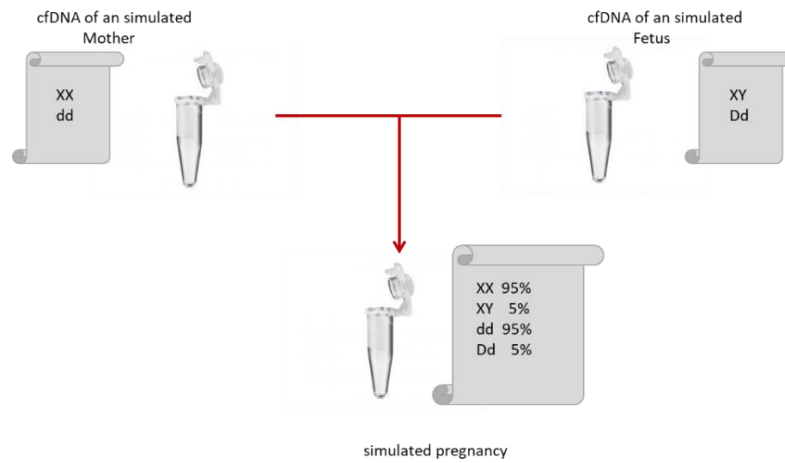


Figure 31: Scheme of the simulation of a pregnancy. Dd: heterozygous for *RHD* gene, dd: *RHD* negative, XY: male. XX: female

The use of plasma from pregnant women was excluded because the content of cell-free DNA between individuals varied. Also, the amount of cfDNA, even in the same week of gestation, varies between different women. Due to this circumstance, it was decided to simulate pregnancies (Figure 31). For the simulation of pregnancy, the plasma of healthy tested volunteers was mixed in the dilution series of heterozygous DNA (5.00 to 0.10 %) in excess of homozygous DNA (95.00 to 99,90 %). With this, a constant amount of cfDNA was expected in all experiments, which were essential for technical validation.

3 RESULTS

This section is subdivided into three subsections. The first describes the development of the protocol for the noninvasive prenatal antigen test using dPCR. In the second part, the technical validation results are presented, and in the third subsection, the first results of a clinical validation are shown.

3.1 Protocol Development for Noninvasive Prenatal Antigen Testing

This section describes the analysis, e.g., the influence of different elution buffers or plasma volume on the dPCR. Furthermore, various cfDNA isolation methods were tested and optimized to reveal a high cfDNA amount as possible. Finally, a suitable molecule density was analyzed for optimal requirements of NIPT analysis with dPCR. Figure 32 gives an overview of the analysis steps during the protocol development.

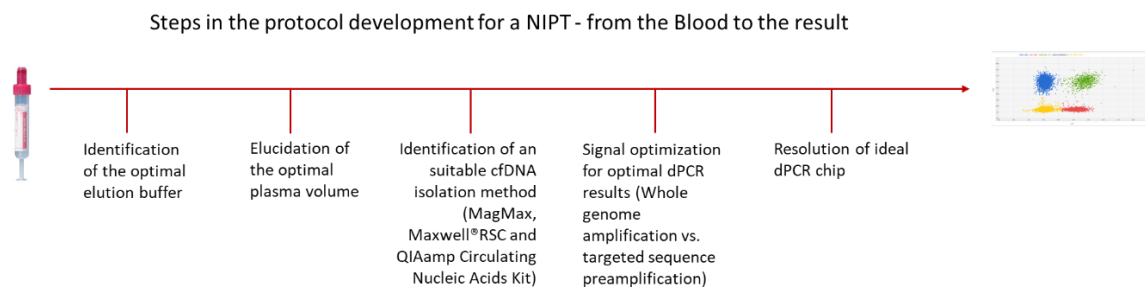


Figure 32: Steps in the protocol development for a NIPT - from the Blood to the result.

3.1.1 Influence of Different Elution Liquids on dPCR Results

In order to test the influence of the AVE buffer, which is included in the QIAamp Circulating Nucleic Acids Kit, on dPCR cell-free DNA from a female volunteer was isolated and eluted once with the AVE buffer and once with ddH₂O, respectively. The influence of the elution buffer compared to ddH₂O was tested with the AMEL-X/Y assay.

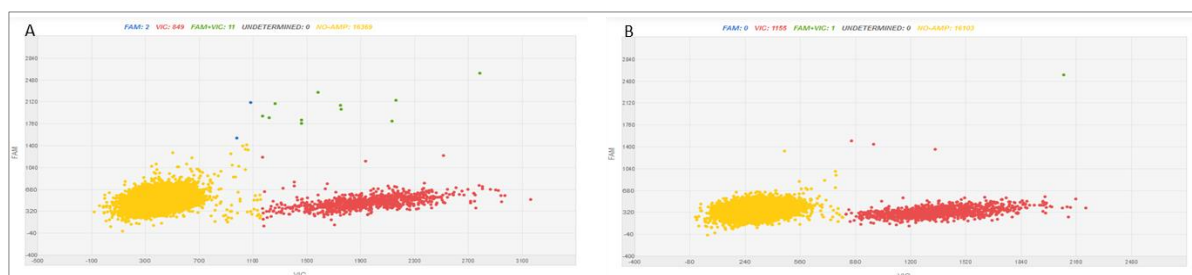


Figure 33: AVE vs. ddH₂O; A: Cell-free DNA from female volunteer eluted in AVE buffer, B: Cell-free DNA from the same female volunteer eluted in ddH₂O. Yellow dots indicated no amplification; red dots are signals of AMEL-X, blue signals of AMEL-Y, and green is the combination of AMEL-X and AMEL-Y. X-axis: VIC color distribution; Y-axis: FAM color distribution; Picture from the QuantStudio™ 3D AnalysisSuite™ Cloud Software.

In Figures 33A and B, the differences between the used elution liquids are depicted. Figure 33B shows the elution with ddH₂O. Here are two clouds visible; one in yellow indicating reaction vessels with no target DNA and one in red for the X-chromosome. The number of false-positive signals is very low compared to Figure 33A, where the cell-free DNA was eluted with the AVE buffer. Figure 33A revealed a larger scatter of false-positive signals resulting in a higher target to total ratio, as shown in table 3.

Table 3: Results of the comparison of AVE elution buffer vs. elution with ddH₂O. After isolation of the cell-free female DNA was analyzed for the false-positive signals of the Y-chromosome. Measurements were conducted in duplicates.

Sample	Target	AVE elution buffer			ddH ₂ O		
		AMEL-X copies/μl [mean ± SD]	AMEL-Y copies/μl [mean ± SD]	Target/total in % [mean ± SD]	AMEL-X copies/μl [mean ± SD]	AMEL-Y copies/μl [mean ± SD]	Target/total in % [mean ± SD]
female	AMEL-Y	64.56±3.26	0.46±0.46	0.67±0.67	93.71±1.89	0.21±0.13	0.22±0.13

The AVE eluted sample indicated a target to a total ratio of 0.67 % and 0.46 copies/μl for AMEL-Y. The target to a total percentage in the elution with ddH₂O was 0.22 %, and the variance was smaller with 0.13 compared to the AVE elution with 0.67. Additionally, it was visible that the X-specific signals were increased by one-third in the elution with ddH₂O compared to the AVE buffer (Table 3).

In summary, because of the higher signals and lower background of the samples eluted with ddH₂O, it was decided to work further on with ddH₂O.

3.1.2 Influence of Plasma Volume on dPCR Results

After the decision to use ddH₂O for the cfDNA elution, it was tested if the use of different plasma volumes shows an impact on cfDNA content resulting in different dPCR outcomes. The idea was that the cfDNA content increases with the volume of plasma. Additionally, an increase of signals was expected in dPCR due to the higher cfDNA amount.

To investigate this hypothesis, cell-free DNA was isolated out of 1, 2, and 4 ml plasma from a female donor and a male donor. In the next step, a simulated pregnancy was analyzed by mixing two individuals' plasma (chapter 2.16). For this investigation, AMEL-Y for the gender, and *RHD* exon 7 was used. In all tests, it was visible that the amount of isolated cfDNA was highest with 4 ml plasma input. The DNA content difference between 1 or 2 ml plasma lay in the range of biological variation and was nearly constant (Table 4).

Regarding the dPCR copies/μl, an increase was found parallel to the plasma volume. It was evident that all signals were increased. So the ratio between target and total cfDNA was not significantly better compared to the used plasma volume.

3 RESULTS

Table 4: Results of the influence of the plasma volume on cfDNA content and dPCR signals. All experiments were conducted in duplicates. *Only one investigation was conducted.

AMEL-X/Y						
Sample	Target	Volume [ml]	DNA [ng/ μ l]	AMEL-X copies/ μ l	AMEL-Y copies/ μ l	Target/total [%]
Female, RhD neg.	AMEL-Y	1.00	10.00	18.95 \pm 8.01	0.27 \pm 0.11	1.42 \pm 0.05
Female, RhD neg.*	AMEL-Y	2.00	5,30	47.02	0.32	0.67
Female, RhD neg.*	AMEL-Y	4.00	33.00	95.06	0.42	0.44
Male, RhD pos.	AMEL-Y	1.00	10.00	12.34 \pm 5.57	11.06 \pm 4.55	47.81 \pm 1.24
Male, RhD pos.	AMEL-Y	2.00	8,70	20.65 \pm 2.92	19.85 \pm 0.03	49.26 \pm 3.51
Male, RhD pos.*	AMEL-Y	4.00	49,30	50.69	54.04	51.60

<i>RHD</i> exon 7						
Sample	Target	Volume [ml]	DNA [ng/ μ l]	GAPDH copies/ μ l	<i>RHD</i> exon 7 copies/ μ l	Target/total [%]
Female, RhD neg.	<i>RHD</i> exon 7	1.00	3.80	17.61 \pm 2.92	0.04 \pm 0.04	0.20 \pm 0.20
Female, RhD neg.*	<i>RHD</i> exon 7	2.00	5.30	45.92	0.63	1.36
Female, RhD neg.	<i>RHD</i> exon 7	4.00	-	-	-	-
Male, RhD pos.	<i>RHD</i> exon 7	1.00	4.00	17.51 \pm 2.16	14.04 \pm 2.21	44.39 \pm 0.86
Male, RhD pos.	<i>RHD</i> exon 7	2.00	8.70	36.66 \pm 6.83	26.86 \pm 4.44	42.38 \pm 0.53
Male, RhD pos.*	<i>RHD</i> exon 7	4.00	49.30	58.80	65.87	52.853

The isolated DNA from table 4 shows the behavior of cfDNA of one person but in the investigation of a pregnant woman is a mixture of two individuals in one sample, whereby the mother's cfDNA is dominant. Therefore, the pregnancy by mixing the plasma from two donors, one was female, RhD negative, and the other male, RhD positive, was simulated. The female's content was 90 -95 %, and the male proportion was 10.00 – 5.00 % (Table 5).

Table 5: Results of the influence of the plasma volume on cfDNA content and dPCR signals in plasma mixtures. All experiments were conducted in duplicates. *Only one investigation was conducted.

Sample	Target	Mixture [%]	AMEL-X/Y				Target/total [%]
			Volume [ml]	DNA [ng/ μ l]	AMEL-X copies/ μ l	AMEL-Y signals / μ l	
Female, RhD neg., 90.00 % Male, RhD pos., 10.00 %	AMEL-X/Y	10.00	1.00	14.75	24.28 \pm 3.18	1.42 \pm 0.55	5.81 \pm 2.74
Female, RhD neg., 90.00 % Male, RhD pos., 10.00 %*	AMEL-X/Y	10.00	2.00	13.60	42.04	3.09	6.85
Female, RhD neg., 95.00 % Male, RhD pos., 5.00 %	AMEL-X/Y	5.00	1.00	21.90	31.22 \pm 6.68	2.06 \pm 1.14	5.71 \pm 2.10
Female, RhD neg., 95.00 % Male, RhD pos., 5.00 %*	AMEL-X/Y	5.00*	2.00	17.70	27.70	1.35	4.63

Sample	Target	Mixture [%]	RHD exon 7				Target/total [%]
			Volume [ml]	DNA [ng/ μ l]	GAPDH copies/ μ l	RHD exon 7 copies/ μ l	
Female, RhD neg., 90.00 % Male, RhD pos., 10.00 %	RHD exon 7	10.00	1.00	14.75	23.96 \pm 2.68	4.14 \pm 1.08	14.49 \pm 1.90
Female, RhD neg., 90.00 %* Male, RhD pos., 10.00 %	RHD exon 7	10.00	2.00	13.60	53.76	3.53	6.16
Female, RhD neg., 95.00 % Male, RhD pos., 5.00 %	RHD exon 7	5.00	1.00	21.90	22.91 \pm 2.67	1.39 \pm 0.42	5.61 \pm 1.03
Female, RhD neg., 95.00 % Male, RhD pos., 5.00 %*	RHD exon 7	5.00	2.00	17.70	27.70	1.35	4.63

It is visible that the plasma volume of isolated cfDNA was independent of the used plasma volume. Furthermore, it can be seen that the signals per μ l are not correlated to the used plasma volume. Additionally, the target to total ratio was not significantly changed with the increased plasma volume.

Due to the non-significant amount of used plasma, a suitable clinical volume of 1 ml was used for further analysis.

3.1.3 Investigation of Different Cell-Free DNA Isolation Methods

After the optimal plasma volume was defined, different methods for the isolation of cell-free DNA was investigated. The various techniques were manual isolation with magnet beads (MagMax, ThermoFisher), column-based manual isolation (QIAmp Circulating Nucleic Acids Kit, Qiagen), and automatic isolation with magnetic beads from Promega (Maxwell[®]RSC, Promega). Every single method is shown in the following.

For this analysis, cell-free DNA from 1 ml plasma was isolated, and 7.10 μ l from the isolated DNA was added to the dPCR chip. The analyzed assays were AMEL-Y and RHD exon 7.

3.1.3.1 Manuel Isolation with MagMax Kit

CfDNA was isolated after the manufacturer's instructions (chapter 2.7.2.1). The cfDNA was analyzed for gender- and RHD status. The amount of isolated cfDNA varied widely from 0.60 – 8.95 ng/ μ l (Table 6). A dPCR analysis of a female sample revealed 0.29 copies/ μ l of AMEL-X and 0.07 copies/ μ l for AMEL-Y, and a ratio of 20.00 % was calculated. The male specimen indicated no signals neither for the X-chromosome nor for the Y-chromosome.

Table 6: Results of the manual cfDNA isolation with MagMax for AMEL-X/Y.

AMEL-X/Y					
Sample	Target	cfDNA [ng/ μ l]	AMEL-X copies / μ l	AMEL-Y copies / μ l	Target/total [%]
Female	AMEL-X	0.60	0.29	0.07	20.00
Male	AMEL-Y	8.95	No signal	No signal	0.00

In Figure 34, an example of the dot plot from the dPCR regarding the X-chromosome is depicted. Most of the reaction vessels contained no amplified target cfDNA (yellow). There are only three red spots for the X-chromosome and one green dot for the X- and Y-chromosome.

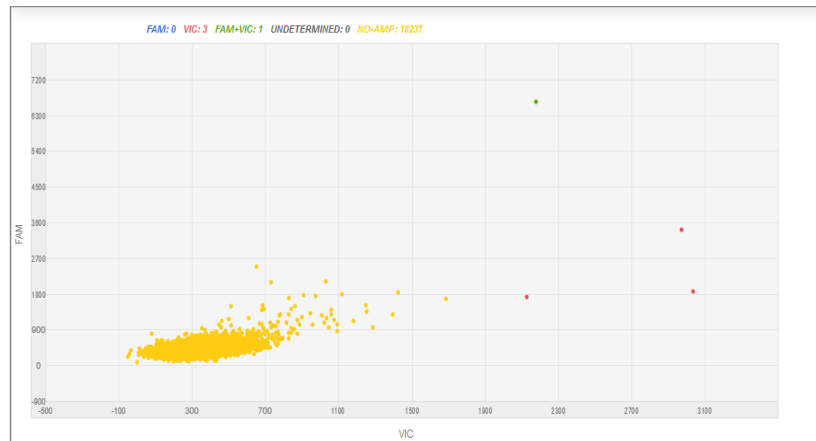


Figure 34: CfDNA isolation with the MagMax. Yellow dots indicated no amplification. red dots are signals of AMEL-X, blue signals of AMEL-Y, and green is the combination of AMEL-X and AMEL-Y. X-axis: VIC color distribution; Y-axis: FAM color distribution; Picture from the QuantStudio™ 3D AnalysisSuite™ Cloud Software.

Further tests concentrated on the identification of the *RHD* status. For the RhD negative sample, no signals were received. Not even a signal from the internal control GAPDH was recognized. The RhD positive specimen indicated 0.12 copies/ μ l for the internal control and 0.16 copies/ μ l for *RHD* exon 7. In general, the target to total ratio was 55.00 % (Table 7).

Table 7: Results of the manual cfDNA isolation with MagMax for *RHD* exon 7.

<i>RHD</i> exon 7					
Sample	Target	cfDNA [ng/ μ l]	GAPDH copies/ μ l	<i>RHD</i> exon 7 copies/ μ l	Target/total [%]
RhD negative	<i>RHD</i> exon 7	0.60	no signal	no signal	0
RhD positive	<i>RHD</i> exon 7	8.95	0.12	0.16	55.00

Figure 35 shows the result of a dPCR after the cfDNA isolation with MagMax. The sample was RhD positive, but no signals for the internal control GAPDH were detected. There are reactions in which the *RHD* and internal control were present (green) and only one signal for the *RHD gene* (blue).

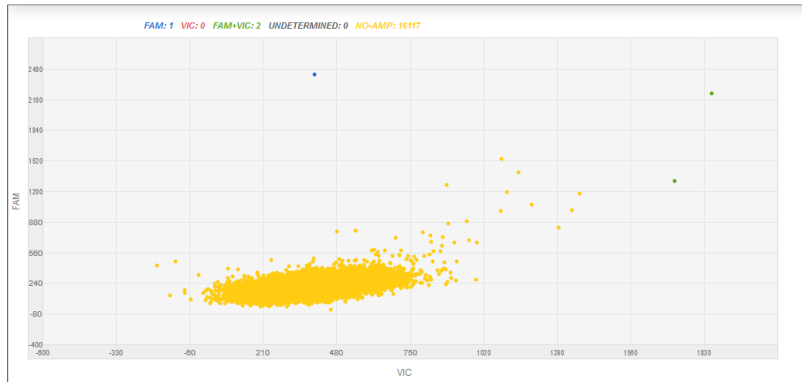


Figure 35: CfDNA isolation with the MagMax from an RhD positive sample. Yellow dots indicated no amplification; red dots are signals of GAPDH, blue signals of *RHD exon 7*, and green is the combination of *RHD exon 7* and GAPDH. X-axis: VIC color distribution; Y-axis: FAM color distribution; Picture from the QuantStudio™ 3D AnalysisSuite™ Cloud Software.

Due to the lack of signals with the manual cfDNA isolation, the MagMax was ruled out for further applications.

3.1.3.2 Automated Isolation with Maxwell®RSC

The Maxwell®RSC is an automated device for the isolation from cfDNA using magnetic beads. One significant advance of automated isolation is that every extraction is always done in the same way, which reduces the probability of contamination and handling mistakes.

The amount of isolated cfDNA was around 0.70 ng/μl. Only a female sample was investigated and an RhD negative sample because the results give enough insight if further experiments are useful. The dPCR results revealed for the female specimen 2.77 copies/μl for the AMEL-X and 0.08 copies/μl for the AMEL-Y, which results in a target and total ratio of 2.70 % (Table 8).

Table 8: Results of the automated cfDNA isolation with Maxwell®RSC analyzed for AMEL-Y marker.

Sample	Target	AMEL-XY			Target/total [%]
		cfDNA [ng/μl]	AMEL-X copies/μl	AMEL-Y copies/μl	
Female	AMEL-Y	0.70	2.77	0.08	2.70

Figure 36 indicates the result of a female sample after cfDNA isolation with the Maxwell®RSC device. The number of vessels containing no DNA is shown in yellow. In red, the reaction wells with a positive amplification of the X-chromosomal marker AMEL-X is indicated. One signal was detected regarding the Y-chromosomal marker (blue).

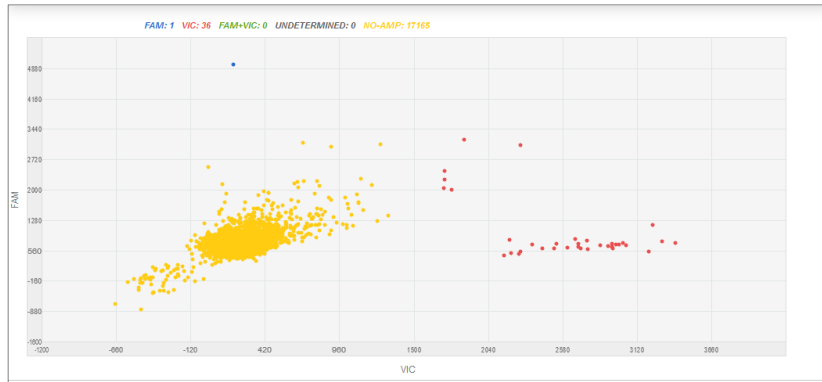


Figure 36: CfDNA isolation with the Maxwell®RSC from a female sample. Yellow dots indicated no amplification; red dots are signals of AMEL-X, blue signals of AMEL-Y, and green is the combination of AMEL-X and AMEL-Y. X-axis: VIC color distribution; Y-axis: FAM color distribution; Picture from the QuantStudio™ 3D AnalysisSuite™ Cloud Software.

Table 9: Results of the automated cfDNA isolation with Maxwell®RSC for *RHD* exon 7.

Sample	Target	<i>RHD</i> exon 7			Target/total [%]
		cfDNA [ng/μl]	GAPDH copies/μl	<i>RHD</i> exon 7 copies/μl	
<i>RHD</i> negative	<i>RHD</i> exon 7	0.70	1.78	0.47	20.68

The dPCR analysis with an RhD negative sample indicated 1.78 copies/μl for the internal control GAPDH and 0.47 copies/μl for the *RHD* exon 7, leading to a 20.68 % ratio for the negative sample (Table 9).

Figure 37 shows one example of the dPCR results after Maxwell®RSC isolation, visualized in a dot plot diagram after dPCR. The sample was RhD negative. The internal control GAPDH is identifiable, and a few signals from cavities containing internal control and *RHD* exon 7 signal.

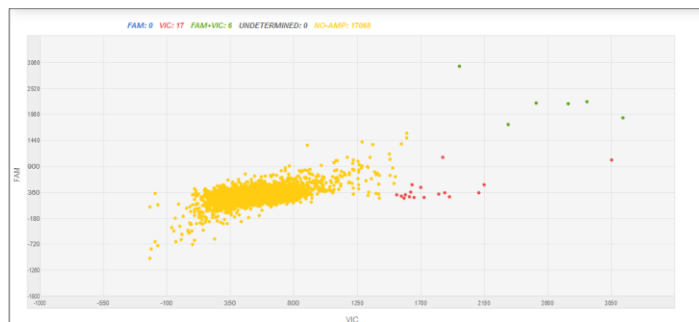


Figure 37: CfDNA isolation with Maxwell®RSC from an RhD negative sample. Yellow dots indicated no amplification; red dots are signals of GAPDH, blue signals of *RHD* exon 7, and green is the combination of *RHD* exon 7 and GAPDH. X-axis: VIC color distribution; Y-axis: FAM color distribution; Picture from the QuantStudio™ 3D AnalysisSuite™ Cloud Software.

In conclusion, the Maxwell®RSC device is an excellent opportunity to isolate cfDNA. However, there are some optimization steps necessary to receive satisfactory results. Because the number of copies/μl signals after dPCR is very low. Under realistic circumstances, e.g., in early pregnancy, this method will not meet our expectations. In order to decide whether the device is suitable, the signal quantity would have to be amplified.

3.1.3.3 Manual Isolation with QIAmp Circulating Nucleic Acids Kit

Besides the MagMax Kit, the QIAmp Circulating Nucleic Acids Kit was tested. This Kit works with a silica membrane instead of magnetic beads. One drawback is that this isolation is manual, which increases the error of handling and contamination.

The cfDNA measurement after isolation indicated a cfDNA content between 3.30-4.40 ng/ μ l. Showing a very stable DNA content, and the cfDNA quality was consistently good (Table 10).

Table 10: Results of the automated cfDNA isolation with QIAmp Circulating Nucleic Acids Kit analyzed for AMEL-X/Y marker.

Sample	Target	AMEL-X/Y			
		cfDNA [ng/ μ l]	AMEL-X copies/ μ l	AMEL-Y copies/ μ l	Target/total [%]
Female	AMEL-Y	3.30	24.04	0.25	1.03
Male	AMEL-Y	4.40	12.08	12.89	51.61

With this isolated cfDNA, the analysis of the gender was performed. The first sample was from a female and was detected with 24.04 copies/ μ l for AMEL-X and only 0.25 copies/ μ l for AMEL-Y. The result was a ratio of 1.03 % target to total and still has a high false-positive signal. The male sample analysis indicated 12.08 copies/ μ l for AMEL-X and 12.89 copies/ μ l for the Y-chromosome, resulting in a ratio of 51.61 % (Table10).

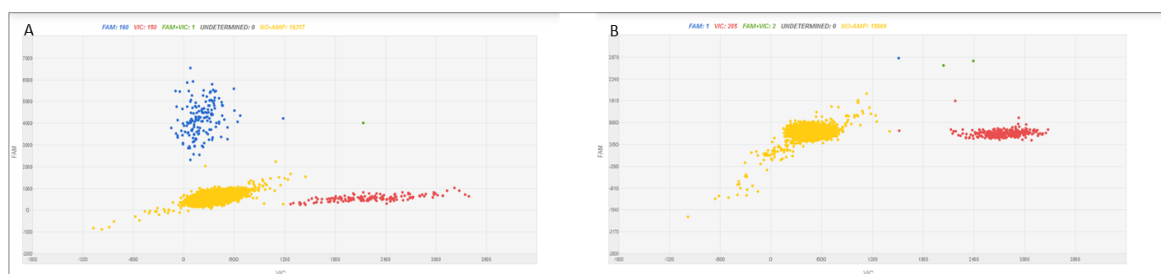


Figure 38: CfDNA isolation with the QIAmp Circulating Nucleic Acids Kit. A: dPCR with a male sample B: dPCR with a female sample. Yellow dots indicated no amplification. red dots are signals of AMEL-X, blue signals of AMEL-Y, and green is the combination of AMEL-X and AMEL-Y. X-axis: VIC color distribution; Y-axis: FAM color distribution; Picture from the QuantStudio™ 3D AnalysisSuite™ Cloud Software.

After a successful dPCR, the dot plot visualizes the results per reaction well. Figure 38A shows a male sample indicated by a balanced ratio of the signals from AMEL-X and AMEL-Y. The absence of the Y-chromosomal signal (blue) indicates the female specimen in Figure 38B. The red dots indicate the AMEL-X in both experiments.

In a second experiment, the rhesus status was tested. The results from the RhD negative individual were indicated by 0.00 copies/ μ l for *RHD* exon 7 and the internal control was detected with 15.37 copies/ μ l. In the case of a RhD positive sample, the internal control and the *RHD* exon 7 signals were equally amplified, with 19.67 copies/ μ l and 16.25 copies/ μ l, respectively (Table 11).

Table 11: Results of the manual cfDNA isolation with QIAmp Circulating Nucleic Acids Kit for *RHD* exon 7.

Sample	Target	<i>RHD</i> exon 7			
		cfDNA [ng/ μ l]	GAPDH copies/ μ l	<i>RHD</i> exon 7 copies/ μ l	Target/total [%]
RhD negative	<i>RHD</i> exon 7	3.30	15.37	0.00	0.00
RhD positive	<i>RHD</i> exon 7	4.40	19.67	16.25	45.26

The visual result of an RhD positive sample in dPCR is depicted in Figure 39. Directly after the cfDNA isolation with the QIAmp Circulating Nucleic Acids Kit, 7.1 µl were used for the dPCR. The result indicated an even amplification of the internal control GAPDH and *RHD* exon 7. This is consistent with the results shown in table 11.

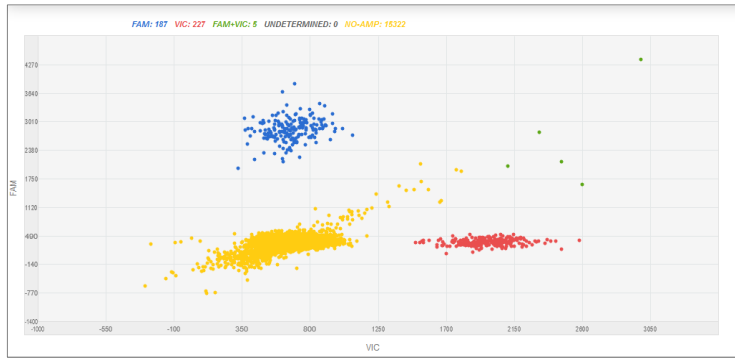


Figure 39: CfDNA isolation with the QIAmp Circulating Nucleic Acids Kit from an RhD positive sample. Yellow dots indicated no amplification; red dots are signals of GAPDH, blue signals of *RHD* exon 7, and green is the combination of *RHD* exon 7 and GAPDH. X-axis: VIC color distribution; Y-axis: FAM color distribution; Picture from the QuantStudio™ 3D AnalysisSuite™ Cloud Software.

In summary, the results with the cfDNA isolation using the QIAmp Circulating Nucleic Acid Kit revealed very confident results. In all tested samples, it was possible to identify the gender or the rhesus gene. But it is to mention that all these samples are from one person. In a pregnancy, there is a mixture of the mother's and child's cfDNA at which the fetus's cfDNA is the minor part. Thus, an increase in the signal intensity to identify little traces of cffDNA is recommended.

3.1.4 Signal Amplification Using Different PCR Methods

In order to increase the signal intensity, different amplification methods were tested. First, the whole genome amplification was tried, and later a targeted DNA amplification was analyzed.

3.1.4.1. Whole Genome Amplification Using the REPLI-g Mini Kit

The REPLI-g Kit is used for purified DNA and is used for a uniform amplification of the whole DNA. The samples were tested for the gender and rhesus gene. Additionally, the isolated cfDNA was tested before and after purification after the amplification. After cfDNA isolation with the QIAmp Circulating Nucleic Acids Kit, a range of around 5.00ng/µl was revealed. After the amplification with the REPLI-g Kit, we measured 499.90 ng/µl. The cfDNA content dropped after purification to 57.30 ng/µl (Table 12).

Table 12: Results of the whole genome amplification with the REPLI-g Kit. The first row is amplified cfDNA. In the second row was the cfDNA purified after amplification. In digital PCR, the gender chromosomes were targeted.

Sample	Treatment	Target	REPLI-g Kit			Target/total [%]
			cfDNA [ng/µl]	AMEL-X copies/µl	AMEL-Y copies/µl	
Male	Amplified + unpurified	AMEL-X/Y	499.90	3.45	3.45	50.00
Male	Amplified + purified	AMEL-X/Y	57.30	0.72	0.24	25.00

The dPCR analysis of a male sample indicated for the unpurified cfDNA an even distribution of the AMEL-X/Y signals (Figure 40A). The purified DNA sample in Figure 40B showed only 0.72 copies/µl for AMEL-X and 0.25 copies/µl for AMEL-Y resulting in a ratio of 25.00 %. The visual investigation revealed an separation of the signals in Figure 40A. The purified DNA revealed after the dPCR just a few signs. Additionally, the signal number was below the amount of the unpurified sample.

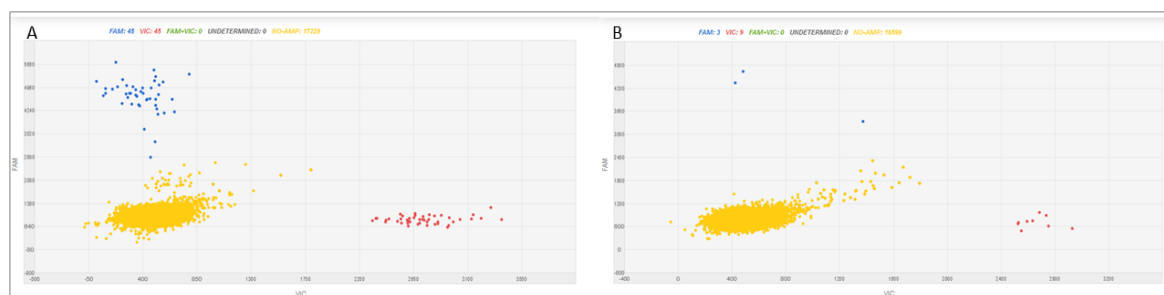


Figure 40: Male Sample isolated with QIAmp Circulating Nucleic Acids Kit and a whole genome amplification with REPLI-g Kit. A: Amplified cfDNA was directly added to dPCR. Signals from the AMEL-X and -Y are identifiable. B: Amplified cfDNA was purified, and subsequently, the dPCR was conducted. A substantial reduction of the AMEL-X- and -Y signals was visible. Yellow dots indicated no amplification; red dots are signals of AMEL-X, blue signals of AMEL-Y, and green is the combination of AMEL-Y and AMEL-X. X-axis: VIC color distribution; Y-axis: FAM color distribution; Picture from the QuantStudio™ 3D AnalysisSuite™ Cloud Software.

In another experiment, it was investigated if the *RHD* signal increase after whole genome amplification. Table 13 shows that the unpurified cfDNA revealed for *RHD* exon 7 2926.26 copies/ μ l but only 12.09 copies/ μ l of the internal control GAPDH. After purification, the *RHD* exon 7 signal decreased to 766.80 copies/ μ l, but the internal control was reduced to 3.03 copies/ μ l. Overall, the ratio between *RHD* exon 7 and GAPDH was in both experiments, around 99.00 %.

Table 13: Results of the whole genome amplification with the REPLI-g Kit. The first row is amplified cfDNA. In the second row was the cfDNA purified after amplification. In digital PCR, the rhesus gene was targeted, and an internal control GAPDH was included.

Sample	Treatment	Target	REPLI-g Kit			
			cfDNA [ng/ μ l]	GAPDH copies/ μ l	<i>RHD</i> exon 7 copies/ μ l	Target/total [%]
<i>Rhd</i> positive,	Amplified unpurified	+ <i>RHD</i> exon 7	499.90	12.09	2926.29	99.59
<i>Rhd</i> positive,	Amplified purified	+ <i>RHD</i> exon 7	57.30	3.03	766.80	99.61

In Figure 41, the results of the purified and unpurified cfDNA after dPCR are depicted. A strong *RHD* signal is identifiable (blue signals), but the internal control in red is very weak.

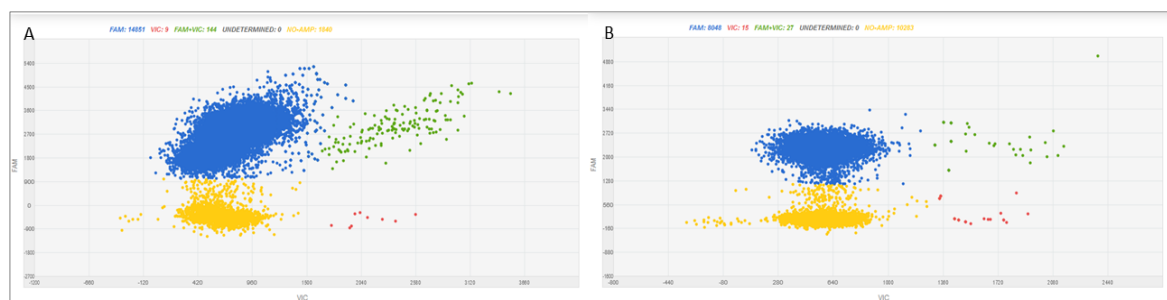


Figure 41: Rhesus positive sample isolated with Qiagen and a whole genome amplification with REPLI-g Kit. A: Amplified cfDNA was directly added to dPCR. Signals from the *RHD* exon 7 were clearly visible. The signal from the internal control just a few signals. B: Amplified cfDNA was purified, and subsequently, the dPCR was conducted. The *RHD* exon 7 signals are strongly represented, while the internal control shows a low amount of signals. Yellow dots indicated no amplification; red dots are signals of GAPDH, blue signals of *RHD* exon 7, and green is the combination of *RHD* exon 7 and GAPDH. X-axis: VIC color distribution; Y-axis: FAM color distribution; Picture from the QuantStudio™ 3D AnalysisSuite™ Cloud Software.

All the used samples are still from a single person. In order to test the applicability of the REPLI-g Kit to identify the *RHD* status or the gender of a fetus, a pregnancy was simulated (chapter 2.16).

Table 14: Results of the whole genome amplification compared with non-amplified cfDNA. All samples are a simulated pregnancy containing 5.00 % male plasma and 95.00 % female plasma.

No.	Sample content	Treatment	REPLI-g Kit				Target/total [%]
			Target	cfDNA [ng/μl]	AMEL-X copies/μl	AMEL-Y copies/μl	
1	95.00 % female, 5.00 % male	untreated	AMEL-X/Y	12.00	97.86	16.80	14.65
2	95.00 % female, 5.00 % male	REPLI-g amplified.	AMEL-X/Y	448.70	24.04	0.99	3.96
3	95.00 % female, 5.00 % male	REPLI-g amplified and purified	AMEL-X/Y	44.60	7.12	0.38	5.04

Table 14 shows the simulated pregnancy results with a 5.00 % male and 95.00 % female proportion. This sample was first isolated, as explained in chapter 2.7.2.3. After isolation, one part was used immediately for dPCR. Another portion was used for the whole genome amplification with the REPLI-g Kit. After amplification, one portion was used for dPCR, and the other was purified and then used for dPCR.

The cfDNA content after isolation was 12.00 ng/μl. After the amplification, the content was 448.70 ng/μl and was reduced after purification to 44.60 ng/μl. The gender analysis for AMEL-X indicated for the untreated sample 97.86 copies/μl and AMEL-Y for 16.80 copies/μl, resulting in a ratio of 14.64 %. The sample 2 showed AMEL-X for 24.04 copies/μl and for AMEL-Y 0.99 copies/μl, which gives a ratio of 3.96 % after amplification. The last sample, was purified after using the REPLI-g Kit, and revealed 7.12 copies/μl for AMEL-X and 0.38 copies/μl for AMEL-Y revealing a ratio of 5.04 %.

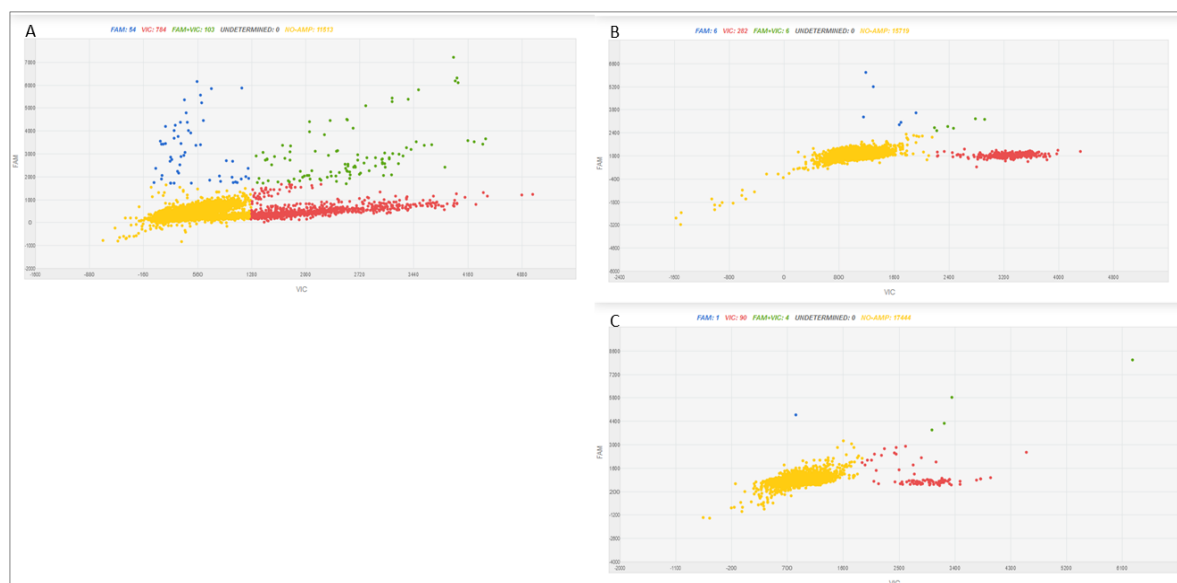


Figure 42: Visual analysis of the whole genome amplification REPLI-g Kit compared with non-amplified cfDNA. The used samples are a simulated pregnancy containing 5.00 % male plasma and 95.00 % female plasma. A: The sample was analyzed after isolation with the QIAmp Circulating Nucleic Acids Kit. B: The specimen was amplified with the REPLI-g Kit after isolation but not purified before dPCR. C: The sample was amplified with the REPLI-g Kit and purified before dPCR. Yellow dots indicated no amplification; red dots are signals of AMEL-X, blue signals of AMEL-Y, and green is the combination of AMEL-X and AMEL-Y. X-axis: VIC color distribution; Y-axis: FAM color distribution; Picture from the QuantStudio™ 3D AnalysisSuite™ Cloud Software.

The visual analysis of the dPCR results in Figure 42A revealed a high number of signals for the untreated sample and reflected the results from table 14. After the whole genome amplification, the signal intensity decreased. The AMEL-X signs are identifiable, but just a few AMEL-Y signals are visible (Figure 42B). After purification of the amplified sample, the signal intensity dropped again, and only a few AMEL-X and AMEL-Y signals were visible (Figure 42C).

Table 15: Results of the whole genome amplification compared with non-amplified cfDNA. All samples are a simulated pregnancy containing 5.00 % of RhD positive plasma and 95.00 % RhD negative plasma. This sample was tested after isolation and after amplification with the REPLI-g Kit without purification and after REPLI-g Kit amplification and purification.

No.	Sample content	Treatment	REPLI-g Kit				
			Target	cfDNA [ng/μl]	GAPDH copies/μl	<i>RHD</i> exon 7 copies/μl	Target/total [%]
4	95.00 % RhD neg., 5.00 % RhD pos.	untreated	RHD exon 7	12.00	121.27	9.24	7.08
5	95.00 % RhD neg., 5.00 % RhD pos.	REPLI-g amplified.	RHD exon 7	448.70	3321.29	4.00	0.12
6	95.00 % RhD neg., 5.00 % RhD pos.	REPLI -g amplified and purified	RHD exon 7	44.60	2138.35	1.42	0.07

The experiment was repeated to test the meaningfulness about the *RHD* status of a possible fetus. Sample 4 was used directly after isolation and indicated 121.26 copies/μl of the internal control and 9.24 copies/μl for *RHD* exon 7 resulting in a ratio of 7.08 %. After isolation, one part was used for whole genome amplification with REPLI-g Kit and revealed 3321.29 copies/μl for GAPDH and 4.00 copies/μl *RHD* exon 7, indicating a target to total of 0.12 %. Sample number 6 was purified after amplification, and signals from GAPDH were around 2138.35 copies/μl, *RHD* exon 7 signals were at 1.42 copies/μl, and the resulting ratio was 0.07 % (Table 15).

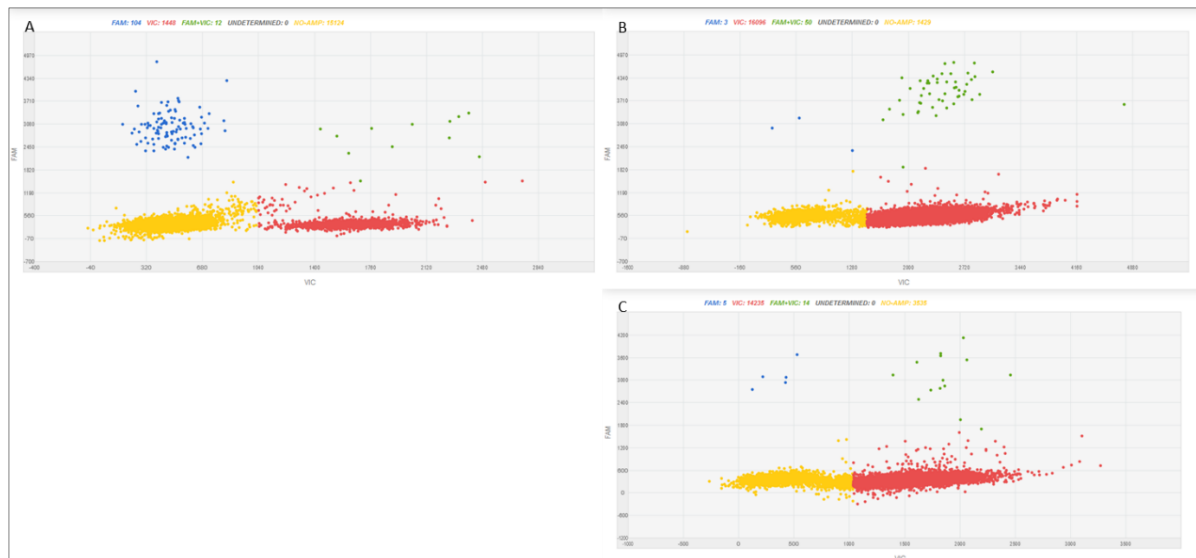


Figure 43: Visual analysis of the whole genome amplification compared with non-amplified cfDNA. The used samples of a simulated pregnancy containing 5.00 % of RhD positive plasma and 95.00 % RhD negative plasma. A: Sample 4 was analyzed after isolation with the QIAmp Circulating Nucleic Acids Kit. B: Sample 5 was amplified with the REPLI-g Kit after isolation but not purified. C: Sample 6 was amplified with the REPLI-g Kit and purified. Yellow dots indicated no amplification; red dots are signals of GAPDH, blue signals of RHD exon 7, and green is the combination of RHD exon 7 and GAPDH. X-axis: VIC color distribution; Y-axis: FAM color distribution; Picture from the QuantStudio™ 3D AnalysisSuite™ Cloud Software.

The dot plot from the results of the dPCR indicated for the used sample 4 right after the isolation a good separated red cloud indicating the internal control GAPDH and a blue cloud showing the signals for the *RHD* exon 7. A few signs from cavities containing both targets are displayed in green (Figure 43A). After amplification with the REPLI-g kit, indicated the signals a strong signal of the internal control (red), a few *RHD* exon 7 signals in blue, and a clear visible cloud of green signals indicating both targets' presence in one reaction compartment (Figure 43B). The last sample was purified after amplification and showed in Figure 43C a good signal in the red channel and only minor signals in the green or blue channel.

The results for the analysis containing two individuals were not satisfying. The REPLI-g Kit concentrates on the amplification more on the longer DNA fragments, and the short, mostly fetal fragments, are not considered. Therefore, another WGA kit was tested, which amplified shorter and strongly fractionated DNA.

3.1.4.2. Whole Genome Amplification Using the REPLI-g FFPE Kit

Besides the REPLI-g Kit, a second Kit for whole genome amplification called REPLI-g FFPE Tissue Kit was tested. This kit is specialized for strong fragmented DNA. Fetal cell-free DNA is regularly degraded with a size between 145-201 bp [141]. Therefore, with this kit, short fragments should be amplified, which was not the case with the REPLI kit.

After cfDNA amplification, the amount was around 1793.90 ng/μl, which was reduced after purification to 128.90 ng/μl.

3 RESULTS

Table 16: Results of the whole genome amplification with the REPLI-g FFPE Tissue Kit. The first row is amplified cfDNA. In the second row is cfDNA, which was purified after amplification. In digital PCR, the gender chromosomes were targeted.

REPLI-g FFPE Tissue Kit							
No.	Sample content	Treatment	Target	cfDNA [ng/μl]	AMEL-X copies/μl	AMEL-Y copies/μl	Target/total [%]
7	Male	Unpurified	AMEL-X/Y	1793.90	882.48	415.02	31.99
8	Male	Purified	AMEL-X/Y	128.90	72.31	31.53	30.36

A male amplified sample revealed after dPCR 882.48 copies/μl for AMEL-X and 415.02 copies/μl for AMEL-Y, resulting in a target to total ratio of 31.99 %. The purified cfDNA indicated for AMEL-X 72.31 copies/μl and for AMEL-Y 31.53 copies/μl, resulting in a ratio of 30.36 %.

The dot plot from the dPCR results displayed strong signals for AMEL-X and AMEL-Y. In the unpurified cfDNA sample 7, many reaction vessels contained both target sequences (green) (Figure 44A). After purification, the results from table 16 are reflected in Figure 44B. The signals from the AMEL-Y (blue) and the AMEL-X (red) are visible in a view reaction cavities containing both targeted sequences (green).

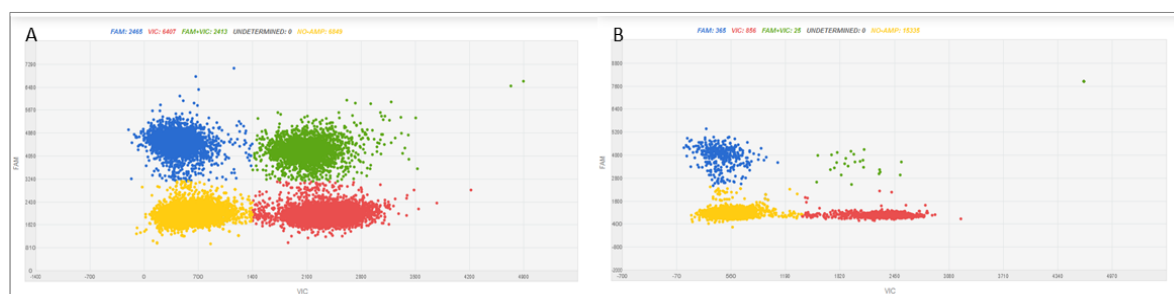


Figure 44: A male sample was isolated with QIAmp Circulating Nucleic Acids Kit and a whole genome amplification with REPLI-g FFPE Kit was conducted. A: Amplified cfDNA was directly added to dPCR. There is an even amplification of AMEL-X- and AMEL-Y visible. B: The amplified DNA was purified before dPCR. This leads to a loss of signals, but the amplification of AMEL-X-and AMEL-Y is visible. Yellow dots indicated no amplification. red dots are signals of AMEL-X, blue signals of AMEL-Y, and green is the combination of AMEL-X and AMEL-Y. X-axis: VIC color distribution; Y-axis: FAM color distribution; Picture from the QuantStudio™ 3D AnalysisSuite™ Cloud Software.

Additionally, the REPLI-g FFPE Tissue Kit was tested for *RHD* exon 7. The used sample was from an RhD positive person. The unpurified cfDNA indicated 4768.10 copies/μl for the internal control GAPDH and 6279.46 copies/μl for *RHD* exon 7, resulting in a target to total ratio of 56.84 %. The purified DNA indicated an even distribution between internal control and *RHD* exon 7 signals (Table 17).

Table 17: Results of the whole genome amplification with the REPLI-g FFPE Tissue Kit. The first row is amplified cfDNA. In the second row was the cfDNA purified after amplification. In digital PCR, the rhesus gene was targeted, and as internal control, GAPDH was included.

REPLI-g FFPE Tissue Kit							
No	Sample content	Treatment	Target	cfDNA [ng/μl]	GAPDH copies/μl	<i>RHD</i> exon 7 copies/μl	Target/total [%]
9	RhD positive	Unpurified	<i>RHD</i> exon 7	1793.90	4768.10	6279.46	56.84
10	RhD positive	Purified	<i>RHD</i> exon 7	128.90	1374.74	1310.48	48.80

The visual analysis of the dPCR results from the unpurified cfDNA indicated a huge amount of cavities containing both targets (green) (Figure 45A), indicating an overloaded chip. The

purified cfDNA revealed robust and evenly distributed signals in all color channels, reflecting the findings in table 17 (Figure 45B).

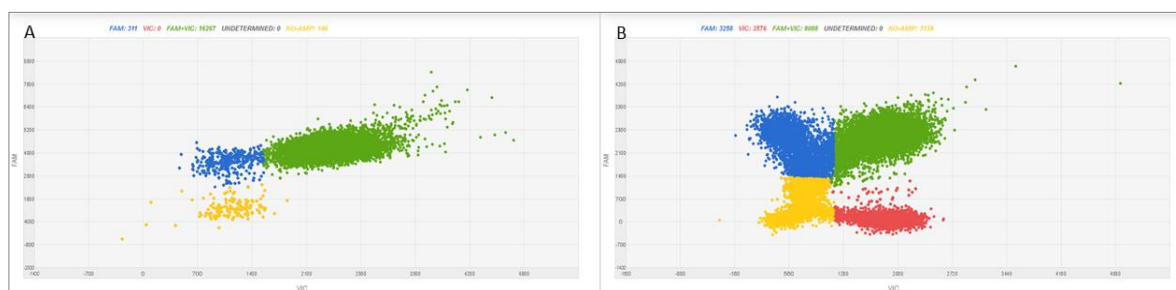


Figure 45: Rhesus positive sample was isolated with QIAmp Circulating Nucleic Acids Kit and a whole genome amplification with REPLI-g was conducted. A: Amplified cfDNA was directly added to dPCR. Most of the reaction cavities contained both targeted genes. Only a few compartments showed the *RHD* exon 7 signals. B: Amplified cfDNA was purified, and subsequently, the dPCR was conducted. The signal for the internal control and *RHD* exon 7 is equal. There were also a lot of reaction cavities, which contained both targeted sequences. Yellow dots indicated no amplification; red dots are signals of GAPDH, blue signals of *RHD* exon 7, and green is the combination of *RHD* exon 7 and GAPDH. X-axis: VIC color distribution; Y-axis: FAM color distribution; Picture from the QuantStudio™ 3D AnalysisSuite™ Cloud Software.

As for the REPLI-g Mini Kit in chapter 3.1.4.1, the REPLI-g FFPE Kit amplification was tested in a simulated pregnancy with a just isolated sample. In the next step, the specimen was amplified with the REPLI-g FFPE Kit, and a dPCR was carried out. Finally, the product of the amplification was purified before dPCR.

Table 18: Results of the whole genome amplification compared with non-amplified cfDNA. All samples are a simulated pregnancy containing 5.00 % male plasma and 95.00 % female plasma. This sample was tested after isolation and after amplification with the REPLI-g FFPE Kit without purification and after REPLI-g FFPE Kit amplification and purification.

No.	Sample content	Treatment	REPLI-g FFPE Kit				
			Target	cfDNA [ng/μl]	AMEL-X copies/μl	AMEL-Y copies/μl	Target/total [%]
11	95.00 % female, 5.00 % male	untreated	AMEL-X/Y	12.00	97.86	16.80	14.65
12	95.00 % female, 5.00 % male	FFPE Tissue Kit amplified	AMEL-X/Y	2163.70	3713.06	12.95	0.35
13	95.00 % female, 5.00 % male	FFPE Tissue Kit amplified+purified	AMEL-X/Y	179.70	3056.16	3.19	0.10

The cfDNA content after isolation was 12.00 ng/μl. After the amplification with the REPLI-g FFPE Tissue Kit, the amount was 2163.07 ng/μl, and after the purification process, there were only 179.70 ng/μl. The first sample in table 18 with number 11 was used for dPCR analysis right after isolation and showed 97.86 copies/μl for AMEL-X and 16.80 copies/μl for AMEL-Y, resulting in a ratio of 14.65 %. After the amplification with the REPLI-g FFPE Tissue Kit, the AMEL-X signals were 3713.06 copies/μl and 12.95 copies/μl for AMEL-Y resulting in a target to total ratio of 0.35 %. Finally, the amplified specimen was purified and indicated for AMEL-X 3056.16 copies/μl and 3.18 copies/μl for AMEL-Y resulting in a ratio of 0.10 %.



Figure 46: Visual analysis of the whole genome amplification compared with non-amplified cfDNA. All samples are a simulated pregnancy containing 5.00 % male plasma and 95.00 % female plasma. A: Sample 11 was analyzed after isolation with the QIAmp Circulating Nucleic Acids Kit. B: Sample 12 was amplified with the REPLI-g FFPE Kit after isolation but not purified. C: Sample 13 was amplified with the REPLI-g FFPE Kit and purified. Yellow dots indicated no amplification. red dots are signals of AMEL-X, blue signals of AMEL-Y, and green is the combination of AMEL-X and AMEL-Y. X-axis: VIC color distribution; Y-axis: FAM color distribution; Picture from the QuantStudio™ 3D AnalysisSuite™ Cloud Software.

The results of the dPCR using the REPLI-g FFPE kit are depicted in Figure 46. The sample in Figure 46A, was just isolated and the dPCR results, indicated a lot signals in the red channel for AMEL-X. In blue, the signals from the AMEL-Y were clearly visible, and even a cloud that contained both targets in one reaction cavity. The dPCR after the genome amplification with the REPLI-g FFPE kit indicated a strong red cloud and an excellent identifiable green cloud. However, there are only a few signals in the blue channel (Figure 46B). The amplified and purified specimen in Figure 46C showed a clear cloud for AMEL-X and a clear visible cloud in the green channel. As for the amplified sample, the purified sample also shows just a few blue channel signals.

Table 19: Results of the whole genome amplification compared with non-amplified cfDNA. All samples are a simulated pregnancy containing 5.00 % of RhD positive plasma and 95.00 % RhD negative plasma. This sample was tested after isolation and after amplification with the REPLI-g FFPE Kit without purification and after REPLI-g FFPE Kit amplification and purification.

No.	Sample content	Treatment	Target	REPLI-g FFPE Kit			
				cfDNA [ng/μl]	GAPDH copies/μl	<i>RHD</i> exon 7 copies/μl	Target/total [%]
14	95.00 % RhD neg., 5.00 % RhD pos.	untreated	<i>RHD</i> exon 7	12.00	121.26	9.24	7.08
15	95.00 % RhD neg., 5.00 % RhD pos.	REPLI-g FFPE Kit amplified	<i>RHD</i> exon 7	2163.70	5870.53	1.98	0.03
16	95.00 % RhD neg., 5.00 % RhD pos.	REPLI-g FFPE Kit amplified+ purified	<i>RHD</i> exon 7	179.70	7625.55	0.51	0.01

The experiment was repeated with *RHD* exon 7 as target, and the results are listed in table 19. As for the gender analysis, the whole genome amplification results were compared with the untreated just isolated raw sample number 14. This sample showed after dPCR 121.26 copies/μl for GAPDH and 9.42 copies/μl for *RHD* exon 7. This leads to a ratio of 7.08 %. After amplification, the number of signals rose to 5870.53 copies/μl for the internal

control, but only 1.98 copies/ μl were detected for *RHD* exon 7 resulting in a ratio of 0.03 %. The conducted dPCR from sample 16 revealed 7925.55 copies/ μl for GAPDH, 0.51 copies/ μl for *RHD* exon 7, and a target to total ratio of 0.01 %.

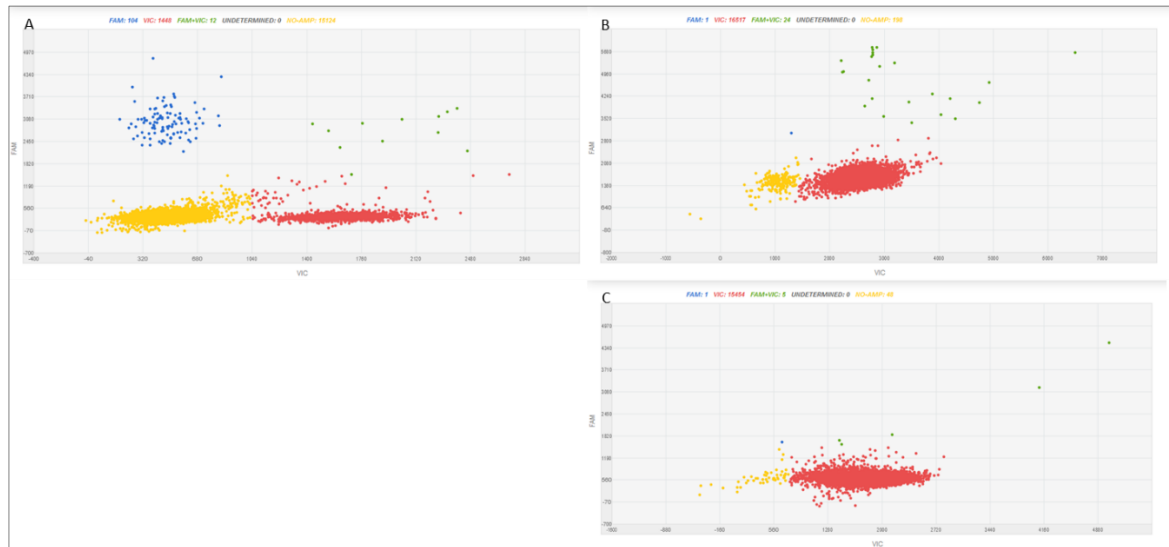


Figure 47: Visual analysis of the whole genome amplification compared with non-amplified cfDNA. All samples are simulated pregnancies containing 5.00 % of RhD positive plasma and 95.00 % RhD negative plasma. A: Sample 14 was analyzed after isolation with the QIAmp Circulating Nucleic Acids Kit. B: Sample 15 was amplified with the REPLI-g FFPE Kit after isolation but not purified. C: Sample 16 was amplified with the REPLI-g FFPE Kit and purified. Yellow dots indicated no amplification. red dots are signals of AMEL-X, blue signals of AMEL-Y, and green is the combination of AMEL-X and AMEL-Y. X-axis: VIC color distribution; Y-axis: FAM color distribution; Picture from the QuantStudio™ 3D AnalysisSuite™ Cloud Software.

The dot-pot results from the dPCR indicated for the untreated sample 14 a red cloud for the GAPDH signals and in blue the signals from *RHD* exon 7. Additionally, there are a few signals in the green channel (Figure 47A). After the whole genome amplification, the internal control signal was powerful, and only a few signs in the green channel were visible (Figure 47B). The dPCR after purification of the amplified sample revealed only signals from the internal control GAPDH (Figure 47C).

With the REPLI-g FFPE Kit, it should be possible to amplify short degraded DNA fragments. However, in the analysis of a mixture containing different individuals, the cfDNA analysis failed. In the next step, a targeted preamplification will be tested.

3.1.4.3 Targeted Preamplification

Because the whole genome amplification didn't work as intended. A specific amplification of the target sequence was tested. As shown for the whole genome amplification, a sample of a single person and a simulated pregnancy was tested.

After cfDNA extraction, the DNA was preamplified for AMEL-X/Y, GAPDH and *RHD* exon 7 (chapter 2.7.2.3, 2.8.4), and the PCR products were purified (chapter 2.9). The outcome was monitored on an agarose gel. In Figure 48, an example of an agarose gel is depicted. In this picture, the size marker MWM2 is shown on line 1. A simulated pregnancy is displayed in line two, and line three is the preamplification result of a single person.

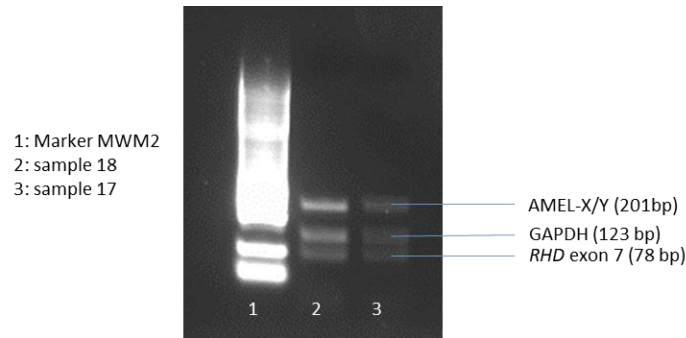


Figure 48: Result of a preamplification of AMEL-X/Y, GAPDH, and *RHD* exon 7. Sample number 17 is an RhD positive, male person and sample 18 was a simulated pregnancy of an RhD negative female with 5.00 % of an RhD positive male. The used marker in line 1 gives information about the size of the PCR products. In both samples, the amplification is clearly visible and separated from each other.

The cfDNA content was measured before and after purification. The specimen from the single person, showed a cfDNA content after extraction of 11.20 ng/μl and rose after amplification to 19,90 ng/μl. The mixture of two individuals had 9.60 ng/μl cfDNA after isolation and 20.50 ng/μl after preamplification.

After the gel analysis, the amplified cfDNA was used for dPCR. The results of the experiment concerning AMEL-X/Y are shown in table 20. Sample number 17 is from a male person, and the results indicated 8045.29 copies/μl for AMEL-X and 81201.00 copies/μl for AMEL-Y resulting in a ratio of 50.23 %. The sample of the simulated pregnancy revealed 9259.23 copies/μl for AMEL-X and 8099.67 copies/μl for AMEL-Y, indicating a ratio of 46.66 %.

Table 20: Results of the dPCR with a targeted preamplification. In the dPCR, the AMEL-X/Y were targeted. Sample number 17 is from a male person. Sample number 18 consists of 95.00 % female and 5.00 % male plasma.

No.	Sample content	Target	DPCR with targeted preamplification				
			cfDNA after isolation [ng/μl]	DNA after preamplification [ng/μl]	AMEL-X copies/μl	AMEL-Y copies/μl	Target/total [%]
17	Male	AMEL-X/Y	11.20	19.90	8045.29	81201.00	50.23
18	95.00 % female, 5.00 % male	AMEL-X/Y	9.60	20.50	9259.23	8099.67	46.66

The dot plot analysis indicated that the majority of the cavities contained signals for AMEL-X and AMEL-Y as well (Figure 49). Furthermore, there are only a few signals for reaction compartments without a reaction or with single reactions for AMEL-X or AMEL-Y.

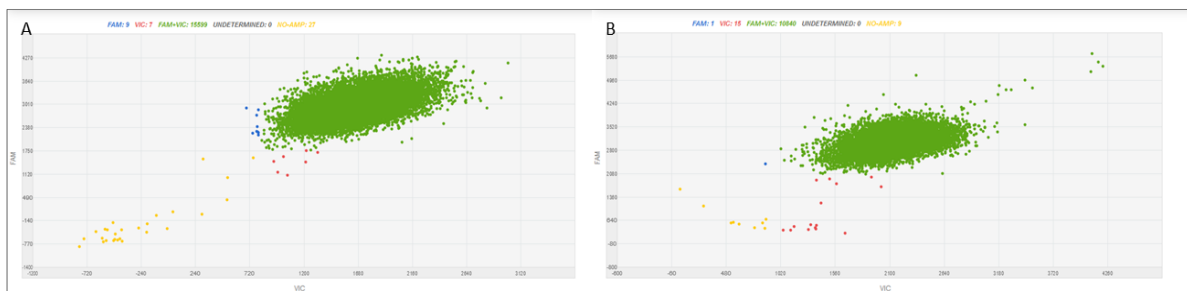


Figure 49: Samples are isolated with Qiagen and preamplified before dPCR. A: DPCR result of sample 17. The primary reaction cavities contained both target sequences. B: DPCR result of the simulated pregnancy sample 18. The main reaction cavities contained both target sequences. Yellow dots indicated no amplification. red dots are signals of AMEL-X, blue signals of AMEL-Y, and green is the combination of AMEL-X and AMEL-Y. X-axis: VIC color distribution; Y-axis: FAM color distribution; Picture from the QuantStudio™ 3D AnalysisSuite™ Cloud Software.

The *RHD* exon 7 identification analysis revealed for the RhD positive sample of a single person, 8870.57 copies/ μ l for GAPDH and 9547.16 copies/ μ l for *RHD* exon 7 resulting in a ratio of 51.84 %. The mixed specimen showed 8917.33 copies/ μ l of the internal control and 9144.95 copies/ μ l for *RHD* exon 7 resulting in a ratio of 50.63 % (Table 21).

Table 21: Results of the dPCR with targeted preamplification. In the dPCR, the *RHD* exon 7 was targeted, and GAPDH was used as an internal control.

No.	Sample content	Target	DPCR with targeted preamplification				
			cfDNA after isolation [ng/ μ l]	DNA after preamplification [ng/ μ l]	GAPDH copies/ μ l	<i>RHD</i> exon 7 copies/ μ l	Target/total [%]
19	RhD positive	<i>RHD</i> exon 7	11.2	19.9	8870.57	9547.16	51.84
20	95.00 % RhD negative, 5.00 % RhD positive	<i>RHD</i> exon 7	9.6	20.5	8917.33	9144.95	50.63

The visual analysis of the *RHD* exon 7 analysis revealed identical results as for gender analysis. Figure 50A depicts the dPCR of sample 19, and Figure 50B is the result of sample 20. In both images are the internal control and the target *RHD* exon 7 mainly in both reaction cavities.

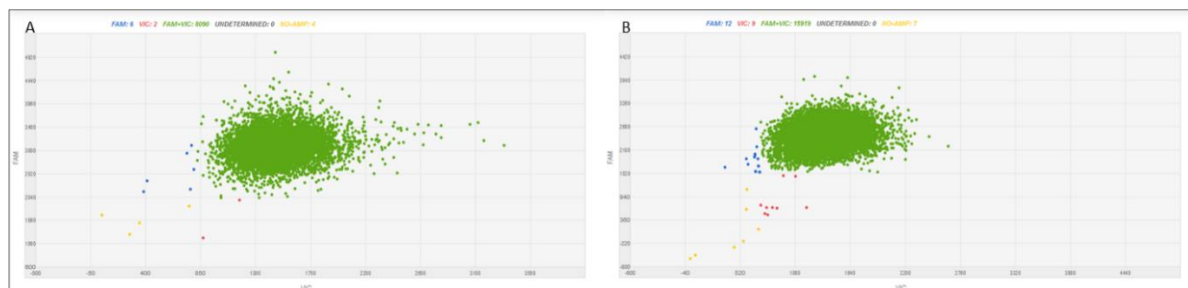


Figure 50: Samples are isolated with Qiagen and preamplified before dPCR. A: DPCR result of sample 19 of a single person. The primary reaction cavities contained both target sequences. B: DPCR result of sample 20, the simulated pregnancy, which consists of 95.00 % RhD negative and 5.00 % RhD positive plasma. Most of the reaction cavities contained both target sequences. Yellow dots indicated no amplification; red dots are signals of GAPDH, blue signals of RHD exon 7, and green is the combination of RHD exon 7 and GAPDH. X-axis: VIC color distribution; Y-axis: FAM color distribution; Picture from the QuantStudio™ 3D AnalysisSuite™ Cloud Software.

Obviously, the chips were overloaded after preamplification, and a separation of the signals from total cfDNA and target is not possible. Therefore, different molecule densities will be tested in order to evaluate the optimal number of molecules per chip.

3.1.5 Optimization of Molecule Density

After the isolation of the cfDNA, which had an average of 4-6 ng/ μ l, the PCR for targeted preamplification increased the DNA concentration up to 7-10 ng/ μ l. The standard protocol from Thermo fisher for dPCR is designed for genomic DNA. Because the preamplification significantly increased the region of interest, the manufacturer's recommended protocol could not be applied. For these reasons, it was decided to conduct a dilution series to identify the best molecule density. For this, a mixture containing 5.00 % of RhD positive sample was used. This sample was diluted from 2×10^7 down to 6,400 molecules.

Cell-free plasma DNA was isolated with the QIAmp Circulating Nucleic Acids Kit and preamplified as described In chapter 2.7.2.3 and chapter 2.8.4. Afterward, the number of molecules was calculated as described in chapter 2.15, and a dPCR was conducted (chapter 2.10).

3 RESULTS

Table 22: Results of the dilution series. All experiments were performed in triplicates.

Number of molecules	<i>RHD</i> exon7 copies/ μ l [mean \pm SD]	GAPDH copies/ μ l [mean \pm SD]	Target/total [%] [mean \pm SD]
2×10^7	295.53 \pm 208.31	4933.45 \pm 1771.31	5.14 \pm 2.13
4×10^6	10.56 \pm 7.84	219.94 \pm 170.41	4.86 \pm 0.87
8×10^5	4.51 \pm 3.52	81.63 \pm 61.71	5.82 \pm 1.79
1.6×10^5	2.15 \pm 1.17	42.15 \pm 18.68	4.44 \pm 0.90
3.2×10^4	0.51 \pm 0.24	4.34 \pm 1.95	10.51 \pm 4.29
6.4×10^3	0.40 \pm 0.02	0.93 \pm 0.17	30.65 \pm 4.40

The investigation of the dilution series revealed for 2×10^7 molecules 295.53 copies/ μ l of *RHD* exon 7 and 4933.45 copies/ μ l for the internal control. This makes a target to total ratio of 5.14 %. The ratio remained stable for 4×10^6 and 8×10^5 molecules, with 4.86 % and 5.82 %, respectively (Table 22).

Also, tests with 1.6×10^5 molecules indicated a ratio in this field. However, investigations with 3.2×10^4 and 6.4×10^3 molecules showed very high percentages with 10.51 % and 30.65 %, which is caused by the small number of detected molecules.

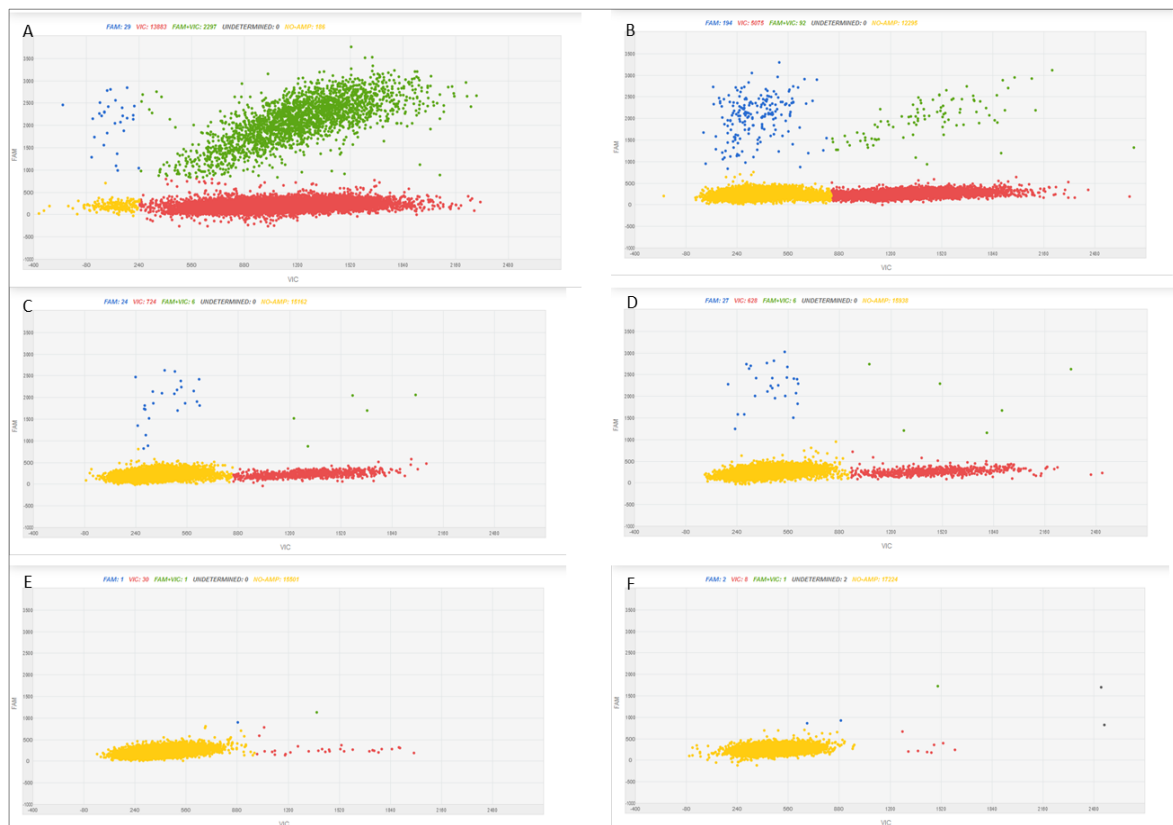


Figure 51: Results of the dilution series.: A: 2×10^7 molecules. B: 4×10^6 molecules. C: 8×10^5 molecules. D: 1.6×10^5 molecules. E: 3.2×10^4 molecules. F: 6.4×10^3 molecules. Yellow dots indicated no amplification; red dots are signals of GAPDH, blue signals of *RHD* exon 7, and green is the combination of *RHD* exon 7 and GAPDH. X-axis: VIC color distribution; Y-axis: FAM color distribution; Picture from the QuantStudio™ 3D AnalysisSuite™ Cloud Software.

The dilution series's visual analysis revealed a reduction of the signal intensity in all color channels from 2×10^7 down to 6.4×10^3 molecules and reflected the results of table 22 very reliable. More precisely, Figure 51A showing 2×10^7 molecules, indicated a strong signal in the green channel, but there are also signals of compartments with *RHD* exon 7 (blue) and

internal control (red). In Figure 51B are 4×10^6 molecules which, show fewer signals in the green channel but more in the blue one. The dPCR result with 8×10^5 molecules revealed a view signals in the green channel but still signals in the blue channel (Figure 51C). In the next Figure 51D 1.6×10^5 molecules indicated some signals for the target sequence, and the internal control is identifiable. For 3.2×10^4 molecules, only two signals for *RHD* exon 7 and a view signals for the internal control GAPDH were detected (Figure 51E). The lowest molecule amount of 6.4×10^3 showed two signs for *RHD* exon 7 and a very low number of internal control (Figure 51F).

According to the results of the molecule dilution, 4×10^6 molecules per chip seemed useful. In the case of a high cfDNA amount, there are still good results possible without overloading the chip. Furthermore, the more probable it is that the cfDNA is low, especially in early pregnancy. 4×10^6 molecules per chip will reveal good results even though the fetal amount is low; it will be detected.

3.1.6 Comparison Between Automatic and Manual Cell-Free DNA Isolation

A dilution series of a simulated pregnancy was designed to test if the molecule density meets our requirements and decide whether Maxwell[®]RSC or QIAmp Circulating Nucleic Acids Kit for cfDNA isolation should be applied. This dilution series consists of plasma of a heterozygous donor (5.00 to 0.10 %) in excess of plasma from an homozygous donor (95.00 to 99.90 %). The samples were isolated with the automated device Maxwell[®]RSC and the QIAmp Circulating Nucleic Acids Kit. As shown in chapter 3.1.3.2 and 3.1.3.3, the isolation with Maxwell[®]RSC and QIAmp Circulating Nucleic Acids Kit revealed both acceptable results. Therefore, both isolation methods were tested with this dilution series to decide the best way for further analysis. After isolation 4×10^6 molecules were loaded onto a chip for dPCR analysis.

Table 23: Results of the dPCR using 4×10^6 molecules. A dilution series of heterozygous plasma (5.00 to 0.10 %) in excess of homozygous plasma (95.00 to 99.90 %) was used to test the detectability and consistency with *RHD* exon 7. The cfDNA was initially isolated with the Maxwell[®]RSC device from Promega.

No	Percentage proportion of RhD pos. plasma	Target	Maxwell [®] RSC				
			cfDNA [ng/μl]	DNA after preamplification [ng/μl]	GAPDH copies/μl	<i>RHD</i> exon 7 copies/μl	Target/total [%]
21	5.00 %	<i>RHD</i> exon 7	3.70	7.30	282.08	6.28	2.18
22	1.00 %	<i>RHD</i> exon 7	5.60	6.30	411.85	20.93	4.84
23	0.50 %	<i>RHD</i> exon 7	3.90	8.90	84.45	0.25	0.29
24	0.10 %	<i>RHD</i> exon 7	2.80	9.30	1073.93	0.79	3.68
25	0.00 %	<i>RHD</i> exon 7	3.10	5.40	396.26	2.11	0.53
26	100.00 %	<i>RHD</i> exon 7	3.20	7.60	271.15	292.88	51.93

The Maxwell[®]RSC isolation revealed an amount of isolated cfDNA in a range of 2.80-5.60 ng/μl and after preamplification 5.40 -9.30 ng/μl. Sample 21 showed a target to total ratio of 2.18 %. Sample 22 contained 1.00 % RhD positive plasma and was detected with 4.84 %, and the example with 0.50 % RhD positive plasma was indicated with 0.29 % target to total. Sample 24 showed a ratio of 3.68 %. The RhD negative sample showed a background signal of 0.53 %, whereas the RhD positive sample was detected with 51.93 % (Table 23).

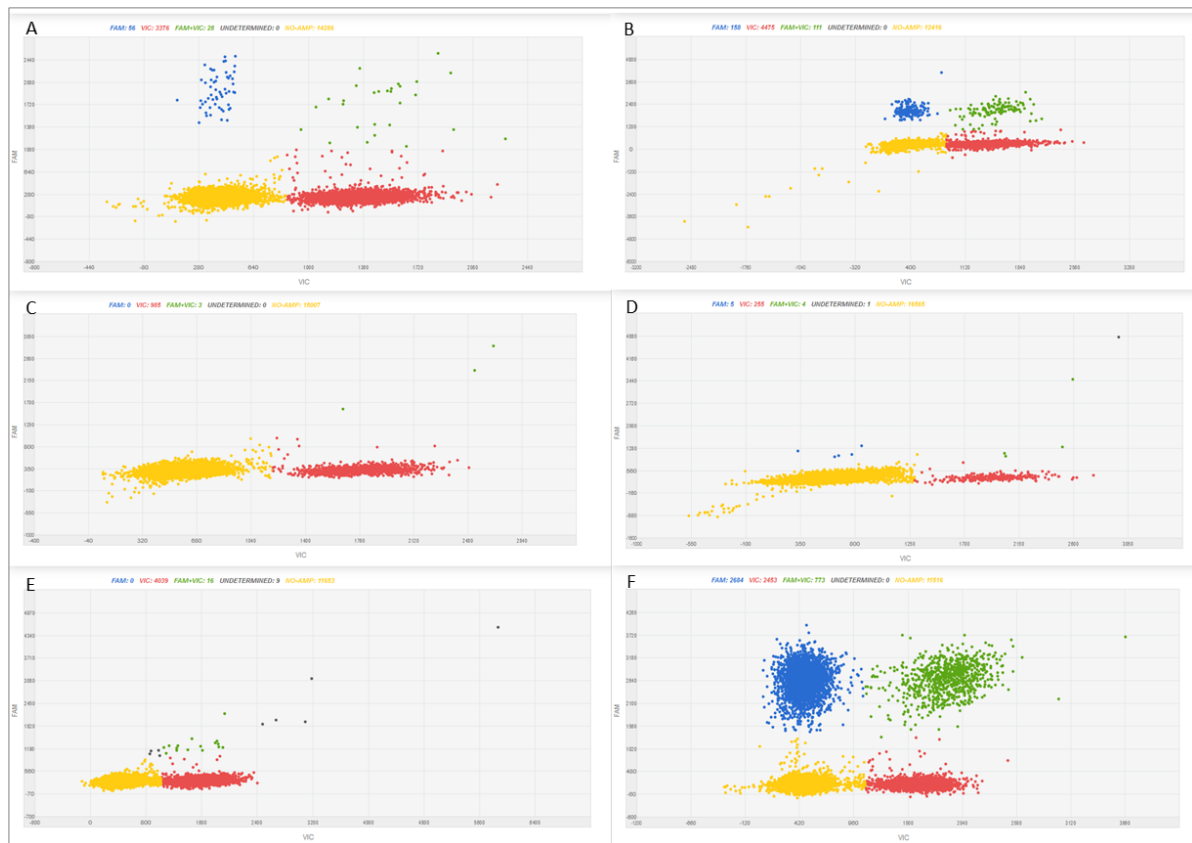


Figure 52: Visual analysis of the dilution series. Plasma was mixed with plasma of a heterozygous donor (5.00 to 0.10 %) in excess of plasma of an homozygous donor (95.00 to 99.90 %). CfDNA was isolated with the Maxwell®RSC. After preamplification, the cfDNA was diluted down to 4×10^6 molecules per dPCR chip. A: The mixture contained 5.00 % RhD positive plasma. B: Results of 1.00 % RhD positive plasma. C: Plasma mixture with 0.50 % RhD positive plasma. D: Sample includes 0.10 % RhD positive plasma. E: RhD negative sample. F: RhD positive sample. Yellow dots indicated no amplification; red dots are signals of GAPDH, blue signals of *RHD* exon 7, and green is the combination of *RHD* exon 7 and GAPDH. X-axis: VIC color distribution; Y-axis: FAM color distribution; Picture from the QuantStudio™ 3D AnalysisSuite™ Cloud Software.

The visual analysis of the dilution series isolated with the Maxwell®RSC device and 4×10^6 molecules per dPCR application reflected the results from table 23. The sample depicted in Figure 52A contained 5.00 % RhD positive material. The *RHD* exon 7 signal was identifiable in the blue cloud and the internal control GAPDH, reflecting the entire cfDNA content, was visible in the red cloud. A few signals in the green channel indicated the presence of both targets in one reaction vessel. In the sample containing 1.00 % RhD positive plasma, the internal control, as well as the *RHD* exon 7 signal, were visible in different clouds. Additionally, the green cloud was strongly represented (Figure 52B). Figure 52C indicated the sample with 0.50 % RhD positive proportion. Only the red signal for the internal control is visible, but no signal for *RHD* exon 7 and just a few in the green channel. The sample signals with 0.10 % RhD positive plasma indicated a small cloud for GAPDH and only a few signals in the green and blue channels (Figure 52D). To compare the results, an RhD negative sample was used to test the background signals. There were a few signals in the green channel and a cloud for internal control visible (Figure 52E). Finally, a pure RhD positive sample was tested, and there was a clear cloud in all color channels visible (Figure 52F).

The sample dilution series was repeated with the QIAmp Circulating Nucleic Acids Kit in order to test if the isolation reveals better results.

3 RESULTS

Table 24: Results of the dPCR using 4×10^6 molecules. A dilution series of heterozygous plasma (5.00 to 0.10 %) in excess of homozygous plasma (95.00 to 99.90 %) was used to test the detectability and consistency with the actual added amount of *RHD* gene. The DNA was initially isolated with the QIAmp Circulating Nucleic Acids Kit.

No.	Percentage proportion of RhD pos. plasma	Target	QIAmp Circulating Nucleic Acids Kit				
			cfDNA [ng/ μ l]	DNA preamplification [ng/ μ l]	GAPDH copies/ μ l	<i>RHD</i> exon 7 copies/ μ l	Target/total [%]
27	5.00 %	RHD exon 7	5.80	8.60	1400.73	59.15	4.05
28	1.00 %	RHD exon 7	4.80	6.60	1063.82	19.54	1.80
29	0.50 %	RHD exon 7	4.80	6.80	487.35	6.94	1.40
30	0.10 %	RHD exon 7	5.20	7.40	1073.93	1.11	0.10
31	0.00 %	RHD exon 7	5.50	8.80	1391.01	0.16	0.01
32	100.00 %	RHD exon 7	5.50	6.90	532.93	389.95	42.25

The cfDNA amount after isolation was between 4.80 -5.80 ng/ μ l and after preamplification between 6.90 and 8.80 ng/ μ l. Sample 27 indicated a ratio of 4.05 % and contained an actual amount of 5.00 %. The sample with 1.00 % *RHD* exon 7 was detected with 1.80 % with the dPCR using only 4×10^6 molecules. The next dilution step was 0.50 %, which was detected with 1.40 %. Interestingly, the sample with a 0.10 % RhD positive sample was shown with an intensity of 0.10 %. For the background test, the RhD negative sample was used and revealed 0.01 % *RHD* exon 7 signals. Additionally, an RhD positive sample was tested and showed a 42.25 % (Table 24).

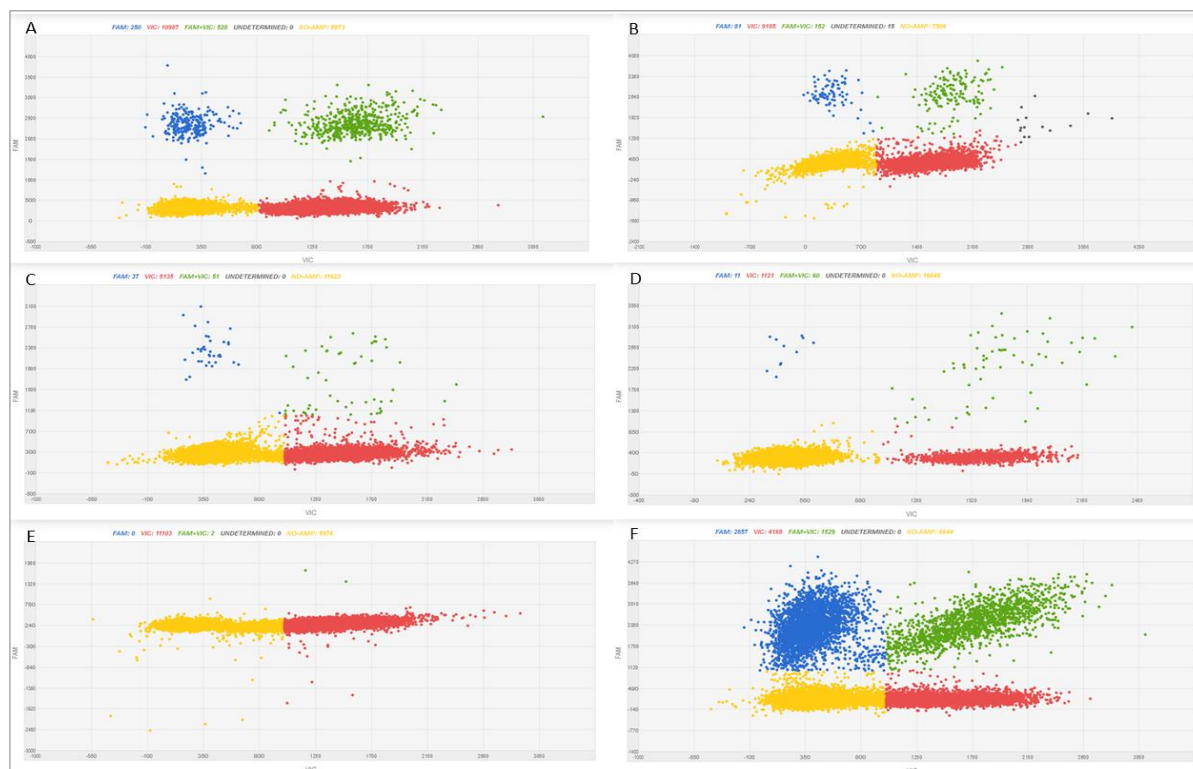


Figure 53: Visual analysis of the dilution series. Plasma was mixed with plasma of an heterozygous donor (5.00 to 0.10 %) in excess of plasma of an homozygous donor (95.00 to 99.90 %). CfDNA was isolated with the QIAmp Circulating Nucleic Acids Kit. After preamplification, the cfDNA was diluted down to 4×10^6 molecules per dPCR chip. A: The mixture contained 5.00 % RhD plasma. B: Indicated an RhD proportion of 1.00 %. C: Plasma mixture with 0.50 % RhD positive sample. D: Sample includes 0.10 % RhD positive proportion. E: RhD negative sample. F: RhD positive sample. Yellow dots indicated no amplification; red dots are signals of GAPDH, blue signals of *RHD* exon 7, and green is the combination of *RHD* exon 7 and GAPDH. X-axis: VIC color distribution; Y-axis: FAM color distribution; Picture from the QuantStudio™ 3D AnalysisSuite™ Cloud Software.

The visual analysis indicated a reduction of the signal intensity from 5.00 % - 0.10 %, as expected. The sample containing 5.00 % plasma of an RhD heterozygous donor showed well separated and unambiguous clouds in each color channel (Figure 53A). This was repeated with a 1.00 % mixture, and the clouds' intensity was a bit reduced (Figure 53B). In Figure 53C is the result of a mixture containing 0.50 % RhD positive plasma depicted. Also, here, the clouds are identifiable, and the intensity was reduced a bit more. This is the same for the sample with 0.10 % RhD positive plasma. Figure 53D indicated the clouds with a further reduced intensity. A test for the background signal showed a strong cloud for the internal control and only sporadic signs in the green or blue channel (Figure 53E). The RhD positive sample analysis indicated a good signal in all color channels, as shown in Figure 53F.

The QIAmp Circulating Nucleic Acids Kit background was small, and the correlation between actual cfDNA content and theoretical content was satisfying. Therefore, the manual cfDNA isolation with the QIAmp Circulating Nucleic Acids Kit will be applied for the standard NIPT protocol.

3.2 Summary of Protocol Development

This thesis aimed to develop a NIPT protocol for the analysis of blood cell- and platelet antigens. In order to create a stable and robust protocol, many small steps are essential to analyze. The first step was to investigate if the elution buffer, which is part of every cfDNA isolation kit, influences the dPCR results. It turned out that the elution buffer has an influence on the signal background and that ddH₂O is most suitable for cfDNA elution for dPCR investigations (chapter 3.1.1).

Furthermore, the plasma volume influence was evaluated, if there is a correlation between volume and signal strength in dPCR and which volume is best in routine use. The results showed that the more plasma volume, the more cfDNA was isolated, but this does not influence the signal strength in dPCR or on the target signal strength. So, the used plasma volume was set to 1 ml per isolation (chapter 3.1.2). After this decision, the most suitable cfDNA isolation method was analyzed. Three different ways were tested. Two were based on magnet beads, one was a fully automated device (Maxwell[®]RSC), and the other was a manual isolation (MagMax). The third method was the manual column-based QIAmp Circulating Nucleic Acids Kit. Auspicious results were gained with the Maxwell[®]RSC and QIAmp Circulating Nucleic Acids Kit. However, the signal strength in dPCR was below the expectations, and it was decided to increase the signals by WGA. The REPLI-g Mini Kit is generally used for the DNA amplification from whole blood and tissue culture cells.

After amplification, the dPCR signals declined compared to the unamplified sample, so another WGA (REPLI-g FFPE Tissue Kit) was tested to amplify strong degraded DNA. It was shown that the cfDNA was strongly amplified, and the signal loss was reduced compared to the REPLI-g Mini Kit. Nevertheless, the signal intensity was lower than the control sample right after isolation (chapter 3.1.4.1 and 3.1.4.2). Consequently, the WGA was ruled out for the use in NIPT. The next try for signal amplification was the targeted preamplification, which worked great (chapter 3.1.4.3). After preamplification, the signal in dPCR was so strong that the chip was completely overloaded. To circumvent this status, a dilution series reducing the molecule amount per chip from 2×10^7 down to 6.4×10^3 was applied in order to identify the optimal molecule density for dPCR. The tests revealed 4×10^6 molecules per chip as an optimal density (chapter 3.1.5).

As mentioned above, the cfDNA isolation with Maxwell[®]RSC and QIAmp Circulating Nucleic Acids Kit revealed promising results. In the last step it was tested which extraction method reveals the best results with the newly designed protocol. A dilution series consisting of plasma of a heterozygous donor (5.00 to 0.10 %) in excess of plasma of a homozygous donor (95.00 to 99.90 %) was produced. It appeared that the QIAmp Circulating Nucleic Acids Kit indicated a low background and the best correlation between actual cfDNA quantity and analyzed cfDNA (chapter 3.1.6).

The final protocol for the NIPT analysis for blood cell- and platelet antigens consists of a manual cfDNA isolation using 1 ml plasma with QIAmp Circulating Nucleic Acids Kit followed by a targeted preamplification and a subsequent dilution to 4×10^6 molecules per dPCR chip and finally, the dPCR with the analysis of the results.

In the following chapter, the technical validation was applied to identify this developed protocol's sensibility and specificity.

3.3 Validation Process of Red Blood Cell and Platelet Antigens

The final protocol consists of the plasma DNA isolation with the QIAmp Circulating Nucleic Acids Kit, a targeted preamplification followed by a dilution to 4×10^6 molecules per dPCR approach. With that established protocol, the technical validation process for *RHD* exon 3, 5, 7, KEL1/KEL2, HPA-1a/b, -2a/b, -3a/b, -5a/b, -15a/b and amelogenin (AMEL-X/Y) was conducted. As indicated in Figure 54, plasma mixes were used to simulate early (first trimester) and late stages of a pregnancy (third trimester) by mixing homozygous and heterozygous plasmas. The results of the technical validation are introduced in this chapter. During the verification, all experiments were conducted in biological triplicates.

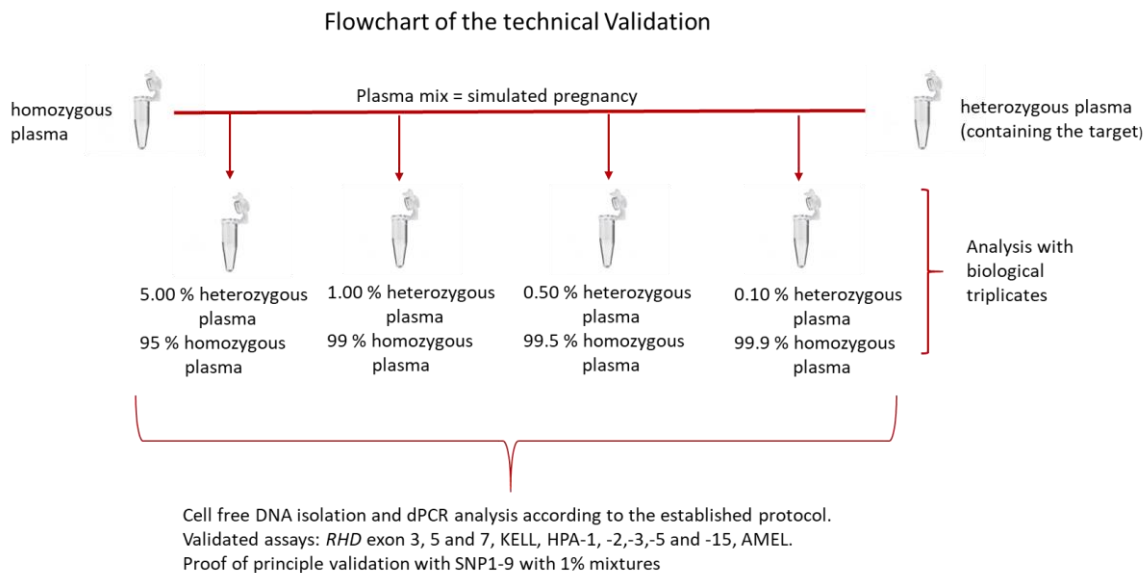


Figure 54: Flowchart of the technical validation.

3.3.1 Validation of the *RHD* Assays

A RhD negative woman's pregnancy with an RhD positive child can lead to Morbus hemolyticus neonatorum (MHN) (chapter 1.2). All RhD negative women receive immunoglobulins regardless of whether they carry an RhD positive child or not. Besides the side effects, only women with an RhD positive child can develop anti-D. Therefore, it aims to reduce the immunoglobulins' administration only to those women who carry an RhD positive child. All RhD negative women with a negative child do not need any treatment in this field. This underlines why it is necessary to elucidate the rhesus status of the fetus. The validation of the *RHD* genotyping focus on the stability and sensitivity of *RHD* gene detection. In order to test the assay's sensitivity, a dilution series from 5.00 % down to 0.10 % in biological triplicates was conducted. The number of loaded molecules per chip was 4×10^6 . For the rhesus gene, the exons 3, 5, and 7 were validated.

3 RESULTS

Table 25: Validation results for *RHD* exon 3 according to the established protocol. All experiments were performed in biological triplicates. SD: standard deviation.

% heterozygous plasma (% target allele)	<i>RHD</i> exon 3		
	Target copies/ μ l [mean \pm SD]	Total copies/ μ l [mean \pm SD]	Target/total in % [mean \pm SD]
5.00 (2.50)	33.56 \pm 13.63	904.20 \pm 327.94	3.54 \pm 0.36
1.00 (0.50)	4.13 \pm 0.91	525.75 \pm 298.63	1.00 \pm 0.44
0.50 (0.25)	5.22 \pm 2.94	1053.87 \pm 456.43	0.49 \pm 0.12
0.10 (0.05)	1.51 \pm 0.38	590.06 \pm 410.35	0.38 \pm 0.19
Background	4.85 \pm 3.13	694.82 \pm 350.91	0.60 \pm 0.20

For calculating the target to total ratio, a reference representing the whole cfDNA quantity was needed. In the case of the *RHD* assay, it was GAPDH whose basic quantity was detected in a range of 525.75-1053.87 copies/ μ l. The *RHD* exon 3 signals decreased with the reduction of the RhD positive portion. While the approach with 5.00 % *RHD*/d heterozygous plasma proportion the target was detected with 33.46 copies/ μ l and the detection in the approach containing 0.10 % RH positive plasma was reduced to 1.51 copies/ μ l. The target to total results of the *RHD* exon 3 assay gives information about the relationship between the basic quantity of the cfDNA and the target *RHD* exon3. A sample with 5.00 % RhD positive plasma revealed a target to total ratio of 3.54 %. The sample containing an RH positive plasma proportion of 1.00 % was detected at an average of 1.00 % in the dPCR, and the approach with 0.50 % RhD positive plasma was detected with 0.49 %. The 0.10 % sample was calculated with a target to total ratio of 0.38 %. However, in this case, the negative control was unexpected high with 0.60 % (Table 25). Therefore, the detection limit for the *RHD* exon 3 assay was set to 1.00 %.

Table 26: Validation results for *RHD* exon 5 according to the established protocol. All experiments were performed in biological triplicates. SD: standard deviation.

% heterozygous plasma (% target allele)	<i>RHD</i> exon 5		
	Target copies/ μ l [mean \pm SD]	Total copies/ μ l [mean \pm SD]	Target/total in % [mean \pm SD]
5.00 (2.50)	18.04 \pm 4.89	310.37 \pm 155.01	6.47 \pm 2.04
1.00 (0.50)	6.33 \pm 4.39	369.34 \pm 342.51	2.06 \pm 0.72
0.50 (0.25)	1.96 \pm 1.13	517.79 \pm 321.33	0.85 \pm 0.77
0.10 (0.05)	2.28 \pm 3.12	581.70 \pm 352.71	0.28 \pm 0.33
Background	0.03 \pm 0.04	281.97 \pm 232.42	0.00 \pm 0.01

The detection of the basic quantity or reference cfDNA was between 281.97-581.70 copies/ μ l in the *RHD* exon 5 assay. As shown in table 26, the target copies reduced from 18.04 copies/ μ l in the approach with 5.00 % RH positive plasma to 2.28 copies/ μ l in the 0.10 % RhD positive plasma experiment. The two parameters target copies and total copies resulting in the target to total ratio. For the mixture containing 5.00 % RhD positive plasma 6.47 % was measured, and the samples with 1.00 % RhD positive plasma were identified on average with 2.06 %. The mix with 0.50 % RhD positive plasma was calculated with 0.85 %, and the mixture containing 0.10 % RhD positive plasma was identified with 0.28 %. The background measurements revealed an intensity of 0.00%. Therefore, the threshold for the *RHD* exon 5 assay was set to 0.10 %.

3 RESULTS

Table 27: Validation results for *RHD* exon 7 according to the established protocol. All experiments were performed in biological triplicates. SD: standard deviation.

% heterozygous plasma (% target allele)	<i>RHD</i> exon 7		
	Target copies/ μ l [mean \pm SD]	Total copies/ μ l [mean \pm SD]	Target/total in % [mean \pm SD]
5.00 (2.50)	82.65 \pm 44.82	1693.48 \pm 555.68	4.36 \pm 0.88
1.00 (0.50)	36.86 \pm 25.27	1494.35 \pm 714.40	2.20 \pm 0.45
0.50 (0.25)	2.47 \pm 3.16	931.34 \pm 390.10	0.48 \pm 0.65
0.10 (0.05)	0.74 \pm 0.32	1027.41 \pm 545.38	0.08 \pm 0.03
Background	0.61 \pm 0.70	1199.90 \pm 285.29	0.04 \pm 0.05

The reference cfDNA GAPDH was detected in a range of 1693.48-931.34 copies/ μ l in the *RHD* exon 7 assay (Table 27). The gradient from 5.00 % down to 0.10 % of RhD positive plasma was clearly recognizable. While in a 5.00 % mixture, *RHD* exon 7 was detected with 82.65 copies/ μ l in a 0.10 % RhD positive plasma proportion were only 0.74 copies/ μ l detected. The two parameters total cfDNA, and target cfDNA results in the target to total ratio. The validation for *RHD* exon 7 revealed for the 5.00 % mixture a 4.36 % target to total, and the 1.00 % mixture was recognized with 2.20 %. Furthermore, the approach containing 0.50 % RhD positive plasma was identified with 0.48 %, and the application with 0.10 % RhD positive plasma was detected with 0.08 %. However, the background was around 0.04 %. For that reason, the detection limit was set to 0.10 %.

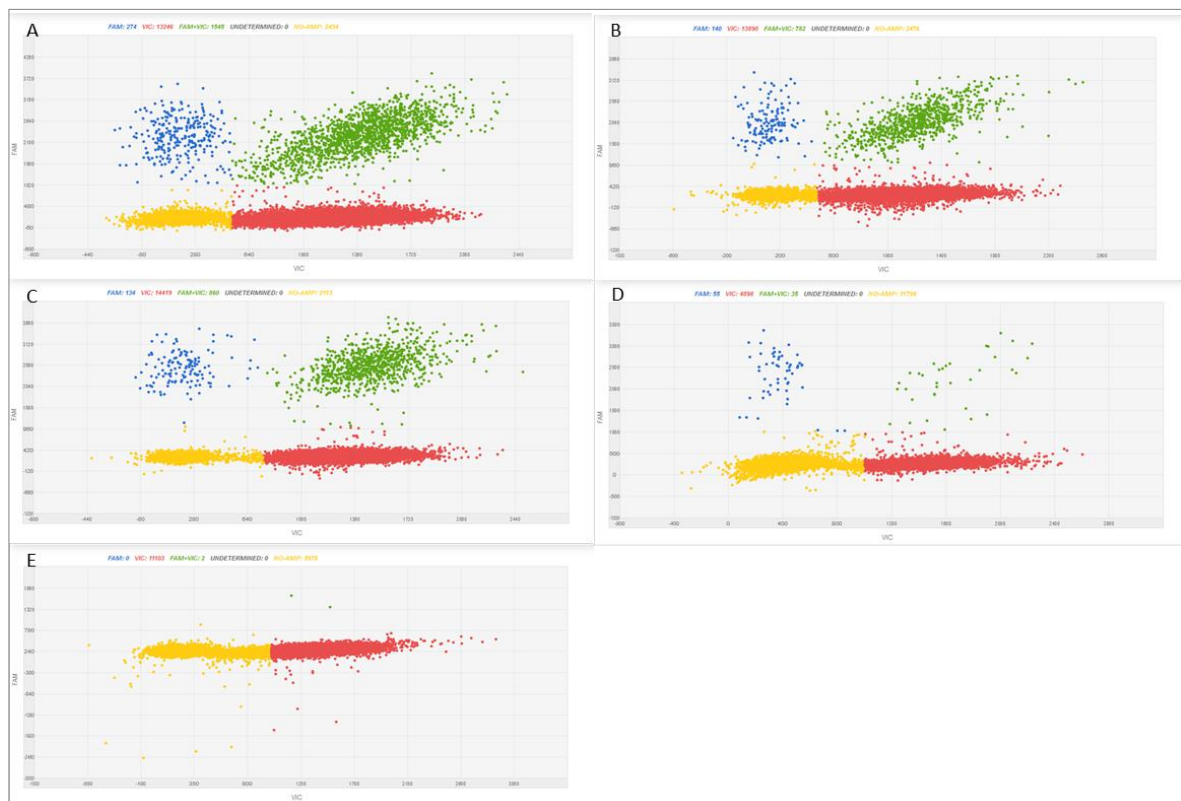


Figure 55: Exemplary visualization of the validation of the *RHD* exon 7 assay in the dilution series. Experiments were performed in biological triplicates. A: The mixture contained 5.00 % RhD positive plasma. B: Indicated an RhD positive plasma proportion of 1.00 %. C: Plasma mixture with 0.50 % RhD positive plasma. D: Sample includes 0.10 % RhD positive plasma. E: RhD negative sample. Yellow dots indicated no amplification; red dots are signals of GAPDH, blue signals of *RHD* exon 7, and green is the combination of *RHD* exon 7 and GAPDH. X-axis: VIC color distribution; Y-axis: FAM color distribution; Picture from the QuantStudio™ 3D AnalysisSuite™ Cloud Software.

The visual results shown in Figure 55 for *RHD* exon 7 are exemplary. A vigorous signal intensity indicated the mixture containing 5.00 % RhD positive plasma in blue, green, and red color channel. The intensity was slightly diminished in the approach with 1.00 % RhD positive plasma but identifiable. This holds for the 0.50 % mixture. Here, the signals for the *RHD* exon 7 (blue), the internal control GAPDH (red), and reaction vessels containing GAPDH and *RHD* exon 7 (green) are well-formed. Finally, in a mixture containing only 0.10 % RhD positive plasma, the signals are clearly evident. The background depicted in Figure 55E showed only the internal control GAPDH and empty compartments.

In summary, it was possible to identify the rare target sequence in a cfDNA mixture. The threshold was set for *RHD* exon 3 to 1.00 % and for *RHD* exon 5 and 7 to 0.10 % RhD positive plasma proportion. The used plasma was from a *RHD/d* heterozygous donor, therefore only 0.50 % of *RHD* exon 3 and 0.05 % of *RHD* exon 5 and 7, are needed for reliable identification.

3.3.2. Validation of the KEL Assay

Another blood cell antigen that can cause MHN is the KEL1 (K) antigen from the KEL system. The anti-K titer gives no information about the disease's severity because the KEL1 antigen is expressed very early in hematopoiesis. Therefore, early knowledge about the KEL1 status is essential. Here, the results of the technical validation are presented.

Table 28: Validation results of the K1/K2 assay according to the established protocol. All experiments were performed in biological triplicates. SD: standard deviation.

% heterozygous plasma (% target allele)	KEL1		
	Target copies/ μ l [mean \pm SD]	Total copies/ μ l [mean \pm SD]	Target/total in % [mean \pm SD]
5.00 (2.50)	33.47 \pm 1.52	1422.92 \pm 191.04	2.33 \pm 0.27
1.00 (0.50)	8.85 \pm 5.28	1446.15 \pm 411.64	0.64 \pm 0.47
0.50 (0.25)	5.40 \pm 5.02	1505.52 \pm 164.49	0.40 \pm 0.40
0.10 (0.05)	1.58 \pm 0.37	2112.22 \pm 593.26	0.08 \pm 0.01
Background	1.55 \pm 0.53	2343.78 \pm 51.91	0.07 \pm 0.02

In this assay is the KEL2 allele was used as reference, which was detected in a range between 2343.78-1422.91 copies/ μ l. The target allele KEL1 was reliably detected with 33.47 copies/ μ l in a mixture containing 5.00 % of heterozygous KEL1/KEL2 plasma and 1.58 copies/ μ l in a mixture with 0.10 % KEL positive plasma. Using the calculations explained in chapter 2.14 the target/total ratio for a mixture with 5.00 % KEL positive plasma was 2.33 %, and the 1.00 % mixture was detected with 0.64 %. The sample containing 0.50 % KEL positive plasma was detected with 0.40%. The mixture containing 0.10% KEL positive plasma was detected with 0.08 %, but the background measurement indicated 0.10 % as well. Therefore, the detection limit of the *KEL* assay was set to 0.50 % KEL positive plasma (Table 28).

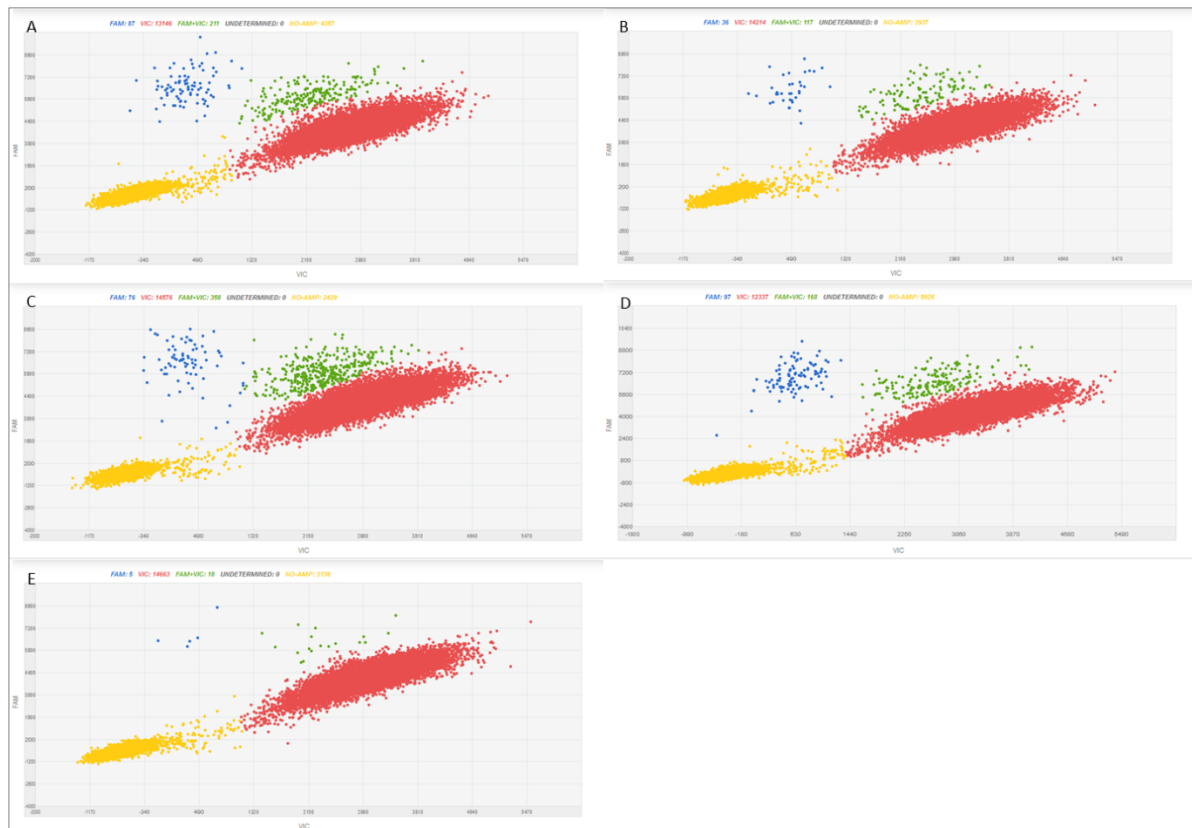


Figure 56: Visualization of the validation of the *KEL* assay in the dilution series. All experiments were performed in biological triplicates. A: cfDNA extracted from plasma mixture with 5.00 % *KEL1/KEL2* heterozygous plasma. B: Plasma mixture with 1.00 % *KEL1/KEL2* proportion. C: Plasma mixture with 0.50 % *KEL1/KEL2* proportion. D: Plasma mixture with 0.10 % *KEL1/KEL2* proportion. E: *KEL1* negative sample. Yellow dots: no amplification; red dots: positive for reference allele *KEL2*; blue dots: positive for target allele *KEL1*; green dots: positive for *KEL1* and *KEL2*. X-axis: VIC signal; Y-axis: FAM signal; Picture from the QuantStudio™ 3D AnalysisSuite™ Cloud Software.

The visual results of the *KEL* assay validation are depicted in Figure 56. The amount of *KEL1/KEL2* heterozygous plasma (5.00 to 0.10 %) was reduced in the exchange of *KEL* negative plasma (95.00 to 99.90 %). In Figure 56A, the result of the 5.00 % mixture is depicted and shows a clear signal in the blue channel for *KEL1*. The green channel, indicates the signal for the internal control and the targeted *KEL1* in one reaction vessel. In the red channel, the *KEL2* signal is displayed. The following dilution steps of 1.00 %, 0.50 %, and 0.10 % showed an identical image with reduced signal intensity in the blue and green channels. In Figure 56E the result of a dPCR with a *KEL* negative sample is depicted. Here, a strong signal for the *KEL2* is visible, and a few signals in the blue and green channels.

In conclusion, the technical validation for the *KEL* assay revealed a background of 0.10 %, and the limit of detection was set to 0.50 % *KEL1/KEL2* heterozygous plasma, which corresponds to a minimum *KEL1* allele presence of 0.25 %.

3.4 Validation of HPA Assays

As described in chapter 1.4, an incompatibility between mother and child regarding the human platelet antigens (HPA) status results in neonatal thrombocytopenia. An early recognition of this intolerance can lead to earlier treatment, and the prevention from bleedings and brain damage. The validation results of the HPA-1, -2, -3, -5, and human platelet antigen 15 are presented in the following. The validation from HPA-1 and HPA-3 was proceeded for the a- as well as the b-allele. For HPA-2, -5, and -15, it was only possible to validate the b-allele due to limited samples regarding the a-variant. The validation experiments for HPA-2, -3, and -15 were conducted as part of a bachelor's thesis from Matthias Lemmer.

3.4.1 Validation of HPA-1

The HPA-1 incomparability is most responsible for neonatal thrombocytopenia formation (chapter 1.3.2 and 1.4). Besides detecting the HPA-1b signal in the background of HPA-1a, the more clinical relevance in the minor combination of a mother with HPA-1bb carrying an HPA-1a child. In this section, both variants were validated, and the results are presented.

Table 29: Validation results for HPA-1a and HPA-1b according to the established protocol. All experiments were performed in biological triplicates. SD: standard deviation.

% heterozygous plasma (% target allele)	HPA-1b			HPA-1a		
	Target copies/ μ l [mean \pm SD]	Total copies/ μ l [mean \pm SD]	Target/total in % [mean \pm SD]	Target copies/ μ l [mean \pm SD]	Total copies/ μ l [mean \pm SD]	Target/total in % [mean \pm SD]
5.00 (2.50)	46.14 \pm 4.20	1725.25 \pm 124.62	2.41 \pm 0.36	83.52 \pm 35.99	3086.29 \pm 730.65	2.32 \pm 1.01
1.00 (0.50)	17.04 \pm 5.90	2355.06 \pm 757.02	0.76 \pm 0.31	22.08 \pm 21.23	2096.32 \pm 600.88	0.63 \pm 0.73
0.50 (0.25)	9.55 \pm 4.45	1644.68 \pm 168.66	0.58 \pm 0.25	8.04 \pm 4.82	2134.79 \pm 1028.72	0.71 \pm 0.37
0.10 (0.05)	6.67 \pm 2.51	2239.56 \pm 994.30	0.31 \pm 0.03	1.38 \pm 0.08	1987.61 \pm 850.59	0.12 \pm 0.03
Background	4.39 \pm 0.17	1815.56 \pm 709.66	0.28 \pm 0.11	0.12 \pm 0.04	2756.70 \pm 2201.27	0.01 \pm 0.01

The validation started with the detection of the HPA-1b signal in a majority of HPA-1a. HPA-1a was used as the reference cfDNA and was detected in a range between 2355.06-1644.68 copies/ μ l. The target HPA-1b in the plasma dilution series containing HPA-1ab in a proportion of 5.00-0.10 % showed an even reduction of the HPA-1b signal from 46.14 copies/ μ l down to 6.67 copies/ μ l. The calculated target to total indicated a background of 0.28 %. A sample containing 5.00 % of HPA-1ab plasma was detected by our measurement with 2.41 %, and a sample with 1.00 % HPA-1ab proportion was identified with 0.76 %. The tests with 0.50 % were shown with 0.58 %, and with 0.31 %, the sample containing 0.10 % HPA-1ab could be detected. The detection limit was set to a minimum HPA-1ab proportion of 0.50 % because the background was similar to the 0.10 % sample at 0.28 % (Table 29).

For the detection of the HPA-1a signal, HPA-1b was used as a reference signal and was in a range of 3086.29-1987.61 copies/ μ l. As for the target recognition of the HPA-1b also the HPA-1a signal showed a regular decrease during the dilution series from 83.52-1.38 copies/ μ l. The calculation of the target to total indicated a background signal of 0.01 % with 0.12 copies/ μ l. The plasma mix containing 5.00 % HPA-1ab plasma, the a-allele was detected with 2.32 % (83.52 copies/ μ l) and the 1.00 % mixture was measured with 0.63 % (22.08 copies/ μ l) HPA-1a signals. The plasma mixtures with 0.50 % and 0.10 % HPA-1ab were detected with 0.71 % (8.04 copies/ μ l) and 0.12 % (1.38 copies/ μ l), respectively (Table 29). The threshold for the detection of HPA-1a in an HPA-1bb background was set to 0.10 % HPA-1a proportion.

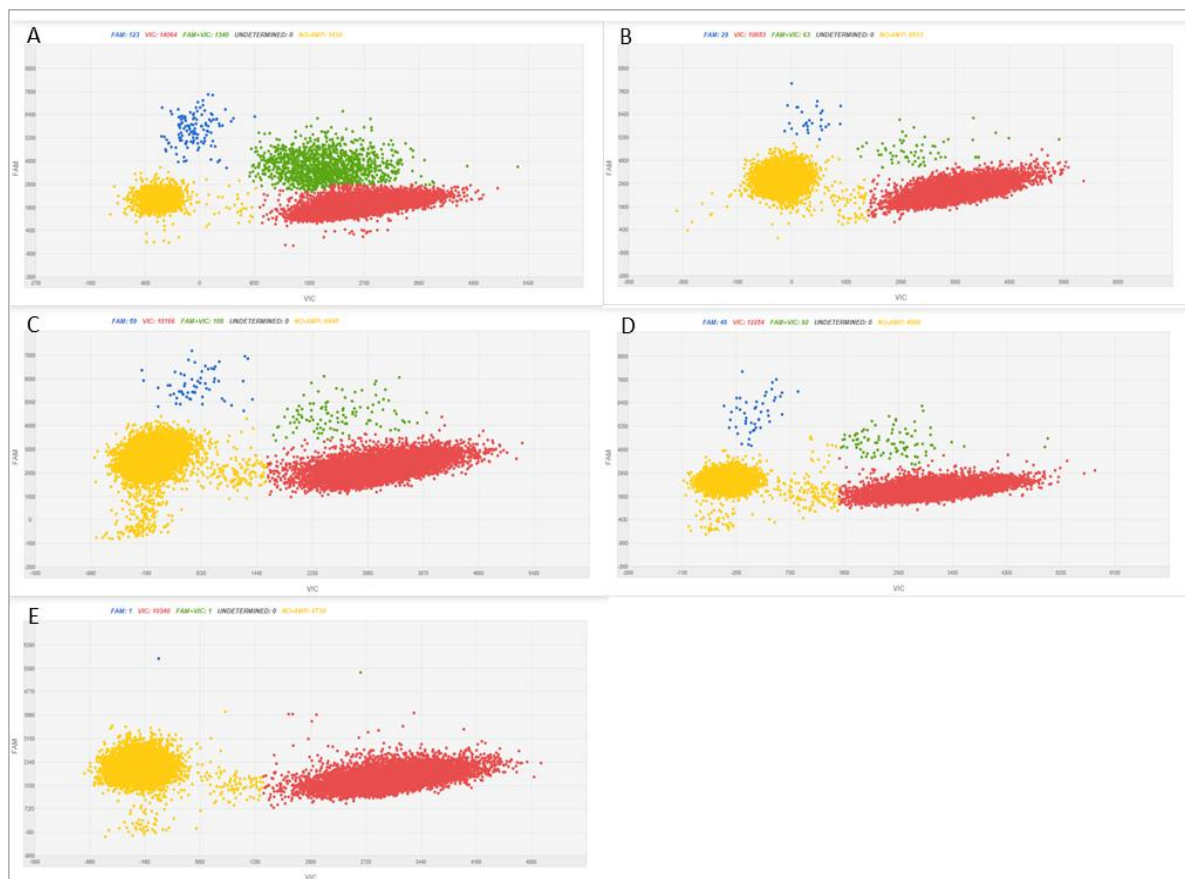


Figure 57: Visualization of the validation of the HPA-1a assay in the dilution series. The background was HPA-1bb, and the signal from HPA-1a was analyzed. All experiments were performed in biological triplicates. A: The mixture contained 5.00 % HPA-1ab DNA. B: Indicated an HPA-1ab proportion of 1.00 %. C: Plasma mixture with 0.50 % HPA-1ab positive proportion. D: The sample includes 0.10 % HPA-1ab positive proportion. E: HPA-1bb sample. Yellow dots indicated no amplification; red dots are signals of HPA-1bb, blue signals of *HPA-1a*, and green is the combination of HPA-1a and *HPA-1b*. X-axis: VIC color distribution; Y-axis: FAM color distribution; Picture from the QuantStudio™ 3D AnalysisSuite™ Cloud Software.

As shown in Figure 57, the signal intensity with reduced HPA-1a content is indicated by the decreased signal intensity in the blue and green channels. The clouds are separated and identifiable in all mixtures from 5.00 % down to 0.10 % (Figure 57A-D). In Figure 57E, a pure HPA-1bb sample is depicted, which shows only a strong signal for the HPA-1b in red but no HPA-1a signals (blue).

Taken together, the threshold for the HPA-1b identification was set to 0.50 % HPA-1ab plasma proportion, which equals an HPA-1b allele of 0.25 %. For the HPA-1a, the detection limit was defined to be 0.10 % HPA-1a plasma proportion corresponding to an HPA-1a allele presence of 0.05 %.

3.4.2 Validation of HPA-2

The HPA-2 is another platelet antigen out of the HPA family known to trigger neonatal thrombocytopenia (chapter 1.3.3 and 1.4). Unfortunately, it was only possible to validate the detection of HPA-2b because suitable plasmas were not available for the validation of HPA-2a.

3 RESULTS

Table 30: Validation results for HPA-2b according to the established protocol. All experiments were performed in biological triplicates. SD: standard deviation.

% heterozygous Plasma (% target allele)	HPA-2b		
	Target copies/ μ l [mean \pm SD]	Total copies/ μ l [mean \pm SD]	Target/total in % [mean \pm SD]
5.00 (2.50)	89.15 \pm 31.13	3914.33 \pm 2236.74	2.63 \pm 0.97
1.00 (0.50)	13.54 \pm 0.98	2616.77 \pm 816.08	0.56 \pm 0.16
0.50 (0.25)	20.24 \pm 3.02	3127.81 \pm 1002.62	0.67 \pm 0.16
0.10 (0.05)	3.57 \pm 0.05	2041.06 \pm 847.65	0.23 \pm 0.13
Background	1.32 \pm 0.83	2577.79 \pm 1555.30	0.05 \pm 0.01

This assay the reference was the HPA-2a signal, which was detected in a range between 3914.33-2041.06 copies/ μ l. For the target signal HPA-2b, the detection was reliable in the dilution series from 89.15 copies/ μ l with 5.00 % heterozygous plasma and 3.57 copies/ μ l for 0.10 % HPA-2ab proportion. The resulting target to total indicated for the 5.00 % mixture 2.63 %. In the mixture with 1.00 % HPA-2ab plasma the identification was around 0.56 % and 0.67 % when 0.50 % HPA-2ab plasma was used. For the detection of samples containing only 0.10 % HPA-2ab plasma, the ratio was 0.23 %. The background signal for this assay was identified with 0.05 % (Table 30).

Altogether, the background was determined with 0.05 %. As a result, the detection limit is 0.10 % HPA-2ab plasma, which corresponds to an HPA-2b presence of 0.05 %.

3.4.3 Validation of HPA-3

The HPA-3 validation was conducted for the a- as well as for the b-variant.

Table 31: Validation results for HPA-3a and HPA-3b according to the established protocol. All experiments were performed in biological triplicates. SD: standard deviation.

% heterozygous plasma (% target allele)	HPA-3b		
	Target copies/ μ l [mean \pm SD]	Total copies/ μ l [mean \pm SD]	Target/total in % [mean \pm SD]
5.00 (2.50)	140.80 \pm 14.81	3794.44 \pm 690.78	3.63 \pm 0.28
1.00 (0.50)	34.76 \pm 5.67	2301.35 \pm 728.79	1.56 \pm 0.24
0.50 (0.25)	2.95 \pm 1.27	6010.56 \pm 1451.59	0.05 \pm 0.02
0.10 (0.05)	1.73 \pm 0.54	5733.97 \pm 417.52	0.03 \pm 0.01
Background	1.76 \pm 1.01	2938.45 \pm 918.34	0.05 \pm 0.02
% heterozygous plasma (% target allele)	HPA-3a		
	Target copies/ μ l [mean \pm SD]	Total copies/ μ l [mean \pm SD]	Target/total in % [mean \pm SD]
5.00 (2.50)	108.15 \pm 9.70	3055.69 \pm 425.20	3.48 \pm 0.52
1.00 (0.50)	21.31 \pm 4.43	2798.59 \pm 578.22	0.76 \pm 0.13
0.50 (0.25)	20.54 \pm 4.60	2792.43 \pm 627.15	0.75 \pm 0.16
0.10 (0.05)	0.60 \pm 0.25	250.83 \pm 304.50	0.03 \pm 0.02
Background	0.56 \pm 0.19	2466.96 \pm 1137.74	0.03 \pm 0.01

As a reference signal in the HPA-3b assay, the HPA-3a signal was used. The detection range was between 2301.35-6010.56 copies/ μ l. Testing the HPA-3b signal's strength of detectability by reducing the HPA-3ab proportion revealed a reduction from 140.80 copies/ μ l in a 5.00 % mixture to 1.73 copies/ μ l in a mixture with 0.10 % HPA-3ab plasma. Out of the two parameters, total copies/ μ l and target copies/ μ l, the target to total ratio was calculated (chapter 2.14). The background for the HPA-3b assay was evaluated with 0.05 %. An approach containing 5.00 % HPA-3ab plasma indicated a ratio of 3.63 % and 1.56 % in the validation using 1.00 % HPA-3ab plasma. The experiments containing 0.50 % target plasma, the ratio was 0.05 %, and the approach containing 0.10 % heterozygous plasma the target was identified with a 0.03 % (Table 31). Due to the SNP's challenging detection from the HPA-3b, the detection limit was set to 1.00 %.

In the HPA-3a validation, signals from HPA-3b were used as basic quantity and were in a range of 3055.69-250.83 copies/ μ l. In a 5.00 % HPA-3ab mixture, the target's detection was 108.15 copies/ μ l and reduced to 0.60 copies/ μ l in samples with 0.10 % HPA-3ab plasma. This results in a detection ratio of 3.48 % in a mixture containing 5.00 % HPA-3ab plasma and 0.76 % for a 1.00 % mixture. This is similar to the validation with 0.50 % heterozygous plasma showing a ratio of 0.75 %, and a mixture with 0.10 % HPA-3ab plasma the a-allele was detected with a 0.03 % which was equal to the background signal (Table 31). Therefore, the detection limit was set to at least 0.50 % of the HPA-3ab proportion.

In summary, the detection limit for identifying the HPA-3b signal was set to 1.00 % HPA-3 heterozygous plasma, corresponding to an allele proportion of 0.50 %. For the evidence of the HPA-3a, at least 0.50 % of heterozygous plasma is needed, which indicates an allele presence of 0.25 %.

3.4.4 Validation of HPA-5

As described in chapter 1.3.5, the HPA-5 is located on GPIa. The validation of this antigen was only possible for the b-allele due to the available plasma restriction.

Table 32: Validation results for HPA-5b according to the established protocol. All experiments were performed in biological triplicates. SD: standard deviation.

% heterozygous plasma	HPA-5b		
	Target copies/ μ l	Total copies/ μ l	Target/total in %
(% target allele)	[mean \pm SD]	[mean \pm SD]	[mean \pm SD]
5.00 (2.50)	25.79 \pm 4.67	1354.06 \pm 151.06	1.91 \pm 0.47
1.00 (0.50)	20.36 \pm 23.14	2633.93 \pm 2730.62	0.55 \pm 0.28
0.50 (0.25)	1.82 \pm 1.12	2289.81 \pm 1388.33	0.08 \pm 0.00
0.10 (0.05)	2.64 \pm 1.59	2252.96 \pm 1224.51	0.13 \pm 0.06
Background	2.09 \pm 1.38	2952.09 \pm 2077.46	0.07 \pm 0.01

This assay's basic quantity is the HPA-5aa, which was detected in a range of 2952.09-1354.06 copies/ μ l. The mixture with 5.00 % HPA-5ab was recognized with 25.79 copies/ μ l, and the 0.10 % mixture was shown with 2.64 copies/ μ l. The background consisting of the HPA-5aa signals was for this approach 0.07 % target to total. A mixture containing 5.00 % HPA-5ab, the b-allele, was identified with 1.91 %. The sample mixture with 1.00 % HPA-5ab positive plasma revealed a b-allele presence of 0.55 %. Mixtures containing 0.50 % or 0.10 % HPA-5ab plasma were both identified with 0.08 % and 0.13 % respectively, which corresponded with the background (Table 32).

Taken together, the detection limit for the HPA-5b assay was set to 1.00 %, corresponding to an HPA-5b allele presence of 0.50 %.

3.4.5 Validation of HPA-15

The HPA-15 is the third most common cause of neonatal thrombocytopenia. Therefore, the early identification of incompatibility between mother and child is essential. A noninvasive blood test stating the fetus's HPA-15 status can help prevent severe damages to the child as early as possible.

Table 33: Validation results for HPA-15b according to the established protocol. All experiments were performed in biological triplicates. SD: standard deviation.

% heterozygous plasma (% target allele)	HPA-15b		
	Target copies/ μ l [mean \pm SD]	Total copies/ μ l [mean \pm SD]	Target/total in % [mean \pm SD]
5.00 (2.50)	97.00 \pm 61.07	2535.28 \pm 1488.39	3.66 \pm 0.38
1.00 (0.50)	44.73 \pm 25.31	1610.40 \pm 735.43	2.58 \pm 1.01
0.50 (0.25)	23.43 \pm 9.97	3152.88 \pm 2030.40	0.85 \pm 0.19
0.10 (0.05)	8.85 \pm 4.74	2865.53 \pm 1528.24	0.31 \pm 0.00
Background	0.25 \pm 0.13	3788.14 \pm 1692.19	0.01 \pm 0.00

The reference signal consisting of HPA-15a was detected in a range between 3788.14-1610.40 copies/ μ l. In the approach containing 5.00 % HPA-15ab positive plasma, around 97.00 copies/ μ l HPA-15b signals were detected, and for the mixture with 0.10 % heterozygous HPA-15 plasma 8.85 copies/ μ l. Calculation of the parameter target copies/ μ l and total copies/ μ l result in the target to total ratio (chapter 2.14). In a mixture containing 5.00 % of HPA-15ab plasma, the b-allele was detected with 3.66 %. For a mixture containing 1.00 % heterozygous target plasma the ratio was 2.58 %. A further reduction of the heterozygous plasma to 0.50 % was still identified with 0.85 %, and in a mixture of 0.10 % HPA-15ab plasma the targeted b-allele was identified with 0.31 %. This assay background was HPA-15a and had a false positive signal for HPA-15b of 0.01 % (Table 33).

In conclusion, due to the little background, a secure detection of a fetus's HPA-15b status can be conducted with a minimum of 0.50 % HPA-15ab plasma proportion in a plasma mixture, which equals an allele frequency of 0.25 %.

3.5 Validation of Gonosomal and Autosomal Markers

Besides identifying the targeted blood cell antigens, in case of a negative test result, it must be ensured that there is really enough cell-free fetal DNA and that it is not degraded too much. In the following chapter, cffDNA markers are validated, one gender-specific and one via autosomal markers.

3.5.1 Validation of Amelogenin

For fetal control, amelogenin (AMEL X/Y) was used as a marker, which usually encodes the enamel. The difference between the female and male variants is indicated by a 6 bp deletion [188].

Table 34: Validation results for AMEL-X/Y according to the established protocol. All experiments were performed in biological triplicates. SD: standard deviation.

% heterozygous plasma	Target copies/ μ l	AMEL-Y	
		Total copies/ μ l	Target/total in %
(% target allele)	[mean \pm SD]	[mean \pm SD]	[mean \pm SD]
5.00 (2.50)	6.44 \pm 2.16	223.10 \pm 186.72	4.20 \pm 1.70
1.00 (0.50)	4.84 \pm 6.19	210.14 \pm 190.64	1.34 \pm 1.01
0.50 (0.25)	0.42 \pm 0.20	332.85 \pm 255.40	0.23 \pm 0.18
0.10 (0.05)	0.24 \pm 0.14	239.14 \pm 256.10	0.23 \pm 0.20
Background	0.16 \pm 0.07	131.77 \pm 83.67	0.14 \pm 0.05

As for the other assays, the validation was conducted with a dilution series containing two individuals by mixing heterozygous plasma from 5.00-0.10 % in exchange for homozygous plasma 95.00-99.90 %. The AMEL-X signals were analyzed for the basis quantity, which was detected between 332.85-131.77 copies/ μ l. In the dilution series, the AMEL-Y target sequence was identified with 6.44 copies/ μ l in a mixture containing 5.00 % male plasma and 0.24 copies/ μ l in a mixture with 0.10 % male plasma. The calculated target to total ratio indicated for the mixture with 5.00 % male proportion a ratio of 4.20 %. The mixture with 1.00 % male fraction was detected with 1.34 %. Samples with 0.50 % and 0.10 % were recognized with 0.23 %. The background measurement using only a female sample indicated false-positive signals of 0.14 % (Table 34). According to this result, the detection limit for this assay was set to 1.00 % male proportion.



Figure 58: Visualization of the validation of the AMEL-X/Y assay in the dilution series. All experiments were performed in biological triplicates. A: The mixture contained 5.00 % AMEL-X/Y DNA. B: Indicated an AMEL-X/Y proportion of 1.00 %. C: Plasma mixture with 0.50 % AMEL-X/Y positive proportion. D: Sample includes 0.10 % AMEL-X/Y positive proportion. E: Female sample only. Yellow dots indicated no amplification. red dots are signals of AMEL-X, blue signals of AMEL-Y, and green is the combination of AMEL-X and AMEL-Y. X-axis: VIC color distribution; Y-axis: FAM color distribution; Picture from the QuantStudio™ 3D AnalysisSuite™ Cloud Software.

The analysis of the dot plots after dPCR showed for the 5.00 % mixture in Figure 58A and for 1.00 % in Figure 58B good separated clouds. The 0.50 % sample shows only a few signals in the blue channel for the AMEL-Y and a low signal in the green channel. In the sample containing a 0.10 % male plasma, one cloud for the Y-chromosome could be identified (Figure 58D). The background shows only signals for of AMEL-X as expected.

Overall, the threshold for identifying the amelogenin signal from a male fetus in a plasma mixture was at a minimum of 1.00 %, which equals an AMEL-Y allele proportion of 0.50 %.

3.5.2 Validation of Autosomal SNPs

The use of the gonosomal marker amelogenin gives only information about a male fetus. In case of a negative result in this assay, it could be a female fetus, or the amount of cell-free fetal DNA was too low in order to identify the fetus. To elucidate this problem, autosomal single-nucleotide polymorphisms (SNP) from the SNPfor1D panel (chapter 1.5.3) were used to identify differences in autosomal SNPs between mother and child and prove that the cfDNA content is sufficient for analysis. Therefore, a negative result does not come from a too low cfDNA amount. The validation of the autosomal marker was intended as a proof of principle. Thus, the a- or b-allele was tested in a 1.00 % plasma mixture and not the hole dilution series, as shown for the other assays. It should be noted that only two samples instead of three could be used for the SNP2a, SNP5a, SNA8a, and SNP9a. For the background validation of SNP4a, only one donor was available.

3 RESULTS

Table 35: Results for anonymous SNPs according to the established protocol. All experiments were performed in biological triplicates. SD: standard deviation, * only two samples for background determination available ** only one sample for background determination available.

Target	% heterozygous plasma (%target allele)	Target copies/ μ l [mean \pm SD]	Total copies/ μ l [mean \pm SD]	Target/Total [% mean \pm SD]
SNP1a	1.00% (0.50%)	3.49 \pm 1,22	760.86 \pm 368.15	0.52 \pm 0.16
rs1357617 (A)	0.00% (0.00%)	0.47 \pm 0,38	5123.21 \pm 926.32	0.01 \pm 0.01
SNP1b	1.00% (0.50%)	16.19 \pm 9.19	915.33 \pm 155.45	0.01 \pm 0.01
rs1357617 (T)	0.00% (0.00%)	0.0 \pm 0.0	6932.50 \pm 1925.80	0.00 \pm 0.00
SNP2a*	1.00% (0.50%)	112.69 \pm 74.5	2795.22 \pm 745.87	3.71 \pm 2.32
rs9171118 (C)	0.00% (0.00%)	0.19 \pm 0.11	3472.24 \pm 259.66	0.01 \pm 0.00
SNP2b	1.00% (0.50%)	16.71 \pm 10,59	2477.79 \pm 422.89	0.71 \pm 0.52
rs9171118 (T)	0.00% (0.00%)	3.53 \pm 3.76	2860.76 \pm 1109.43	0.11 \pm 0.09
SNP3a	1.00% (0.50%)	32.01 \pm 6.45	1204.24 \pm 245.95	2.72 \pm 0.78
rs1015250 (G)	0.00% (0.00%)	24.56 \pm 24.02	2449.89 \pm 130.78	1.04 \pm 1.02
SNP3b	1.00% (0.50%)	10.25 \pm 6.37	1339.12 \pm 854.07	1.60 \pm 0.90
rs1015250 (C)	0.00% (0.00%)	1.75 \pm 2.42	2708.91 \pm 1202.85	0.06 \pm 0.07
SNP4a**	1.00% (0.50%)	5.84 \pm 3.05	1477.93 \pm 817.52	0.41 \pm 0.22
rs722098 (A)	0.00% (0.00%)	0.08	2289.95	0.00
SNP4b	1.00% (0.50%)	11.32 \pm 6.57	737.27 \pm 97.23	1.51 \pm 0.95
rs722098 (G)	0.00% (0.00%)	1.17 \pm 0.54	1434.48 \pm 440.99	0.09 \pm 0.05
SNP5a*	1.00% (0.50%)	35.77 \pm 17.14	2129.60 \pm 1232.58	1.76 \pm 0.22
rs733164 (G)	0.00% (0.00%)	111.13 \pm 94.92	1792.22 \pm 1528.68	5.82 \pm 0.03
SNP5b	1.00% (0.50%)	41.13 \pm 34.84	2797.28 \pm 538.88	1.26 \pm 0.95
rs733164 (A)	0.00% (0.00%)	0.10 \pm 0.04	2461.87 \pm 1213.22	0.01 \pm 0.00
SNP6b	1.00% (0.50%)	17.13 \pm 11.60	1639.44 \pm 1370.28	1.16 \pm 0.35
rs2056277 (T)	0.00% (0.00%)	0.18 \pm 0.04	2796.08 \pm 907.23	0.01 \pm 0.00
SNP7b	1.00% (0.50%)	3.57 \pm 1.23	2054.77 \pm 932.61	0.19 \pm 0.08
rs2056277 (C)	0.00% (0.00%)	2.01 \pm 2.68	2885.55 \pm 1175.44	0.14 \pm 0.20
SNP8a*	1.00% (0.50%)	8.92 \pm 4.33	609.67 \pm 64.06	1.52 \pm 0.80
rs2830795 (A)	0.00% (0.00%)	0.07 \pm 0.00	5968.09 \pm 2807.85	0.00 \pm 0.00
SNP8b	1.00% (0.50%)	27.05 \pm 7.66	735.51 \pm 270.65	3.72 \pm 0.93
rs2830795 (G)	0.00% (0.00%)	0.37 \pm 0.28	6654.74 \pm 2251.76	0.01 \pm 0.01
SNP9a*	1.00% (0.50%)	18.13 \pm 11.62	1090.37 \pm 70.30	1.57 \pm 0.93
rs1028528 (A)	0.00% (0.00%)	0.97 \pm 0.52	3622.20 \pm 573.33	0.03 \pm 0,01
SNP9b	1.00% (0.50%)	5.98 \pm 5.34	952.00 \pm 375.65	0.63 \pm 0.55
rs1028528 (G)	0.00% (0.00%)	1.60 \pm 1.51	4795.94 \pm 364.84	0.03 \pm 0.03

The background of SNP1a was indicated by 0.47 copies/ μ l, which results in a target to total of 0.01 %. Samples containing 0.50 % of the targeted a-allele were indicated by a ratio of 0.52 %, with an average of 3.49 copies/ μ l. For the SNP1b allele, a ratio of 0.01 % with 16.19 copies/ μ l was detected while the background signal was defined with 0.00 copies/ μ l; consequently, the target to total ratio is 0.00 %. The background signals for SNP2a and SNP2b were 0.01 % and 0.11 % with false-positive signals of 0.19 copies/ μ l and 3.53 copies/ μ l, respectively. Tests containing 1.00 % plasma of the SNP2ab indicated a ratio of 3.71 % with 112.69 copies/ μ l for SNP2a and 16.71 copies/ μ l for SNP2b. SNP3a and SNP3b were indicated with a background ratio of 1.04 % with 24.56 copies/ μ l and 0.06 % with 1.75 copies/ μ l, respectively. Investigations with 1.00 % plasma proportions containing SNP3a revealed 32.01 copies/ μ l and a ratio of 2.72 %. The SNP3b showed 10.25 copies/ μ l and a ratio of 1.60 %. For the background determination of SNP4a, only one sample was available and showed a ratio of 0.00 % with 0.08 copies/ μ l. The SNP4b background was registered with a ratio of 0.09 % and 1.17 copies/ μ l. The test with a 0.50 % SNP4a- allele revealed 5.84 copies/ μ l and a ratio of 0.41 % and SNP4b showed 11.32 copies/ μ l with a ratio of 1.51 %. During the SNP5a allele analysis, a background of 5.82 % with 111.13 copies/ μ l was identified, and the 1.00 % SNP5ab plasma mixture was recognized with 35.77 copies/ μ l for SNP5a and a ratio of 1.76 %. The SNP5b showed a background of 0.01 % with 0.10 copies/ μ l, and the analysis with a 1.00 % plasma mixture demonstrated a ratio of 1.26 % and 41.13 copies/ μ l for SNP5b. SNP6b was documented with a background of 0.00 % and 0.18 copies/ μ l. The test with 1.00 % SNP6ab plasma was identified with 17.13 copies/ μ l for SNP6b resulting in a target to total ratio of 1.16 %. The background validation of SNP7b revealed a ratio of 0.14 % with 2.01 copies/ μ l. A 1.00 % mixture indicated a ratio of 0.19 % with 3.57 copies/ μ l for SNP7b. During the validation of the background of SNP8a and SNP8b, a ratio of 0.00 % with 0.07 copies/ μ l was found for SNP8a and 0.01 % with 0.37 copies/ μ l for SNP8b. Tests concerning the target allele showed a 1.52 % ratio with 8.92 copies/ μ l and 3.72 % with 27.05 copies/ μ l, respectively. SNP9a and SNP9b were indicated with a background ratio of 0.03 % and 0.97 copies/ μ l and 1.60 copies/ μ l, respectively. The target allele was detected with 1.57 % and 18.13 copies/ μ l for SNP9a. SNP9b was shown with 0.63 % and 5.98 copies/ μ l (Table 35).

In summary, the proof of principle analysis for nine SNPs with their two different alleles from the *SNPforID* penal was successful. In 14 assays, the target was identified in a 1.00 % plasma mixture, which corresponds to a target allele presence of 0.50 %.

3.6 Summary of Technical Validation

After the protocol development was completed, a technical validation was conducted to analyze sensitivity and specificity for the various blood cell and platelet antigens'. Dilutions were made for all tests with heterozygous plasma from 5.00-0.10 % in exchange for homozygous plasma 95.00-99.90 %. All tests were conducted in biological triplicates.

The first validation series was made with the rhesus system. Here, the *RHD* exons 3, 5, and 7 were validated. The identified detection limit in a plasma mixture containing an *RHD/d* heterozygous donor was for exon 5, and 7 0.10 %, which corresponds to an *RHD* allele presence of 0.05 %. *RHD* exon 3 showed a higher threshold with 1.00 % indicating that at least 0.50 % *RHD* exon3 allele is needed for reliable detection.

The validation for the *KEL* assay revealed a detection limit 0.50 % plasma of a *KEL1/KEL2* heterozygous donor. This equals a *KEL1* allele proportion of 0.25 %.

For the platelet analysis, the five most common antigens, which can induce FNAIT, were tested. The assays for HPA-3b and 5b showed a threshold of 1.00 %, corresponding to an allele presence of 0.50 %, HPA-1b, and 3a indicated a detection limit of 0.50 %, indicating a target allele frequency of 0.25 %. The lowest detection limit in a plasma mixture was gained for the assays HPA-1a, -2b, and 15b with 0.10 %, which is comparable to a target allele presence of 0.05 %.

To show that cfDNA was analyzed, amelogenin was used as a gender marker and showed a detection limit of 1.00 % in a plasma mixture, which equals a Y-allele presence of 0.50 %. However, this marker only works for a male fetus. In the case of a female fetus, the signal melts with the X-chromosomal signal of the mother. Therefore, nine autosomal markers with their two alleles from the SNP *forID* panel were analyzed in a proof of principle test. Meaning, only the background and a plasma mixture containing 1.00 % target allele was analyzed. From the 16 assays, it was possible to identify the rare allele in 14 assays.

In conclusion, the technical validation showed assays with low detection limits. Now it is the challenge to confirm these promising results in a clinical validation.

3.7 Preliminary Results from Clinical Validation

The last section of this thesis is about clinical validation. The outcome of the technical validation showed promising results. However, the cell-free DNA origin differs from the cell-free fetal DNA (cffDNA) (chapter 1.5). To verify the robustness and sensitivity of the developed assays, a small clinical validation was conducted. The focus was on how the assays work with a stronger degraded fetal DNA and if the technical validation results could be confirmed. For the study, a network of resident gynecologists was set up to recruit 50 pregnant women. EDTA blood was collected, and mothers were pretyped for all assays. In the case of a homozygous result, the cfDNA from the mothers' plasma was extracted and analyzed with dPCR according to the developed protocol to predict the genotype of the unborn children (Figure 59). In 12 cases, buccal swabs or cord blood from the newborn children have been sent back and were used to verify the dPCR test results.

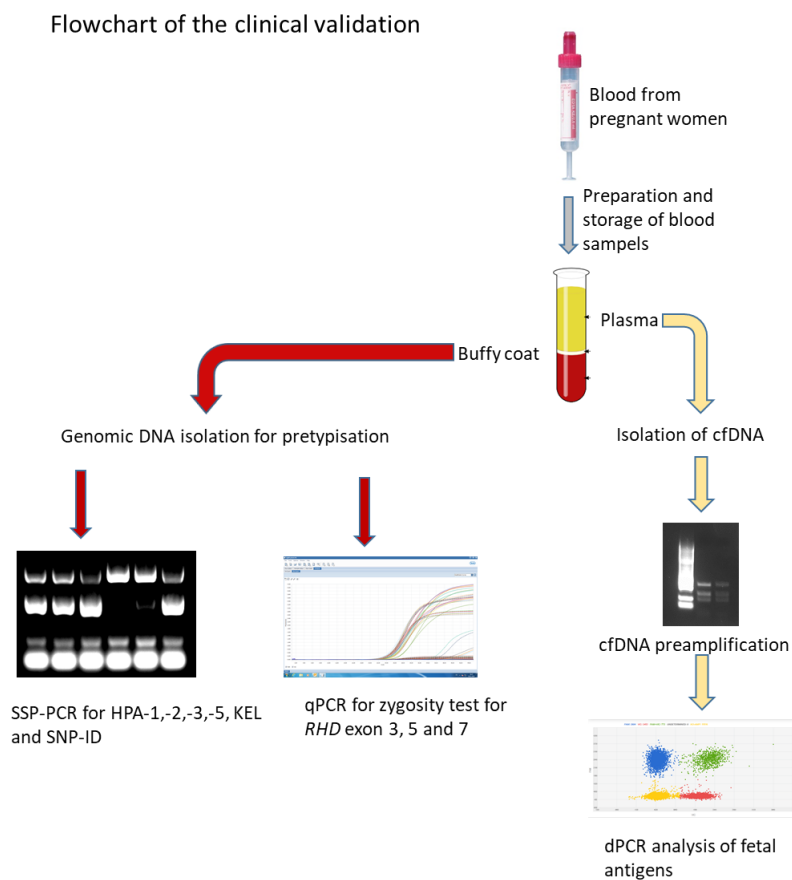


Figure 59: Flowchart of the clinical validation.

3.7.1 Clinical Validation of the *RHD* Assays

The clinical validation of the *RHD* genotype identification included exons 3, 5, and 7. In the first step, the mother's *RHD* status was tested by zygosity test (chapter 2.12). In the case of a D-negative woman, dPCR was conducted to identify the fetus's rhesus status.

Table 36: Overview of the clinical validation of the *RHD* assay. DPCR results from plasma DNA given in copies/ μ l (% target/total), GA, gestational age, nt, not tested.

Case No.	GA, week	<i>RHD</i> exon 3	<i>RHD</i> exon 5	<i>RHD</i> exon 7	Proposed Result	Tested genotype newborns
		dPCR result from plasma DNA	dPCR result from plasma DNA	dPCR result from plasma DNA		
1	38	207.95 (8.567)	1104.3 (14.003)	493.37 (11.887)	Dd	nt
2	34	0.0733 (0.353)	1.095 (0.12)	0 (0)	dd	nt
5	-	644.39 (9.18)	825.99 (9.787)	4513.8 (46.5)	Dd	nt
7	36	45.825 (1.555)	221.81 (3.042)	412.01 (13.582)	Dd	nt
8	33	17.779 (0.216)	20.217 (0.425)	65.333 (2.096)	Dd	nt
23	25	1.018 (1.055)	20.117 (0.372)	9.11 (3.17)	Dd	nt
25	9	21.996 (1.186)	16.108 (0.435)	15.664 (0.558)	Dd	nt
28	9	2.97 (15.888)	40.359 (1.236)	4.721 (20.541)	Dd	nt
32	24	3.0 (0.147)	54.161 (1.707)	82.615 (1.847)	Dd	nt
33	37	2.764 (22.983)	12.476 (0.439)	5.605 (29.011)	Dd	nt
34	13	113.12 (19.552)	1449.3 (35.183)	833.67 (41.498)	Dd	nt
36	-	73.747 (2.08)	0.218 (0.00289)	146.28 (12.153)	Dd	nt
39	26	4.334 (2.871)	1624.5 (52.716)	247.62 (9.476)	Dd	nt
44	33	0.0781 (0.00620)	0.922 (0.0259)	1.368 (0.0337)	dd	nt

The background determination was for *RHD* exon 3 around 0.08 copies/ μ l with a ratio of 0.18 %. For *RHD* exon 5, the average background was 0.75 copies/ μ l with 0.05 %, and in *RHD* exon 7, 0.68 copies/ μ l with a 0.02 % ratio. Two tests indicated a D-negative fetus (No. 1, No. 44). The number of detected target copies was in the middle 94.90 copies/ μ l, with a ratio of 7.11 % for *RHD* exon 3. *RHD* exon 5 was detected on average with 489.94 copies/ μ l and 10.85 % ratio, and *RHD* exon 7 was identified on average with 569.15 copies/ μ l and 16.03 %.

Of all tested pregnant women, 14 were tested as D-negative. Further analysis revealed 12 *RHD* positive fetuses and 2 *RHD* negative fetuses (Table 36). The test results were consistent in all investigated exons except number 36. Here the result of the exon 5 analysis indicated a negative outcome. But the other tests (*RHD* exon 3 and 7) were clear positive, so the *RHD* positive phenotype is proven. The decision between *RHD* positive and *RHD* negative was unambiguously visible in the copies/ μ l as well as the target/ total ratio.

A *RHD* negative result was indicated by a little copy number between 0.00 - 1.37copies/ μ l, and the percentage was always below 0 %. In the statistical analysis for the copies/ μ l in the *RHD* assays, the t-test was not applicable. Because the *RHD* negative fetuses' sample size was relatively small, and the dispersion of values in the *RHD* positive group was huge. Therefore, the Mann-Whitney-Test was applied. This test analyses if two independent groups have different tendencies. For the *RHD* exon 3 and 7 assays, a p-value of 0.02 was identified under clinical circumstances, which is significant at the 5.00 % level. The analysis of the *RHD* exon 5 revealed a p-value of 0.01, indicating that the difference between the background and *RHD* copies/ μ l are significantly different.

In conclusion the low background in the technical validation was confirmed in the clinical validation for *RHD* assays. *RHD* detection reliability revealed three tests with a high significance under clinical circumstances (exon 3 p = 0.02; exon 5 p = 0.01 exon 7 p = 0.02).

3.7.2 Clinical Validation of the KEL Assay

All 50 pregnant women were analyzed concerning their *KEL* status, and 49 were tested *KEL*1 negative. From all these women, a dPCR was conducted to evaluate the *KEL*1 status of the fetus.

Table 37: Overview of the clinical validation of the K1/K2 assay . DPCR results from plasma DNA given in copies/ μ l (% target/total), GA, gestational age, nt, not tested.

Case No.	GA, week	KEL1		
		dPCR result from plasma DNA	Proposed fetal genotype	Tested genotype newborns
1	38	0.22 (0.01)	kk	nt
2	34	0.08 (0.01)	kk	nt
3	9	0.00 (0.00)	kk	nt
4	39	0.00 (0.00)	kk	nt
5	-	0.00 (0.00)	kk	nt
6	23	0.07 (0.00)	kk	kk
7	36	0.15 (0.00)	kk	nt
8	33	0.08 (0.00)	kk	nt
9	29	0.26 (0.01)	kk	nt
10	11	0.30 (0.02)	kk	kk
11	21	0.08 (0.00)	kk	kk
12	23	0.00 (0.00)	kk	kk
13	26	0.07 (0.00)	kk	kk
14	18	0.41 (0.00)	kk	nt
15	39	0.51 (0.01)	kk	kk
17	10	0.07 (0.00)	kk	nt
18	33	0.34 (0.02)	kk	kk
19	25	0.30 (0.02)	kk	nt
20	26	0.00 (0.00)	kk	nt
21	25	0.08 (0.00)	kk	nt
22	24	0.00 (0.00)	kk	nt
23	25	0.28 (0.01)	kk	nt
24	9	0.14 (0.00)	kk	nt
25	9	1.32 (0.04)	kk	nt
26	24	0.49 (0.02)	kk	nt
27	9	0.67 (0.06)	kk	nt
28	9	0.00 (0.00)	kk	kk
29	6	0.00 (0.00)	kk	nt
30	24	0.08 (0.02)	kk	nt
31	24	0.10 (0.02)	kk	nt
32	24	0.08 (0.00)	kk	nt
33	37	0.13 (0.01)	kk	nt
34	13	0.74 (0.06)	kk	nt
35	12	0.07 (0.00)	kk	nt
36	-	0.00 (0.00)	kk	nt
37	20	0.06 (0.00)	kk	nt
38	25	0.29 (0.02)	kk	nt
39	26	0.07 (0.00)	kk	nt

41	26	0.18 (0.00)	kk	nt
42	27	0.33 (0.00)	kk	kk
43	26	0.59 (0.05)	kk	nt
44	33	0.83 (0.05)	kk	nt
45	25	0.08 (0.00)	kk	nt
46	12	0.33 (0.01)	kk	nt
47	-	0.40 (0.03)	kk	nt
48	15	0.00 (0.00)	kk	nt
49	23	0.00 (0.00)	kk	kk
50		0.40 (0.01)	kk	nt

In all tested plasmas, the fetal status was negative for KEL1. The target to total ratio was, on average, 0.01 % with 0.21 copies/ μ l for KEL1. From the 49 test results, it was possible to verify the plasma results with genomic DNA of ten newborn. All test results have been confirmed as correct (Table 37, gray shading). The test results were correctly determined independently from the gestational week. However, the earliest week for *KEL* assay analysis was the 6th week, but the most premature pregnancy with a confirmed result was the 9th week.

Taken together, the background determined in the clinical validation was significantly lower as in the technical validation ($p = 2.27 \cdot 10^{-10}$).

3.7.3 Clinical Validation of the HPA Assays

As already introduced is an incomparability between mother and child for HPA (human platelet antigen), a reason for the development of Fetal and neonatal alloimmune thrombocytopenia (FNAIT) (chapter 1.4). On the contrary to the rhesus test, which is already established as routine screening in some countries, for now, there is no test for HPA-1,2,3 and 5 in the routine available to estimate the fetal risk for FNAIT [156-158, 160, 161, 169]. In the technical validation, it was possible to develop assays for HPA-1, -2, -3, and -5. The results of the clinical validation are presented in the following section. It is to mention that the results from the HPA-2, and -3 are gained during a bachelor thesis from M. Lemmer.

3.7.3.1 HPA-1

The analysis regarding the identification of the human platelet antigen 1b (HPA-1b) in a majority of HPA-1a is shown in table 38. 30 out of the 50 pregnant women were tested HPA-1a homozygous, and their plasma was further analyzed with dPCR to identify the fetal HPA-1 status.

Table 38: Overview of the clinical validation of the HPA-1b allele. DPCR results from plasma DNA given in copies/ μ l (% target/total), GA, gestational age, nt, not tested.

Case No.	GA, week	HPA-1b		
		dPCR result from plasma DNA	Proposed fetal genotype	tested genotype newborns
3	9	0.44 (0.01)	HPA-1aa	nt
5	-	0.07 (0.00)	HPA-1aa	nt
6	23	0.37 (0.02)	HPA-1aa	HPA-1aa
7	36	0.07 (0.00)	HPA-1aa	nt
9	29	2.24 (0.21)	HPA-1aa	nt
10	11	1.04 (0.34)	HPA-1aa	HPA-1aa
12	23	0.29 (0.01)	HPA-1aa	HPA-1aa
14	18	0.71 (0.01)	HPA-1aa	nt

3 RESULTS

15	39	3.46 (0.08)	HPA-1ab	HPA-1ab
17	10	1.60 (0.09)	HPA-1aa	nt
19	25	0.79 (0.13)	HPA-1aa	nt
20	26	0.56 (0.02)	HPA-1aa	nt
25	9	0.91 (0.12)	HPA-1aa	nt
26	24	3.60 (0.34)	HPA-1ab	nt
27	9	0.74 (0.27)	HPA-1aa	nt
28	9	0.67 (0.17)	HPA-1aa	HPA-1aa
29	6	1.88 (0.58)	HPA-1aa	nt
30	24	1.29 (0.24)	HPA-1aa	nt
32	24	0.78 (0.07)	HPA-1aa	nt
33	37	0.60 (0.23)	HPA-1aa	nt
35	12	93.37 (13.84)	HPA-1ab	nt
39	26	2.02 (0.19)	HPA-1aa	nt
40	28	0.78 (0.01)	HPA-1aa	nt
44	33	1.35 (0.95)	HPA-1aa	nt
45	25	2.75 (0.16)	HPA-1ab	nt
46	12	1.28 (0.13)	HPA-1aa	nt
47	-	2.85 (0.14)	HPA-1aa	nt
48	15	0.60 (0.03)	HPA-1aa	nt
49	23	0.15 (0.01)	HPA-1aa	HPA-1aa
50		0.32 (0.01)	HPA-1aa	nt

The determination of the background out of the 26 HPA-1aa fetuses was, on average, 0.94 copies/ μ l with 0.15 %. Four women showed a signal for HPA-1ab with 25.80 copies/ μ l resulting in a ratio of 3.60 %. The earliest pregnancy week for the identified HPA-1b allele was the 12th week (no 35). In six cases, the dPCR results were verified with genomic DNA from born children (grey shading). All tested children matched the proposed fetal genotype regarding the HPA-1 status. For statistical analysis, the t-test was used. The hypothesis that the background of the data from HPA-1aa is different from the HPA-1ab data, is significant at the 5.00 % level with $p = 0.002$.

To investigate the HPA-1a allele recognition in the clinical application, the number of test subjects was minor. Only three of the 50 mothers were tested HPA-1bb.

Table 39: Overview of the clinical validation of the HPA-1a allele. DPCR results from plasma DNA given in copies/ μ l (% target/total), GA, gestational age, nt, not tested.

Case No.	GA, week	HPA-1-a		
		dPCR result from plasma DNA	Proposed fetal genotype	Tested genotype newborns
23	25	5.18 (0.24)	HPA-1-ab	nt
24	9	0.82 (0.02)	HPA-1-bb	nt
37	20	0.08 (0.01)	HPA-1-bb	nt

The results of the dPCR from the cfDNA indicated two HPA-1bb and one HPA-1ab fetus. Unfortunately, a verification of the results was not possible. However, as shown in table 39, the difference between the homozygous result and the HPA-1ab result was clearly identifiable in target to total ratio and copies/ μ l. However, the number of test results was too small to determine meaningful results.

In conclusion, the HPA-1b assay background was in the clinical validation unambiguously lower than in the technical validation ($p = 2.87 \cdot 10^{-9}$). The detection of the b-allele in the

clinical validation was very reliable, so that the target signal was significantly higher than the background ($p = 0.002$).

3.7.3.2 HPA-2

Out of the 50 study participants, 40 were tested as human platelet antigen 2a (HPA-2a) homozygous. From these women, the cfDNA was analyzed with dPCR regarding the HPA-2b allele.

Table 40: Overview of the clinical validation of the HPA-2b allele. DPCR results from plasma DNA given in copies/ μ l (% target/total), GA, gestational age, nt, not tested.

Case No.	GA, week	HPA-2b		
		dPCR result from plasma DNA	Proposed fetal genotype	Tested genotype newborns
1	38	2.19 (0.05)	HPA-2-aa	nt
2	34	0.15 (0.00)	HPA-2-aa	nt
3	9	1.40 (0.03)	HPA-2-aa	nt
4	39	0.08 (0.00)	HPA-2-aa	nt
5	-	0.00 (0.00)	HPA-2-aa	nt
6	23	1.76 (0.07)	HPA-2-aa	aa
7	36	0.00 (0.00)	HPA-2-aa	nt
8	33	0.15 (0.01)	HPA-2-aa	nt
9	29	0.48 (0.01)	HPA-2-aa	nt
10	11	1.36 (0.09)	HPA-2-aa	aa
11	21	0.24 (0.00)	HPA-2-aa	aa
12	23	22.96 (0.29)	HPA-2-ab	ab
13	26	2.60 (0.08)	HPA-2-aa	aa
15	39	0.77 (0.04)	HPA-2-aa	aa
16	7	1.54 (0.15)	HPA-2-aa	aa
17	10	2.17 (0.10)	HPA-2-aa	nt
18	33	2.55 (0.06)	HPA-2-aa	aa
19	25	1.17 (0.09)	HPA-2-aa	nt
20	26	3.02 (0.10)	HPA-2-aa	nt
21	25	130.77 (1.45)	HPA-2-ab	nt
22	24	1.00 (0.06)	HPA-2-aa	nt
23	25	11.60 (0.46)	HPA-2-ab	nt
24	9	2.84 (0.06)	HPA-2-aa	nt
25	9	1.71 (0.05)	HPA-2-aa	nt
28	9	0.78 (0.08)	HPA-2-aa	aa
29	6	1.57 (0.12)	HPA-2-aa	nt
31	24	1.48 (0.06)	HPA-2-aa	nt
32	24	1.56 (0.04)	HPA-2-aa	nt
33	37	1.96 (0.06)	HPA-2-aa	nt
35	12	0.48 (0.10)	HPA-2-aa	nt
36	-	0.08 (0.01)	HPA-2-aa	nt
37	20	25.81 (0.45)	HPA-2-ab	nt
38	25	6.24 (0.50)	HPA-2-ab	nt
41	26	6.65 (0.09)	HPA-2-aa	nt
42	27	1.24 (0.04)	HPA-2-aa	aa

3 RESULTS

43	26	1.34 (0.11)	HPA-2-aa	nt
45	25	1.61 (0.03)	HPA-2-aa	nt
47	-	1.76 (0.09)	HPA-2-aa	nt
48	15	0.27 (0.01)	HPA-2-aa	nt
49	23	0.08 (0.00)	HPA-2-aa	ab

The background was estimated from the 35 HPA-2aa results and indicated an average of 1.37 copies/ μ l with 0.05 % ratio. Whereas the amount of b-allele was identified on average with 39.47 copies/ μ l and 0.65 %. From the 40 tested mothers, it was possible to verify the dPCR results with genomic DNA from 11 born children. One of the children, No. 12, revealed a test result of HPA-2ab, which could be confirmed (Table 40). In nine cases, the predicted genotype HPA-2aa was approved by the genetic material of the children. In case No. 49, an inconsistent result was identified. The dPCR stated a clear signal for HPA-2aa, but in the PCR-SSP, which was used to analyze the genomic DNA, a heterozygous signal for HPA-2ab was identified. Nevertheless, the statistical analysis revealed a p-value of 8.37×10^{-6} which is significant at the 5.00 % level.

Table 41: Overview of the clinical validation of the HPA-2a allele. DPCR results from plasma DNA given in copies/ μ l (% target/total), GA, gestational age, nt, not tested.

HPA-2a				
Case No.	GA, week	dPCR result from plasma DNA	Proposed fetal genotype	Tested genotype newborns
27	9	6.09 (0.30)	HPA-2-ab	nt

For the HPA-2a allele analysis, only one test participant with HPA-2bb was identified (Table 41). The analysis identified a proposed genotype of HPA-2ab for the fetus, but it was impossible to verify this result with genomic DNA.

Taken together, the background measurement in the clinical study confirmed the value from the technical validation for the HPA-2b assay ($p = 0.49$). The identification of the targeted HPA-2b allele in the clinical analysis had a high strength ($p = 8.37 \times 10^{-6}$).

3.7.3.3 HPA-3

Sixteen participants of the NIPT study were tested homozygous for human platelet antigen 3a (HPA-3a). The subsequent analysis with dPCR identified 13 predicted genotypes with HPA-3aa and three with HPA-3ab (Table 42).

Table 42: Overview of the clinical validation of the HPA-3b allele. DPCR results from plasma DNA given in copies/ μ l (% target/total), GA, gestational age, nt, not tested.

HPA-3b				
Case No.	GA, week	dPCR result from plasma DNA	Proposed fetal genotype	Tested genotype newborns
2	34	0.07 (0.00)	HPA-3-aa	nt
4	39	0.94 (0.03)	HPA-3-aa	nt
5	-	0.90 (0.01)	HPA-3-aa	nt
7	36	0.47 (0.01)	HPA-3-aa	nt
8	33	0.90 (0.03)	HPA-3-aa	nt
9	29	0.08 (0.01)	HPA-3-aa	nt
11	21	3.96 (0.11)	HPA-3-ab	HPA-3-ab
12	23	1.07 (0.04)	HPA-3-aa	HPA-3-aa
13	26	0.64 (0.02)	HPA-3-aa	HPA-3-aa
22	24	1.56 (0.94)	HPA-3-ab	nt
23	25	3.42 (0.15)	HPA-3-aa	nt
35	12	0.41 (0.08)	HPA-3-aa	nt
36	-	0.17 (0.02)	HPA-3-aa	nt
45	25	0.45 (0.02)	HPA-3-aa	nt
47	-	7.20 (0.31)	HPA-3-ab	nt
49	23	1.42 (0.02)	HPA-3-aa	HPA-3-aa

In this assay, a background of 0.03 % with 0.84 copies/ μ l was determined. The proof of the b-allele showed, on average, 4.24 copies/ μ l and a ratio of 0.46 %. From the 16 predicted fetal genotypes, it was possible to verify four (gray shading). All proposed genotypes matched the genotype of the children. The earliest week of a verified analysis was the 21th week of gestation. The t-test revealed a highly significant result at the 5.00 % level with $p = 0.001$.

The distribution of HPA-3bb individuuum is lower than for HPA-3aa. Therefore, 6 of our participants were tested homozygous for the minor genotype.

Table 43: Overview of the clinical validation of the HPA-3a allele. DPCR results from plasma DNA given in copies/ μ l (% target/total), GA, gestational age, nt, not tested.

HPA-3a				
Case No.	GA, week	dPCR result from plasma DNA	Proposed fetal genotype	Tested genotype newborns
1	38	523.90 (8.79)	HPA-3-ab	nt
17	10	2.45 (0.13)	HPA-3-bb	nt
19	25	13.57 (2.43)	HPA-3-ab	nt
20	26	21.30 (1.55)	HPA-3-ab	nt
24	9	31.01 (1.64)	HPA-3-ab	nt
38	25	63.69 (8.50)	HPA-3-ab	nt

DPCR analysis of these six cases revealed one HPA-3bb fetus and five HPA-3ab fetuses. The difference between the HPA-3bb and HPA-3ab genotype was identifiable in the copies/ μ l and target/total ratio (Table 43). For the b-allele identification, an average of 130.70 copies/ μ l and a 4.58 % ratio was calculated.

Finally, comparing the HPA 3b background between the clinical and technical validation indicated no significant difference ($p = 0.07$). The proof of the b-allele detection in the clinical analysis was very robust with $p = 0.001$.

3.7.3.4 HPA-5

Participants of the NIPT study were tested for their human platelet antigen 5 (HPA-5) status, and 40 were HPA-5a homozygous. The fetal analysis results revealed 38 proposed fetal phenotypes with HPA-5aa and two with HPA-5ab (Table 44).

Table 44: Overview of the clinical validation of the HPA-5b allele. DPCR results from plasma DNA given in copies/ μ l (% target/total), GA, gestational age, nt, not tested.

Case No.	GA, week	HPA-5b		
		dPCR result from plasma DNA	Proposed fetal genotype	Tested genotype newborns
2	34	0.61 (0.01)	HPA-5aa	nt
3	9	0.37 (0.00)	HPA-5aa	nt
5	-	0.78 (0.02)	HPA-5aa	nt
6	23	1.94 (0.06)	HPA-5aa	HPA-5aa
8	33	1.53 (0.03)	HPA-5aa	nt
9	29	5.12 (0.06)	HPA-5aa	nt
10	11	6.41 (1.92)	HPA-5ab	HPA-5aa
11	21	0.47 (0.01)	HPA-5aa	HPA-5aa
12	23	0.31 (0.01)	HPA-5aa	HPA-5aa
13	26	0.51 (0.04)	HPA-5aa	HPA-5aa
14	18	0.25 (0.00)	HPA-5aa	nt
15	39	0.30 (0.01)	HPA-5aa	HPA-5aa
16	7	8.84 (0.23)	HPA-5aa	HPA-5aa
17	10	1.35 (0.11)	HPA-5aa	nt
18	33	0.55 (0.01)	HPA-5aa	HPA-5aa
19	25	3.44 (0.08)	HPA-5aa	nt
20	26	1.09 (0.03)	HPA-5aa	nt
21	25	0.07 (0.00)	HPA-5aa	nt
22	24	7.23 (0.37)	HPA-5aa	nt
23	25	0.68 (0.02)	HPA-5aa	nt
24	9	1.21 (0.02)	HPA-5aa	nt
26	24	1.73 (0.04)	HPA-5aa	nt
27	9	1.28 (0.08)	HPA-5aa	nt
28	9	0.55 (0.08)5	HPA-5aa	HPA-5aa
29	6	1.88 (0.04)	HPA-5aa	nt
30	24	1.96 (0.05)	HPA-5aa	nt
31	24	0.67 (0.08)	HPA-5aa	nt
32	24	2.44 (0.04)	HPA-5aa	nt
33	37	0.37 (0.00)	HPA-5aa	nt
34	12	45.60 (2.66)	HPA-5ab	nt

37	20	0.32 (0.01)	HPA-5aa	nt
40	28	5.56 (0.30)	HPA-5aa	nt
41	26	0.08 (0.00)	HPA-5aa	nt
43	26	0.47 (0.90)	HPA-5aa	nt
44	33	0.15 (0.08)	HPA-5aa	nt
45	25	0.86 (0.06)	HPA-5aa	nt
46	12	1.04 (0.14)	HPA-5aa	nt
47	-	1.72 (0.10)	HPA-5aa	nt
49	23	0.65 (0.01)	HPA-5aa	HPA-5aa
50	-	0.94 (0.08)	HPA-5aa	nt

For the background determination, the results of the 38 HPA-5-aa were used and indicated a ratio of 0.08 % with 1.56 copies/ μ l. The b-allele signal was identified on average with 26.00 copies/ μ l and a percentage of 2.29 %. Ten dPCR results could be verified by PCR-SSP analysis of the genomic material of the newborn children. Nine of them are in accordance with the predicted fetal genotype of the dPCR analysis. In case 10, a discrepancy was identified. The dPCR stated an HPA-5ab genotype and the PCR-SSP an HPA-5aa genotype.

Altogether, the background result of the technical validation corresponded with the clinical validation ($p = 0.33$). A statistical analysis of the clinical values regarding b-allele identification was significant ($p = 1.82 \cdot 10^{-8}$).

3.7.4 Clinical Validation of Amelogenin

During the analysis of blood cell antigens, a negative result must be secured to circumvent false-negative results. So, a negative outcome could be due to a too low amount of cfDNA, or the sample was too old, and the cfDNA was highly degraded, and no result could be gained. This must be considered when a negative result occurs. Therefore, the use of fetal markers is recommended. With the proof of the presence of a suitable amount of fetal DNA, a negative result could be trusted. In this thesis, ten fetal markers are applied. One is proof of gender, and the others are autosomal markers.

For the fetal gender test, the marker amelogenin (AMEL-X/Y) was used (chapter 1.5.3). The difference between X- and Y-chromosome is a 6 bp deletion in the female gene. All study participants were tested for fetal gender.

Table 45: Overview of the clinical validation of AMEL-X/Y. DPCR results from plasma DNA given in copies/ μ l (% target/total), GA, gestational age, nt, not tested.

Case No.	GA, week	AMEL-Y		
		dPCR result from plasma DNA	Proposed fetal genotype	Tested genotype newborns
1	38	0.54 (0.01)	XX	nt
2	34	46.87 (0.82)	XY	nt
3	9	0.55 (0.01)	XX	nt
4	39	2.52 (0.03)	XX	nt
5	-	0.17 (0.00)	XX	nt
6	23	0.29 (0.01)	XX	XX
7	36	7.99 (0.15)	XY	nt
8	33	0.38 (0.01)	XX	nt
9	29	0.15 (0.01)	XX	XX
10	11	15.91 (1.71)	XY	XY

3 RESULTS

11	21	20.13 (0.30)	XY	XY
12	23	0.32 (0.00)	XX	XX
13	26	15.87 (0.89)	XY	XY
14	18	0.32 (0.00)	XX	nt
15	39	101.70 (1.32)	XY	XY
16	7	0.29 (0.00)	XX	XY
17	10	0.95 (0.02)	XX	nt
18	33	5.71 (0.41)	XY	XX
19	25	0.23 (0.06)	XX	nt
20	26	0.49 (0.01)	XX	nt
21	25	0.87 (0.01)	XX	nt
22	24	0.65 (0.02)	XX	nt
23	25	0.38 (0.02)	XX	nt
24	9	0.72 (0.00)	XX	nt
25	9	0.76 (0.05)	XX	nt
26	24	0.14 (0.02)	XX	nt
27	9	0.14 (0.04)	XX	nt
28	9	9.43 (1.23)	XY	XY
29	6	0.09 (0.02)	XX	nt
30	24	8.73 (0.78)	XY	nt
31	24	0.20 (0.10)	XX	nt
32	24	0.15 (0.01)	XX	nt
33	37	25.01 (9.61)	XY	nt
34	13	0.26 (0.08)	XX	nt
35	12	193.12 (7.10)	XY	nt
36	-	0.59 (0.16)	XX	nt
37	20	0.00 (0.00)	XX	nt
38	25	22.58 (0.94)	XY	nt
39	26	0.34 (0.01)	XX	nt
40	28	0.15 (0.00)	XX	nt
41	26	42.73 (0.53)	XY	nt
42	27	6.20 (0.84)	XY	XY
43	26	1.39 (0.76)	XY	nt
44	33	0.07 (0.03)	XX	nt
45	25	3.82 (0.11)	XY	nt
46	12	4.18 (0.19)	XY	nt
47	-	92.36 (1.71)	XY	nt
48	15	0.00 (0.00)	XX	nt
49	23	0.32 (0.01)	XX	XX
50	-	0.33 (0.01)	XX	nt

18 male and 32 female fetuses were proposed. As shown in table 45, the difference between the X- and Y-specific signal was identifiable. For the X-signal, an average of 0.42 copies/ μ l resulting in a 0.02 % ratio, was gained. In a male fetus, the average copies were 34.65 copies/ μ l and a 1.63 % ratio. In 12 cases, the predicted gender was verified by the genomic DNA from the children. In 10 cases, the expected genotype matched the tested genotype. However, in cases 16 and 18, there was a discrepancy detected. Patient 16 showed a predicted female gender, but the verification with PCR-SSP showed a male genotype. In case 18, it's the other way around; the proposed gender was male, and the

PCR-SSP stated female. Despite the two different results, the statistical analysis was significant at the 5.00 % level, with a p-value of 0.0001.

Taken together, the background was in the clinical validation significantly lower compared to the technical verification ($p = 0.007$). The t-test analysis of the clinical results indicated a very significant difference between AMEL-X- and Y signals ($p = 0.0001$).

3.7.5 Clinical Validation of the Autosomal SNP Assays

The use of a gonosomal fetal marker has one huge disadvantage. In case of a AMEL-Y negative or female result with the amelogenin assay, it is the question if the fetus is really female. It could be possible that the DNA amount was too low, or the blood sample was too old, and therefore the cfDNA was strongly degraded. To answer this question, it was decided to test nine autosomal markers of the SNPforID panel for cfDNA proof.

3.7.5.1 SNP1

The pregnant women's analysis regarding their single nucleotide polymorphism 1 (SNP1) status indicated 18 women as SNP1b homozygous. Cell-free DNA of this woman was tested in order to identify the fetal SNP1 status.

Table 46: Overview of the clinical validation of SNP1a. DPCR results from plasma DNA given in copies/ μ l (% target/total), GA, gestational age, nt, not tested.

Case No.	GA, week	SNP1a		
		dPCR result from plasma DNA	Proposed fetal genotype	Tested genotype newborns
3	9	0.45 (0.02)	SNP1bb	nt
4	39	0.31 (0.01)	SNP1bb	nt
12	23	1.40 (0.08)	SNP1bb	SNP1bb
13	26	49.69 (3.52)	SNP1ab	SNP1ab
16	7	1.01 (0.054)	SNP1bb	SNP1bb
20	26	0.26 (0.00)	SNP1bb	nt
27	9	0.92 (0.02)	SNP1bb	nt
29	6	0.37 (0.01)	SNP1bb	nt
32	24	0.61 (0.02)	SNP1bb	nt
35	12	11.47 (0.21)	SNP1ab	nt
39	26	0.22 (0.00)	SNP1bb	nt
41	26	0.05 (0.00)	SNP1bb	SNP1bb
42	27	0.78 (0.02)	SNP1bb	SNP1bb
43	26	40.74 (8.31)	SNP1ab	nt
44	33	0.39 (0.00)	SNP1bb	nt
45	25	0.08 (0.00)	SNP1abb	nt
48	15	0.25 (0.00)	SNP1bb	nt
49	23	0.64 (0.01)	SNP1bb	SNP1bb

From all 18 tested participants, three fetuses were proposed as SNP1ab, and 15 were expected as SNP1bb (Table 46). The SNP1bb showed an average ratio of 0.02 %, and SNP1ab was identified in the mean with 4.01 %. The copy numbers/ μ l for SNP1ab were in the middle detected with 33.97 copies/ μ l, and in the case of homozygous SNP1b 0.52 copies/ μ l were found. In six cases, the results of the dPCR were verified (gray shading) and matched in all cases. The earliest week of gestation with a verified result was the 7th

week (case 16). A t-test assuming the same variance in the two groups indicated a $p = 6.61 \cdot 10^{-7}$ which is significant at the 5.00 % level.

During the clinical validation, six women with the SNP1aa were analyzed. The results are depicted in table 47 and show that in 6 tests, four cases are proposed as heterozygous and two as SNP1a homozygous.

Table 47: Overview of the clinical validation of SNP1b. DPCR results from plasma DNA given in copies/ μ l (% target/total), GA, gestational age, nt, not tested.

SNP1b				
Case No.	GA, week	dPCR result from plasma DNA	Proposed fetal genotype	Tested genotype newborns
8	33	1.28 (0.045)	SNP1aa	nt
18	33	510.01 (45.71)	SNP1ab	SNP1ab
24	9	1.97 (0.02)	SNP1aa	nt
28	9	2.53 (0.09)	SNP1ab	SNP1ab
30	24	0.08 (0.00)	SNP1ab	nt
40	28	177.14 (2.42)	SNP1ab	nt

The background was collected from the two SNP1aa values and showed a mean of 1.63 copies/ μ l and a 0.03 % ratio. The targeted b-allele showed, on average, 172.44 copies/ μ l and a ratio of 12.05 %. It was possible to confirm the predicted fetal genotype in two cases (Table 47, gray shading). Both matched with the tested genotype of the newborn. Due to the small number of samples, no statistical analysis was conducted.

In summary, the background for the SNP1a-assay in the clinical validation was identical to the technical validation value ($p = 0.42$). The statistical analysis from the data of the clinical study regarding the a-allele identification revealed a very significant difference between background and target ($p = 6.61 \cdot 10^{-7}$).

3.7.5.2 SNP2

Of the 50 participants, 26 were tested SNP2a homozygous, and the fetus's status was analyzed with dPCR according to the established protocol.

Table 48: Overview of the clinical validation of SNP2b. DPCR results from plasma DNA given in copies/ μ l (% target/total), GA, gestational age, nt, not tested.

SNP2b				
Case No.	GA, week	dPCR result from plasma DNA	Proposed fetal genotype	Tested genotype newborns
2	34	0.46 (0.01)	SNP2aa	nt
3	9	0.97 (0.01)	SNP2aa	nt
7	36	0.52 (0.01)	SNP2aa	nt
8	33	0.45 (0.01)	SNP2aa	nt
12	23	1.61 (0.33)	SNP2ab	SNP2ab
18	33	5.30 (0.34)	SNP2ab	SNP2ab
21	25	4.16 (0.07)	SNP2aa	nt
22	24	3.30 (0.31)	SNP2ab	nt
24	9	1.37 (0.02)	SNP2aa	nt
25	9	0.69 (0.06)	SNP2aa	nt

3 RESULTS

26	24	1.62 (0.33)	SNP2ab	nt
27	9	0.08 (0.04)	SNP2aa	nt
29	6	0.09 (0.03)	SNP2aa	nt
30	24	2.47 (0.24)	SNP2ab	nt
32	24	0.38 (0.03)	SNP2aa	nt
33	37	0.84 (0.07)	SNP2aa	nt
37	20	0.00 (0.00)	SNP2aa	nt
38	25	6.90 (0.55)	SNP2ab	nt
39	26	2.10 (0.77)	SNP2ab	nt
40	28	1.99 (0.07)	SNP2ab	nt
41	26	0.33 (0.02)	SNP2aa	SNP2aa
43	26	29.57 (7.05)	SNP2ab	nt
45	25	0.00 (0.00)	SNP2aa	nt
47	-	1.34 (0.08)	SNP2aa	nt
49	23	0.09 (0.00)	SNP2aa	SNP2aa
50	-	0.00 (0.00)	SNP2aa	nt

As shown in table 48, nine cases revealed a SNP2ab status. Analysis of the data showed a mean background signal of 0.03 % with 0.69 copies/ μ l. The identification of the b-allele was determined with an average of 1.11 % and 6.09 copies/ μ l. It was possible to check four cases (gray shading) with genomic DNA and compared the results with the proposed fetal genotype. In all cases, the presumptions were confirmed. The test of statistical significance at the 5.00 % level indicated a $p = 0.01$.

For the SNP2a identification, only two participants were identified, and the cfDNA was further tested.

Table 49: Overview of the clinical validation of SNP2a. DPCR results from plasma DNA given in copies/ μ l (% target/total), GA, gestational age, nt, not tested.

SNP2a				
Case No.	GA, week	dPCR result from plasma DNA	Proposed fetal genotype	Tested genotype newborns
1	39	16.90 (0.52)	SNP2ab	nt
36	-	0.88 (0.66)	SNP2bb	nt

As depicted in table 49, one test showed a SNP2ab and one an SNP2bb genotype. Since there was only one case of SNP2bb and SNP2ab, no average values could be collected. Unfortunately, there was no genomic material from children available to verify the results.

Altogether, the comparison of the background of the clinical and technical validation in the SNP2b assay indicated a significantly lower background in the clinic ($p = 0.01$). The t-test analysis between the SNP2aa and SNP2ab groups revealed a p-value of 0.01.

3.7.5.3 SNP3

Twenty-five pregnant women were tested SNP3a homozygous a further analysis of the cfDNA revealed 9 cases with SNP3ab and 16 SNP3aa.

Table 50: Overview of the clinical validation of SNP3b. DPCR results from plasma DNA given in copies/ μ l (% target/total), GA, gestational age, nt, not tested.

Case No.	GA, week	SNP3b		
		dPCR result from plasma DNA	Proposed fetal genotype	Tested genotype newborns
3	9	0.08 (0.01)	SNP3aa	nt
6	23	0.46 (0.74)	SNP3aa	SNP3aa
14	18	0.91 (0.13)	SNP3aa	nt
16	7	3.00 (0.52)	SNP3ab	SNP3ab
17	10	6.96 (0.62)	SNP3ab	nt
19	25	0.44 (0.27)	SNP3aa	SNP3aa
20	26	0.61 (0.90)	SNP3aa	nt
21	25	10.91 (0.29)	SNP3ab	nt
22	24	1.30 (0.27)	SNP3aa	nt
23	25	6.73 (0.88)	SNP3ab	nt
24	9	0.44 (0.01)	SNP3aa	nt
25	9	3.13 (0.45)	SNP3ab	nt
28	9	1.13 (0.26)	SNP3aa	SNP3aa
30	24	0.73 (0.08)	SNP3aa	nt
31	24	0.64 (1.36)	SNP3aa	nt
33	37	0.08 (0.00)	SNP3aa	nt
38	25	15.72 (2.82)	SNP3ab	nt
39	26	0.51 (0.42)	SNP3aa	nt
40	28	0.75 (0.04)	SNP3aa	nt
43	26	4.11 (1.54)	SNP3ab	nt
45	25	0.50 (0.10)	SNP3aa	nt
46	12	0.49 (0.11)	SNP3aa	nt
47	-	1.61 (0.18)	SNP3ab	nt
48	15	7.79 (0.20)	SNP3ab	nt
50	-	0.09 (0.00)	SNP3aa	nt

It can be seen that the copy number/ μ l in heterozygous cases is higher than in homozygous individuals (Table 50). In the middle, 6.58 copies/ μ l and 0.57 copies/ μ l, respectively. The mean ratio for a heterozygous SNP3 was around 0.83 %, and for homozygous SNP3 0.29 %. In four cases the predicted genotype was verified by genomic DNA and revealed a match in all cases (gray shading). The earliest confirmed investigation was in the 7th week of gestation. Also, here the t-test revealed a highly sensitive test with $p = 7.48 \cdot 10^{-6}$.

The analysis of the SNP3a revealed two cases out of 50, and the predicted genotype was for one fetus homozygous for the b-allele, and the other was heterozygous (Table 51).

Table 51: Overview of the clinical validation of SNP3a. DPCR results from plasma DNA given in copies/ μ l (% target/total), GA, gestational age, nt, not tested.

SNP3a				
Case No.	GA, week	dPCR result from plasma DNA	Proposed fetal genotype	Tested genotype newborns
7	36	2.22 (0.08)	SNP3bb	nt
11	21	1.86 (0.21)	SNP3ab	SNP3ab

Due to the small sample size, it was not possible to determine meaningful average values. The hetero- and homozygous type difference was identifiable by the target/total ratio (Table 51). For the homozygous, the ratio was 0.08 % and thus determined the background signal. The signal for the a-allele was identified with 0.21 %. It was possible to verify the proposed results successfully from case 11 with genomic DNA.

In conclusion, was the background in the technical validation identical to the clinical validation ($p = 0.05$). But the analysis between the homozygous and heterozygous groups in the clinical validation revealed a highly significant difference ($p = 7.48 \cdot 10^{-6}$).

3.7.5.4 SNP4

The for the SNP4 analysis women 23 were identified as homozygous for SNP4a. Thirteen children were proposed as SNP4ab and 10 with SNP4aa.

Table 52: Overview of the clinical validation of SNP4b. DPCR results from plasma DNA given in copies/ μ l (% target/total), GA, gestational age, nt, not tested.

SNP4b				
Case No.	GA, week	dPCR result from plasma DNA	Proposed fetal genotype	Tested genotype newborns
1	38	127.97 (6.14)	SNP4ab	nt
3	9	5.44 (0.28)	SNP4ab	nt
8	33	2.45 (0.03)	SNP4aa	nt
10	11	4.23 (7.11)	SNP4ab	SNP4ab
11	21	2.96 (0.33)	SNP4aa	SNP4aa
12	23	3.33 (1.06)	SNP4ab	SNP4ab
13	26	8.82 (1.75)	SNP4ab	SNP4ab
14	28	5.16 (0.22)	SNP4ab	nt
19	25	2.08 (1.18)	SNP4aa	SNP4aa
21	25	9.96 (0.22)	SNP4aa	nt
23	25	1.49 (0.45)	SNP4ab	nt
24	9	8.35 (0.23)	SNP4ab	nt
25	9	2.04 (0.34)	SNP4aa	nt
27	9	0.90 (0.47)	SNP4aa	nt
28	9	0.76 (0.27)	SNP4aa	SNP4aa
29	6	1.20 (0.84)	SNP4ab	nt
34	13	15.49 (5.40)	SNP4ab	nt
36	-	0.95 (0.50)	SNP4aa	nt
37	20	0.83 (0.01)	SNP4aa	nt
40	28	5.06 (0.24)	SNP4ab	nt
45	25	4.40 (0.33)	SNP4ab	nt

3 RESULTS

48	15	1.63 (0.02)	SNP4aa	nt
49	23	0.29 (0.00)	SNP4aa	SNP4aa

It was visible that in all heterozygous cases, the number of copies/ μ l were higher as in homozygous cases (Table 52). The mean copies for SNP4ab were 15.45 copies/ μ l, and the target/total ratio was 1.87 %. In SNP4aa cases, the mean ratio was 0.32 % with 1.49 copies/ μ l. It was possible to prove the predicted fetal genotype in 7 cases (gray shading), and all tests matched the assumption. The earliest verified test was in the 9th gestational week. The statistical analysis revealed a p-value of 0.08, which is not significant at the 5.00 % level.

For the SNP4b analysis, only two participants were found and analyzed. In both cases, a heterozygous fetal genotype was predicted. It is to mention that one pregnancy is 12th week and the other 37th week (Table 53). It could be seen, that in the late pregnancy the copies/ μ l, and the target to total ratio was higher. Due to the low number of test objects, it was not possible to determine meaningful average values.

Table 53: Overview of the clinical validation of SNP4a. DPCR results from plasma DNA given in copies/ μ l (% target/total), GA, gestational age, nt, not tested.

SNP4a				
Case No.	GA, week	dPCR result from plasma DNA	Proposed fetal genotype	Tested genotype newborns
33	37	A 34.39 (3.65)	SNP4ab	nt
46	12	A 5.39 (0.49)	SNP4ab	nt

In Summary, the comparison of the copies/ μ l of the background in the clinical and technical validation indicated $p = 0.29$. The t-test analysis of the clinical results revealed no significant differences between the background and the target ($p = 0.08$).

3.7.5.5 SNP5

Of the 50 study participants, 29 were tested SNP5aa, and the cfDNA was further analyzed in order to propose the fetal genotype.

Table 54: Overview of the clinical validation of SNP5b. DPCR results from plasma DNA given in copies/ μ l (% target/total), GA, gestational age, nt, not tested.

SNP5b				
Case No.	GA, week	dPCR result from plasma DNA	Proposed fetal genotype	Tested genotype newborns
3	9	0.47 (0.01)	SNP5aa	nt
4	39	0.66 (0.01)	SNP5aa	nt
5	-	0.15 (0.00)	SNP5aa	nt
7	36	0.32 (0.01)	SNP5aa	nt
8	33	0.27 (0.00)	SNP5aa	nt
10	11	18.92 (4.18)	SNP5ab	SNP5ab
11	21	1.09 (0.03)	SNP5aa	SNP5aa
12	23	2.90 (0.44)	SNP5ab	SNP5ab
13	26	0.78 (0.04)	SNP5aa	SNP5aa
15	39	1.16 (0.05)	SNP5aa	SNP5aa
16	7	1.74 (0.13)	SNP5aa	SNP5aa

17	10	11.31 (0.61)	SNP5ab	nt
19	25	10.37 (1.66)	SNP5ab	SNP5ab
21	25	4.92 (0.09)	SNP5aa	nt
22	24	15.08 (0.62)	SNP5ab	nt
25	9	9.39 (0.96)	SNP5ab	nt
27	9	0.24 (0.04)	SNP5aa	nt
28	9	4.55 (0.55)	SNP5ab	SNP5ab
30	24	0.41 (0.02)	SNP5aa	nt
31	24	21.19 (3.32)	SNP5ab	nt
32	24	0.08 (0.00)	SNP5aa	nt
33	37	54.47 (3.48)	SNP5ab	nt
35	12	34.05 (24.56)	SNP5ab	SNP5aa
36	-	0.40 (0.12)	SNP5aa	nt
38	25	1.62 (0.13)	SNP5aa	nt
40	28	0.30 (0.01)	SNP5aa	nt
46	12	4.56 (0.19)	SNP5ab	nt
47	-	0.83 (0.05)	SNP5aa	nt
49	23	1.47 (0.03)	SNP5aa	SNP5ab

Out of these 29 tests, 11 fetuses were predicted as SNP5ab and 18 as SNP5aa (Table 54). The background examination showed a mean of 0.94 copies/ μ l, which corresponds to a target to total of 0.04 %. The signal intensity for the SNP5ab allele was identified with an average of 16.98 copies/ μ l, resulting in a ratio of 3.69 %. It was possible to verify the test results from 10 children. In eight cases, the results were confirmed, but in two cases, No. 35 and 49, differences occurred. A closer look to case 35 revealed for the dPCR analysis an unusually high signal for SNP5ab. This test was proceeded twice with the same outcome. The genomic DNA analysis of the child revealed an SNP5aa genotype. The other inconsistency was found in case 49. Here, the dPCR analysis stated SNP5aa while the genomic DNA analysis with the PCR-SSP pointed to SNP5ab. Nevertheless, the t-test revealed a very significant test ($p = 6.49 \cdot 10^{-5}$).

For the investigation concerning the a-allele, two participants were typed with SNP5bb, and the research with dPCR lead to the predicted fetal genotype SNP5ab in both cases (Table 55). Due to the low number of tests, the average determination was not considered as meaningful.

Table 55: Overview of the clinical validation of SNP5a. DPCR results from plasma DNA given in copies/ μ l (% target/total), GA, gestational age, nt, not tested.

SNP5a				
Case No.	GA, week	dPCR result from plasma DNA	Proposed fetal genotype	Tested genotype newborns
24	9	49.04 (1.11)	SNP5ab	nt
29	6	2.28 (0.43)	SNP5ab	nt

Taken together, revealed the background comparison between the technical and clinical validation for the SNP5b assay a lower background in the technical validation ($p = 0.003$). The t-test analysis of the copies/ μ l regarding the identification of the b-allele indicated a very significant difference between background and target ($p = 6.49 \cdot 10^{-5}$).

3.7.5.6 SNP6

For the analysis of SNP6, 24 women were indicated as SNP6aa. Further investigations showed eight predicted fetal genotypes with SNP6ab and 16 with SNP6aa.

Table 56: Overview of the clinical validation of SNP6b. dPCR results from plasma DNA given in copies/ μ l (% target/total), GA, gestational age, nt, not tested.

SNP6b				
Case No.	GA, week	dPCR result from plasma DNA	Proposed fetal genotype	Tested genotype newborns
1	38	0.39 (0.01)	SNP6aa	nt
4	39	0.29 (0.01)	SNP6aa	nt
5	-	0.58 (0.02)	SNP6aa	nt
8	33	0.079 (0.00)	SNP6aa	nt
10	11	8.50 (3.96)	SNP6ab	SNP6ab
13	26	1.78 (0.07)	SNP6aa	SNP6aa
15	39	0.69 (0.01)	SNP6aa	SNP6aa
16	7	0.84 (0.16)	SNP6ab	SNP6ab
19	25	0.39 (0.11)	SNP6aa	SNP6aa
21	25	0.52 (0.01)	SNP6aa	nt
22	24	44.77 (1.17)	SNP6ab	nt
23	25	1.41 (0.12)	SNP6aa	nt
27	9	0.85 (0.08)	SNP6aa	nt
29	6	1.29 (0.14)	SNP6ab	nt
30	24	3.40 (0.12)	SNP6ab	nt
31	24	19.00 (1.81)	SNP6ab	nt
36	-	10.53 (3.23)	SNP6ab	nt
37	20	0.52 (0.01)	SNP6aa	nt
38	25	11.47 (0.46)	SNP6ab	nt
39	26	1.87 (0.05)	SNP6aa	nt
40	28	1.02 (0.02)	SNP6aa	nt
41	26	0.33 (0.01)	SNP6aa	SNP6aa
46	12	2.65 (0.07)	SNP6aa	nt
50	-	0.40 (0.01)	SNP6aa	nt

The difference between heterozygous and homozygous was often evident. The heterozygous genotype showed in the middle 12.47 copies/ μ l for the b-allele with a ratio of 1.38 %. In the case of a homozygous genotype, 0.86 copies/ μ l identified and a ratio of 0.04 %. In six cases, the verification with genomic material from the children matched the predicted genotype completely. The earliest week for a positive match was the 7th week of gestation (Table 56). A t-test with a level of significance of 5.00 % indicated a p-value of 0.002.

In two cases, the pregnant women were tested SNP6bb, and the dPCR analysis revealed a proposed fetal genotype of SNP6ab in both cases. It was possible to verify the test in case 18 with genomic DNA, which matched the results of the dPCR (Table 57). Based on the low number of tests, a mean was not calculated.

Table 57: Overview of the clinical validation of SNP6a. DPCR results from plasma DNA given in copies/ μ l (% target/total), GA, gestational age, nt, not tested.

SNP6a				
Case No.	GA, week	dPCR result from plasma DNA	Proposed fetal genotype	Tested genotype newborns
18	33	3.59 (0.14)	SNP6ab	SNP6ab
26	24	30.36 (6.67)	SNP6ab	nt

In conclusion, the background comparison between the two SNP6b validations revealed a lower background in the technical validation ($p = 3.21 \cdot 10^{-5}$). The statistical analysis of the clinical data showed a very reliable identification of the b-allele with $p = 0.002$.

3.7.5.7 SNP7

In the 50 participants in the NIPT-study, 39 were tested to be SNP7a homozygous. Further analysis with dPCR indicated eight fetuses with SNP7ab and 31 with SNP7aa (Table 58).

Table 58: Overview of the clinical validation of SNP7b. DPCR results from plasma DNA given in copies/ μ l (% target/total), GA, gestational age, nt, not tested.

SNP7b				
Case No.	GA, week	dPCR result from plasma DNA	Proposed fetal genotype	Tested genotype newborns
1	38	3.02 (0.11)	SNP7ab	nt
3	9	0.22 (0.01)	SNP7aa	nt
5	-	0.37 (0.01)	SNP7aa	nt
6	23	0.65 (0.07)	SNP7aa	SNP7aa
7	36	0.44 (0.02)	SNP7aa	nt
8	33	0.07 (0.00)	SNP7aa	nt
9	29	9.23 (1.32)	SNP7ab	SNP7ab
10	11	0.80 (0.16)	SNP7aa	SNP7aa
11	21	0.88 (0.02)	SNP7aa	SNP7aa
12	23	0.30 (0.03)	SNP7aa	SNP7aa
13	26	0.75 (0.02)	SNP7aa	SNP7aa
15	39	0.085 (0.00)	SNP7aa	SNP7aa
16	7	1.96 (0.09)	SNP7aa	SNP7aa
17	10	15.96 (0.46)	SNP7ab	nt
18	33	1.54 (0.11)	SNP7aa	SNP7aa
19	25	0.62 (0.57)	SNP7aa	SNP7aa
20	26	9.45 (0.89)	SNP7ab	SNP7ab
21	25	0.24 (0.00)	SNP7aa	nt
22	25	7.70 (0.37)	SNP7ab	nt
24	9	0.51 (0.01)	SNP7aa	nt
25	9	1.35 (0.07)	SNP7aa	nt
26	24	1.23 (0.10)	SNP7aa	nt
28	9	1.12 (0.13)	SNP7aa	SNP7aa
29	6	1.18 (0.14)	SNP7aa	nt
30	24	2.02 (0.10)	SNP7aa	nt
32	24	2.53 (0.06)	SNP7aa	nt

33	37	3.40 (0.13)	SNP7ab	nt
36	-	0.46 (0.18)	SNP7aa	nt
37	20	0.14 (0.01)	SNP7aa	nt
38	25	1.23 (0.06)	SNP7aa	nt
39	26	0.76 (0.03)	SNP7aa	nt
40	28	0.44 (0.02)	SNP7aa	nt
41	26	0.37 (0.02)	SNP7aa	SNP7aa
43	26	32.76 (3.07)	SNP7ab	nt
45	25	3.37 (0.12)	SNP7ab	nt
46	12	1.94 (0.07)	SNP7aa	nt
48	15	0.29 (0.01)	SNP7aa	nt
49	23	0.76 (0.03)	SNP7aa	SNP7aa
50	-	0.079 (0.00)	SNP7aa	nt

The background determination value was, on average, 0.82 copies/ μ l, and a ratio of 0.07 %. The b-allele signals were detected with a mean of 10.61 copies/ μ l and a ratio of 0.80 %. It was possible to prove the test results with the newborn children's genomic DNA in 14 cases. The result of this analysis was a full match. The statistical analysis with the assumption of the same variance between the two groups showed a highly significant test ($p = 9.18 \cdot 10^{-7}$).

Of all tested participants, only one was identified with SNP7bb and further analyzed with dPCR (Table 59). The predicted fetal genotype was heterozygous, but it was impossible to prove the results with genomic DNA.

Table 59: Overview of the clinical validation of SNP7a. DPCR results from plasma DNA given in copies/ μ l (% target/total), GA, gestational age, nt, not tested.

SNP7a				
Case No.	GA, week	dPCR result from plasma DNA	Proposed fetal genotype	Tested genotype newborns
34	13	18.47 (1.56)	SNP7ab	nt

Finally, it was shown that the background in the SNP7b assay was in the clinical validation lower as in the technical validation ($p = 0.03$). The identification of the targeted b-allele was compared to the background and indicated a significant difference ($p = 9.18 \cdot 10^{-7}$).

3.7.5.8 SNP8

To analyze the single nucleotide polymorphism 8b (SNP8b), it was possible to identify 27 study participants with SNP8aa. Further analysis indicated 18 proposed SNP8ab and 9 SNP8aa fetuses (Table 60).

Table 60: Overview of the clinical validation of SNP8b. DPCR results from plasma DNA given in copies/ μ l (% target/total), GA, gestational age, nt, not tested.

SNP8b				
Case No.	GA, week	dPCR result from plasma DNA	Proposed fetal genotype	Tested genotype newborns
1	38	14.20 (0.34)	SNP8ab	nt
2	34	2.49 (0.06)	SNP8aa	nt
3	9	0.65 (0.02)	SNP8aa	nt
4	39	0.77 (0.02)	SNP8aa	nt

5	-	0.08 (0.00)	SNP8aa	nt
7	36	3.13 (0.06)	SNP8aa	nt
9	29	32.91 (2.12)	SNP8ab	nt
10	11	1.99 (1.62)	SNP8ab	SNP8ab
11	21	4.68 (0.31)	SNP8ab	SNP8ab
16	7	8.94 (0.56)	SNP8ab	SNP8ab
18	33	9.37 (1.07)	SNP8ab	SNP8ab
21	25	1.24 (0.056)	SNP8aa	nt
22	25	23.94 (1.20)	SNP8ab	nt
24	9	0.98 (0.04)	SNP8aa	nt
25	9	7.14 (0.33)	SNP8ab	nt
26	24	21.55 (1.17)	SNP8ab	nt
27	9	12.47 (0.69)	SNP8ab	nt
28	9	10.76 (0.45)	SNP8ab	SNP8ab
29	6	7.45 (0.40)	SNP8ab	nt
30	24	16.67 (0.31)	SNP8ab	nt
31	24	10.82 (0.72)	SNP8ab	nt
33	37	30.56 (0.45)	SNP8ab	nt
34	13	7.88 (0.37)	SNP8ab	nt
35	12	17.24 (12.42)	SNP8ab	nt
41	26	2.25 (0.04)	SNP8aa	SNP8aa
42	27	8.55 (0.32)	SNP8ab	SNP8ab
50	-	1.22 (0.02)	SNP8aa	nt

The background was estimated from the average values of the SNP8aa results and indicated 1.42 copies/ μ l with a ratio of 0.03 %. The signal strength for the b-allele was around 13.73 copies/ μ l and a ratio of 1.38 %. In nine cases, the predicted fetal genotype was proved by genomic DNA and agreed perfectly. The earliest identification of a SNP8ab was received in the 7th week of gestation. The p-value was calculated with 0.0001, which is significant at the 5.00 % level.

The clinical validation of the a-allele revealed only two cases with SNP8bb. The tests with the dPCR indicated one genotype with SNP8ab and one with SNP8bb (Table 61). Genomic DNA could prove the homozygous test result from the born child.

Table 61: Overview of the clinical validation of SNP8a. DPCR results from plasma DNA given in copies/ μ l (% target/total), GA, gestational age, nt, not tested.

Case No.	GA, week	SNP8a		
		dPCR result from plasma DNA	Proposed fetal genotype	Tested genotype newborns
6	23	0.67 (0.04)	SNP8bb	SNP8-bb
46	12	6.70 (0.92)	SNP8ab	nt

Altogether, was the background in the technical validation compared to the clinical validation of the SNP8b assay lower ($p = 0.01$), but the comparison of the background and target b-allele in the clinical validation was very significant ($p = 0.0001$).

3.7.5.9 SNP9

For the SNP9, 24 participants were identified as single nucleotide polymorphism 9a (SNP9a) homozygous. The fetal analysis with dPCR indicated 17 proposed fetal genotypes with SNP9ab and 7 with SNP9aa (Table 62).

Table 62: Overview of the clinical validation of SNP9b. DPCR results from plasma DNA given in copies/ μ l (% target/total), GA, gestational age, nt, not tested.

SNP9b				
Case No.	GA, week	dPCR result from plasma DNA	Proposed fetal genotype	Tested genotype newborns
6	23	0.55 (0.18)	SNP9aa	SNP9aa
7	36	0.52 (0.01)	SNP9aa	nt
10	11	3.02 (0.40)	SNP9ab	SNP9ab
11	21	0.29 (0.00)	SNP9aa	SNP9aa
12	23	95.82 (2.77)	SNP9ab	SNP9ab
14	18	0.03 (1.56)	SNP9aa	nt
16	7	3.17 (0.77)	SNP9ab	SNP9ab
17	10	12.72 (0.36)	SNP9ab	nt
19	25	5.10 (0.23)	SNP9ab	SNP9ab
21	25	1.05 (0.02)	SNP9aa	nt
23	25	10.16 (0.23)	SNP9ab	nt
25	9	7.26 (0.21)	SNP9ab	nt
27	9	7.92 (0.28)	SNP9ab	nt
29	6	9.72 (0.27)	SNP9ab	nt
31	24	6.37 (0.41)	SNP9ab	nt
35	12	16.17 (0.57)	SNP9ab	nt
36	-	1.23 (0.41)	SNP9ab	nt
41	26	1.51 (0.04)	SNP9aa	SNP9aa
42	27	32.85 (1.32)	SNP9ab	SNP9ab
44	33	4.53 (0.61)	SNP9ab	nt
45	25	6.82 (0.29)	SNP9ab	nt
46	12	9.97 (0.94)	SNP9ab	nt
47	-	5.74 (0.43)	SNP9ab	nt
49	23	1.10 (0.00)	SNP9aa	SNP9aa

Out of the nine predicted SNP9aa fetuses, a background was estimated with 0.72 copies/ μ l and a ratio of 0.26 %. The mean signal strength for the b-allele was 14.03 copies/ μ l, and a ratio of 0.62 %. In nine cases, the predicted results could be successfully confirmed by the children's genetic material (gray shading). The earliest proven result was the 7th week of gestation. A t-test revealed the significance of $p = 0.013$.

For the analysis of SNP9bb women, three cases were tested. Two were predicted to be SNP9bb and one SNP9ab, which could be confirmed by genomic DNA (Table 63). Out of the low number of tests, an average was not calculated.

Table 63: Overview of the clinical validation of SNP9a. DPCR results from plasma DNA given in copies/ μ l (% target/total), GA, gestational age, nt, not tested.

Case No.	GA, week	SNP9a		
		dPCR result from plasma DNA	Proposed fetal genotype	Tested genotype newborns
9	29	7.36 (0.16)	SNP9ab	SNP9ab
20	26	1.57 (0.03)	SNP9bb	nt
24	9	0.07 (0.00)	SNP9bb	nt

Taken together, the number of copies/ μ l in the background of the SNP9b assay in the clinical validation was not significantly different to the technical validation ($p = 0.13$). In the clinical validation was the b-allele identification substantially different from the background ($p = 0.01$).

3.8 Summary of Clinical Validation

During the clinical validation, blood samples of 50 women were investigated regarding their fetal status with the various assays. The participants were between 6-39 weeks of pregnancy, giving an average of 20.8 weeks. A 9 ml EDTA blood tube was collected, and the genomic DNA was used to create a genetic profile from the mother for all assays. In assays in which the mothers were homozygous, the cfDNA was isolated from the plasma according to the developed protocol. The determination of the *RHD* status was conducted by determining the presence of *RHD* exons 3, 5, and 7. The background was between 0.75 copies/ μ l (*RHD* exon 5) and 0.02 % for *RHD* exon 7. The signal for the presence of the *RHD* gene was shown in 12 cases. Here, *RHD* exon 3 showed the lowest target to total ratio and, additionally, the lowest number of detected copies/ μ l. The highest target to total ratio was *RHD* exon 7 with 16.03 % and 569.15 copies/ μ l. In case 36, the test results were positive for *RHD* exon 3 and 7 and negative for *RHD* exon 5. Overall, the discrepancy between negative and positive was very high ($p = 0.02$ for exon 3 and 7; exon 5 $p = 0.006$) in this assays and showed that this assays have the potential to be used at the end of the first trimester onwards due to the low background.

The second blood antigen, which was validated, was KEL. Here, KEL1 differs from KEL2 by an SNP. Since around 92% of the population is KEL1 negative, it was impossible to detect a KEL1 positive fetus in the sample size of 50 pregnant women. Therefore, only the low background could be determined, which theoretically makes it possible to recognize a KEL1 fetus already in early pregnancy.

Furthermore, platelet antigens 1,2,3, and 5 were examined by detection of different SNPs. A low background characterized the assays regarding the a-allele detection, ranging from 0.15-0.03 %; the number of target copies ranged from 1.56-0.84 copies/ μ l. In the case of the detection of the b-allele, the target to total ratio was between 0.46-3.60 % with 4.24-39.47 copies/ μ l. The statistical analysis with t-test showed that in all tests, the identification of the targeted allele was significantly higher as the background (HPA-1b $p = 0.02$; HPA-2b $p = 8.37 \cdot 10^{-6}$; HPA-3b $p = 0.001$ and HAP-5b $p = 1.83 \cdot 10^{-8}$) The earliest gestational age of a correct predicted SNP was the 7th week of gestation in the HPA-5 assay. A total of 31 tests to verify the cfDNA analysis were carried out in all HPA assays. In two cases, discrepancies were identified. First, in the HPA-2 assay, a homozygous genotype was proposed in case 49, and a heterozygous genotype was identified with PCR-SSP with the child's genetic material. The second was in case 11 in the HPA-5 assay. A heterozygous genotype was predicted with dPCR, and a homozygous was detected with PCR-SSP using genomic material of the child.

For the fetal markers the gonosomal marker, amelogenin, and nine autosomal markers from the SNPforID panel were used. The gender-related fetal marker amelogenin detects a 6 bp deletion, which is located on the X-chromosome. All 50 test participants were examined for

the gender of the child. A girl's value was equivalent to the background and was, on average, 0.08 % and 1.56 copies/ μ l. In a male fetus, the numbers were significantly higher (34.65 copies/ μ l and 2.63 %), revealing a p-value of 0.0001. Of the 50 tests, 12 could be verified. The suspected genotype was confirmed in 10 participants. However, there were discrepancies in the two tests. In case 16, a girl was identified in the cfDNA, and the cross-check indicated a boy. In case 18, it was precisely the opposite. Possible causes are discussed in detail in the discussion section (chapter 4.3).

Since a negative value in the amelogenin assay is not necessarily a female fetus, it could also be that the cffDNA content was too low or too degraded. It is therefore advisable to use a gender-independent marker. For this purpose, nine markers from the SNPforID panel were used in this work. It turned out that this SNP analysis is also useful as a fetal marker for early pregnancy. The background for analyzing the b-alleles of the different SNPs was between 0.02 % for SNP1 and 0.32 % for SNP4. The number of copies/ μ l was between 0.52 copies/ μ l for SNP1 and SNP3 and 1.49 copies/ μ l for SNP4. The signal strength of the b-allele was between 0.62 % (SNP9) and 4.01 % (SNP1), and the detected copy number was between 6.09 copies/ μ l for SNP2 and 33.97 copies/ μ l for SNP1. The statistical investigation indicated that besides the SNP1 and SNP4 assay, all others had had low p-values, which were significant at the 5.00 % level. In all 257 SNP examinations, 70 could be checked. There were discrepancies in two cases. One in SNP5 case 35, the genotype SNP5ab, was predicted in the dPCR, but the PCR-SSP revealed SNP5aa. Another inconsistency was found in SNP5 case 49. Here, a homozygous genotype was proposed via dPCR, but a heterozygote genotype was identified in the verification.

Nevertheless, this assay is highly applicable for early pregnancy use because, in 7 SNP-assays, it was possible to get verified results in the 7th week of gestation.

A total of 535 dPCR tests were performed during the clinical validation, of which 126 could be checked using genomic DNA from the children. In 6 cases (4.76%), there were different results. But with a few adaptations this error rate could be reduced.

4 DISCUSSION

In the following section the results of the protocol development, assay validation and the results of the clinical validation are critically discussed.

4.1 Optimization of the Protocol

Many small steps were analyzed and checked in the development of the protocol. For example, it turned out that it is better to elute the cfDNA with ddH₂O than AVE buffer. Because the composition of the AVE buffer, which stabilizes the DNA, influences the dPCR. It was shown that cffDNA eluted with AVE buffer generated in the dPCR more unspecific signals. Furthermore, it was investigated which plasma volume is most suitable. In the end, no significant difference between plasma volume and dPCR result was identified. However, there was a connection between cfDNA yield and used plasma volume, in unmixed samples, the cfDNA content increased the more plasma was used. This is in accordance with Devonshire et al.'s results, which showed a linear relationship between volume and yield [243].

Of course, various cfDNA isolation methods were also investigated. MagMAX kit from Thermo Fisher, QIAmp Circulating Nucleic Acids Kit from Qiagen, and Maxwell[®]RSC from Promega were analyzed. Isolation with the MagMAX kit appears to be the most unsuitable one. On the one hand, the cfDNA yield was very fluctuating, and a downstream analysis showed hardly any signals in the dPCR. The other method was the Maxwell[®]RSC Instrument. The cfDNA yield was lower compared to QIAmp Circulating Nucleic Acids Kit, but promising results were achieved in the dPCR. Therefore, the Maxwell[®]RSC is an excellent alternative to QIAmp Circulating Nucleic Acids Kit when small optimizations are carried out since the Maxwell[®]RSC works fully automatically, which is a huge advantage. The QIAmp Circulating Nucleic Acid Kit isolation performed best. The cfDNA content was the highest compared to the other methods. The test results in the dPCR were excellent without further optimizations.

Several working groups compared different isolation methods. They agreed that QIAmp Circulating Nucleic Acid Kit showed the best results in efficiency and that the yield was always one of the best. Followed by Maxwell[®]RSC, which was similar in the DNA yield to QIAmp Circulating Nucleic Acids Kit. In comparison, the MagMAX kit performed worst [243-246]. Overall, when using the same plasma, it was found that isolation with different methods made a clear difference in yield and efficiency [243].

However, the signal strength in dPCR was still too low in our tests to allow fetal analysis in early pregnancy, so a signal enhancement by whole genome amplification was tried. Unfortunately, this did not succeed. A successful signal amplification using whole genome amplification was achieved by Reid et al. with very high sensitivity. They used circulating tumor cells instead of cffDNA [247]. Unluckily, no cfDNA tests were found with whole genome amplification, but other cfDNA tests were very successful due to targeted preamplification. It was thus possible to detect multiple cancer-relevant mutations within tumor-derived samples with a sensitivity of up to 0.01 %, as well as high reproducibility and accuracy [248, 249]. Also, in this work, the targeted preamplification showed the desired results. However, the chips for the dPCR were overloaded, and the optimal number of molecules per chip were determined using a dilution series, which indicated $4 \cdot 10^6$ molecules as optimal.

Although the developed protocol works excellently, it is possible to carry out further optimizations. Firstly, the blood collection should be revised because the EDTA tubes used in this work have the disadvantage that genomic DNA is released by lysis of the cells very soon. A direct comparison between EDTA tubes and special blood collection tubes (BCT) showed that the cffDNA fraction in BCTs was significantly higher (4-24 %) than in EDTA tubes (0.1-2 %) [250]. The longer the storage period, the higher the genomic DNA content, which shifts the outcome, as it is more challenging to identify the fetal DNA. It was shown that storage at 4 °C for 72 h in sodium citrate tubes is well suited too [251]. For blood storage

from 7 to 14 days, Streck cell-free DNA BCT and Cell-Free DNA Collection Tubes from Roche should be mentioned. Many studies have shown that BCTs can prevent an increase of cfDNA during storage at room temperature [252-256]. It has been demonstrated that cell-free DNA BCT from Streck stabilizes the blood cells without formaldehyde and does not affect the existing cfDNA [256]. Therefore it is expected that there will be no problems with the dPCR.

Using BCTs it could be investigated whether a preamplification is still necessary or how the target to total ratio may change. Maybe the number of cycles can be reduced during preamplification. One goal should be to eliminate the need to dilute the sample after preamplification. Therefore, a reduced number of cycles in the preamplification or the use of BCTs could also be useful because such preamplification and dilution steps are a potential source of errors. During the development of the protocol, but also later in the validation process, it was noticed that the same sample showed different strengths of false-positive signals in several dPCR runs. Such a phenomenon was also identified by Jackson et al. and could be remedied by replacing the TaqMan polymerase with a high-fidelity polymerase [248]. Such an exchange should at least be considered for the assays, in which the sensitivity was low. Because by reducing the false positive signals, the target to total ratio will be shifted, and the test becomes more sensitive. The development of new dPCR devices should also be pursued further. For example, there are already dPCR devices on the market that have a 3-color detection system, and thus it would be possible to run two assays on one chip [257].

The gold standard in the NIPT is currently the use of qPCR. However, especially in early pregnancy or in samples where the fetal fraction is low, qPCR is not suitable. In a study by Sillence et al., it was shown that in samples with a suboptimal fetal fraction (< 2 %), the use of qPCR for single-copy targets (like RHD exon 5) is rather unsuitable. In comparison, the dPCR achieved 100 % sensitivity for these targets [250].

4.2 Technical Validation of the Assays

After the protocol development was accomplished, the sensitivity and specificity was analyzed in a technical validation for the various blood cell and platelet antigen assays. Dilutions were made for all tests with heterozygous plasma from 5.00-0.10 % in exchange for homozygous plasma 95.00-99.90 %. All tests were conducted in biological triplicates. A total of 4×10^6 molecules were used per dPCR analysis.

The first validation series was made with the rhesus system. One reason for the development of MHN is the mother and child's incompatibility regarding the rhesus gene (chapter 1.1.1 and 1.2). To circumvent MHN, all RhD negative pregnant women receive immunoglobulins. However, treatment is only necessary for women who expect an RhD positive child. Thus, RhD negative women with a RhD negative child are unnecessarily exposed to IgG treatment's side effects or risks. Therefore, it is recommended to develop a test to identify whether the fetus is RhD positive or RhD negative. So only women carrying an RhD positive child receive the treatment. This *RHD*-assay shows the presence or absence of an entire gene. Here, the RHD exons 3, 5, and 7 were validated.

The identified detection limit for *RHD* exon 5 and 7 was 0.05 %. This means that, it is possible to identify with the dPCR in an volume of 1,000 μ l plasma in which are 999.00 μ l homozygous material the 1.00 μ l with heterozygous material. Only *RHD* exon 3 had a relatively low sensitivity with 0.50 %.

RHD genotyping is already a standard application in many countries. E.g., in Denmark and parts of England, pregnant women in the 25th gestational week are examined for the fetuses' rhesus status. These tests are carried out with qPCR. However, there is no published sensitivity to such a test. Thus, the high sensitivities obtained with the dPCR cannot be compared with the literature in this area. So only the standard sensitivity of 2 % of the qPCR can be assumed [250]. The data of this validation indicate a sensitivity far below this 2 % between 0.5-0.05 % depending on the assay.

Morbus haemolyticus neonatorum (MHN) can also be caused by the antibody formation against KEL1. Compared to MHN induced by anti-D, the titer level is not related to the

disease's severity. Were the RhD positive or negative phenotype is due to the presence or absence of the rhesus gene, the Kell phenotype is caused by an SNP (chapter 1.1.2). The identification of this base exchange could be worked out excellently with the developed protocol. KEL1 was reliably identified with a detection limit of 0.25 %. For the *KEL* assay validation, KEL2 served as an internal control.

A working group has also created a dilution series for *KEL* genotyping. Dilutions of 15, 10, and 5 % were created, and the 5 % could be reliably detected with the qPCR [170]. This is far beyond this thesis's results because a mixture of 5.00 % heterozygous KEL1/KEL2 plasma was the highest concentration used. A danish group analyzed spiked DNA with NGS and postulated a sensitivity of 0.5 % to detect the polymorphism behind the KEL blood group [183]. With the digital PCR's help, it was possible to identify KEL1 in a mix containing 0.25 % KEL1. This shows how sensitive the dPCR can identify SNPs and opens up many other areas of application for this method.

An incompatibility between mother and child regarding the platelet antigens can induce neonatal alloimmune thrombocytopenia (FNAIT). An untreated FNAIT leads to bleedings and brain damage or even the child's death (chapter 1.4). With an early identification, bleedings can be circumvented by immunoglobulin administration or platelet transfusions [126-131]. The leading cause for FNAIT is the HPA-1 incomparability, followed by HPA-2 and -15. Compared to the RH blood group, where the risk of having an MHN starts with the 2nd pregnancy, a platelet intolerance is already a problem in the 1st pregnancy.

Besides, the difference between the HPA-a and b-variant is only one base. This is more difficult to detect, as the deletion from several bases, e.g., in amelogenin or of an entire gene, like *RHD*. This is why such assays can quickly lead to incorrect results if the primer does not bind optimally. However, it is to mention that the target HPA is always heterozygous in this validation, which means if a 1.00 % mixture was set up, the maximum of the available target was 0.50 %. From this point of view, the observed values agree very well with the theoretical values.

For the platelet antigens analysis, the five most common antigens known to induce FNAIT were tested. The assays for HPA-3b and -5b showed a sensitivity of 0.50 %, HPA-1b, -2b, and -3a indicated a detection limit of 0.25 %. The lowest limit of detection was gained for the assays HPA-1a and -15b with 0.05 %. Unfortunately, in literature there are no validations described and could therefore not compared with these results.

In addition to the validation of the blood cells and platelet antigens, it is always necessary to test that fetal DNA has been analyzed with sufficient DNA quality. Therefore, the NPIT was also validated for fetal markers. For the gender dependent fetal identification amelogenin was used. Amelogenin (AMEL) encodes for the enamel, and it is distinguished between male and female by a 6 bp deletion in the female gene [187, 188]. When validating amelogenin as a fetal marker, the signal of the X-chromosome serves as the total DNA, and the Y-chromosome signal indicates the male fetus. The validation revealed a detection limit for the AMEL-Y of 0.50 %. This is the first description of the detection measurement of amelogenin with dPCR. So a comparison with other publications is not possible. However, this marker only works with male fetuses. In the case of a female fetus, the signal melts with the AMEL-X signal from the mother. Besides the amelogenin, it is also possible to use the SRY gen for gender analysis, which some laboratories do in the *RHD* analysis [168]. SRY stands for sex-determining region Y and is responsible for developing the male phenotype [239]. This gen could be established in case of difficulties in the results with the amelogenin test.

As already mentioned, the use of AMEL-X/Y as a fetal marker is only suitable for a male fetus. In the case of a female fetus, the fetus's X-chromosomal signal melts with the AMEL-X signal from the mother. In case of a AMEL-Y negative result, it is crucial to exclude the possibility of the absence of cffDNA or that the cfDNA is not sufficient before a female fetus is diagnosed. Therefore, nine autosomal markers out of the SNP*for*ID panel were tested as a fetal marker (chapter 3.5.2). These markers distinguish between the autosomal SNP between mother and child if there is a difference. A result differing from the mother for an SNP marker proves the presence of an fetus and secured sufficient cffDNA. These nine markers were analyzed in a proof of principle test. Meaning only the background and a

mixture containing 1.00 % target plasma were analyzed and revealed a detection limit of 0.50 % target allele.

SNPforID marker were already tested as a fetal marker in 2013. A dilution series of 1000-10 pg was made here, and a reliable identification of the SNPs with 10 pg using qPCR was shown [200]. In comparison, this dissertation showed that a dPCR chip loaded with only 4×10^6 molecules, which is a concentration of 0.43 ag/ μ l, leads to reproducible results.

In literature, many other gender-independent markers are discussed, like epigenetic markers or RNA markers. One of these markers is the RASSF1A. This tumor suppressor gene's promoter is hypermethylated in the placenta and hypomethylated in the maternal cells [258]. Through the use of methylation-sensitive restriction enzymes, the maternal RASSF1A sequences are degraded, and thus the fetal RASSF1A sequences remain [258, 259]. However, the digestion step is quite time-consuming and has not been established as a standard in the routine.

The use of autosomal SNPs also has the potential to identify an early transplant rejection or it is possible to check parentage during pregnancy, which could be an essential tool in case of a pregnancy as a result of a sexual assault. Since the use of dPCR is very sensitive, an analysis is possible even in early pregnancy. However, to be able to apply this, approximately 52 SNPs are required to be equivalent to the gold standard of the STR analysis [193]. Compared to STR, SNP's use is accompanied by fewer mutations [191, 196].

4.3 Clinical Validation of the Assays

If the results which we gained during the technical validation could be repeated under real circumstances, a clinical validation was conducted. The used cfDNA in the technical validation was from volunteers, and the plasma was mixed as described in chapter 2.16 to simulate a pregnancy. In the clinical validation, blood from real pregnant women was used. This cfDNA is more degraded, and it was analyzed if it is possible to receive similar results. The local ethics committee approved the procedure of the study (Vote No. 2017-665N-MA).

In the beginning, a network of resident gynecologists was established for the recruitment of pregnant women. Blood from 50 pregnant women was collected, and their genomic DNA was used for a pretyping for all assays from the technical validation. If a woman was homozygous in an assay, e.g., HPA-1bb, the cfDNA was isolated with the developed protocol, and the fetus's genotype was proposed with dPCR. Overall, genetic material from 12 children, was returned to prove the expected results.

Around 35 % of the population are RhD negative. The description of an incompatibility of an RhD negative woman carrying an RhD positive fetus was made in 1939 [2]. A few years later, Landsteiner and Wiener identified the rhesus gene as a cause of the antigen formation [4]. MHN's occurrence was significantly reduced by introducing immunoglobulins to RhD negative pregnant women in the 1960s (chapter 1.1.1). However, not all women need this treatment. Only RhD negative women who would expect an RhD positive child should be treated. But, the immunoglobulins' targeted administration is only possible if the child's *RHD* status is known

In *RHD* exon 3, a statistical analysis indicated that the values concerning the *RHD* gene in the technical and clinical validation were identical ($p = 0.84$). Comparing background of the clinical and technical validation no significant differences were found ($p = 0.08$). This indicates that the values from the technical validation were confirmed in the clinical study.

The investigation regarding *RHD* exon 5 showed that the *RHD* identification in a real pregnant woman was similar distributed as in the technical validation ($p = 0.17$). The clinical validation of the background did not differ from the values from the technical validation ($p = 0.1$).

Examination of *RHD* exon 7 identification showed similar results in clinical and technical validation ($p = 0.63$). The comparison of the background in the two validations revealed again identical distributions ($p = 0.80$).

The analysis of the clinical study revealed in all assays significant differences between the background and target signal intensity (*RHD* exon 3 and 7 $p = 0.02$; *RHD* exon 5 $p = 0.01$). In case 36, there was a failure regarding the dPCR with *RHD* exon 5. However, since three

loci were analyzed, one assay's failure can be compensated if the other two assays indicate the same result, which was the case in this example. Such a procedure is legitimate and is followed internationally in many laboratories [168]. Fetal material was not used for verification here since a matching result of 2 exons was classified as meaningful. With this assay, we have been successfully participating in an international quality assurance test since 2018 [168].

Clinical investigations were accomplished by many researchers using qPCR. In 2008, a study with 1,113 RhD negative women was carried out in Germany. The sensitivity of the *RHD* genotyping was 99.7 % and the specificity 99.2 % [260]. In the Netherlands a huge study with 25,798 RhD negative pregnant women indicated a sensitivity of 99.94 % and a specificity of 97.4 % [157]. Denmark, one of the first countries who established the *RHD* screening in the clinical routine, showed in 12,668 women a sensitivity of 99.9 % and specificity of 99.1 % [156]. Another study from Finland with 10,814 participants indicated a sensitivity and specificity above 99 % [158]. Further countries like Norway, Sweden and England, revealed identical results [161, 162, 164].

It should be noted that the sample size in this study was only 14. Therefore, only a rough estimate was made. With an increased number of cases, a reliable analysis for sensitivity and specificity could be conducted. It is tempting to speculate; that the results will be in no way inferior to those of the studies that have already been carried out.

In Germany is the *RHD* genotyping offered to all RhD negative women since November 2020 [166]. The use of a noninvasive *RHD* test is already part of routine pregnancy exams in many countries. Denmark, Norway, the Netherlands, England, and Finland, only RhD negative women expecting an RhD positive child are administered immunoglobulins [156-158, 160, 161, 169]. However, in these countries, the examination is carried out with qPCR and is therefore significantly less sensitive than the dPCR because all studies were conducted on average around the 25th week of pregnancy. Thus, the dPCR is particularly suitable in high-risk pregnancies in which it is crucial to determine an antigen intolerance as early as possible.

In addition to the rhesus system, the KEL blood group is also able to trigger MHN. 92.00 % of the population is KEL1 negative. If a KEL2 homozygous woman is pregnant with a KEL1 heterozygous child, MHN can develop. In MHN caused by a rhesus incompatibility, the anti-D antibodies bind to mature erythrocytes and destroy them. In the case of an anti-KEL1 induced MHN, the antibodies bind to the KEL1 positive erythroid progenitor cells (erythroid burst-forming units and colony-forming units). Thus, mature erythrocytes can't develop, and hematopoiesis is interrupted early, resulting in anemia [30].

All 49 fetuses examined were KEL1 negative. Compared to the technical validation, a significantly lower background was identified in the clinical validation ($p = 2.27 \cdot 10^{-10}$). Since the difference between KEL1 and KEL2 is an SNP, the stronger degradation of the cfDNA in the clinical validation could be advantageous in the analysis. The cfDNA used in the technical validation process consists of mixed plasma, and the cfDNA contained therein is known to be longer (chapter 1.5) than the fetal, which is in the range between 145-201 bp [141, 142]. Due to shorter fragments, incorrect bindings may have been reduced and lower the background positively. It would be interesting to examine a KEL1 positive fetus in a larger number of cases and then possibly be able to compare the results with other publications.

The first report of a *KEL* genotyping comes from England. The test is based on the qPCR with a sensitivity of 25 pg per well KEL1/KEL2 heterozygous sample in a background of 5 ng per well KEL2 homozygous sample [169]. The investigations in this work have shown that reproducible results can be obtained with the dPCR with a concentration of 0.43 ag/ μ l, which corresponds to approximately $4 \cdot 10^6$ molecules in 15 μ l.

A recent study by the Australian Red Cross with dPCR was able to identify a KEL1 heterozygous fetus as early as the 13th week of gestation. For this analysis, the blood was collected in a Streck Cell-Free DNA BCT, which means that the fetal proportion was significantly higher (16.8 %). The KEL1 was identified with 0.34 copies/ μ l [261]. Since no positive fetus could be identified in this work, the values, unfortunately, cannot be compared. In addition to the use of dPCR or qPCR for fetal *KEL* status, an NGS-based protocol is used in Denmark to identify the fetal blood group [262]. Tests with spiked DNA showed a sensitivity

of 1.00 %, but the authors postulated a sensitivity of 0.50 % to detect polymorphisms with NGS [183]. The fetal *KEL* genotyping is offered in Denmark, England, Germany, and the Netherlands to immunized women [165].

The human platelet antigens (HPA) are transmembrane glycoproteins, which are expressed on the platelets' surface. Especially important in this work are five of the six biallelic systems, namely HPA-1-5 and HPA-15. Here the a-allele differs from the b-allele only by one SNP (chapter 1.3). If a woman who is, e.g., homozygous for the a-allele is pregnant, and the child inherits the b-allele from the father, this can lead to the formation of antibodies by the mother against the child. As a result, the child's platelets are diminished, leading to severe bleeding or, in the worst case, to the child's death. Particularly feared are hemorrhages in the brain, which can result in severe disabilities. Until now, suspected FNAIT could only be confirmed by invasive methods, such as taking blood from the umbilical cord. But this intervention is always associated with considerable risks for the mother and child. A NIPT for HPA is offered to immunized women in Germany, the Netherlands and Spain using dPCR [165].

In the clinical validation of HPA-1b, four children were predicted as positive for the b-allele. The copy number/ μ l in the background in the clinical validation was clearly below the technical validation ($p = 2.87 \cdot 10^{-9}$). The reason for this could be the more degraded fetal DNA (and the reduced amount of cfDNA). The plasma DNA used in the technical validation was of genomic origin and was, therefore, longer and has a higher number of copies, which favors increased bindings or false bindings. The statistical analysis of the clinical data revealed a significant difference between the homozygous and heterozygous groups ($p = 0.002$), indicating reliable test results.

Genetic material from six newborns was sent back after birth, and was compared with the HPA-1b results from dPCR revealing 100 % accordance. The earliest confirmed evidence of HPA-1b was in the 12th week of gestation. The data in this clinical study show that the NIPT for the fetal HPA-1b determination is, according to statistical analysis, highly reliable and can be used in the first trimester.

The identification of the fetal HPA-1 status of the fetus has already been investigated using many methods, e.g., classic qPCR, some groups work with targeted massively parallel sequencing or COLD PCR [184, 263, 264].

In the most extensive study to date, 100,448 pregnant women were examined. 2.1 % of these women were HPA-1a negative. This group was tested for antibodies, and 10.6 % were positive. A total of 161 HPA-1a positive children were born, of which 55 were diagnosed with FNAIT. Two of these children showed an ICH [265]. During this examination, the doctors were able to prepare for an FNAIT based on the antibody status. Unfortunately, this publication focusses on the antibody status and not noninvasive fetal testing. However, if they were aware of the fetal HPA-1a status, they could already counteract an FNAIT during pregnancy by giving immunoglobulins or intrauterine transfusion, thus preventing the risk of bleeding and the associated health risks. However, this study shows the importance of identifying fetal HPA status. Implementation of routine screening for fetal HPA status is already being discussed in Norway, Denmark, England, and the Netherlands [266]. In 2012 the PROFNAIT consortium, which is a European Union-funded project, started their work to develop a polyclonal antibody-based prophylaxis against HPA-1a induced FNAIT [267].

A study from Poland shows 4.00 % false positive detection of HPA-1a, meaning that these women did not risk FNAIT but were treated as such. But this test is still offered to all HPA-1a negative pregnant women [268]. In addition to the classic qPCR, Ferro et al. determined the fetal HPA status using the co-amplification at lower denaturation temperature (COLD) HRM PCR method. Out of 142 study participants, 4 HPA-1bb women were identified who were pregnant with an HPA-1ab fetus. The authors could identify them in the 12th week of gestation onwards [264].

A large-scale study to identify high-risk pregnancies for FNAIT is currently underway in the Netherlands. It is planned to type HPA serologically and to search for antibodies. A NIPT to determine the fetal HPA status is not planned. The study is scheduled for 2.5 years [269]. It should be noted that the level of the antibodies varies during the pregnancy, which is why it

is recommended, if incompatibility is suspected, to measure repeatedly at different times during the pregnancy [270].

In this work, the fetal signal was preamplified in order to identify the fetal status against the high maternal signal. Another way is the pre-PCR digestion of the cell-free DNA with the Msp1 restriction enzyme to enhance the fetal signal. This enzyme degrades the maternal HPA-1b and leaves the fetal HPA-1a intact. As a result the background is reduced and makes the fetal signal more recognizable [263]. This method could also be of interest for use with the dPCR.

The background data from the technical validation from HPA-2 were compared with the clinical values and showed that both data sets are similar ($p = 0.49$). With this result from the statistical analysis, the technical study's values are confirmed in the clinical validation.

In the clinical validation were in all HPA-2ab cases, the number of copies/ μ l significantly increased compared to the HPA-2aa cases ($p = 8.37 \cdot 10^{-6}$), indicating that the data sets are very different.

A total of 11 test results could be checked in this assay with the genomic DNA of born children. 10 of these tests agreed with the expected genotype of the dPCR. In one case, No. 49, there were discrepancies. The results of the dPCR indicated an HPA-2aa genotype, whereas the PCR-SSP analysis indicated HPA-2ab. To rule out sample mix-ups, the analyses was repeated, and the results were confirmed. It should be noted that the PCR-SSP is a non-validated method, which may also give false-positive results. In the case of the dPCR, we had no case with a false negative or positive result in the validation procedure. To find out which method has been determined correctly, NGS could be used. A resolution of the sequence in its base pairs could provide information about the child's correct genotype and possibly offer valuable improvements for further analysis of cfDNA and genomic DNA.

The determination of the background in the HPA-3b assay indicated that the values from technical and clinical validation underlie a similar distribution ($p = 0.07$).

The statistical data analysis of the clinical data revealed a highly significant difference between HPA-3aa and HPA-3ab signals ($p = 0.001$). In four cases, the results were approved using the children's genomic DNA, and the accordance was 100.00 %.

The average number of copies for the HPA-3a-allele showed similar results as in the technical validation with the 5.00 % plasma mixture ($p = 0.43$), indicating that these two groups are identical. Unfortunately, there was no genetic material from the born children to check these results.

For the HPA-5b identification, the background from the technical validation was compared with clinical background. It turned out that these two groups were identical in their results ($p = 0.33$). The statistical analysis of clinical data revealed a highly significant difference between the HPA-5aa and HPA-5ab groups ($p = 1.82 \cdot 10^{-8}$), indicating a reliable test.

The analysis of the genomic material made it possible to verify 10 cases. There were nine matches, but in case 10, there was an inconsistency. The result of the dPCR showed a heterozygous genotype, while the PCR-SSP showed a homozygous result for the a-allele. To rule out confusion, the tests were repeated, and the results were confirmed in both cases. To determine the child's genotype, NGS could be used here. A clarification of the genotype of case 10 could provide valuable improvements for further dPCR and PCR-SSP analysis.

For the HPA-2, -3, and -5 assays, there are no published studies with which the results could be compared. Thus, the data from this clinical investigation are the first- NIPT data for fetal HPA determination. The assays described here impress with their high sensitivity and are suitable for use in early pregnancy. Due to the promising results, the clinical examination should be expanded to offer this test to risk pregnancies as soon as possible.

The gender analysis was done with the amelogenin marker (AMEL) (chapter 1.5.3). It is advantageous that the X-specific signal also serves as a basic quantity at the same time. The DNA sequence from amelogenin in males and females can be distinguished by a 6 bp deletion in the female sequence. The gender assay was applied to all study participants. Eighteen boys and 32 girls were determined with the newly developed protocol.

The statistical analysis revealed a significantly lower background in the clinical validation compared to the technical validation with $p = 0.007$. In the technical validation, the cfDNA of volunteers was used in biological triplicates, but it is known that cfDNA and cffDNA differ in the fragment size [143]. It is tempting to speculate that the number of false bindings is reduced due to the more degraded DNA.

The Y-specific signal detection from the clinical study was compared with the technical validation data and indicated significantly higher target copies under real circumstances ($p = 0.01$). One reason could be the increased number of cffDNA in late pregnancies or a better primer binding on the more degraded fetal DNA.

A comparison of the clinical validation results revealed a highly significant difference regarding male identification and the background ($p = 0.0001$).

In 10 cases, the predicted result was confirmed by the child's DNA. However, there were differences in two cases; in case 16, a girl was identified with dPCR, and the buccal swap analysis revealed a boy. One reason for this could be that this was a very early pregnancy, and there was not enough fetal material to determine the Y-chromosome. The dPCR looked for AMEL-Y, whereas the genomic DNA was proceeded with PCR-SSP for the SRY gen. It is known in forensics that in rare cases the AMEL analysis incorrectly identifies men as women because they also have a deletion resulting in a band at 106 bp [271, 272].

Already in 1998, it was described for the first time that men were typed as women by deleting the Y-chromosomal copy in the amelogenin gene [273]. The frequency of such deletion varies in different populations. In Sri Lanka, for example, it is 8 %, whereas in India it is 0.23 %, Malaysia 0.6 %, and in China 0.227 % [273-276]. The frequency of deletion in Y-chromosomes of the amelogenin gene in the Caucasian population was 0.018 % in a study of 28,182 individuals [277]. In addition to Y-chromosomal microdeletions, mutations in the primer's binding region can lead to the incorrect classification of a man as a woman [275, 278, 279].

In case 18, a boy was identified using the amelogenin assay, and a girl was determined using the PCR-SSP. Since it is a late pregnancy, there should be enough cffDNA. One possibility could be that the girl has no deletion and was wrongly identified as a boy in the dPCR. However, the SRY gene could be detected in the PCR-SSP, which points to a male. It is also possible that we have a rare mutation in which the SRY has jumped to the X-chromosome. In this case, it is an XX male who is phenotypically male and genotypically female. When the genetic material returned, there was no information about the phenotype, only the blood. A check with NGS could clarify these two cases and bring essential knowledge for the further development of the prenatal test.

Already in 2008, a case was described in which three women in a family carried both variants of amelogenin [280]. In summary, the cause of an X-null is often a mutation in the primer region, whereas a deletion causes a Y-null in the Y-variant [279]. However, other amplification problems with the amelogenin gene have also been described, so it happens that the X-variant is not amplified [281]. The cause can be a point mutation in intron 1 from C to G in the primer-binding region of the amelogenin sequence [281-283]. The occurrence of an X-null variant of amelogenin is very rare. Only one in 43,000 is affected. In addition, this mutation was only found in the Caucasus population [283]. Discrepancies in the use of amelogenin as a gender marker are well known in forensics. Therefore, to use amelogenin is questionable, and a combination of amelogenin with SRY gen is recommended [271].

It should be noted that the origin of the cfDNA comes from the trophoblasts. The differentiation between trophoblast and embryoblast takes place very early after fertilization. A mutation can now take place in the trophoblasts, but this does not affect the embryo. This could be a reason for the different outcomes in cases 10 and 18. To check this, one could examine the child's genomic DNA with the dPCR. If the results in the amelogenin match, then a check of the cfDNA in the dPCR for the SRY gene is recommended. If the results match, there is a deletion or a mutation in the primer binding site of amelogenin. But there was no mutation in this area between embryoblast and trophoblast. If, e.g., in case 16, the SRY assay in dPCR is negative, the trophoblasts are different from the embryoblasts, probably due to a mutation or because one of the samples was not from the child. However, the easiest and most time-saving method would be to sequence the child's cfDNA and genomic DNA to rule

out or confirm a mutation. The probability of such a situation in one of the two cases is low, but such events must be considered in a biological system.

Fetal sex testing is used in some NIPT laboratories to control the presence of fetal DNA [165, 200].

The disadvantage of the amelogenin assay is the uncertainty with a negative test result. Here the question arises whether the fetus is female or whether no cfDNA was present. It is, therefore, advantageous to use an autosomal marker for fetal identification. Thus, nine autosomal markers from the SNPforID panel were tested to prove the presence of cfDNA. To accomplish that, the genomic DNA from the mother was pretested for the SNP status of the nine SNPs. In case of a homozygous result, the cfDNA was investigated to identify a heterozygous signal from the fetus.

The SNP5b values obtained for the presumed genotypes were statistically examined within the clinical study and showed a very significant difference between background and target ($p = 6.49 \cdot 10^{-5}$). Ten of the suspected genotypes could be checked using the genetic material sent in after birth. Here a match was found in eight cases. However, in two cases, a different result was obtained. The first interesting circumstance was that in case 35, an unusually high target to total ratio for the 12th week of pregnancy was noticed. This could indicate a contamination. However, the test was repeated two times, and the result was confirmed. It might be possible that a mutation at a different site in the child's genome is present, whereby the primer could also bind to other sites and thus lead to falsified results. In the PCR-SSP, the suspected SNP5ab could not be confirmed. However, the sensitivity of dPCR is very high, and therefore small changes can be identified. The PCR-SSP results are analyzed via agarose gel. Consequently, the sensitivity is very low because a slight signal in the gel is quickly overlooked or neglected as not strong enough. Besides, the primer sequences of PCR-SSP and dPCR are different, which is why this mutation went unnoticed in PCR-SSP or was not detected due to the lower sensitivity.

In case 49, SNP5aa was identified in the plasma, but the PCR-SSP clearly showed a heterozygous genotype. Here too, the tests were repeated, and the results were confirmed. In both cases, the methods could have been determined correctly. It is possible that during early pregnancy, a mutation in the trophoblast cell line may have developed, which is not related to the embryo. Therefore, it could be that in the cfDNA, which comes from the trophoblasts, the genotype was different from the genome of the born child. This can be checked by analyzing the cfDNA and the genomic DNA with NGS.

Altogether, seventy-one results in the SNP examinations could be checked by the genomic DNA of the newborns. In two cases where the results controversial. Here a sequencing is recommended to finally clarify whether the dPCR or PCR-SSP displayed the correct result. The earliest gestational age with a proofed result was the 7th gestational week.

After a statistical analysis of the clinical data, nine analyzed SNP assays revealed a significant difference between background and target signal in eight tests. A comparison of this clinical data with other literature is unfortunately not possible.

Until today there is no gender independent cfDNA marker established. Besides in literature were often epigenetic markers, RASSF1A, and SNPs discussed as a fetal marker. The results in this thesis recommend SNPs as very promising marker for gender independent fetal DNA identification.

In a study that including 223 samples, 97.8 % had at least one SNP that differed between mother and child [200]. In this study, at least one SNP was found in all the examined participants in that mother and child differed. However, a disadvantage of this method is that the mother must be pretyped for the SNPs with PCR-SSP in order to identify the homozygotes SNPs. These SNPs are then used to check whether the fetus is heterozygote or not. This is time-consuming since SNPs are first analyzed individually and then tested specifically using dPCR. But, an SNP match is sufficient to show that fetal DNA is suitable for analysis. To circumvent a false-positive result, it is recommended to use at least two SNPs to reveal the fetus's presence. This recommendation agrees with Doescher et al. [200].

The weak point of these protocols is the low level of automation. This increases the probability of user errors in the routine in the form of, e.g., a sample exchange, pipetting errors, and

contamination. In particular, the latter is fatal because if someone works improperly, even the smallest amounts are enough to get the wrong result. On the one hand, the dPCR is very sensitive, as only $4 * 10^6$ molecules need to be loaded in one chip. This corresponds to a concentration of 0.43 ag/ μ l. It has not yet been described that such a small number of molecules can be worked so sensitively. The data from this little clinical investigation impressively show that the NIPT is a valuable tool for clarifying fetal blood groups and platelet antigens to replace the invasive procedure. However, more data is needed, so a more extensive study in cooperation with the women's and children's clinic is recommended.

4.4 Conclusion and Outlook

The aim of this thesis was the development of a noninvasive test to determine the status of the fetal blood cell antigens from the blood groups RH and KEL and platelet antigens from five biallelic platelet antigens HPA-1, -2, -3, -5, and -15. Besides these antigens, a gender-dependent marker, amelogenin, and nine SNPs from the SNPforID panel as a gender-independent fetal marker were investigated.

All these targets should be analyzed with digital PCR. Therefore, a new protocol from cfDNA isolation until dPCR set up had to be developed. The aim was to establish a protocol with which it is possible to analyze the small amount of cffDNA reliably, and it should be suitable for routine use. This aim was successfully achieved. Only 0.43 ag/μl or 4×10^6 molecules per analysis are needed after preamplification to receive unambiguous results. This low amount of required DNA is unique in literature.

To show that with this low amount could be gained precise results, a technical validation was conducted. A pregnancy was simulated by mixing different plasmas before cfDNA isolation. The plasma of tested heterozygous volunteers was mixed from 5.00% down to 0.1% with homozygous plasma to identify the limit of detection with the dPCR for every single assay in biological triplicates. The results indicated a detection limit of 0.10% heterozygous plasma for many assays, which is a sensitivity of 0.05% for targeted alleles *RHD* exon 5 and 7, KEL 1, HPA-1a, and HPA-15b. Therefore the second work package of this dissertation was successful too.

With such a low detection limit, the developed protocol has the potential to give meaningful results in the 1st trimester. To prove this assumption, the third work package concerns the results of a clinical investigation of 50 women, which was approved by the local ethics committee (Vote No. 2017-665N-MA). Significant results were gained in the assays from *RHD* exon 3, 5, and 7, HPA-1,-2,-3, and -5, amelogenin, and from nine analyzed SNP assays, eight were significant. The earliest confirmed result was in the 7th week of pregnancy and showed that the third work package was also successfully completed.

Taken together, this protocol is not only exceptionally robust and can easily be transferred to other NIPT targets. It has a huge potential for further applications like early graft rejection identification and of course as an early test for cancer detection.

5 ABSTRACT

Morbus haemolyticus neonatorum is caused by intolerance of blood group antigens, e.g., the rhesus D protein or KEL1 protein between mother and child. A rhesus D or KEL1 negative mother can produce antibodies against the foreign antigens on the child's erythrocytes' surface inherited from the father. In the case of rhesus D, this antibody formation can be prevented by administering immunoglobulins to all pregnant rhesus D negative women. But a targeted treatment of women who are expecting a rhesus positive child would relieve the health insurance companies and reduce the possibly unnecessary treatment of women who might suffer from side effects like anaphylactic reactions. No protective immunoglobulin treatment is available for the KEL blood group, and only continuous ultrasound examinations and blood transfusions can safely protect the child from severe damage to health. Early knowledge about the child's antigen status could help to initiate these important examinations early and reduce the likelihood of disabilities or stillbirths.

However, with blood platelets, incompatibilities can occur between mother and child, resulting in fetal/neonatal alloimmune thrombocytopenia. So far, the probability for fetal alloimmune thrombocytopenia has been determined using the antibody titer but only at later pregnancy stages. In case of a diagnosed fetal/neonatal alloimmune thrombocytopenia, a continuous ultrasound examination has to be carried out in combination with platelet transfusions or immunoglobulin administration to prevent an intracranial hemorrhage during pregnancy. As for the blood group antigens, early knowledge of the fetal status could avoid severe damage to the child's health.

In all described cases, a noninvasive method could determine the child's antigen status from the mother's blood and thus protect the child from health damage. The term noninvasive refers to the fact that the examination is noninvasive for the fetus. In several countries like Denmark or Netherlands, the noninvasive determination of the fetal rhesus D status is already in routine use. But these tests are conducted during the second trimester in pregnancy using qPCR. Especially for the KEL blood group and platelet complications, no standard tests are in the routine use.

Therefore, this work aims to develop a noninvasive prenatal blood test to identify blood cell and platelet antigens from the fetus only using a blood sample from the mother. The test should have a high sensitivity so that it can already be used at the stage of early pregnancy. To achieve this, a further development of quantitative polymerase chain reaction, namely digital polymerase chain reaction, was used. To implement this relatively new technique in a protocol for routine use and analyze its potential, this work has been divided into three main parts. The first part describes the protocol's development from cell-free deoxyribonucleic acid isolation to completing the digital polymerase chain reaction.

In the second part, the protocol was subjected to a technical validation for sensitivity and specificity. For this, attempts were made to simulate pregnancies in various stages using plasma mixtures consisting of a homogeneous carrier (mother) and a small amount of heterogeneous plasma (child). Mixes of 5.00 % down to 0.10 %, referring to the fact that the target allele is included with 2.50 to 0.05 %, respectively, were prepared. The 0.1 % mixture represents a very early pregnancy, and 5.00 % mixture means pregnancy in the third trimester. During this validation, it was shown that it was possible to reliably identify a proportion of as low as 0.05 % of the rhesus D exon 5 and exon 7. For the KEL blood group, a detection limit of 0.25 % was evaluated. In addition, the test was also validated for the human platelet antigens -1, -2, -3, -5, and -15. Here the test for human platelet antigens -1a and -15b showed a detection limit of 0.05 %, and the threshold value for the human platelet antigens -1b, -2b, and -3a was determined at 0.25 %. Only for the human platelet antigens -1a and -15b the test indicated a threshold of 0.50%. As a fetal marker, amelogenin was used, and for this, the test indicated a detection limit of 0.50 %. However, this marker only identifies male fetuses because, during analysis, the female fetus's signal cannot be distinguished from the mother's signal. Therefore, nine autosomal markers from the single nucleotide

polymorphism for identification panel were tested as fetal markers with 1.00 % mixtures indicating 0.50 % target proportion. In all tested assays, the target could be identified.

In the third part of this thesis, real pregnant women were investigated in a small clinical study, and the results were compared with the technical validation. With approval by a local ethics committee, blood samples from 50 pregnant women were analyzed with the newly developed tests. It was possible to confirm the results of the technical validation. An statistical analysis indicated that from all 17 analyzed assays, 13 revealed significant results ($p > 0.05$). To further confirm the results, the accuracy of the collected genomic desoxyribonucleic acid of children after birth could be tested and compared to the prenatal results in 126 cases. There was a discrepancy in 6 cases, which could be corrected through small test protocol optimizations. Overall, the study shows how reliable the developed protocol can be used in early stages of pregnancy, starting from week seven after conception. Therefore as a next step, it is recommended to carry out a more extensive confirmation study to possibly offer this very sensitive method to women with a high-risk pregnancy for fetal/neonatal alloimmune thrombocytopenia or Morbus haemolyticus neonatorum.

6 LITERATURE LIST

1. Gogri, H., et al., *Molecular genotyping of Indian blood group system antigens in Indian blood donors*. *Transfus Apher Sci*, 2018. **57**(3): p. 388-390.
2. Levine, P. and R.E. Stetson, *Landmark article July 8, 1939. An unusual case of intra-group agglutination. By Philip Levine and Rufus E Stetson*. *JAMA*, 1984. **251**(10): p. 1316-7.
3. Daniels, G., *Human blood groups*. 2nd ed. 2002, Malden, MA: Blackwell Science. x, 560 p.
4. Landsteiner, K.W., A., *An Agglutinable Factor in Human Blood Recognized by Immune Sera for Rhesus Blood*. *Exp Biol Med.*, 1940. **43**().
5. Colin, Y., et al., *Genetic basis of the RhD-positive and RhD-negative blood group polymorphism as determined by Southern analysis*. *Blood*, 1991. **78**(10): p. 2747-52.
6. Cherif-Zahar, B., et al., *Organization of the gene (RHCE) encoding the human blood group RhCcEe antigens and characterization of the promoter region*. *Genomics*, 1994. **19**(1): p. 68-74.
7. Cherif-Zahar, B., et al., *Localization of the human Rh blood group gene structure to chromosome region 1p34.3-1p36.1 by in situ hybridization*. *Hum Genet*, 1991. **86**(4): p. 398-400.
8. Suto, Y., et al., *Gene organization and rearrangements at the human Rhesus blood group locus revealed by fiber-FISH analysis*. *Hum Genet*, 2000. **106**(2): p. 164-71.
9. Wagner, F.F. and W.A. Flegel, *RHD gene deletion occurred in the Rhesus box*. *Blood*, 2000. **95**(12): p. 3662-8.
10. Landsteiner, K. and A.S. Wiener, *STUDIES ON AN AGGLUTINOGEN (Rh) IN HUMAN BLOOD REACTING WITH ANTI-RHESUS SERA AND WITH HUMAN ISOANTIBODIES*. *J Exp Med*, 1941. **74**(4): p. 309-20.
11. Cherif-Zahar, B., et al., *Molecular cloning and protein structure of a human blood group Rh polypeptide*. *Proc Natl Acad Sci U S A*, 1990. **87**(16): p. 6243-7.
12. Le van Kim, C., et al., *Molecular cloning and primary structure of the human blood group RhD polypeptide*. *Proc Natl Acad Sci U S A*, 1992. **89**(22): p. 10925-9.
13. Avent, N.D., et al., *cDNA cloning of a 30 kDa erythrocyte membrane protein associated with Rh (Rhesus)-blood-group-antigen expression*. *Biochem J*, 1990. **271**(3): p. 821-5.
14. Southcott, M.J., M.J. Tanner, and D.J. Anstee, *The expression of human blood group antigens during erythropoiesis in a cell culture system*. *Blood*, 1999. **93**(12): p. 4425-35.
15. Tippett, P. and R. Sanger, *Observations on subdivisions of the Rh antigen D*. *Vox Sang*, 1962. **7**: p. 9-13.
16. Rouillac, C., et al., *Transcript analysis of D category phenotypes predicts hybrid Rh D-CE-D proteins associated with alteration of D epitopes*. *Blood*, 1995. **85**(10): p. 2937-44.
17. Stratton, F., *A new Rh allelomorph*. *Nature*, 1946. **158**: p. 25.
18. Tippett, P., *Depressed Rh phenotypes*. *Rev Fr Transfus Immunohematol*, 1978. **21**(1): p. 135-50.
19. Wagner, F.F., et al., *Molecular basis of weak D phenotypes*. *Blood*, 1999. **93**(1): p. 385-93.

20. Wagner, F.F., et al., *Weak D alleles express distinct phenotypes*. Blood, 2000. **95**(8): p. 2699-708.
21. Daniels, G., Bromilow, I., *Essential Guide to Blood Groups*. Third Edition ed. 2014: Wiley-Blackwell (John Wiley & Sons, Ltd).
22. Coombs, R.R., A.E. Mourant, and R.R. Race, *In-vivo isosensitisation of red cells in babies with haemolytic disease*. Lancet, 1946. **1**(6391): p. 264-6.
23. Levine, P., et al., *A New Human Hereditary Blood Property (Cellano) Present in 99.8% of all Bloods*. Science, 1949. **109**(2836): p. 464-6.
24. Zelinski, T., et al., *Genetic linkage between the Kell blood group system and prolactin-inducible protein loci: provisional assignment of KEL to chromosome 7*. Ann Hum Genet, 1991. **55**(2): p. 137-40.
25. Lee, S., et al., *The human Kell blood group gene maps to chromosome 7q33 and its expression is restricted to erythroid cells*. Blood, 1993. **81**(10): p. 2804-9.
26. Murphy, M.T., et al., *Regional chromosomal assignment of the Kell blood group locus (KEL) to chromosome 7q33-q35 by fluorescence in situ hybridization: evidence for the polypeptide nature of antigenic variation*. Hum Genet, 1993. **91**(6): p. 585-8.
27. Lee, S., et al., *Molecular basis of the Kell (K1) phenotype*. Blood, 1995. **85**(4): p. 912-6.
28. Lee, S., et al., *Molecular cloning and primary structure of Kell blood group protein*. Proc Natl Acad Sci U S A, 1991. **88**(14): p. 6353-7.
29. Toivanen, P. and T. Hirvonen, *Antigens Duffy, Kell, Kidd, Lutheran and Xg a on fetal red cells*. Vox Sang, 1973. **24**(4): p. 372-6.
30. Vaughan, J.I., et al., *Inhibition of erythroid progenitor cells by anti-Kell antibodies in fetal alloimmune anemia*. N Engl J Med, 1998. **338**(12): p. 798-803.
31. Weiner, C.P. and J.A. Widness, *Decreased fetal erythropoiesis and hemolysis in Kell hemolytic anemia*. Am J Obstet Gynecol, 1996. **174**(2): p. 547-51.
32. Bowman, J.M., *RhD hemolytic disease of the newborn*. N Engl J Med, 1998. **339**(24): p. 1775-7.
33. Louis K.Diamond, K.D.B., James M.Baty, *Erythroblastosis fetalis and its association with universal edema of the fetus, icterus gravis neonatorum and anemia of the newborn*. The Journal of Pediatrics, 1932. **1**(3): p. Pages 269-276.
34. Darrow, R., *Icterus gravis (erythroblastosis) neonatorum*. Arch. Pathol., 1938. **25**: p. 378-417.
35. Philip Levine, M.D., Newark, N.J., Lyman Burnham, M.D., Englewood, N.J., E.M. Katzin, M.D., Newark, N.J., Peter Vogel, M.D., New York, N. Y, *The role of iso-immunization in the pathogenesis of erythroblastosis fetalis*. AJOG, 1941. **42**: p. 925-937.
36. Stern K, G.H., Berger M., *Experimental Isoimmunization to Hemoantigens in Man*. J Immunol, 1961. **97**: p. 1245-57.
37. Finn, R., et al., *Experimental studies on the prevention of Rh haemolytic disease*. Br Med J, 1961. **1**(5238): p. 1486-90.
38. Freda V. J., G.G., *Antepartum management and prevention of Rh isoimmunization*. Bull. Sloane Hosp., 1962. **Wommen 8**: p. 147.
39. Clarke, C.A., et al., *Further experimental studies on the prevention of Rh haemolytic disease*. Br Med J, 1963. **1**(5336): p. 979-84.
40. Bowman, J., *Rh-immunoglobulin: Rh prophylaxis*. Best Pract Res Clin Haematol, 2006. **19**(1): p. 27-34.

41. Bowman, J.M. and J.M. Pollock, *Antenatal prophylaxis of Rh isoimmunization: 28-weeks'-gestation service program*. Can Med Assoc J, 1978. **118**(6): p. 627-30.
42. *Prevention of primary Rh immunization: first report of the Western Canadian trial, 1966-1968*. Can Med Assoc J, 1969. **100**(22): p. 1021-4.
43. Benirschke K., B.G.J., Baergen R.N., *Erythroblastosis Fetalis and Hydrops Fetalis*. In: *Pathology of the Human Placenta*. Springer, Berlin, Heidelberg, 2012.
44. Kumpel, B.M., *Lessons learnt from many years of experience using anti-D in humans for prevention of RhD immunization and haemolytic disease of the fetus and newborn*. Clin Exp Immunol, 2008. **154**(1): p. 1-5.
45. O'Riordan, J.P., *The preparation and production of anti-D immunoglobulin*. Ir J Med Sci, 1968. **7**(6): p. 263-7.
46. Schreier, E., et al., *Hepatitis GBV-C sequences in patients infected with HCV contaminated anti-D immunoglobulin and among i.v. drug users in Germany*. J Hepatol, 1996. **25**(3): p. 385-9.
47. Kent, J., A.M. Farrell, and P. Soothill, *Routine administration of Anti-D: the ethical case for offering pregnant women fetal RHD genotyping and a review of policy and practice*. BMC Pregnancy Childbirth, 2014. **14**: p. 87.
48. Rutkowski, K. and S.M. Nasser, *Management of hypersensitivity reactions to anti-D immunoglobulin preparations*. Allergy, 2014. **69**(11): p. 1560-3.
49. O'Brien, K., et al., *Reaction to anti-D immunoglobulin - can we manage it?* Obstet Med, 2009. **2**(1): p. 38-9.
50. Henseler, O., et al., *[Report on notifications pursuant to section sign21 German Transfusion Act for 2010 and 2011]*. Bundesgesundheitsblatt Gesundheitsforschung Gesundheitsschutz, 2013. **56**(10): p. 1352-67.
51. Bundesauschuss, G., *Richtlinien des Gemeinsamen Bundesausschusses über die ärztliche Betreuung während der Schwangerschaft und nach der Entbindung („Mutterschafts-Richtlinien“)*. Bundesanzeiger, 2016. **AT 19.07.2016 B5**.
52. Alberts B, J.A., Lewis J, et al., *Molecular Biology of the Cell. 4th edition*. New York: Garland Science, 2002(Integrins).
53. Curtis, B.R. and J.G. McFarland, *Human platelet antigens - 2013*. Vox Sang, 2014. **106**(2): p. 93-102.
54. von dem Borne, A.E. and F. Decary, *Nomenclature of platelet-specific antigens*. Transfusion, 1990. **30**(5): p. 477.
55. Metcalfe, P., et al., *Nomenclature of human platelet antigens*. Vox Sang, 2003. **85**(3): p. 240-5.
56. Veldhuisen, B., et al., *Molecular typing of human platelet and neutrophil antigens (HPA and HNA)*. Transfus Apher Sci, 2014. **50**(2): p. 189-99.
57. Mueller-Eckhardt, *Transfusionsmedizin*. 2 ed. 1996, Berlin: Springer-Verlag. 634.
58. Kelton, J.G., et al., *Gova/b alloantigen system on human platelets*. Blood, 1990. **75**(11): p. 2172-6.
59. Zucker, M.B., et al., *Thrombocytopenia with a circulating platelet agglutinin, platelet agglutinin, platelet lysin and clot retraction inhibitor*. Blood, 1959. **14**(2): p. 148-61.
60. Van Loghem Jj, J., et al., *Serological and genetical studies on a platelet antigen (Zw)*. Vox Sang, 1959. **4**(2): p. 161-9.
61. Shulman, N.R., et al., *Immunoreactions Involving Platelets. V. Post-Transfusion Purpura Due to a Complement-Fixing Antibody against a*

- Genetically Controlled Platelet Antigen. A Proposed Mechanism for Thrombocytopenia and Its Relevance in "Autoimmunity".* J Clin Invest, 1961. **40**(9): p. 1597-620.
62. Kunicki, T.J. and R.H. Aster, *Deletion of the platelet-specific alloantigen PIA1 from platelets in Glanzmann's thrombasthenia.* J Clin Invest, 1978. **61**(5): p. 1225-31.
63. Kunicki, T.J. and R.H. Aster, *Isolation and immunologic characterization of the human platelet alloantigen, P1A1.* Mol Immunol, 1979. **16**(6): p. 353-60.
64. Bennett, J.S., et al., *Inhibition of fibrinogen binding to stimulated human platelets by a monoclonal antibody.* Proc Natl Acad Sci U S A, 1983. **80**(9): p. 2417-21.
65. Marguerie, G.A., et al., *The platelet-fibrinogen interaction. Evidence for proximity of the A alpha chain of fibrinogen to platelet membrane glycoproteins IIb/III.* Eur J Biochem, 1984. **139**(1): p. 5-11.
66. Gardner, J.M. and R.O. Hynes, *Interaction of fibronectin with its receptor on platelets.* Cell, 1985. **42**(2): p. 439-48.
67. Plow, E.F., et al., *Related binding mechanisms for fibrinogen, fibronectin, von Willebrand factor, and thrombospondin on thrombin-stimulated human platelets.* Blood, 1985. **66**(3): p. 724-7.
68. Plow, E.F., et al., *The effect of Arg-Gly-Asp-containing peptides on fibrinogen and von Willebrand factor binding to platelets.* Proc Natl Acad Sci U S A, 1985. **82**(23): p. 8057-61.
69. Pytela, R., et al., *Platelet membrane glycoprotein IIb/IIIa: member of a family of Arg-Gly-Asp--specific adhesion receptors.* Science, 1986. **231**(4745): p. 1559-62.
70. Fitzgerald, L.A., et al., *Protein sequence of endothelial glycoprotein IIIa derived from a cDNA clone. Identity with platelet glycoprotein IIIa and similarity to "integrin".* J Biol Chem, 1987. **262**(9): p. 3936-9.
71. Newman, P.J., R.S. Derbes, and R.H. Aster, *The human platelet alloantigens, PIA1 and PIA2, are associated with a leucine33/proline33 amino acid polymorphism in membrane glycoprotein IIIa, and are distinguishable by DNA typing.* J Clin Invest, 1989. **83**(5): p. 1778-81.
72. Kumpel, B.M., et al., *Ultrastructural localization of glycoprotein IIIa (GPIIIa, beta 3 integrin) on placental syncytiotrophoblast microvilli: implications for platelet alloimmunization during pregnancy.* Transfusion, 2008. **48**(10): p. 2077-86.
73. Greer, F., Rodgers, *Wintrobe's Clinical Hematology.* Lippincott Williams & Wilkins, a Wolters Kluwer business, 2009. **12th ed.**
74. van der Weerd CM, v.d.W.-D.H., Engelfriet CP, van Loghem JJ, *A new platelet antigen, Proceedings of the 8th Congress of the European Society of Haematology.* S. Karger, 1961: p. 379.
75. Van Der Weerd, C.M., et al., *The Zw Blood Group System in Platelets.* Vox Sang, 1963. **8**: p. 513-30.
76. Saji, H., et al., *New platelet antigen, Siba, involved in platelet transfusion refractoriness in a Japanese man.* Vox Sang, 1989. **56**(4): p. 283-7.
77. Kuijpers, R.W., et al., *Localization of the platelet-specific HPA-2 (Ko) alloantigens on the N-terminal globular fragment of platelet glycoprotein Ib alpha.* Blood, 1992. **79**(1): p. 283-8.
78. Okumura, I., C. Lombart, and G.A. Jamieson, *Platelet glycoprotein IIb. Purification and characterization.* J Biol Chem, 1976. **251**(19): p. 5950-5.

79. Wenger, R.H., et al., *The 5' flanking region and chromosomal localization of the gene encoding human platelet membrane glycoprotein Ib alpha*. *Gene*, 1989. **85**(2): p. 517-24.
80. Yamamoto, K., et al., *Localization of a thrombin-binding site on human platelet membrane glycoprotein Ib determined by a monoclonal antibody*. *Thromb Haemost*, 1986. **55**(2): p. 162-7.
81. Wicki, A.N. and K.J. Clemetson, *Structure and function of platelet membrane glycoproteins Ib and V. Effects of leukocyte elastase and other proteases on platelets response to von Willebrand factor and thrombin*. *Eur J Biochem*, 1985. **153**(1): p. 1-11.
82. Handa, M., et al., *The von Willebrand factor-binding domain of platelet membrane glycoprotein Ib. Characterization by monoclonal antibodies and partial amino acid sequence analysis of proteolytic fragments*. *J Biol Chem*, 1986. **261**(27): p. 12579-85.
83. Lopez, J.A., et al., *Cloning of the alpha chain of human platelet glycoprotein Ib: a transmembrane protein with homology to leucine-rich alpha 2-glycoprotein*. *Proc Natl Acad Sci U S A*, 1987. **84**(16): p. 5615-9.
84. Kuijpers, R.W., et al., *NH2-terminal globular domain of human platelet glycoprotein Ib alpha has a methionine 145/threonine145 amino acid polymorphism, which is associated with the HPA-2 (Ko) alloantigens*. *J Clin Invest*, 1992. **89**(2): p. 381-4.
85. von dem Borne, A.E., et al., *Baka, a new platelet-specific antigen involved in neonatal allo-immune thrombocytopenia*. *Vox Sang*, 1980. **39**(2): p. 113-20.
86. Keimowitz, R.M., et al., *Post-transfusion purpura associated with alloimmunization against the platelet-specific antigen, Baka*. *Am J Hematol*, 1986. **21**(1): p. 79-88.
87. Boizard, B. and J.L. Wautier, *Lek a, a new platelet antigen absent in Glanzmann's thrombasthenia*. *Vox Sang*, 1984. **46**(1): p. 47-54.
88. Kickler, T.S., et al., *Identification of Bakb, a new platelet-specific antigen associated with posttransfusion purpura*. *Blood*, 1988. **71**(4): p. 894-8.
89. Kieffer, N., et al., *Immunochemical characterization of the platelet-specific alloantigen Leka: a comparative study with the PIA1 alloantigen*. *Blood*, 1984. **64**(6): p. 1212-9.
90. van der Schoot, C.E., et al., *Characterization of platelet-specific alloantigens by immunoblotting: localization of Zw and Bak antigens*. *Br J Haematol*, 1986. **64**(4): p. 715-23.
91. Bray, P.F., et al., *Physical linkage of the genes for platelet membrane glycoproteins IIb and IIIa*. *Proc Natl Acad Sci U S A*, 1988. **85**(22): p. 8683-7.
92. Poncz, M., et al., *Structure of the platelet membrane glycoprotein IIb. Homology to the alpha subunits of the vitronectin and fibronectin membrane receptors*. *J Biol Chem*, 1987. **262**(18): p. 8476-82.
93. Lyman, S., et al., *Polymorphism of human platelet membrane glycoprotein IIb associated with the Baka/Bakb alloantigen system*. *Blood*, 1990. **75**(12): p. 2343-8.
94. Kiefel, V., et al., *A new platelet-specific alloantigen Bra. Report of 4 cases with neonatal alloimmune thrombocytopenia*. *Vox Sang*, 1988. **54**(2): p. 101-6.
95. Mueller-Eckhardt, C., et al., *348 cases of suspected neonatal alloimmune thrombocytopenia*. *Lancet*, 1989. **1**(8634): p. 363-6.
96. Bettaieb, A., et al., *Brb, a platelet alloantigen involved in neonatal alloimmune thrombocytopenia*. *Vox Sang*, 1991. **60**(4): p. 230-4.

97. Smith, J.W., et al., *Platelet specific alloantigens on the platelet glycoprotein Ia/IIa complex*. Br J Haematol, 1989. **72**(4): p. 534-8.
98. Woods, V.L., Jr., et al., *Antigenic polymorphism of human very late activation protein-2 (platelet glycoprotein Ia-IIa). Platelet alloantigen Hca*. J Clin Invest, 1989. **83**(3): p. 978-85.
99. Kiefel, V., et al., *The Bra/Brb alloantigen system on human platelets*. Blood, 1989. **73**(8): p. 2219-23.
100. McEver, R.P., E.M. Bennett, and M.N. Martin, *Identification of two structurally and functionally distinct sites on human platelet membrane glycoprotein IIb-IIIa using monoclonal antibodies*. J Biol Chem, 1983. **258**(8): p. 5269-75.
101. Santoso, S., V. Kiefel, and C. Mueller-Eckhardt, *Human platelet alloantigens Bra/Brb are expressed on the very late activation antigen 2 (VLA-2) of T lymphocytes*. Hum Immunol, 1989. **25**(4): p. 237-46.
102. Giltay, J.C., et al., *The platelet glycoprotein Ia-IIa-associated Br-alloantigen system is expressed by cultured endothelial cells*. Br J Haematol, 1990. **75**(4): p. 557-60.
103. Santoso, S., V. Kiefel, and C. Mueller-Eckhardt, *Immunochemical characterization of the new platelet alloantigen system Bra/Brb*. Br J Haematol, 1989. **72**(2): p. 191-8.
104. Nieuwenhuis, H.K., et al., *Human blood platelets showing no response to collagen fail to express surface glycoprotein Ia*. Nature, 1985. **318**(6045): p. 470-2.
105. Kunicki, T.J., et al., *The human fibroblast class II extracellular matrix receptor mediates platelet adhesion to collagen and is identical to the platelet glycoprotein Ia-IIa complex*. J Biol Chem, 1988. **263**(10): p. 4516-9.
106. Santoro, S.A., *Identification of a 160,000 dalton platelet membrane protein that mediates the initial divalent cation-dependent adhesion of platelets to collagen*. Cell, 1986. **46**(6): p. 913-20.
107. Takada, Y. and M.E. Hemler, *The primary structure of the VLA-2/collagen receptor alpha 2 subunit (platelet GPIa): homology to other integrins and the presence of a possible collagen-binding domain*. J Cell Biol, 1989. **109**(1): p. 397-407.
108. Santoso, S., et al., *The human platelet alloantigens Br(a) and Brb are associated with a single amino acid polymorphism on glycoprotein Ia (integrin subunit alpha 2)*. J Clin Invest, 1993. **92**(5): p. 2427-32.
109. Ertel, K., et al., *Relevance of the HPA-15 (Gv) polymorphism on CD109 in alloimmune thrombocytopenic syndromes*. Transfusion, 2005. **45**(3): p. 366-73.
110. Sutherland, D.R., et al., *Identification of a cell-surface antigen associated with activated T lymphoblasts and activated platelets*. Blood, 1991. **77**(1): p. 84-93.
111. Smith, J.W., et al., *Characterization and localization of the Gova/b alloantigens to the glycosylphosphatidylinositol-anchored protein CDw109 on human platelets*. Blood, 1995. **86**(7): p. 2807-14.
112. Murray LJ, B.E., Uchida N, Hoffman R, Nayar R, Yeo EL, Schuh AC, Sutherland DR, *CD109 is expressed on a subpopulation of CD34+ cells enriched in hematopoietic stem and progenitor cells*. Experimental Hematology, 1999. **27**(8): p. 1282-1294.
113. Haregewoin, A., et al., *Cellular expression of a GPI-linked T cell activation protein*. Cell Immunol, 1994. **156**(2): p. 357-70.

114. Lin, M., et al., *Cell surface antigen CD109 is a novel member of the alpha(2) macroglobulin/C3, C4, C5 family of thioester-containing proteins*. *Blood*, 2002. **99**(5): p. 1683-91.
115. Schuh, A.C., et al., *A tyrosine703serine polymorphism of CD109 defines the Gov platelet alloantigens*. *Blood*, 2002. **99**(5): p. 1692-8.
116. Harrington, W.J., et al., *Immunologic mechanisms in idiopathic and neonatal thrombocytopenic purpura*. *Ann Intern Med*, 1953. **38**(3): p. 433-69.
117. Shulman, N.R., *Immunoreactions involving platelets. IV. Studies on the pathogenesis of thrombocytopenia in drug purpura using test doses of quinidine in sensitized individuals; their implications in idiopathic thrombocytopenic purpura*. *J Exp Med*, 1958. **107**(5): p. 711-29.
118. Bertrand, G., et al., *Prediction of the fetal status in noninvasive management of alloimmune thrombocytopenia*. *Blood*, 2011. **117**(11): p. 3209-13.
119. Kaplan, C., *Foetal and neonatal alloimmune thrombocytopenia*. *Orphanet J Rare Dis*, 2006. **1**: p. 39.
120. Michelson, A.D., *Platelets*. Academic Press, 2013.
121. Pahal, G.S., et al., *Normal development of human fetal hematopoiesis between eight and seventeen weeks' gestation*. *Am J Obstet Gynecol*, 2000. **183**(4): p. 1029-34.
122. Forestier, F., et al., *Hematological values of 163 normal fetuses between 18 and 30 weeks of gestation*. *Pediatr Res*, 1986. **20**(4): p. 342-6.
123. Hohlfeld, P., et al., *Fetal thrombocytopenia: a retrospective survey of 5,194 fetal blood samplings*. *Blood*, 1994. **84**(6): p. 1851-6.
124. Dreyfus, M., et al., *Frequency of immune thrombocytopenia in newborns: a prospective study*. *Immune Thrombocytopenia Working Group*. *Blood*, 1997. **89**(12): p. 4402-6.
125. Rayment, R., et al., *Neonatal alloimmune thrombocytopenia*. *BMJ*, 2003. **327**(7410): p. 331-2.
126. Kaplan, C., et al., *Feto-maternal alloimmune thrombocytopenia: antenatal therapy with IvIgG and steroids--more questions than answers*. *European Working Group on FMAIT*. *Br J Haematol*, 1998. **100**(1): p. 62-5.
127. Bussel, J.B., et al., *Antenatal management of alloimmune thrombocytopenia with intravenous gamma-globulin: a randomized trial of the addition of low-dose steroid to intravenous gamma-globulin*. *Am J Obstet Gynecol*, 1996. **174**(5): p. 1414-23.
128. Kaplan, C., et al., *Management of alloimmune thrombocytopenia: antenatal diagnosis and in utero transfusion of maternal platelets*. *Blood*, 1988. **72**(1): p. 340-3.
129. Daffos, F., et al., *Prenatal treatment of alloimmune thrombocytopenia*. *Lancet*, 1984. **2**(8403): p. 632.
130. Nicolini, U., et al., *In-utero platelet transfusion for alloimmune thrombocytopenia*. *Lancet*, 1988. **2**(8609): p. 506.
131. Murphy, M.F., et al., *Antenatal management of severe feto-maternal alloimmune thrombocytopenia: HLA incompatibility may affect responses to fetal platelet transfusions*. *Blood*, 1993. **81**(8): p. 2174-9.
132. Gruel, Y., et al., *Determination of platelet antigens and glycoproteins in the human fetus*. *Blood*, 1986. **68**(2): p. 488-92.
133. Silver, R.M., et al., *Neonatal alloimmune thrombocytopenia: antenatal management*. *Am J Obstet Gynecol*, 2000. **182**(5): p. 1233-8.
134. Giovangrandi, Y., et al., *Very early intracranial haemorrhage in alloimmune fetal thrombocytopenia*. *Lancet*, 1990. **336**(8710): p. 310.

135. Mandel, P.a.M., P., *Les acides nucléiques du plasma sanguin chez l'Homme*. Comptes Rendus des Seances de la Societe de Biologie et de ses Filiales, 1948. **142**: p. 241-243.
136. Tan, E.M., et al., *Deoxybonucleic acid (DNA) and antibodies to DNA in the serum of patients with systemic lupus erythematosus*. J Clin Invest, 1966. **45**(11): p. 1732-40.
137. Leon, S.A., et al., *Free DNA in the serum of cancer patients and the effect of therapy*. Cancer Res, 1977. **37**(3): p. 646-50.
138. Lo, Y.M., et al., *Presence of fetal DNA in maternal plasma and serum*. Lancet, 1997. **350**(9076): p. 485-7.
139. Lo, Y.M., et al., *Quantitative analysis of fetal DNA in maternal plasma and serum: implications for noninvasive prenatal diagnosis*. Am J Hum Genet, 1998. **62**(4): p. 768-75.
140. Alberry, M., et al., *Free fetal DNA in maternal plasma in anembryonic pregnancies: confirmation that the origin is the trophoblast*. Prenat Diagn, 2007. **27**(5): p. 415-8.
141. Chan, K.C., et al., *Size distributions of maternal and fetal DNA in maternal plasma*. Clin Chem, 2004. **50**(1): p. 88-92.
142. Li, Y., et al., *Size separation of circulatory DNA in maternal plasma permits ready detection of fetal DNA polymorphisms*. Clin Chem, 2004. **50**(6): p. 1002-11.
143. Lo, Y.M., et al., *Maternal plasma DNA sequencing reveals the genome-wide genetic and mutational profile of the fetus*. Sci Transl Med, 2010. **2**(61): p. 61ra91.
144. Holdenrieder, S., et al., *Circulating nucleosomes in serum*. Ann N Y Acad Sci, 2001. **945**: p. 93-102.
145. Sun, K., et al., *Size-tagged preferred ends in maternal plasma DNA shed light on the production mechanism and show utility in noninvasive prenatal testing*. Proc Natl Acad Sci U S A, 2018. **115**(22): p. E5106-E5114.
146. Lo, Y.M., et al., *Rapid clearance of fetal DNA from maternal plasma*. Am J Hum Genet, 1999. **64**(1): p. 218-24.
147. Kotsopoulou, I., et al., *Non-invasive prenatal testing (NIPT): limitations on the way to become diagnosis*. Diagnosis (Berl), 2015. **2**(3): p. 141-158.
148. Jakobsen, T.R., et al., *High levels of fetal DNA are associated with increased risk of spontaneous preterm delivery*. Prenat Diagn, 2012. **32**(9): p. 840-5.
149. Leung, T.N., et al., *Maternal plasma fetal DNA as a marker for preterm labour*. Lancet, 1998. **352**(9144): p. 1904-5.
150. Lo, Y.M., et al., *Quantitative abnormalities of fetal DNA in maternal serum in preeclampsia*. Clin Chem, 1999. **45**(2): p. 184-8.
151. Zhong, X.Y., et al., *Elevation of both maternal and fetal extracellular circulating deoxyribonucleic acid concentrations in the plasma of pregnant women with preeclampsia*. Am J Obstet Gynecol, 2001. **184**(3): p. 414-9.
152. Lo, Y.M., et al., *Increased fetal DNA concentrations in the plasma of pregnant women carrying fetuses with trisomy 21*. Clin Chem, 1999. **45**(10): p. 1747-51.
153. Zhong, X.Y., et al., *Fetal DNA in maternal plasma is elevated in pregnancies with aneuploid fetuses*. Prenat Diagn, 2000. **20**(10): p. 795-8.
154. Lo, Y.M., *Fetal RhD genotyping from maternal plasma*. Ann Med, 1999. **31**(5): p. 308-12.
155. Lo, Y.M., et al., *Prenatal diagnosis of fetal RhD status by molecular analysis of maternal plasma*. N Engl J Med, 1998. **339**(24): p. 1734-8.

156. Clausen, F.B., et al., *Routine noninvasive prenatal screening for fetal RHD in plasma of RhD-negative pregnant women-2 years of screening experience from Denmark*. Prenat Diagn, 2014. **34**(10): p. 1000-5.
157. de Haas, M., et al., *Sensitivity of fetal RHD screening for safe guidance of targeted anti-D immunoglobulin prophylaxis: prospective cohort study of a nationwide programme in the Netherlands*. BMJ, 2016. **355**: p. i5789.
158. Haimila, K., et al., *Targeted antenatal anti-D prophylaxis program for RhD-negative pregnant women - outcome of the first two years of a national program in Finland*. Acta Obstet Gynecol Scand, 2017. **96**(10): p. 1228-1233.
159. Clausen, F.B., et al., *Pre-analytical conditions in non-invasive prenatal testing of cell-free fetal RHD*. PLoS One, 2013. **8**(10): p. e76990.
160. Clausen, F.B., et al., *Report of the first nationally implemented clinical routine screening for fetal RHD in D- pregnant women to ascertain the requirement for antenatal RhD prophylaxis*. Transfusion, 2012. **52**(4): p. 752-8.
161. Sorensen, K., et al., *Determination of fetal RHD type in plasma of RhD negative pregnant women*. Scand J Clin Lab Invest, 2018. **78**(5): p. 411-416.
162. Chitty, L.S., et al., *Diagnostic accuracy of routine antenatal determination of fetal RHD status across gestation: population based cohort study*. BMJ, 2014. **349**: p. g5243.
163. Soothill, P.W., et al., *Use of cffDNA to avoid administration of anti-D to pregnant women when the fetus is RhD-negative: implementation in the NHS*. BJOG, 2015. **122**(12): p. 1682-6.
164. Wikman, A.T., et al., *Noninvasive single-exon fetal RHD determination in a routine screening program in early pregnancy*. Obstet Gynecol, 2012. **120**(2 Pt 1): p. 227-34.
165. Daniels, G., et al., *Vox Sanguinis International Forum on application of fetal blood grouping: summary*. Vox Sang, 2018. **113**(2): p. 198-201.
166. Entbindung, G.B.ü.d.ä.B.w.d.S.u.n.d., *Mutterschafts-Richtlinien*. 2020, Bundesanzeiger AT 23.11.2020 B3.
167. Clausen, F.B., et al., *Non-invasive foetal RhD genotyping to guide anti-D prophylaxis: an external quality assurance workshop*. Blood Transfus, 2018. **16**(4): p. 359-362.
168. Clausen, F.B. and A. Hellberg, *External quality assessment of noninvasive fetal RHD genotyping*. Vox Sang, 2020. **115**(5): p. 466-471.
169. Finning, K., et al., *Fetal genotyping for the K (Kell) and Rh C, c, and E blood groups on cell-free fetal DNA in maternal plasma*. Transfusion, 2007. **47**(11): p. 2126-33.
170. Cro, F., et al., *An innovative test for non-invasive Kell genotyping on circulating fetal DNA by means of the allelic discrimination of K1 and K2 antigens*. Am J Reprod Immunol, 2016. **76**(6): p. 499-503.
171. Wu, R., *Nucleotide sequence analysis of DNA. I. Partial sequence of the cohesive ends of bacteriophage lambda and 186 DNA*. J Mol Biol, 1970. **51**(3): p. 501-21.
172. Sanger, F., S. Nicklen, and A.R. Coulson, *DNA sequencing with chain-terminating inhibitors*. Proc Natl Acad Sci U S A, 1977. **74**(12): p. 5463-7.
173. Maxam, A.M. and W. Gilbert, *A new method for sequencing DNA*. Proc Natl Acad Sci U S A, 1977. **74**(2): p. 560-4.
174. Kasianowicz, J.J., et al., *Characterization of individual polynucleotide molecules using a membrane channel*. Proc Natl Acad Sci U S A, 1996. **93**(24): p. 13770-3.

175. Shendure, J., et al., *Accurate multiplex polony sequencing of an evolved bacterial genome*. *Science*, 2005. **309**(5741): p. 1728-32.
176. Margulies, M., et al., *Genome sequencing in microfabricated high-density picolitre reactors*. *Nature*, 2005. **437**(7057): p. 376-80.
177. Rothberg, J.M., et al., *An integrated semiconductor device enabling non-optical genome sequencing*. *Nature*, 2011. **475**(7356): p. 348-52.
178. Hyman, E.D., *A new method of sequencing DNA*. *Anal Biochem*, 1988. **174**(2): p. 423-36.
179. Seo, T.S., et al., *Photocleavable fluorescent nucleotides for DNA sequencing on a chip constructed by site-specific coupling chemistry*. *Proc Natl Acad Sci U S A*, 2004. **101**(15): p. 5488-93.
180. Ju, J., et al., *Four-color DNA sequencing by synthesis using cleavable fluorescent nucleotide reversible terminators*. *Proc Natl Acad Sci U S A*, 2006. **103**(52): p. 19635-40.
181. Bentley, D.R., et al., *Accurate whole human genome sequencing using reversible terminator chemistry*. *Nature*, 2008. **456**(7218): p. 53-9.
182. Mardis, E.R., *Next-generation DNA sequencing methods*. *Annu Rev Genomics Hum Genet*, 2008. **9**: p. 387-402.
183. Rieneck, K., et al., *Next-generation sequencing: proof of concept for antenatal prediction of the fetal Kell blood group phenotype from cell-free fetal DNA in maternal plasma*. *Transfusion*, 2013. **53**(11 Suppl 2): p. 2892-8.
184. Wienzek-Lischka, S., et al., *Noninvasive fetal genotyping of human platelet antigen-1a using targeted massively parallel sequencing*. *Transfusion*, 2015. **55**(6 Pt 2): p. 1538-44.
185. Johnson, K.L., et al., *Interlaboratory comparison of fetal male DNA detection from common maternal plasma samples by real-time PCR*. *Clin Chem*, 2004. **50**(3): p. 516-21.
186. Lau, E.C., et al., *Human and mouse amelogenin gene loci are on the sex chromosomes*. *Genomics*, 1989. **4**(2): p. 162-8.
187. Nakahori, Y., O. Takenaka, and Y. Nakagome, *A human X-Y homologous region encodes "amelogenin"*. *Genomics*, 1991. **9**(2): p. 264-9.
188. Sullivan, K.M., et al., *A rapid and quantitative DNA sex test: fluorescence-based PCR analysis of X-Y homologous gene amelogenin*. *Biotechniques*, 1993. **15**(4): p. 636-8, 640-1.
189. Mannucci, A., et al., *Forensic application of a rapid and quantitative DNA sex test by amplification of the X-Y homologous gene amelogenin*. *Int J Legal Med*, 1994. **106**(4): p. 190-3.
190. C Phillips, M.L., J Sanchez, M Brion, B Sobrino, N Morling, P Schneider, D Syndercombe Court, A Carracedo, *Selecting single nucleotide polymorphisms for forensic applications*. Elsevier, 2004. **1261**: p. 18-20.
191. Sanchez, J.J., et al., *A multiplex assay with 52 single nucleotide polymorphisms for human identification*. *Electrophoresis*, 2006. **27**(9): p. 1713-24.
192. Houck, M.M., *Forensic Biology* 1st ed. Elsevier, ed. M.M. Houck. 2015.
193. Gill, P., *An assessment of the utility of single nucleotide polymorphisms (SNPs) for forensic purposes*. *Int J Legal Med*, 2001. **114**(4-5): p. 204-10.
194. Pontes, M.L., et al., *SNP Markers as Additional Information to Resolve Complex Kinship Cases*. *Transfus Med Hemother*, 2015. **42**(6): p. 385-8.
195. Schwark, T., et al., *The SNPforID Assay as a Supplementary Method in Kinship and Trace Analysis*. *Transfus Med Hemother*, 2012. **39**(3): p. 187-193.

196. Borsting, C., et al., *Performance of the SNPforID 52 SNP-plex assay in paternity testing*. Forensic Sci Int Genet, 2008. **2**(4): p. 292-300.
197. Musgrave-Brown, E., et al., *Forensic validation of the SNPforID 52-plex assay*. Forensic Sci Int Genet, 2007. **1**(2): p. 186-90.
198. S. Alimat, S.H., W. Goodwin, *SNP genotyping of forensic casework samples using the 52 SNPforID markers*. Forensic Science International: Genetics Supplement Series, 2013. **4**: p. 178-179.
199. P.Dario, A.R.O., T.Ribeiro, M.J.Porto, J.Costa Santos, D.Dias, F.Corte Real, *SNPforID 52-plex in casework samples: "Cracking" bones and other difficult samples*. Forensic Science International: Genetics Supplement Series, 2015. **5**: p. 118-120.
200. Doescher, A., et al., *Evaluation of single-nucleotide polymorphisms as internal controls in prenatal diagnosis of fetal blood groups*. Transfusion, 2013. **53**(2): p. 353-62.
201. Li, Y., et al., *Determination of RHD zygosity using real-time quantitative PCR*. Swiss Med Wkly, 2003. **133**(31-32): p. 442-5.
202. Krog, G.R., F.B. Clausen, and M.H. Dziegiel, *Quantitation of RHD by real-time polymerase chain reaction for determination of RHD zygosity and RHD mosaicism/chimerism: an evaluation of four quantitative methods*. Transfusion, 2007. **47**(4): p. 715-22.
203. Svobodova, I., et al., *Performance of Droplet Digital PCR in Non-Invasive Fetal RHD Genotyping - Comparison with a Routine Real-Time PCR Based Approach*. PLoS One, 2015. **10**(11): p. e0142572.
204. Squidonius. *Qiagen Mini Spin Column*. 2008; Available from: https://commons.wikimedia.org/wiki/File:Qiagen_Mini_Spin_Column.svg, Status 18.12.20.
205. Boom, R., et al., *Rapid and simple method for purification of nucleic acids*. J Clin Microbiol, 1990. **28**(3): p. 495-503.
206. Borodina, T.A., H. Lehrach, and A.V. Soldatov, *DNA purification on homemade silica spin-columns*. Anal Biochem, 2003. **321**(1): p. 135-7.
207. Promega, *Maxwell*. 2020: p. permission granted on 11/11/20 by email.
208. Dean, F.B., et al., *Comprehensive human genome amplification using multiple displacement amplification*. Proc Natl Acad Sci U S A, 2002. **99**(8): p. 5261-6.
209. Lizardi, P.M., *U.S. Patent 6,124,120*. 2000.
210. Blanco, L. and M. Salas, *Characterization and purification of a phage phi 29-encoded DNA polymerase required for the initiation of replication*. Proc Natl Acad Sci U S A, 1984. **81**(17): p. 5325-9.
211. Dean, F.B., et al., *Rapid amplification of plasmid and phage DNA using Phi 29 DNA polymerase and multiply-primed rolling circle amplification*. Genome Res, 2001. **11**(6): p. 1095-9.
212. Lasken, R.S., *Genomic DNA amplification by the multiple displacement amplification (MDA) method*. Biochem Soc Trans, 2009. **37**(Pt 2): p. 450-3.
213. Qianlim. *MDA reaction steps*. 2009; Available from: https://commons.wikimedia.org/wiki/File:MDA_reaction_steps.JPG, Status 18.12.20.
214. Müller HJ., P.D.R., *Nested PCR*. In: *PCR - Polymerase-Kettenreaktion*. Springer Spektrum, Berlin, Heidelberg, 2016.
215. Mülhardt, C., *Der Experimentator: Molekularbiologie/Genomics*. 2003. **4. Auflage**: p. 86.

216. Singh, J., Birbian², N., Sinha, S., Goswami, A., *A critical review on PCR, its types and applications*. International Journal of Advanced Research in Biological Sciences, 2014.
217. Arneemann, J., *PCR-Aufreinigung*. In: Gressner A.M., Arndt T. (eds) *Lexikon der Medizinischen Laboratoriumsdiagnostik*. Springer Reference Medizin. Springer, Berlin, Heidelberg, 2019.
218. Sykes, P.J., et al., *Quantitation of targets for PCR by use of limiting dilution*. Biotechniques, 1992. **13**(3): p. 444-9.
219. Kalinina, O., et al., *Nanoliter scale PCR with TaqMan detection*. Nucleic Acids Res, 1997. **25**(10): p. 1999-2004.
220. Vogelstein, B. and K.W. Kinzler, *Digital PCR*. Proc Natl Acad Sci U S A, 1999. **96**(16): p. 9236-41.
221. Quan, P.L., M. Sauzade, and E. Brouzes, *dPCR: A Technology Review*. Sensors (Basel), 2018. **18**(4).
222. Holland, P.M., et al., *Detection of specific polymerase chain reaction product by utilizing the 5'----3' exonuclease activity of Thermus aquaticus DNA polymerase*. Proc Natl Acad Sci U S A, 1991. **88**(16): p. 7276-80.
223. Lyamichev, V., M.A. Brow, and J.E. Dahlberg, *Structure-specific endonucleolytic cleavage of nucleic acids by eubacterial DNA polymerases*. Science, 1993. **260**(5109): p. 778-83.
224. Lee, L.G., C.R. Connell, and W. Bloch, *Allelic discrimination by nick-translation PCR with fluorogenic probes*. Nucleic Acids Res, 1993. **21**(16): p. 3761-6.
225. Livak, K.J., et al., *Oligonucleotides with fluorescent dyes at opposite ends provide a quenched probe system useful for detecting PCR product and nucleic acid hybridization*. PCR Methods Appl, 1995. **4**(6): p. 357-62.
226. Förster, *Zwischenmolekulare Energiewanderung und Fluoreszenz*. Annalen der Physik, 1948. **437**(1-2): p. 55-75.
227. Braindamaged. *Taqman*. 2009; Available from: <https://en.wikipedia.org/w/index.php?title=File:Taqman.png>, Status 11.11.20.
228. Sanders, R., et al., *Evaluation of digital PCR for absolute DNA quantification*. Anal Chem, 2011. **83**(17): p. 6474-84.
229. White, R.A., 3rd, et al., *Digital PCR provides sensitive and absolute calibration for high throughput sequencing*. BMC Genomics, 2009. **10**: p. 116.
230. Hoshino, T. and F. Inagaki, *Molecular quantification of environmental DNA using microfluidics and digital PCR*. Syst Appl Microbiol, 2012. **35**(6): p. 390-5.
231. Whale, A.S., et al., *Comparison of microfluidic digital PCR and conventional quantitative PCR for measuring copy number variation*. Nucleic Acids Res, 2012. **40**(11): p. e82.
232. Mullis, K., et al., *Specific enzymatic amplification of DNA in vitro: the polymerase chain reaction*. Cold Spring Harb Symp Quant Biol, 1986. **51 Pt 1**: p. 263-73.
233. Saiki, R.K., et al., *Enzymatic amplification of beta-globin genomic sequences and restriction site analysis for diagnosis of sickle cell anemia*. Science, 1985. **230**(4732): p. 1350-4.
234. Newton, C.R., et al., *Analysis of any point mutation in DNA. The amplification refractory mutation system (ARMS)*. Nucleic Acids Res, 1989. **17**(7): p. 2503-16.
235. Wu, D.Y., et al., *Allele-specific enzymatic amplification of beta-globin genomic DNA for diagnosis of sickle cell anemia*. Proc Natl Acad Sci U S A, 1989. **86**(8): p. 2757-60.

236. Pignatelli, D., et al., *The Complexities in Genotyping of Congenital Adrenal Hyperplasia: 21-Hydroxylase Deficiency*. *Front Endocrinol (Lausanne)*, 2019. **10**: p. 432.
237. Heid, C.A., et al., *Real time quantitative PCR*. *Genome Res*, 1996. **6**(10): p. 986-94.
238. Chiu, R.W., et al., *Determination of RhD zygosity: comparison of a double amplification refractory mutation system approach and a multiplex real-time quantitative PCR approach*. *Clin Chem*, 2001. **47**(4): p. 667-72.
239. Sinclair, A.H., et al., *A gene from the human sex-determining region encodes a protein with homology to a conserved DNA-binding motif*. *Nature*, 1990. **346**(6281): p. 240-4.
240. Lovell-Badge, R., *The role of Sry in mammalian sex determination*. *Ciba Found Symp*, 1992. **165**: p. 162-79; discussion 179-82.
241. Scheffer, P.G., et al., *Noninvasive fetal blood group genotyping of rhesus D, c, E and of K in alloimmunised pregnant women: evaluation of a 7-year clinical experience*. *BJOG*, 2011. **118**(11): p. 1340-8.
242. Fazekas de St, G., *The evaluation of limiting dilution assays*. *J Immunol Methods*, 1982. **49**(2): p. R11-23.
243. Devonshire, A.S., et al., *Towards standardisation of cell-free DNA measurement in plasma: controls for extraction efficiency, fragment size bias and quantification*. *Anal Bioanal Chem*, 2014. **406**(26): p. 6499-512.
244. Sorber, L., et al., *A Comparison of Cell-Free DNA Isolation Kits: Isolation and Quantification of Cell-Free DNA in Plasma*. *J Mol Diagn*, 2017. **19**(1): p. 162-168.
245. Perez-Barrios, C., et al., *Comparison of methods for circulating cell-free DNA isolation using blood from cancer patients: impact on biomarker testing*. *Transl Lung Cancer Res*, 2016. **5**(6): p. 665-672.
246. Diefenbach, R.J., et al., *Evaluation of commercial kits for purification of circulating free DNA*. *Cancer Genet*, 2018. **228-229**: p. 21-27.
247. Reid, A.L., et al., *Detection of BRAF-V600E and V600K in melanoma circulating tumour cells by droplet digital PCR*. *Clin Biochem*, 2015. **48**(15): p. 999-1002.
248. Jackson, J.B., et al., *Multiplex Pre-amplification of Serum DNA to Facilitate Reliable Detection of Extremely Rare Cancer Mutations in Circulating DNA by Digital PCR*. *J Mol Diagn*, 2016. **18**(2): p. 235-43.
249. Yao, H., et al., *Coupling multiplex pre-amplification and droplet digital PCR for longitudinal monitoring of *ESR1* and *PIK3CA* mutations from plasma cell-free DNA*. *bioRxiv*, 2019: p. 598847.
250. Sillence, K.A., et al., *Fetal Sex and RHD Genotyping with Digital PCR Demonstrates Greater Sensitivity than Real-time PCR*. *Clin Chem*, 2015. **61**(11): p. 1399-407.
251. Sato, A., et al., *Investigation of appropriate pre-analytical procedure for circulating free DNA from liquid biopsy*. *Oncotarget*, 2018. **9**(61): p. 31904-31914.
252. Norton, S.E., et al., *A new blood collection device minimizes cellular DNA release during sample storage and shipping when compared to a standard device*. *J Clin Lab Anal*, 2013. **27**(4): p. 305-11.
253. Parackal, S., et al., *Comparison of Roche Cell-Free DNA collection Tubes ((R)) to Streck Cell-Free DNA BCT ((R)) s for sample stability using healthy volunteers*. *Pract Lab Med*, 2019. **16**: p. e00125.

254. Fernando, M.R., et al., *A new methodology to preserve the original proportion and integrity of cell-free fetal DNA in maternal plasma during sample processing and storage*. Prenat Diagn, 2010. **30**(5): p. 418-24.
255. Norton, S.E., et al., *A stabilizing reagent prevents cell-free DNA contamination by cellular DNA in plasma during blood sample storage and shipping as determined by digital PCR*. Clin Biochem, 2013. **46**(15): p. 1561-5.
256. Zhao, Y., et al., *Performance comparison of blood collection tubes as liquid biopsy storage system for minimizing cfDNA contamination from genomic DNA*. J Clin Lab Anal, 2019. **33**(2): p. e22670.
257. Madic, J., et al., *Three-color crystal digital PCR*. Biomol Detect Quantif, 2016. **10**: p. 34-46.
258. Chan, K.C., et al., *Hypermethylated RASSF1A in maternal plasma: A universal fetal DNA marker that improves the reliability of noninvasive prenatal diagnosis*. Clin Chem, 2006. **52**(12): p. 2211-8.
259. White, H.E., et al., *Evaluation of a novel assay for detection of the fetal marker RASSF1A: facilitating improved diagnostic reliability of noninvasive prenatal diagnosis*. PLoS One, 2012. **7**(9): p. e45073.
260. Muller, S.P., et al., *The determination of the fetal D status from maternal plasma for decision making on Rh prophylaxis is feasible*. Transfusion, 2008. **48**(11): p. 2292-301.
261. O'Brien, H., et al., *Non-invasive prenatal testing (NIPT) for fetal Kell, Duffy and Rh blood group antigen prediction in alloimmunised pregnant women: power of droplet digital PCR*. Br J Haematol, 2020. **189**(3): p. e90-e94.
262. Rieneck, K., F.B. Clausen, and M.H. Dziegiel, *Noninvasive Antenatal Determination of Fetal Blood Group Using Next-Generation Sequencing*. Cold Spring Harb Perspect Med, 2015. **6**(1): p. a023093.
263. Scheffer, P.G., et al., *Noninvasive fetal genotyping of human platelet antigen-1a*. BJOG, 2011. **118**(11): p. 1392-5.
264. Ferro, M., et al., *Noninvasive prenatal diagnosis by cell-free DNA screening for fetomaternal HPA-1a platelet incompatibility*. Transfusion, 2018. **58**(10): p. 2272-2279.
265. Kjeldsen-Kragh, J., et al., *A screening and intervention program aimed to reduce mortality and serious morbidity associated with severe neonatal alloimmune thrombocytopenia*. Blood, 2007. **110**(3): p. 833-9.
266. Nogues, N., *Recent advances in non-invasive fetal HPA-1a typing*. Transfus Apher Sci, 2020. **59**(1): p. 102708.
267. Järås, K., *Prophylactic treatment to prevent immunisation against human platelet antigen (HPA) 1a – a new approach for prevention of foetal and neonatal alloimmune thrombocytopenia*. Z Geburtshilfe Neonatol, 2013. **V25_5**: p. 217.
268. Orzinska, A., et al., *Noninvasive prenatal HPA-1 typing in HPA-1a negative pregnancies selected in the Polish PREVFNAIT screening program*. Transfusion, 2018. **58**(11): p. 2705-2711.
269. Winkelhorst, D., et al., *HIP (HPA-screening in pregnancy) study: protocol of a nationwide, prospective and observational study to assess incidence and natural history of fetal/neonatal alloimmune thrombocytopenia and identifying pregnancies at risk*. BMJ Open, 2020. **10**(7): p. e034071.
270. Jaegtvik, S., et al., *Neonatal alloimmune thrombocytopenia due to anti-HPA 1a antibodies; the level of maternal antibodies predicts the severity of thrombocytopenia in the newborn*. BJOG, 2000. **107**(5): p. 691-4.

271. Tozzo, P., et al., *Deletion of amelogenin Y-locus in forensics: literature revision and description of a novel method for sex confirmation*. J Forensic Leg Med, 2013. **20**(5): p. 387-91.
272. Zehethofer, K. and B. Rolf, *A molecular analysis of three amelogenin negative males in two routine paternity tests*. Forensic Sci Int Genet, 2011. **5**(5): p. 550-1.
273. Santos, F.R., A. Pandya, and C. Tyler-Smith, *Reliability of DNA-based sex tests*. Nat Genet, 1998. **18**(2): p. 103.
274. Chang, Y.M., et al., *A distinct Y-STR haplotype for Amelogenin negative males characterized by a large Y(p)11.2 (DYS458-MSY1-AMEL-Y) deletion*. Forensic Sci Int, 2007. **166**(2-3): p. 115-20.
275. Ma, Y., et al., *Y chromosome interstitial deletion induced Y-STR allele dropout in AMELY-negative individuals*. Int J Legal Med, 2012. **126**(5): p. 713-24.
276. Kashyap, V.K., et al., *Deletions in the Y-derived amelogenin gene fragment in the Indian population*. BMC Med Genet, 2006. **7**: p. 37.
277. Steinlechner, M., et al., *Rare failures in the amelogenin sex test*. Int J Legal Med, 2002. **116**(2): p. 117-20.
278. Roffey, P.E., C.I. Eckhoff, and J.L. Kuhl, *A rare mutation in the amelogenin gene and its potential investigative ramifications*. J Forensic Sci, 2000. **45**(5): p. 1016-9.
279. Ou, X., et al., *Null alleles of the X and Y chromosomal amelogenin gene in a Chinese population*. Int J Legal Med, 2012. **126**(4): p. 513-8.
280. P.M.Stapleton, D.L., C.D. Millar, E. Wu, M. Andres, D.R. Love, *Discovery of three related females who type XY at the amelogenin locus*. Forensic Science International: Genetics Supplement Series, 2008. **1**(1): p. 577-579.
281. Maciejewska, A. and R. Pawlowski, *A rare mutation in the primer binding region of the Amelogenin X homologue gene*. Forensic Sci Int Genet, 2009. **3**(4): p. 265-7.
282. Shadrach, B., et al., *A rare mutation in the primer binding region of the amelogenin gene can interfere with gender identification*. J Mol Diagn, 2004. **6**(4): p. 401-5.
283. Caratti, S., et al., *Amplification failure of the amelogenin gene (AMELX) caused by a primer binding site mutation*. Prenat Diagn, 2009. **29**(12): p. 1180-2.

7 SUPPLEMENTAL MATERIAL

Chapter 3.3 shows the technical validation of the various assays. But the tables already show the summary of the data from the biological triplicates. To show how these values arose, the evaluation is shown here using the RHD exon 7 and HPA1a assay as an example. The values for Rox, neg. FAM and neg. VIC were output by the QuantStudio™ 3D AnalysisSuite™ cloud software. The formulas for further calculations can be found in chapter 2.14.

Table 44: Example of the raw data during technical validation of the RHD exon 7 assay. SD: standard deviation

Mixture	Volunteer RHD neg	Volunteer RHD pos.	RHD exon 7																		
			RHD negative Volumen in µl	RHD positive Volumen in µl	ROX	neg Fam	neg VIC	P(Fam)	λ (Fam)	FAM copies/µl	Mean FAM copies/µl	SD	P(Vic)	λ(Vic)	VIC copies/µl	Mean VIC copies/µl	SD	Target/Total [%]	Mean Target/Total [%]	SD	
5%	39	91	950	50	17630	16860	6123	0.96	0.04	59.15				0.35	1.06	1400.73			4.05		
	67	90	950	50	15846	15335	6364	0.97	0.03	43.42				0.40	0.91	1208.29			3.47		
	39	113	950	50	17499	15680	2708	0.90	0.11	145.37	82.65	44.82	0.15	1.87	2471.43	1693.48	555.68	5.56	4.36	0.88	
1%	39	91	990	10	16939	16691	7587	0.99	0.01	19.54				0.45	0.80	1063.82			1.80		
	67	90	990	10	17204	16966	8602	0.99	0.01	18.45				0.50	0.69	918.08			1.97		
	39	113	990	10	17288	16366	2616	0.95	0.05	72.59	36.86	25.27	0.15	1.89	2501.15	1494.35	714.40	2.82	2.20	0.45	
0.50%	39	91	995	5	16846	16758	11660	0.99	0.01	6.94				0.69	0.37	487.35			1.40		
	67	90	995	5	16576	16572	8596	1.00	0.00	0.32				0.52	0.66	869.75			0.04		
	39	113	995	5	17781	17779	6009	1.00	0.00	0.15	2.47	3.16	0.34	1.08	1436.92	931.34	390.10	0.01	0.48	0.65	
0.10%	39	91	999	1	17845	17830	7932	1.00	0.00	1.11				0.44	0.81	1073.93			0.10		
	67	90	999	1	15550	15546	12053	1.00	0.00	0.34				0.78	0.25	337.41			0.10		
	39	113	999	1	17368	17358	4919	1.00	0.00	0.76	0.74	0.32	0.28	1.26	1670.89	1027.41	545.38	0.05	0.08	0.03	
RHD neg.	39		1000	0	16649	16629	5733	1.00	0.00	1.59				0.34	1.07	1412.07			0.11		
RHD neg.	67		1000	0	17308	17307	9485	1.00	0.00	0.08				0.55	0.60	796.63			0.01		
RHD neg.	39		1000	0	17081	17079	5976	1.00	0.00	0.16	0.61	0.70	0.35	1.05	1391.01	1199.90	285.29	0.01	0.04	0.05	
RHD pos.		91	0	1000	17198	12812	11501	0.74	0.29	389.95				0.67	0.40	532.93			42.25		
RHD pos.		90	0	1000	16573	8406	7285	0.51	0.68	899.11				0.44	0.82	1088.69			45.23		
RHD pos.		113	0	1000	17283	5123	4105	0.30	1.22	1610.57	966.54	500.59	0.24	1.44	1904.00	1175.20	563.07	45.83	44.44	1.56	

SUPPLEMENTAL MATERIAL

Table 45: Example of the raw data during technical validation of the HPA-1a assay. SD: standard deviation

Mixture	Volunteer RHD neg	Volunteer RHD pos.	RHD negative Volumen in µl	RHD positive Volumen in µl	HPA-1a																
					ROX	neg Fam	neg VIC	P(Fam)	λ (Fam)	FAM copies/µl	Mean FAM copies /µl	SD	P(Vic)	λ(Vic)	VIC copies/µl	Mean VIC copies/µl	SD	Target/Total [%]	Mean Target/Total [%]	SD	
5%	HPA1bb-1	125	950	50	17077	16475	3358	0.96	0.04	47.53				0.20	1.63	2154.15			2.16		
	HPA1bb-2	84	950	50	16957	15494	1553	0.91	0.09	119.51				0.09	2.39	3166.21			3.64		
	HPA1bb-3	113	950	50	16784	16205	858	0.97	0.04	46.50	83.52	35.99		0.05	2.97	3938.51	3086.29	730.65	1.17	2.32	1.01
1%	HPA1bb-1	125	990	10	17103	17092	6667	1.00	0.00	0.85				0.39	0.94	1247.79			0.07		
	HPA1bb-2	84	990	10	16599	16065	2402	0.97	0.03	43.31				0.14	1.93	2560.32			1.66		
	HPA1bb-3	113	990	10	15229	15183	2340	1.00	0.00	4.01	22.08	21.23		0.15	1.87	2480.86	2096.32	600.88	0.16	0.63	0.73
0.50%	HPA1bb-1	125	995	5	17278	17111	7004	0.99	0.01	12.86				0.41	0.90	1195.96			1.06		
	HPA1bb-2	84	995	5	17273	17231	5001	1.00	0.00	3.22				0.29	1.24	1641.73			0.20		
	HPA1bb-3	113	995	5	17152	16754	1161	0.98	0.02	31.10	8.04	4.82		0.07	2.69	3566.67	2134.79	1028.72	0.86	0.71	0.37
0.10%	HPA1bb-1	125	999	1	17362	17345	6024	1.00	0.00	1.30				0.35	1.06	1402.03			0.09		
	HPA1bb-2	84	999	1	15461	15444	5494	1.00	0.00	1.46				0.36	1.03	1370.42			0.11		
	HPA1bb-3	113	999	1	16502	16441	1484	1.00	0.00	4.91	1.38	0.08		0.09	2.41	3190.38	1987.61	850.59	0.15	0.12	0.03
HPA-1bb.	HPA1bb-1		1000	0	16265	16264	6735	1.00	0.00	0.08				0.41	0.88	1167.81			0.01		
	HPA1bb-2		1000	0	17072	17070	6731	1.00	0.00	0.16				0.39	0.93	1232.74			0.01		
	HPA1bb-3		1000	0	17484	17469	208	1.00	0.00	1.14	0.12	0.04		0.01	4.43	5869.54	2756.70	2201.27	0.02	0.01	0.01
HPA-1ab		125	0	1000	17241	11103	11384	0.64	0.44	582.88				0.66	0.42	549.78			51.46		
		84	0	1000	16798	5463	6612	0.33	1.12	1487.76				0.39	0.93	1234.93			54.64		
HPA-1ab		113	0	1000	15768	6335	6546	0.40	0.91	1207.80	1092.8 16523	378.25 931		0.42	0.88	1164.41	983.04	307.71	50.91	52.3396898	1.643 93581 5

8 CURRICULUM VITAE

Name and first name Eryilmaz, Marion
Date of birth 26. März 1979
Place of birth Neustadt in Holstein

EDUCATION

08/2013 – 02/2016 Hochschule Mannheim University of Applied Sciences, Mannheim
Master of Science Biomedical Science and Technology (1.4) (31.10.2015)
Masterarbeit at the Kirchhoff-Institut for physics in Heidelberg (2015):
Investigation of DNA damage after ionizing radiation using Spatial Position
Determination Microscopy (SPDM) (1.0)

03/2009 – 07/2013 Hochschule Mannheim University of Applied Sciences, Mannheim
Bachelor of Science in Biological Chemistry (1.5) (01.07.2013)
Bachelor thesis at the German Cancer Research Center in Heidelberg (2013):
Effects of ionizing radiation on the regulation and organization of human
telomeres changes (1.0)

08/1999 – 07/2000 Gewerbeschule I, Lübeck
Acquisition of the technical college entrance qualification

08/1996 – 01/1999 Company Elektro Knop and Elektro Michalzik, Neustadt in Holstein
Training as an electrician

WORK EXPERIENCE

04/2020 – currently Parental leave

06/2017 – 03/2020 Institute for Transfusion Medicine and Immunology,
Medical Faculty Mannheim of Heidelberg University
Aiming for a dissertation

- Topic: Development of a noninvasive prenatal test for the determination of fetal blood cell antigens

09/2016 – 05/2017 Parental leave

03/2015 – 12/2016 Kirchhoff Institute for Physics, Heidelberg
Experimental Biophysics Department, Prof. Hausmann

10/2010 – 12/2015 German Cancer-research Center, Heidelberg
Department of Genetics of Skin Carcinogenesis, Prof. Boukamp
Student Assistant

01/2001 – 02/2009 Schleswig-Holstein Musik Festival e.V., Lübeck
Management assistant

FURTHER EDUCATION

06/2012-11/2013 Medical physics for physicists
University of Heidelberg Scientific advanced training in cooperation with
the German Cancer Research Center

ABSTRACTS

- Technical validation of noninvasive prenatal testing for blood group and platelet antigens from cell-free plasma DNA using digital PCR, cfDNA 2019
- Digital PCR in noninvasive prenatal diagnostics (2018)
- Digital PCR for the noninvasive prenatal diagnosis of blood group antigens from cell-free maternal plasma DNA, DGTI 2018
- Digital PCR for noninvasive prenatal diagnosis of blood group antigens from cell-free plasma DNA, DGTI 2017
- Influence of ionizing radiation on telomeres and genomic changes, AEK Conference 2013
- Genomic changes induced by ionizing radiation, Global Conference on Radiation 2013

Publications

- Introduction of Noninvasive Prenatal Testing for Blood Group and Platelet Antigens from Cell-Free Plasma DNA Using Digital PCR; *Transfus Med Hemother* 2019; doi: 10.1159/000504348
- Localization Microscopy Analyses of MRE11 Clusters in 3D-Conserved Cell Nuclei of Different Cell Lines; *Cancers* 2018, 10, 25; doi:10.3390/cancers10010025

Congress lectures:

- Noninvasive prenatal parentage testing using SNP*for*ID markers in digital PCR, German Society for Parentage Assessment (DGAB); 2019
- Fully integrated microfluidic lab-on-a-disk system for DNA extraction and HLA genotyping (DGTI); 2019
- Digital PCR for noninvasive prenatal diagnosis of blood group antigens from cell-free maternal plasma DNA (DGTI); 2018

Award:

- DGAB Research Competition 2018; Noninvasive prenatal parentage testing using SNP*for*ID markers in digital PCR, 2018
-

9 ACKNOWLEDGEMENTS

At first, I thank Prof. Dr. Harald Klüter for enabling this dissertation in his institute. I thank Prof. Dr. Peter Bugert for giving me this wonderful topic and the chance to work in this outstanding group.

Furthermore, I thank Gabi Rink and Katharina Kemp for their supervision and discussions. I also thank the members of inno-train Diagnostik GmbH for constructive discussions.

Finally, I thank the members of the Institute for Transfusion Medicine and Immunology as well as the members of the DRK-Blutspendedienst Baden-Württemberg - Hessen gGmbH for helpfulness, good discussions, and friendly working atmosphere.